Fishery Bulletin 105(1) Contents

Click on page numbers to go to PDF version of article.

Articles

1
Wexler, Jeanne B., Seinen Chow, Toshie Wakabayashi, Kenji Nohara, and Daniel Margulies
Temporal variation in growth of yellowfin tuna (*Thunnus albacares*) larvae in the Panama Bight, 1990-97

19
McDermott, Susanne F., Katherine P. Maslenikov, and Donald R. Gunderson
Annual fecundity, batch fecundity, and oocyte atresia of Atka mackerel (*Pleurogrammus monopterygius*) in Alaskan waters

30
Hobbs, James A., William A Bennett, Jessica E Burton, and Bradd Baskerville-Bridges
Modification of the biological intercept model to account for ontogenetic effects in laboratory-reared delta smelt (*Hypomesus transpacificus*)

39
Laidig, Thomas E., James R. Chess, and Daniel F. Howard
Relationship between abundance of juvenile rockfishes (*Sebastes* spp.) and environmental variables documented off northern California and potential mechanisms for the covariation

49
Harley, Shelton J., and Jenny M. Suter
The potential use of time-area closures to reduce catches of bigeye tuna (*Thunnus obesus*) in the purse-seine fishery of the eastern Pacific Ocean

62
Secor, David H., and Philip M. Piccoli
Oceanic migration rates of Upper Chesapeake Bay striped bass (*Morone saxatilis*), determined by otolith microchemical analysis

74
Matkin, Craig O., Lance G. Barrett-Lennard, Harald Yurk, David Ellifrit, and Andrew W. Trites
Ecotypic variation and predatory behavior among killer whales (*Orcinus orca*) off the eastern Aleutian Islands, Alaska

88
Stockhausen, William T., and Michael Fogarty
Removing observational noise from fisheries-independent time series data using ARIMA models

102
Pitcher, Kenneth W., Peter F. Olesiuk, Robin F. Brown, Mark S. Lowry,. Steven J.

Jeffries, John L. Sease, Wayne L. Perryman, Charles E. Stinchcomb, Lloyd F. Lowry
Abundance and distribution of the eastern North Pacific Steller sea lion (*Eumetopias jubatus*) population

116
Gerritsen, Hans D., and David McGrath
Precision estimates and suggested sample sizes for length-frequency data

121
Farley, Edward V. Jr, James M. Murphy, Milo D. Adkison, Lisa B. Eisner, John H. Helle, Jamal H. Moss, and Jennifer Nielsen
Early marine growth in relation to marine-stage survival rates for Alaska sockeye salmon (*Oncorhynchus nerka*)

131
Ganias, Konstantinos, Cristina Nunes, and Yorgos Stratoudakis
Degeneration of postovulatory follicles in the Iberian sardine *Sardina pilchardus*: structural changes and factors affecting resorption

Notes

140
Arrizabalaga, Haritz, Victoria López-Rodas, Eduardo Costas, and Alberto González-Garcés
Use of genetic data to assess the uncertainty in stock assessments due to the assumed stock structure: the case of albacore (*Thunnus alalunga*) from the Atlantic Ocean

147
Cherel, Yves, Richard Sabatié, Michel Potier, Francis Marsac, and Frédéric Ménard
New information from fish diets on the importance of glassy flying squid (*Hyaloteuthis pelagica*) (Teuthoidea: Ommastrephidae) in the epipelagic cephalopod community of the tropical Atlantic Ocean

153
Conti, Stéphane G., Benjamin D. Maurer, Mark A. Drawbridge, and David A. Demer
Measurements of total scattering spectra from bocaccio (*Sebastes paucispinis*)

158
Guidelines for authors

Subscription form

U.S. Department of Commerce
Carlos M. Gutierrez
Secretary

National Oceanic and Atmospheric Administration
Vice Admiral
Conrad C. Lautenbacher Jr., USN (ret.)
Under Secretary for Oceans and Atmosphere

National Marine Fisheries Service
William T. Hogarth
Assistant Administrator for Fisheries

Scientific Editor
Adam Moles, Ph.D.

Associate Editor
Elizabeth Siddon

Ted Stevens Marine Research Institute
Auke Bay Laboratories
Alaska Fisheries Science Center
17109 Pt. Lena Loop Road
Juneau, Alaska 99801

Managing Editor
Sharyn Matriotti

National Marine Fisheries Service
Scientific Publications Office
7600 Sand Point Way NE, BIN C1570
Seattle, Washington 98115-0070

Editorial Committee

Jeffrey M. Leis	Australian Museum, S
Thomas Shirley	Texas A&M Universit
David Somerton	National Marine Fishe
Mark Terceiro	National Marine Fishe

Temporal variation in growth of yellowfin tuna (*Thunnus albacares*) larvae in the Panama Bight, 1990–97

Jeanne B. Wexler (contact author)[1]
Seinen Chow[2]
Toshie Wakabayashi[3]
Kenji Nohara[3]
Daniel Margulies[1]

Email address for J. B. Wexler: jwexler@iattc.org

[1] Inter-American Tropical Tuna Commission
8604 La Jolla Shores Drive
La Jolla, California 92037-1508

[2] National Research Institute of Fisheries Science Nagai
6-31-1 Yokosuka
Kanagawa 283-0316 Japan

[3] National Research Institute of Far Seas Fisheries
5-7-1 Shimizu-Orido
Shizuoka 424-8633 Japan

Abstract—Tuna larvae (at flexion, postflexion, and transformation stages) were collected by dip net and light traps at night in the northwestern Panama Bight during the season of reduced upwelling (June–September) of 1990, 1991, 1992, and 1997. The larvae were identified as yellowfin tuna (*Thunnus albacares*) by mtDNA analysis. Ichthyoplankton data from bongo and Tucker trawl tows were used to examine the potential prey abundance in relation to the mean size-at-age and growth rates of the yellowfin tuna larvae and their otoliths. The most rapid growth rates occurred during June 1990 when plankton volumes were at their highest levels. The lowest plankton volumes coincided with the lowest growth rates and mean sizes-at-age during the August–September 1991 period. High densities of larval fish were prevalent in the ichthyoplankton tows during the 1991 period; therefore intra- and interspecific competition for limited food resources may have been the cause of slower growth (density-dependent growth) in yellowfin tuna larvae The highest mean sea-surface temperature and the lowest mean wind stress occurred during an El Niño-Southern Oscillation (ENSO) event during the 1997 period. There appeared to be no clear association between these environmental factors and larval growth rates, but the higher temperatures may have caused an increase in the short-term growth of otoliths in relation to larval fish size.

Manuscript submitted 22 October 2004 to the Scientific Editor's Office.

Manuscript accepted 14 March 2006 by the Scientific Editor.

Fish. Bull. 105:1–18 (2007).

Yellowfin tuna (*Thunnus albacares*) larvae inhabit the mixed layer of all tropical and subtropical oceans of the world (Ueyanagi, 1969; Nishikawa et al., 1985). When recruited to the commercial fishery, yellowfin tuna are one of the most important tuna species worldwide (Collette and Nauen, 1983; FAO, 2004). Near-daily spawning of yellowfin tuna, and the subsequent dispersal of fertilized eggs, appears to be largely dependent on the occurrence of surface water temperatures equal to or greater than 24°C (Schaefer, 1998). In the eastern Pacific Ocean (EPO), yellowfin tuna spawn continuously between 0° and 20°N (Schaefer, 2001). Despite widespread spawning of yellowfin tuna throughout the EPO, the larvae are patchy in distribution (Ahlstrom, 1971), and relatively large numbers have been collected only near islands (Graves et al., 1988; this study) and near shore (González Armas, 2002).

The larvae of *Thunnus* are difficult to identify by meristic, morphological, or pigmentation characteristics (Matsumoto et al., 1972; Potthoff, 1974; Richards et al., 1990; Lang et al., 1994). In the EPO, the late-larval and early-juvenile stages of yellowfin and bigeye (*T. obesus*) tuna co-exist and cannot be differentiated by these conventional methods. However, allozyme (Graves, et al., 1988) and recent molecular (Takeyama et al., 2001; Chow et al., 2003) analyses have made it feasible to identify larvae of these two species that inhabit the EPO.

The growth dynamics of yellowfin tuna during early life stages may have a profound effect on cohort strength (Houde, 1987), but growth rates have not been described for the larvae in the Pacific Ocean. Larval and juvenile stage durations and corresponding growth rates (Houde, 1989), starvation rates (Margulies, 1993), and larval transport and predation (Grimes, 2001) may be strongly influenced by biological and physical processes that would affect prerecruit survival in yellowfin tuna. Standing stocks of phytoplankton and zooplankton in the EPO, where yellowfin tuna larvae are found are seasonally variable (Blackburn et al., 1970; Owen and Zeitschel, 1970; Lauth and Olson, 1996; González Armas, 2002) and influenced by interannual events such as El Niño-Southern Oscillation (ENSO) conditions (Dessier and Donguy, 1987; Fiedler, 1992; Chavez et al., 1999; Strutton and Chavez, 2000). In the northwestern Panama Bight of the EPO, nearshore ichthyoplankton surveys (from 1989 to 1993)

Table 1

Collections of yellowfin tuna larvae by night-lighting (NL) and light traps (LT) near Frailes del Sur in the northwestern Panama Bight, 1990–1997.

Sampling period	Number of sampling dates	Number of larvae collected	Number used for age and growth analyses	Number used for ( ) and identified as *T. albacares* by PCR-RFLP analysis	Age range (days)	Standard length range (mm)
21–26 June 1990	3	97 (NL)	25	(5) 1	8–18	6.2–19.6
5–25 July 1991	5	13 (NL) 9 (LT)	13	(13) 10	11–15	9.1–12.7
4–7 September 1991	2	126 (NL)	43	(34) 26	12–20	7.1–12.4
24 June–3 July 1992	3	47 (NL)	22	(34) 19	10–14	7.6–12.0
7 August 1997	1	98 (NL)	69	(71) 69	11–18	8.7–14.5

(IATTC[1]; IATTC[2]; Lauth and Olson, 1996; Owen[3]) and experiments with captured scombrid larvae (from 1986 to 1997) at the Achotines Laboratory of the Inter-American Tropical Tuna Commission (IATTC) (Olson and Scholey, 1990; Margulies, 1993; Scholey, 1993; Wexler, 1993) have provided an opportunity to explore factors controlling prerecruit growth and survival of scombrids. These small- and fine-scale studies may provide some understanding of the recruitment variability of yellowfin tuna in the Panama Bight, considering that yellowfin tuna exhibit limited, small-scale movements within the EPO (Schaefer, 1991; Wild, 1994) and that processes important to recruitment probably occur at small scales (Fortier and Leggett, 1985).

The Panama Bight is characterized by distinct seasonal and interannual variations in atmospheric and oceanic conditions (Wooster, 1959; Smayda, 1963, 1966; Forsbergh, 1963, 1969). The climatological and physical oceanographic properties that occur within the Panama Bight are determined by the north-south seasonal movement of the northeast trade winds of the Atlantic Ocean, the equatorial calm belt (i.e., the doldrums), the southeast trade winds of the Pacific Ocean, and the convergence of these trade wind systems within the doldrums (i.e., the intertropical convergence zone, ITCZ) (Smayda, 1966). From January through April, the ITCZ is displaced to the south and strong northerly trade winds create a dry season and produce local upwelling. From about May through December, the ITCZ is displaced to the north and the Panama Bight is dominated by southeast trade winds and a rainy season characterized by reduced upwelling, higher sea-surface temperatures (SSTs), lower ocean salinities, and a deeper thermocline and mixed layer (Lauth and Olson, 1996). The growth and subsequent survival of yellowfin tuna larvae that occur during the reduced upwelling season may be regulated more by the spatial patchiness of prey organisms coincident with lower plankton volumes (Owen, 1989). ENSO events could further affect the seasonal availability of nutrients and food organisms during this period (Barber and Chavez, 1986; Dessier and Donguy, 1987; Fiedler, 1992; Chavez et al., 1999). A mild ENSO event occurred during our sampling periods in 1991–92 (Barber et al., 1996) and a strong event occurred in late 1997 (Chavez et al., 1999; Strutton and Chavez, 2000; Glynn et al., 2001).

The objectives of this study were 1) to identify the species of *Thunnus* sampled in the northwestern Panama Bight by molecular analysis, 2) to determine ages and compare the size-at-age data of yellowfin tuna larvae collected during the periods of reduced upwelling of 1990, 1991, 1992, and 1997, and 3) to explore relationships between the temporal variation in growth rates and measured levels of plankton and physical processes in the Panama Bight.

Materials and methods

Larval fish collections

Fish larvae were collected in the northwestern Panama Bight (Fig. 1) during the seasons of reduced upwelling in June 1990, July and September 1991, June and July 1992, and August 1997 (Table 1). Most of the larvae were collected with a dipnet just below the ocean surface after they were attracted with an underwater light at night (night-lighting, NL) (Olson and Scholey, 1990) near Frailes del Sur in the vicinity of the 100- and 200-meter isobaths. Larvae were also collected in this area in July 1991 by a light trap (LT) (design described in Thorrold,

[1] IATTC (Inter-American Tropical Tuna Commission). 1992. Annual report of the Inter-American Tropical Tuna Commission 1990, 261 p. IATTC, 8604 La Jolla Shores Drive, La Jolla, CA 92037.

[2] IATTC (Inter-American Tropical Tuna Commission). 1992. Annual report of the Inter-American Tropical Tuna Commission 1991, 271 p. IATTC, 8604 La Jolla Shores Drive, La Jolla, CA 92037.

[3] Owen, R. W. 1997. Oceanographic atlas of habitats of larval tunas in the Pacific Ocean off the Azuero Peninsula, Panama, 32 p. Inter-American Tropical Tuna Commission Data Report 9. IATTC, 8604 La Jolla Shores Drive, La Jolla, CA 92037.

1993) deployed near the surface. All larvae were fixed in 95% ethyl alcohol shortly after capture, except for some that were caught alive and used in laboratory experiments. Fish used in laboratory experiments were not used for the age and growth analyses. SSTs were recorded with a bucket thermometer, and the salinity of a sample of water taken just below the surface was measured with a handheld salinometer. Visual observations of environmental conditions (e.g., wind, currents, and weather) were recorded at the time of sampling.

Laboratory procedures and analyses

Larvae of the genus *Thunnus* were sorted from other scombrid larvae by the morphological features and meristics described in Nishikawa and Rimmer (1987) and Ambrose (1996). The standard length (SL) of each larva was measured in distilled water before the sagittal otoliths were removed for aging and before the remaining tissue of each individual was placed in 95% ethyl alcohol for species identification. The sagittae were removed, cleaned of tissue with chlorine bleach, rinsed in distilled water, dried, and embedded distal side up with Eukitt (O. Kindler, Freiberg, Germany) mounting medium on a glass slide. The diameter along the longest axis of each sagitta was measured with an ocular micrometer and light microscope. The sagittae were polished at the surface until the increments were clearly visible with transmitted light at a magnification of 480 or 720×. Daily increments (previously validated in Wexler et al., 2001) of the left and right sagittae were counted "blindly" (i.e., repeated counts were made without prior knowledge of the previous counts) by the first author until the same number of increments were counted at least three times in one of the sagittae. The number of increments in the sagitta that was more clearly read (which usually resulted in a higher count) was used as a direct estimate of age for that fish.

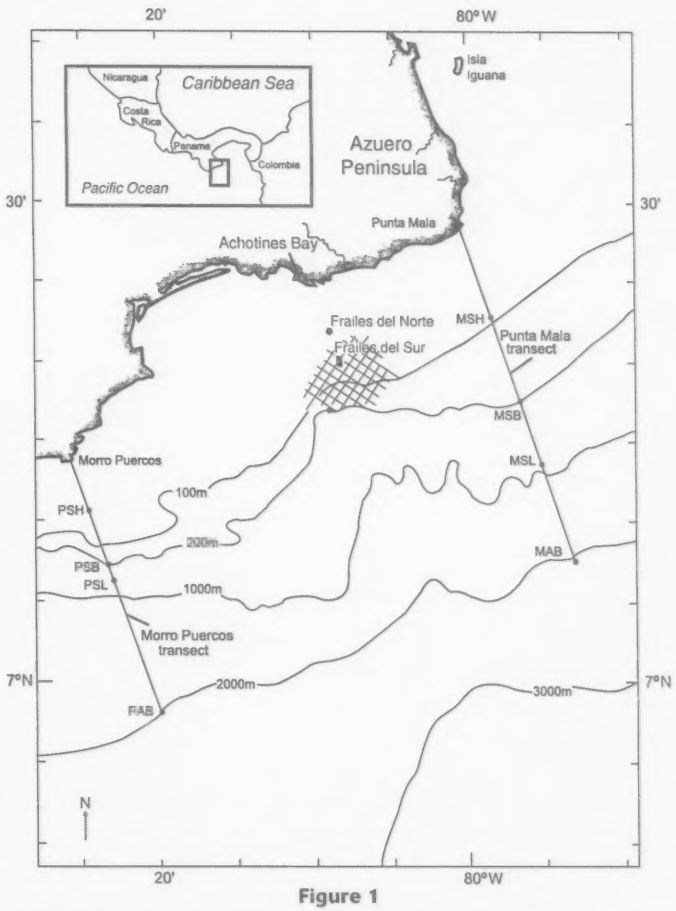

Figure 1

Locations where yellowfin tuna (*Thunnus albacares*) larvae were collected with an underwater light at night (cross hatched; from 1990–92 and 1997) and where ichthyoplankton sampling occurred (during 1990–92) near the Achotines Laboratory, on the Azuero Peninsula of the northwestern Panama Bight. Ichthyoplankton sampling stations along the Punta Mala and Morro Puercos transects are the following: Mala abyss (MAB), Mala slope (MSL), Mala shelf break (MSB), Mala shelf (MSH), Puercos abyss (PAB), Puercos slope (PSL), Puercos shelf break (PSB), Puercos shelf (PSH).

The temporal variation in growth was examined by comparing the size-at-age data of the larvae and their otoliths among collection periods through analysis of covariance (ANCOVA) and a multiple range comparison test (Tukey HSD) (XLSTAT vers. 7.5.2, Addinsoft USA, New York, NY) (α=0.05).

DNA analysis and species identification

The flanking region between ATPase 6 and cytochrome oxidase subunit I (COI) genes of mtDNA was amplified by using the polymerase chain reaction (PCR), and restriction fragment length polymorphism (RFLP) patterns were used to identify the species of *Thunnus* larvae according to protocols of Takeyama et al. (2001) and Chow et al. (2003). Albacore (*T. alalunga*), yellowfin, and bigeye tunas in the Pacific Ocean can be identified by the diagnostic restriction profile of *Mse* I digestion (Chow and Inoue, 1993), and this enzyme assay was used to identify the species of larvae collected in 1990–92. Chow et al. (2000) found, however, that many specimens of bigeye tuna in the Atlantic Ocean shared the same restriction profile with yellowfin tuna; this also occurred in the Pacific Ocean, but at a much lower frequency (1 out of 144 individuals examined). Takeyama et al.

Table 2

Maximum distances traveled for each collection group of yellowfin tuna larvae recruited to the sampling area based on back-calculated spawning dates, the period of time over which the larvae were exposed to environmental conditions during their life history, and an average, maximum current speed and direction for the Panama Bight region (Fiedler, 2002). The average latitudinal and longitudinal degrees traveled were used to estimate an area occupied by larvae of all collection groups. The mean sea surface temperature (SST) is based on monthly averages within 1- by 1.5-degree ares for each collection group period within the estimated area.

Collection group	First spawn date	Last sample date	Monthly mean SST (SE) and ranges (°C)	Time period exposed to ambient SST (days)	Number of days feeding	Maximum meters traveled @ .25 m/sec	Maximum nautical miles traveled	Degrees
I	6/6/1990	6/26/1990	27.84 (0.090) 26.4–28.7	20	17	432,000	233	3.89
II	6/19/1991	7/25/1991	27.90 (0.063) 26.6–28.7	36	33	777,600	420	7.00
III	8/14/1991	9/7/1991	27.60 (0.059) 26.5–28.4	24	21	518,400	280	4.66
IV	6/9/1992	7/3/1992	28.00 (0.066) 26.4–29.0	24	21	518,400	280	4.66
V	7/19/1997	8/7/1997	29.10 (0.046) 28.3–30.0	19	16	410,400	222	3.69
							mean degrees	4.78

(2001) found another restriction enzyme (*Tsp* 509I) that was diagnostic for bigeye tuna regardless of where the specimens came from. Therefore, in addition to using *Mse* I digestion, *Tsp* 509I was also used for all individuals collected in 1997.

Back-calculated dates

Spawning dates were back-calculated for each larva by subtracting the number of otolith increments counted from the date the larva was collected. An additional day was also subtracted because the first increment in yellowfin tuna is present at hatching approximately 20 hours after fertilization (senior author, personal commun.) and the second increment does not form until the third day after fertilization (approximately two days after hatching); increments are formed daily thereafter (Wexler et al., 2001). During the reduced upwelling season when SSTs are warmer, first feeding of the larvae occurs at first light, approximately three days after hatching (Margulies et al., in press) when, on average, three increments are present in the sagittae. Therefore, three days were subtracted from the estimated spawning date to estimate the time period that the larvae of each collection group were feeding until they were collected (Table 2). "Collection-group period" is defined as the time period from the time of first spawning to the time when larvae were sampled.

Estimated area occupied by larval cohorts

The yellowfin tuna larvae that were collected near the Frailes Islands may be recruited locally from offshore areas; this conjecture is based on measurements of the mean monthly fields of velocity and direction of the North Equatorial Countercurrent (NECC) (up to 0.25 m/s) (Fiedler, 2002), southerly surface winds (up to 5 m/s) (Fiedler, 2002), and the location and proportion of reproductively active female yellowfin tuna (Schaefer, 1998) that are found during June–September in the Panama Bight area (Fig. 2). The earliest back-calculated spawning date for a larva within each collection group was used to estimate the maximum amount of time the larvae within that group were exposed to environmental and feeding conditions (Table 2). This amount of time and the maximum current speed and direction during this season were used to calculate maximum average distances traveled and the potential area occupied by each collection group until sampled at the Frailes Islands (Table 2, Fig. 2).

Ichthyoplankton and oceanographic surveys

During 1990–92 ichthyoplankton and oceanographic sampling were conducted from a 25-ft Boston whaler along the Morro Puercos (P) and Punta Mala (M) transects (Fig. 1) (IATTC[1]; IATTC [2]; Lauth and Olson, 1996). Data collected from these surveys were used to describe the temporal variation of conditions within the planktonic community that may correspond to that of larval yellowfin tuna growth rates. In 1990, oblique bongo tows were made from the surface to 50 m along both transects with 335-μm mesh nets (Lauth and Olson, 1996). As a measure of relative abundance, standardized plankton volumes under 10 m^2 of sea surface were calculated by following procedures of Smith and Richardson (1977), and the estimates for each side of the

bongo were averaged. Beginning in 1991, a 0.6-m^2 Tucker trawl equipped with a 335-mm mesh net, flow meter, and temperature-depth logger was used to sample ichthyoplankton at discrete depths at only the Punta Mala shelf break (MSB). These surveys were designed to study the vertical distribution and *in situ* growth and starvation rates of tuna larvae and the abundance of their zooplankton prey (IATTC[1]; IATTC[2]). Two replicate tows of 4 to 5 minutes were made at each of three or four depth strata: 0–5 (stratum 1), 5–20 (stratum 2), 20–40 (stratum 3), and 40–60 m (stratum 4). Plankton volumes were standardized (Smith and Richardson, 1977) at each depth stratum and were added together for each sampling day to compare the mean plankton volumes collected by the Tucker trawl with those collected by the bongo tows of the previous year. Mean plankton volumes were compared between collection group periods by using a one-way analysis of variance (ANOVA), the Student-Newman-Keuls multiple range comparison test (SNK test), and a *t*-test for unequal variance (α=0.05) when appropriate (Zar, 1984). In 1991, all four depth strata were sampled, but in 1992 only the first three strata were sampled. Additionally, a 73-μm mesh net with a mouth area of 0.014 m^2 was nested inside the Tucker trawl in 1992 to collect microzooplankton simultaneously with all other plankters. The displaced volume of the microzooplankton was included in the total standardized plankton volume for each sampling day. Water temperatures, surface wind speeds (m/s), and salinity values (psu) were measured (described in Lauth and Olson, 1996) during each sampling day.

Plankton displacement volumes for all years were also standardized as plankton volume per volume of water filtered (mL/m^3) to compare mean values between years and with literature values. The mean of each standardized volume for the 1990 oblique tows (0–50 m) and for discrete depths between 0 and 40 m of the 1991 and 1992 data were compared between collection group periods by using ANOVA, the SNK test, and a *t*-test for unequal variance (α=0.05) (Zar, 1984).

Sea-surface temperatures and wind stress climatology

The oceanographic surveys provided physical data within a limited portion of the area where *Thunnus* larvae potentially occurred since hatching. Therefore, area- and time-specific (monthly averages within 1- by 1.5-degree areas) SSTs to 5 m depth and wind stress climatology data (all data sets based on a hindcast ocean analysis system model described by Ji et al. [1995]) for the estimated area of each collection group period (Table 2, Fig. 2) were accessed from the internet (IRI[4]). Wind velocities in m/s were calculated from wind stress values based on a constant drag coefficient of 1.3×10^{-3} (Sverdrup et al., 1942; Large and Pond, 1981; Ji et al.,

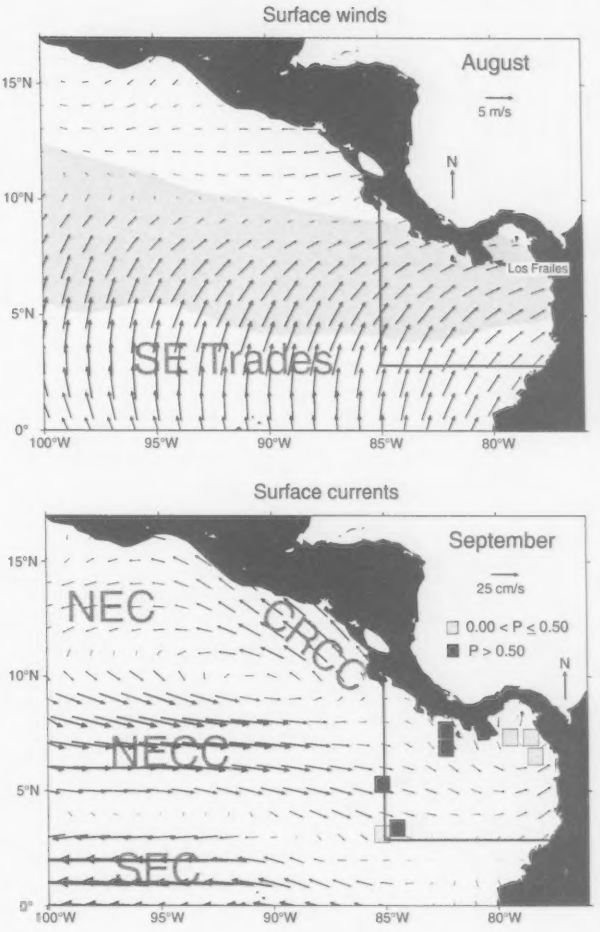

Figure 2

Monthly fields of surface wind velocity (for August) and surface current velocity (for September) representative of the seasonal extremes during the reduced upwelling period in the Panama Bight (after Figure 3 of Fiedler, 2002). Shading indicates surface wind divergence (intertropical convergence zone) during August, NEC = North Equatorial Current, SEC = South Equatorial Current, NECC = North Equatorial Counter Current, and CRCC = Costa Rica Coastal Current. The area between the vertical and horizontal lines and the land mass represents the estimated maximum average area (in degrees) (see Table 2) potentially occupied by each larval yellowfin tuna cohort during its life history. The spawning distribution of yellowfin tuna within the area is presented as the proportions (P) of reproductively active females in relation to the total numbers of mature females captured within 1-degree areas during the second and third quarters between 1987 and 1989 (from Schaefer, 1998).

[4] International Research Institute for Climate Prediction (IRI). 2006. Website: http://ingrid.ldeo.columbia.edu/SOURCES/.NOAA/.NCEP/.EMC/.CMB/.Pacific/.monthly/ (accessed on 14 October 2005).

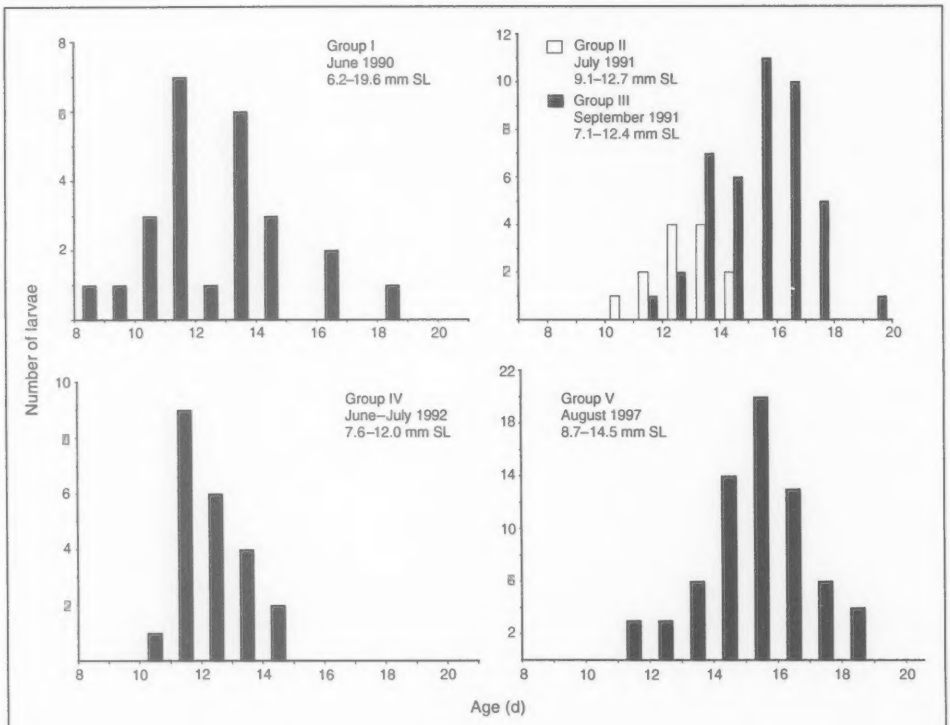

Figure 3

Age distributions and standard length ranges of yellowfin tuna (*Thunnus albacares*) larvae for each collection group period during 1990–92 and 1997. Larvae were collected near the Frailes Islands in the Panama Bight.

1995). Physical data were compared between collection group periods using ANOVA and the SNK test.

Results

Collections and identification

The occurrence of fairly large numbers (approximately 100 or more) of larval and early-stage juvenile *Thunnus* was sporadic, but not uncommon, in night-light collections during certain months of each year of the reduced upwelling season (Table 1). Based on back-calculated spawning dates and the average surface current speed, the collection site within an 8-degree latitude by 8-degree longitude area (between 2–10°N and 77–85°W) was estimated as the average maximum area potentially occupied by yellowfin tuna larvae of each collection group during their early life history (Table 2, Fig. 2). At the time of collection, sizes of larvae ranged from 6.2 to 19.6 mm SL (Table 1), and all were either in the flexion, postflexion, or transformation stages of development (stages described in Ambrose, 1996). Other scombrid species (i.e., *Auxis* sp., *Euthynnus lineatus*, and *Scomberomorous sierra*) were also found when *Thunnus* larvae were collected, but were not usually predominant in the collections.

Successful PCR amplification occurred in 80% of the larvae analyzed, and subsequent RFLP analysis indicated that the *Thunnus* larvae collected near the Frailes Islands were *T. albacares* (Table 1).

Size-at-age and growth

The ages of yellowfin tuna larvae collected ranged from 8 to 20 days (Table 1, Fig. 3). The age range was mostly limited between 11 and 14 days for the larvae collected in July 1991 (collection group II) and in June–July 1992 (collection group IV); therefore growth models were not fitted to the data (Figs. 3 and 4). However, a comparison of the size-at-age between all five groups within this limited age range indicated that both SLs and otoliths were significantly smaller for larvae collected in September 1991 (collection group III) (ANCOVA and Tukey multiple comparison test, $P<0.0001$), and that SLs were similar between the larvae of 1990 (collection group I) and July

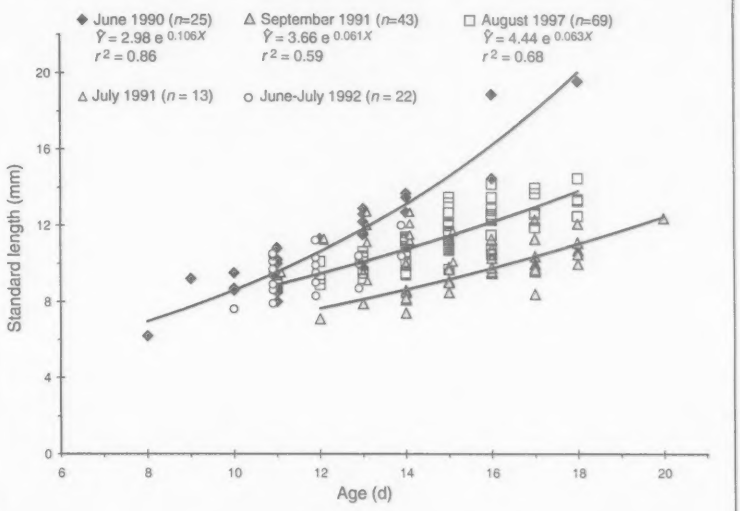

Figure 4

Exponential relationships between standard length and age in days estimated from otolith increment counts of larval yellowfin tuna (*Thunnus albacares*) collected during June 1990, September 1991, and August 1997. Data are also presented for yellowfin tuna larvae collected during July 1991 and June–July 1992, but growth models were not fitted to the limited range of data.

1991 (collection group II) and between those of 1992 and 1997 (collection groups IV and V).

The length-at-age data were used to examine and compare growth relationships of all yellowfin tuna larvae collected in June 1990, September 1991, and August 1997 (collection groups I, III, and V, respectively). An exponential model provided the best fit to each of the three groups of data (Fig. 4). The variances were homogeneous after log transformation of the length data for each group, and the slopes were compared. The slope and the average growth rate obtained through differentiation of the exponential equation of the 1990 data (1.28 mm/d, SE=0.134) were significantly greater than those of the September 1991 (0.60 mm/d, SE=0.033) and 1997 (0.71 mm/d, SE=0.038) data (ANCOVA, $P<0.0001$, Tukey multiple comparison test). The elevations (i.e., adjusted means or intercepts) of the 1991 and 1997 data were significantly different ($P<0.0001$) and indicated that the mean length-at-age was significantly smaller for larvae of the September 1991 collection group (Fig. 4).

Similar results were obtained for otolith growth rates (based on the exponential relationships between otolith diameter and age) for the three years (Fig. 5). The slopes were compared after log transformation of the otolith data for each group. The growth rate of the 1990 data was significantly faster than that of the 1991 and 1997 data (ANCOVA, $P<0.0001$, Tukey multiple comparison test), and the elevations were different between the 1991 and 1997 data, indicating that otoliths were significantly smaller for larvae of the September 1991 collection group (Fig. 5).

A comparison of the linear relationships between otolith diameter and SL (ANCOVA, $P<0.0001$, Tukey multiple comparison test; Fig. 6) revealed that the otoliths of the 1997 group were larger and grew significantly faster in relation to fish size than those of the 1990 and 1991 groups. Otoliths of the fastest (1990 group) and slowest (1991 group) growth periods were growing at the same rate in relation to fish length, but the slower-growing group had significantly larger otoliths in relation to fish size than those of the faster-growing group ($P<0.0001$; Fig. 6).

Standing stocks of ichthyoplankton

Ichthyoplankton and physical parameters were measured at four stations along the P and M transects on two sampling days in June 1990 (16 tows total, each to 50 m), at the MSB station on the M transect on six sampling days in June and July 1991 (12 tows each depth strata 1–4), at the MSB station on three sampling days in August 1991 (six tows each strata 1–4 and four tows each strata 1–3), and at the MSB station on two sampling days in June and July 1992 (six tows each strata 1–3) (Table 3, Fig. 1). The sampling days lay within the

period of time when each collection group of larvae could have been feeding in the estimated area of occurrence (Table 2, Fig. 2). Ichthyoplankton tows were not made in the Panama Bight during 1997.

Mean standardized plankton volumes were variable and significantly different (ANOVA, $P<0.001$) among collection-group periods (Fig. 7). The mean plankton volume (±SE) in 1990 (157.3 ±13.53 mL) when the fastest larval growth rate occurred was greater and different from all other sampling or collection periods (SNK test), and ranged from 106.5 to 310.4 mL under 10 m^2 of sea surface (Table 3, Fig. 7). The mean plankton volumes during June–July 1991 (82.3 ±3.46 mL) and during August–September 1991 (62.8 ±5.86 mL), when the slowest growth rate occurred, were similar and less than those for all other periods (SNK test); volumes ranged from 43.7 to 102.4 mL under 10 m^2 of sea surface (Table 3, Fig. 7).

Mean plankton volumes, expressed as the amount filtered per volume of water sampled within the first three depth strata, were also significantly different (ANOVA, $P<0.001$) among collection group periods. Means were similar between the 1990 and 1992 groups and between the two 1991 groups (SNK test). Volumes ranged from 0.199 to 0.559 mL/m^3 during 1990 and 1992 and from 0.075 to 0.235 mL/m^3 during the two 1991 periods (Table 3).

Plankton volumes included relatively large numbers of fish larvae (predominantly preflexion stages) during the least (August–September 1991) and most (June 1990) rapid growth periods, and mean values were not significantly different (t-test for unequal variances, $P>0.20$). Numbers of larvae under 10 m^2 of sea surface ranged from 686.8 to 4786.1 and from 934.5 to 2685.6 in 1990 and 1991, respectively. Few scombrid larvae occurred in the ichthyoplankton samples for each of the two years, but were greatest during the 1991 period. The number of scombrid larvae under 10 m^2 ranged from 0 to 2.7 and from 0 to 12.7 in 1990 and 1991, respectively. *Thunnus* larvae (preflexion stage) were collected only in August 1991, and the numbers ranged from 0.5 to 5.5 larvae under 10 m^2 of sea surface.

Environmental effects

Mean SSTs were significantly different among all collection group periods (ANOVA, $P<0.0001$). SSTs were similar between the local sampling area (Fig. 1) and the estimated region of each collection group (Fig. 2) in that they were significantly lower for the August–September 1991 period (group III) and higher for the July–August 1997 period (group V) (ANOVA, $P<0.0001$, SNK test; Table 2, Fig. 7).

The mean wind stress was significantly lower for the 1997 collection-group period (group V) when compared with all other group periods (ANOVA, $P<0.0001$, SNK test; Fig.7). The monthly means within each 1- by 1.5-degree area were similar and ranged from 0.084 to 0.517 dynes/cm^2 for group-collection periods I–IV, and for the 1997 period (group V), they ranged from 0.027 to 0.462 dynes/cm^2. Wind velocities calculated from the wind stress values were low to moderate, ranging from 1.59 to 3.94 m/s (modes of 2.45 and 2.60 m/s) for groups I–IV and from 0.90 to 3.72 m/s (modes of 1.2 and 1.7 m/s) for group V.

Higher salinity values, ranging from 33 to 34 psu, occurred during July–August 1997 (group V) during an ENSO event, and during the 1990–92 collection-group periods (I–IV) values ranged from 29 to 32 psu, when both the fastest and slowest growth rates of yellowfin tuna larvae occurred.

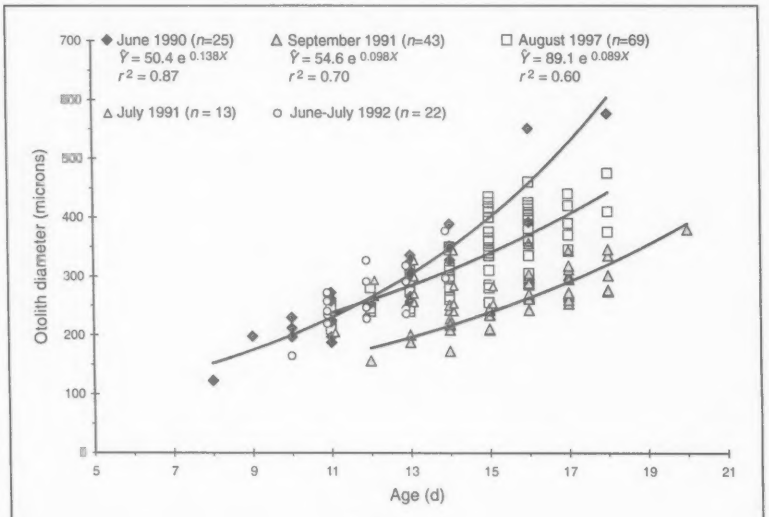

Figure 5

Exponential relationships between sagittal otolith diameter and estimated age in days of larval yellowfin tuna (*Thunnus albacares*) collected during June 1990, September 1991, and August 1997. Data are also presented for yellowfin tuna larvae collected during July 1991 and June–July 1992, but growth models were not fitted to the limited range of data.

Discussion

This study describes the first *in situ* growth rates for yellowfin tuna larvae occurring in the Pacific Ocean. Previous efforts to age and describe growth of yellowfin tuna during the early stages of develop-

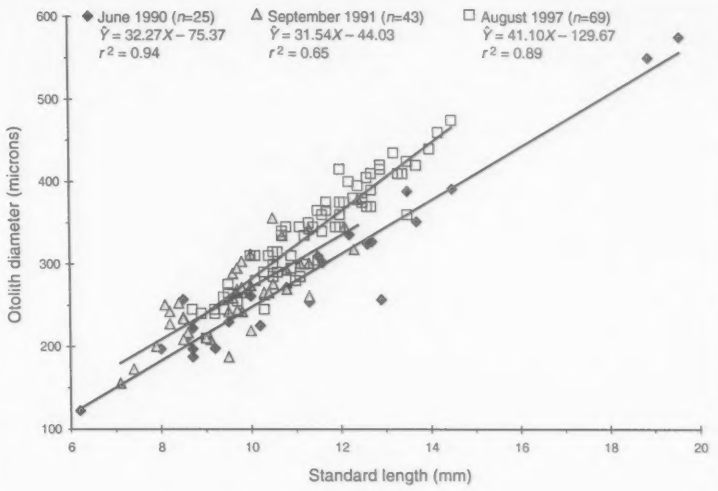

Figure 6

Linear relationships between otolith diameter and standard length for larval yellowfin tuna (*Thunnus albacares*) collected during June 1990, September 1991, and August 1997.

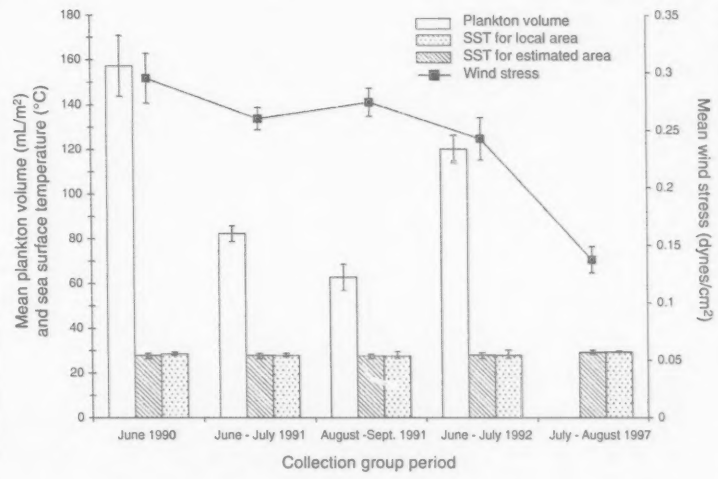

Figure 7

Standardized mean plankton volumes and monthly mean wind stress and sea surface temperature data for the local sampling area (Fig. 1) and the estimated area (Fig. 2) potentially occupied by each larval yellowfin tuna (*Thunnus albacares*) cohort during its life history. The standard errors of the means are indicated for plankton and wind stress, and the ranges for the mean water temperatures are also indicated. Plankton data were collected from ichthyoplankton tows in the vicinity of the Frailes Islands (see Fig. 1) and area- and time-specific physical data were extracted from the internet (IRI[4]).

Table 3

Standardized plankton displacement volumes collected from ichthyoplankton surveys conducted along the Punta Mala (M) and Morro Puercos (P) transects during 1990–1992 in the Panama Bight. Station definitions are described in Figure 1.

Sampling date	Transect	Station	Tow depth (m)	mL plankton volume/10m^2 of sea surface	mL/m^3	Sum of depth strata 1–4	Sum of depth strata 1–3
19 June 1990	M	MAB	0–50	121.3	0.219		
		MAB	0–50	242.3	0.425		
		MSL	0–50	123.9	0.226		
		MSL	0–50	118.5	0.208		
		MSB	0–50	143.0	0.260		
		MSB	0–50	156.0	0.280		
		MSH	0–50	167.6	0.328		
		MSH	0–50	310.4	0.559		
20 June 1990	P	PAB	0–50	140.9	0.252		
		PAB	0–50	129.1	0.264		
		PSL	0–50	205.8	0.393		
		PSL	0–50	163.6	0.301		
		PSB	0–50	113.2	0.199		
		PSB	0–50	125.6	0.240		
20 June 1990	P	PSH	0–40	106.5	0.245		
		PSH	0–40	149.5	0.333		
17 June 1991	M	MSB	0–5.7	6.6	0.117		
			5.3–25.8	21.5	0.105		
			21.2–27.0	39.6	0.147		
			43.1–48.1	2.4	0.049	70.1	67.7
		MSB	0–5.4	8.4	0.155		
			5.2–21.9	20.9	0.125		
			21.2–48.2	38.2	0.142		
			42.5–67.2	10.2	0.041	77.7	67.5
12 July 1991	M	MSB	0–5.7	13.0	0.229		
			5.4–21.9	31.5	0.190		
			22.9–44.5	23.9	0.111		
			43.8–67.2	10.5	0.045	96.9	68.4
		MSB	0–6.1	14.4	0.235		
			4.9–23.7	32.8	0.175		
			22.9–48.2	32.0	0.127		
			43.8–67.2	10.5	0.045	89.6	79.1
16 July 1991	M	MSB	0–5.7	9.9	0.176		
			4.9–21.9	19.9	0.117		
			21.2–44.5	24.7	0.106		
			40.2–67.2	12.4	0.046	67.0	54.5
		MSB	0–5.7	4.6	0.081		
			5.3–23.7	19.7	0.107		
			21.2–44.5	25.9	0.111		
			40.2–67.2	12.5	0.046	62.8	50.3
19 July 1991	M	MSB	0–5.4	6.2	0.114		
			5.2–21.9	24.4	0.146		
			20.2–44.5	36.4	0.150		
			40.2–64.0	15.5	0.065	82.5	67.0
		MSB	0–5.4	5.2	0.096		
			5.3–20.9	31.6	0.203		
			21.2–46.0	31.3	0.126		
			43.1–70.1	13.2	0.049	81.3	68.0

continued

Table 3 (continued)

Sampling date	Transect	Station	Tow depth (m)	mL plankton volume/10m² of sea surface	mL/m³	Sum of depth strata 1–4	Sum of depth strata 1–3
23 July 1991	M	MSB	0–5.4	7.9	0.147		
			5.5–20.9	21.0	0.137		
			21.2–46.5	40.2	0.159		
			43.1–61.8	11.4	0.061	80.6	69.1
		MSB	0–5.7	9.7	0.171		
			5.5–22.9	18.5	0.116		
			21.2–46.5	40.8	0.162		
			41.8–67.2	15.0	0.059	83.9	68.9
25 July 1991	M	MSB	0–5.7	9.2	0.163		
			5.3–25.8	30.9	0.150		
			22.1–46.5	44.9	0.184		
			43.1–70.1	17.4	0.065	102.4	84.9
		MSB	0–5.4	9.4	0.174		
			5.1–20.9	23.3	0.147		
			21.2–38.9	34.5	0.195		
			43.1–62.3	25.9	0.135	93.2	67.2
15 August 1991	M	MSB	0–5.7	5.7	0.101		
			5.3–19.2	15.4	0.111		
			21.2–44.5	32.0	0.137		53.1
15 August 1991	M	MSB	0–6.7	8.6	0.129		
			5.3–21.9	24.3	0.146		
			21.2–44.5	29.5	0.126		
			36.0–56.5	15.6	0.076	78.0	62.4
		MSB	0–5.7	9.3	0.165		
			5.3–21.9	18.8	0.113		
			21.2–40.2	22.5	0.119		
			43.8–67.2	15.3	0.066	66.0	50.6
		MSB	0–5.7	8.6	0.151		
			5.7–21.9	20.2	0.125		
			22.9–43.8	27.7	0.133		56.5
		MSB	0–6.1	8.4	0.138		
			5.3–21.9	22.2	0.134		
			21.2–44.5	36.0	0.154		66.6
		MSB	0–5.7	12.3	0.217		
			6.1–19.2	18.5	0.142		
			21.2–48.2	53.6	0.199		84.3
21 August 1991	M	MSB	0–5.7	6.5	0.115		
			5.3–21.9	12.8	0.077		
			21.2–44.5	19.2	0.082		
			45.0–67.2	7.9	0.035	46.3	38.4
		MSB	0–6.4	5.4	0.084		
			5.5–21.9	12.3	0.075		
			21.2–44.5	18.5	0.079		
			43.8–67.2	7.5	0.032	43.7	36.2
23 August 1991	M	MSB	0–5.7	8.1	0.143		
			5.3–21.9	19.7	0.119		
			21.2–44.5	32.6	0.140		

continued

Table 3 (continued)

Sampling date	Transect	Station	Tow depth (m)	mL plankton volume/10m² of sea surface	mL/m³	Sum of depth strata 1–4	Sum of depth strata 1–3
23 August 1991 (continued)			45.9–67.2	9.5	0.044	69.9	60.4
		MSB	0–5.7	7.3	0.128		
			5.3–23.7	23.4	0.127		
			21.2–44.5	31.2	0.134		
			43.1–67.2	10.9	0.046	72.9	61.9
22 June 1992	M	MSB	0–5.0	14.6	0.294		
			5.4–20.2	34.6	0.234		
			20.2–40.0	60.0	0.303		109.2
		MSB	0–5.0	11.5	0.233		
			5.0–20.2	39.3	0.259		
			20.2–40.0	52.4	0.264		103.3
		MSB	0–5.0	16.9	0.342		
			5.0–20.2	56.3	0.370		
			20.2–40.0	70.9	0.358		144.1
		MSB	0–5.0	23.4	0.473		
			5.0–20.2	54.5	0.359		
			20.2–40.0	54.2	0.274		132.1
2 July 1992	M	MSB	0–5.0	19.7	0.397		
			4.5–20.2	48.9	0.312		
			20.2–40.0	49.8	0.252		118.4
		MSB	0–5.0	10.7	0.216		
			5.4–18.7	37.5	0.280		
			20.2–40.0	65.9	0.333		114.0

ment may have been precluded by the patchiness in their distribution and the difficulties in species identification. The only other growth study done on yellowfin tuna larvae was conducted in the Gulf of Mexico (Lang et al., 1994), but the species identifications were based on morphology and meristics, and the larvae were younger than those in our study. Results from our mtDNA analysis enabled us to examine species-specific growth rates of older larval stages of yellowfin tuna and associated factors affecting their growth and distribution.

Distribution

Yellowfin tuna larvae have consistently appeared in the night-light collections near the Frailes Islands during the reduced upwelling season, but not during the season when strong upwelling occurs and other species of scombrid larvae and plankton levels are more abundant (Smayda, 1966; Forsbergh, 1969; Lauth and Olson, 1996). The absence of yellowfin tuna larvae from our sampling area during the upwelling season may be associated with a cessation of spawning by yellowfin tuna during this period (Schaefer 1998, 2001; Margulies et al., in press) and with the temperature threshold of their larvae. Lower mean water temperatures typically occur during the upwelling season (Lauth and Olson, 1996) and have ranged from 17.3° to 25.8°C within the upper 50 m (Owen[3]). In the laboratory, survival of first-feeding yellowfin tuna larvae is poor at ambient water temperatures of <21°C and at dissolved oxygen levels <2.2 mg/L (<33.0 % of oxygen saturation) (Margulies et al.[5]). These temperature and dissolved oxygen requirements probably determine and limit the distribution of yellowfin tuna larvae within the mixed layer and determine whether or not they can survive during the upwelling season when water temperatures are lower. The distribution of yellowfin tuna larvae during the upwelling season may also be strongly influenced by the occurrence of strong westerly directed currents and northerly winds resulting in larval transport away from the coastal areas of the Panama Bight during this season.

The area of larval distribution since hatching may actually be smaller or larger than what we have estimated, depending on the amount of passive transport and

[5] Margulies, D., V. P. Scholey, J. B. Wexler, R. J. Olson, J. M. Suter, and S. Hunt. In press. A review of IATTC research on the early life history and reproductive biology of scombrids conducted at the Achotines Laboratory from 1985 to 2005. Inter-American Tropical Tuna Commission, Special Report 16. IATTC, 8604 La Jolla Shores Drive, La Jolla, CA 92037.

the swimming behavior of the larvae within the mixed layer. Passive transport would probably occur only during the egg, yolk-sac, and first-feeding stages (the first 8–10 days after fertilization) because yellowfin tuna larvae are competent swimmers and can hold their position against strong currents in the laboratory beginning at around 8–10 mm SL (D. Margulies, personal commun.). Although the maximum average area of larval yellowfin tuna distribution from the time of hatching is probably our best estimate, the physical and biological processes that occur in such a large area may not be representative of processes occurring on much smaller scales that may be more specific to conditions affecting larval transport, growth, and survival (Owen, 1989).

Prey abundance

Our ichthyoplankton data were collected within a 0.5-degree area that included the Frailes Islands where larvae were sampled and may provide an index of prey abundance (at least for the first one or two weeks of feeding until piscivory occurs). Although our data were spatially limited, the measured plankton volumes provide the only available estimates of zooplankton levels for the periods of interest.

The use of different gear types (i.e., the bongo and Tucker trawl) for ichthyoplankton collections during 1990–92 may have affected the amount of microzooplankton sampled during the different years. Microzooplankton abundance has not been compared between these two types of sampling nets. However, Shima and Bailey (1994) reported that the bongo and 1-m Tucker nets caught similar numbers and size distribution of larval walleye pollock (*Theragra chalcogramma*). The higher plankton volumes collected by the bongo in 1990 may be an underestimate of plankton abundance compared to the volumes of water being sampled by the Tucker trawl with a larger mouth opening (McGowan and Fraundorf, 1966). Given that plankton volumes were probably under-represented in the bongo tows, the difference in magnitude between the amounts of plankton sampled by each net type may actually be greater.

Another potential bias in comparing plankton volumes among the different years was that more areas (stations) were sampled with the bongo in 1990 than with the Tucker trawl in other years (MSB station only). However, the mean plankton volume would have been similar in 1990 if only the MSB station had been used in the analysis (Table 3).

Growth

Daily growth rates estimated from the exponential models for each of the three years (1990, 1991, and 1997) ranged from 0.46 to 2.06 mm/d and were generally greater than those reported for other congeners (Jenkins and Davis, 1990; Lang et al., 1994). However, the larvae represented in those studies were predominantly younger and in earlier stages of development (and thus would exhibit slower absolute growth) than the flexion and postflexion larvae and transitional juvenile stages of yellowfin tuna collected in our sampling area. The slower growth rates observed in southern bluefin tuna (*Thunnus maccoyii*) larvae were also associated with density-dependent and oligotrophic conditions in the East Indian Ocean (Rochford, 1962; Jenkins and Davis, 1990; Young and Davis, 1990). Our growth rates, however, were comparable to similar developmental stages of other scombrids that inhabit relatively similar, productive nearshore waters, such as king and Spanish mackerels (*Scomberomorus cavalla* and *S. maculates*, respectively; DeVries et al., 1990), black skipjack (*Euthynnus lineatus*; Wexler, 1993), and little tunny (*Euthynnus alletteratus*; Allman and Grimes, 1998).

Distinct differences in the average size-at-age and growth rates were very apparent between our 1990 and September 1991 collections of yellowfin tuna larvae. Size-dependent processes (i.e., predation and starvation; Pepin, 1988; Grimes and Isely, 1996) or density-dependent growth and survival (Jenkins et al., 1991) may affect the size-frequency distributions of surviving larvae. A simulation model (Pepin, 1988) demonstrated that with increased food abundance, the mean and variance in larval growth rates increases, but, as predator abundance increases, the variance in growth rates decreases for any given mean. Instantaneous growth rates for yellowfin tuna larvae of a similar age in 1990 were 2 to 3 times higher than those in 1991, and plankton volumes were 2 to 7 times higher than those in 1991. Increases in food availability, such as that during 1990, may also attract predators and result in greater rates of mortality of the slowest-growing individuals, so that they are not represented in the sampled population. Although the larvae in 1991 were growing more slowly than those in 1990, they probably do not represent the slowest-growing larvae of their cohort. Typically, postflexion larval and early-stage juvenile scombrids collected during the reduced upwelling season in our sampling area have exhibited more variable growth (Wexler, 1993), but have been predominantly healthy (Margulies, 1993). Therefore, slower or faster growing survivors at this stage may be independent of their nutritional condition, and larvae collected by the sampling method we used represent the survivors and most competent individuals of their cohort.

Growth may have been slower in 1991 because of higher larval densities, limited food availability, and available prey composition. A strong inverse relationship exists between growth rates and stocking densities of yellowfin tuna larvae and early-stage juveniles (up to 18 days after hatching) fed a constant food supply in the laboratory (IATTC[6], IATTC[7]; Margulies et al.[5]). The re-

[6] IATTC (Inter-American Tropical Tuna Commission). 2000. Annual report of the Inter-American Tropical Tuna Commission 1998, 357 p. IATTC, 8604 La Jolla Shores Drive, La Jolla, CA 92037.

[7] IATTC (Inter-American Tropical Tuna Commission). 2002. Annual report of the Inter-American Tropical Tuna Commission 2001, 148 p. IATTC, 8604 La Jolla Shores Drive, La Jolla, CA 92037.

lationship may be even more pronounced under limited food conditions (Jenkins et al., 1991). Although we have only indirect evidence for density-dependent growth of the 1991 cohorts, the occurrence of more yellowfin tuna larvae sampled at the surface with the night light and the large numbers of other fish larvae collected in the ichthyoplankton tows coincident with the lower plankton volumes may indicate growth-limited conditions during this period. The slower growth of the late-stage larvae in 1991, when plankton abundance was much lower, may also be indicative of the types or species of preferred prey (zooplankters and fish larvae) that were available in the area that the larvae occupied. In the laboratory, yellowfin tuna larvae have predominantly selected all stages of cyclopoids over other types of copepods when offered a mixed assemblage of zooplankton prey (Margulies et al., 2001) and have become piscivorous beginning at approximately 6–7 mm in SL (Margulies et al.[5]). During this transitional stage in their diet, growth becomes much more rapid and variable (Kaji et al., 1999; Margulies et al.[5]), and the availability of specific types of fish larvae may influence their ability to switch to piscivory in the ocean. Yellowfin tuna larvae readily consume other, smaller conspecifics in the laboratory, but it is not known if there is a preference or growth advantage for consuming certain species of fish larvae during the transition to a more piscivorous diet. Although the available prey composition could affect the growth of late-stage yellowfin tuna larvae, intra- and interspecific competition for limited food resources during the 1991 period may have been the principal cause of slower growth.

The temporal variation in size-at-age within the same season and year (1991) may be related to the physical and biological characteristics of the area occupied by each group of larvae since hatching. Larval distribution could be determined by the location and timing of yellowfin tuna spawning and the small- and large-scale dynamics of physical oceanographic processes. Average sizes of the larvae and their otoliths of the 1991 August–September group were distinctly and significantly smaller than those of all other groups. The back-calculated first-feeding dates of this group coincided with the lowest plankton volumes measured in our local sampling area and with the only collection of first-feeding yellowfin tuna larvae from our ichthyoplankton tows. In contrast, the mean sizes of larvae and otoliths of the 1991 July group were similar to those of the fastest-growing group of 1990, despite low plankton volumes similar to those of the September 1991 period. We believe that the September 1991 group may have been spawned nearer to our local sampling area (Fig. 2) and that they were more exposed to feeding conditions in the vicinity of the Frailes Islands than were the faster-growing larvae of the July 1991 group.

Physical effects on growth

The probability of feeding success in marine larvae, and subsequent growth rates and survival, may increase with moderate levels of wind-induced microscale turbulence in their feeding environment (Rothschild and Osborn, 1988; Cury and Roy, 1989; Ware and Thomson, 1991; MacKenzie et al., 1994; IATTC[8], IATTC[9]). Preliminary estimates of wind speeds that produce optimal turbulent velocities and maximum survival of first-feeding yellowfin tuna larvae in the laboratory are moderate to high (D. Margulies, personal commun.) compared to wind speeds measured in the Panama Bight during this study. This estimate of optimal wind speeds is based on the assumption that maximum abundances of yellowfin tuna larvae in the EPO occur at depths of 0 to 20 m. However, the data on wind stress and velocities in the estimated area of larval distribution may not represent the frequency of optimal wind speeds associated with areas where first feeding of each cohort occurred. Additionally, wind event durations and frequencies, for which data were not available, may also play a significant role in the optimal survival of marine larvae (Wroblewski et al., 1989). Although moderate to high wind-induced turbulence may enhance early larval survival, growth rates may actually be slower during a portion of the larval phase as a result of higher larval densities and increased competition for limited resources.

Temperature-limited or -enhanced growth was not clear from our analyses of the yellowfin tuna larvae collected. Although a parabolic relationship between growth rates and SSTs was evident, it is unlikely that the two slowest-growing groups represented by the upper (29.1°C; group V) and lower (27.6°C; group III) mean temperatures in our study (Table 2) are approaching thermal tolerance limits for yellowfin tuna larvae. In the laboratory, successful hatching of yellowfin tuna larvae still occurs at upper temperatures of 32–34°C and first-feeding larvae are able to survive and feed between temperatures of 21° and 32°C (Margulies et al.[5]). Lower temperatures during the August–September 1991 (group III) period (Table 2) may have resulted in slower growth than that of the other collection periods, but we have only found significantly slower growth rates and differences in the mean sizes at first feeding when mean temperatures were less than 27°C in the laboratory (senior author, personal commun.). In contrast to the most rapid growth rate in 1990, the larvae in 1997 were growing more slowly when a strong ENSO event and the highest SSTs occurred. The optimum temperature range for growth of yellowfin tuna larvae in the Gulf of Mexico was 29–29.5°C (Lang et al., 1994), which was a similar temperature range for larvae of the 1997 period in our study. We do not, however, have information on relative food abundances during this

[8] IATTC (Inter-American Tropical Tuna Commission). 2001. Annual report of the Inter-American Tropical Tuna Commission 1999, 183 p. IATTC, 8604 La Jolla Shores Drive, La Jolla, CA 92037.

[9] IATTC (Inter-American Tropical Tuna Commission). 2002. Annual report of the Inter-American Tropical Tuna Commission 2000, 171 p. IATTC, 8604 La Jolla Shores Drive, La Jolla, CA 92037.

time. Interactive effects of food availability and temperature may have a profound effect on growth, and we would expect that energetic demands become greater at the higher water temperatures, in which case the potential for faster growth would be attained through increased food consumption (Houde, 1989), providing food resources are not limited. Thus, it may be more reasonable to assume that food availability has a more significant impact on growth than SSTs during the reduced upwelling season when temperatures are consistently greater than 27°C.

Although water temperature has been shown to regulate the formation and short-term growth of otoliths in some marine fish species (Barber and Jenkins, 2001), the causal factor affecting otolith growth could also be associated with food availability (Govoni et al., 1985; Johnson et al., 2002) and composition (Woodbury, 1999). Otolith growth appears to be a conservative measure of somatic growth (i.e., otoliths continue to grow even with decreases in somatic growth; Campana and Neilson, 1985); therefore a significant change in otolith growth could signal a dramatic change in the larval feeding environment. We observed significant interannual differences between relationships of otolith size and fish size. Otoliths were disproportionately larger in slower growing groups of larvae, but additionally, during the period of 1997 when SSTs were abnormally high, otoliths were growing at a greater rate in relation to fish size (Fig. 6). Elevated water temperatures have been shown to increase short-term otolith growth (Hoff and Fuiman, 1993; Barber and Jenkins, 2001). Althoughtemperature may have affected otolith growth in 1997, lower food levels may have been the causal factor for a significantly slower otolith growth rate and the smaller mean otolith diameter of the 1991 group.

Recruitment implications

The probability of survival from early stages of development to recruitment in marine fishes is thought to be influenced by prerecruit starvation and predation mortality associated with slower growing and nutritionally weakened individuals (Cushing, 1975; Houde, 1987; Margulies, 2001) and predator-prey interactions and densities (Cowan and Houde, 1992). However, Peterman et al. (1988) have demonstrated that the survival rate of prerecruits older than 19 days of age is more variable than earlier life stages, and it is this stage that determines recruitment strength in northern anchovy (*Engraulis mordax*). Yellowfin tuna in the Pacific Ocean exhibit a pattern of reproduction that has strong potential for regulation of recruitment during prejuvenile stages, when initial numbers in a cohort are quite large and vital rates (e.g., growth, mortality) are high (Houde, 1987; Margulies, 2001). However, the potential for recruitment fluctuations is also high for the relatively long juvenile stage of yellowfin tuna as well (Houde, 1987; Margulies, 2001). In the EPO, yellowfin tuna are recruited to the fishery at a fork length of about 30 cm and at an age of approximately 6 months (Wild, 1994; Maunder and Harley[10]). Recruitment estimates calculated at quarterly intervals for yellowfin tuna in the EPO are variable and may be influenced by environmental fluctuations (Maunder and Harley[10]). It is not clear what effect slower or faster growing cohorts may have on recruitment, but the growth- and stage-specific mortality rates (Houde, 1987; Pepin, 1991; Comyns et al., 2003) of a cohort may determine whether it survives to recruitment or when it enters the fishery. We were unable to estimate mortality rates for the larvae collected in each of the three years because during some years they were collected on single sampling dates (Essig and Cole, 1986). Nonetheless, the recruitment estimate (ca. 1.44×10^7 individuals) following the period in 1991, when the smallest size-at-age and the slowest-growing larvae were present was approximately half the amount estimated (ca. 3.11×0^7 individuals) following the period in 1990 (Maunder and Harley[10]; Maunder[11]), when larvae were larger and growing more rapidly. The recruitment estimate following the 1997 period (ca. 3.06×10^7 individuals) was slightly less than that following the 1990 period. Larvae of the 1997 group were growing at a rate similar to that of the 1991 group, but the mean size-at-age was significantly greater, which may indicate a size advantage favorable for prerecruit survival (Miller et al., 1988). The growth rates and conditions estimated for yellowfin tuna larvae within the small scale area of our study may apply to localized recruitment estimates within the Panama Bight and not those of the entire EPO, given that restricted movements of yellowfin tuna occur in the EPO (Schaefer, 1991; Wild, 1994). Although these inferences may be applicable only to recruitment within the Panama Bight, they may still indicate that growth rates and the mean size-at-age during the larval and early-juvenile stages are a contributing factor to recruitment variability of yellowfin tuna in the EPO.

Our study provides the first examination of factors affecting larval growth and possibly prerecruit survival of yellowfin tuna in the Pacific Ocean. Future research is necessary to better understand small-scale variability in growth and mortality rates of yellowfin tuna larvae within their feeding environment. To that end, we are conducting further studies at the Achotines Laboratory in Panama to examine vital rates of this species and the interactions of these vital rates with biological and physical processes to complement our field measurements and to gain more insight into prerecruit survival of yellowfin tuna.

---

[10] Maunder, M. N., and S. J. Harley. 2004. Status of yellowfin tuna in the eastern Pacific Ocean in 2002 and outlook for 2003, p. 5–119. Inter-American Tropical Tuna Commission, stock assessment report 4. IATTC, 8604 La Jolla Shores Drive, La Jolla, CA 92037.

[11] Maunder, M. 2004. Personal commun. Inter-American Tropical Tuna Commission, 8604 La Jolla Shores Drive, La Jolla, CA 92037.

Acknowledgments

We are grateful to the entire staff of the IATTC's Achotines Laboratory who made this study possible. We especially thank R. Lauth, D. Soliz, M. Samaniego, A. Cano, J. Stadler, and M. Vergara, the principal crew members of the *Achotines III* during frequently hazardous field sampling. We also thank I. Díaz, D. Domínguez, K. Herrera, and A. García for processing and sorting ichthyoplankton samples. T. Foreman, R. Owen, E. Espinoza, D. Ballesteros, Y. Ballesteros, and P. Vergara also assisted in the field sampling. Logistic and maintenance support was provided by J. Budria, V. Scholey, and E. Espinoza. T. Foreman, R. Olson, R. Lauth, and R. Owen were principally involved in the development of the ichthyoplankton and oceanographic sampling program, and the raw data were processed by R. Lauth, J. Stadler, R. Owen, and R. Olson. We also thank M. Samaniego, E. Espinoza, D. Mancilla, S. Thorrold, R. Jope, C. Vergara, D. Soliz, P. Vergara, B. Ballesteros, Y. Ballesteros, D. Ballesteros, and A. Cano, who assisted with or conducted night-light and light-trap operations. Helpful discussions were appreciated and provided by D. Ambrose, R. Deriso, P. Fiedler, S. Harley, R. Olson, R. Owen, P. Smith, and P. Tomlinson. M. Maunder provided the quarterly recruitment estimates. C. Patnode helped with final preparations of the figures. W. Bayliff, S. Harley, R. Owen, K. Schaefer, and two anonymous reviewers provided helpful review comments. Finally, we thank the former and present directors, J. Joseph and R. Allen, and the chief scientist of the Tuna-Billfish Program, R. Deriso, of the IATTC for their continued support of this research.

Literature cited

Ahlstrom, E. H.
1971. Kinds and abundance of fish larvae in the eastern tropical Pacific, based on collections made on EASTROPAC I. Fish. Bull. 69:3–77.

Allman, R. J., and C. B. Grimes.
1998. Growth and mortality of little tunny (*Euthynnus alletteratus*) larvae off the Mississippi River plume and Panama City, Florida. Bull. Mar. Sci. 62:189–197.

Ambrose, D. A.
1996. Scombridae: Mackerels and tunas. *In* Guide to the early stages of fishes in the California Current region (H. G. Moser, ed.), p. 1270–1285. Calif. Coop. Ocean. Fish. Inves., CALCOFI Atlas 33.

Barber, M. C., and G. P. Jenkins.
2001. Differential effects of food and temperature lead to decoupling of short-term otolith and somatic growth rates in juvenile King George whiting. J. Fish Biol. 58:1320–1330.

Barber, R. T., and F. P. Chavez.
1986. Ocean variability in relation to living resources during the 1982–83 El Niño. Nature 319:279–285.

Barber, R. T., M. P. Sanderson, S. T. Lindley, F. Chai, J. Newton, C. C. Trees, D. G. Foley, and F. P. Chavez.
1996. Primary productivity and its regulation in the equatorial Pacific during and following the 1991–1992 El Nino. Deep-Sea Res. II 43:933–969.

Blackburn, M., R. M. Laurs, R. W. Owen, and B. Zietzschel.
1970. Seasonal and areal changes in standing stocks of phytoplankton, zooplankton and micronekton in the eastern tropical Pacific. Mar. Biol. 7:14–31.

Campana, S. E., and J. D. Neilson.
1985. Microstructure of fish otoliths. Can. J. Fish. Aquat. Sci. 42:101–1032.

Chavez, F. P., P. G. Strutton, G. E. Friederich, R. A. Feely, G. C. Feldman, D. G. Foley, and M. J. McPhaden.
1999. Biological and chemical response of the equatorial Pacific Ocean to the 1997–98 El Niño. Science 286:2126–2131.

Chow, S. and S. Inoue.
1993. Intra- and interspecific restriction fragment length polymorphism in mitochondrial genes of *Thunnus* tuna species. Bull. Nat. Res. Inst. Far Seas Fish. 30:207–224.

Chow, S., H. Okamoto, N. Miyabe, K. Hiramatsu, and N. Barut.
2000. Genetic divergence between Atlantic and Indo-Pacific stocks of bigeye tuna (*Thunnus obesus*) and admixture around South Africa. Mol. Ecol. 9:221–227.

Chow, S., K. Nohara, T. Tanabe, T. Itoh, S. Tsuji, Y. Nishikawa, S. Ueyanagi, and K. Uchikawa.
2003. Genetic and morphological identification of larval and small juvenile tunas (Pisces: Scombridae) caught by a mid-water trawl in the western Pacific. Bull. Fish. Res. Agency 8:1–14.

Collette, B. B., and C. E. Nauen.
1983. FAO species catalogue. Vol. 2, Scombrids of the world. An annotated and illustrated catalogue of tunas, mackerels, bonitos, and related species known to date. FAO Fish. Synop. 125, 137 p. FAO, Rome.

Comyns, B. H., R. F. Shaw, and J. Lyczkowski-Schultz.
2003. Small-scale spatial and temporal variability in growth and mortality of fish larvae in the subtropical northcentral Gulf of Mexico: implications for assessing recruitment success. Fish. Bull. 101:10–21.

Cowan, J. H., Jr., and E. D. Houde.
1992. Size-dependent predation on marine fish larvae by ctenophores, scyphomedusae and planktivorous fish. Fish. Oceanogr.1:113–126.

Cury, P., and C. Roy.
1989. Optimal environmental window and pelagic fish recruitment success in upwelling areas. Can. J. Fish. Aquat. Sci. 46:670–680.

Cushing, D. H.
1975. Marine ecology and fisheries, 278 p. Cambridge Univ. Press, Cambridge, England.

Dessier, A., and J. R. Donguy.
1987. Response to El Niño signals of the epiplanktonic copepod populations in the eastern tropical Pacific. J. Geophys. Res. 92:14,393–14,403.

De Vries, D. A., C. B. Grimes, K. L. Lang, and D. B. White.
1990. Age and growth of king and Spanish mackerel larvae and juveniles from the Gulf of Mexico and U.S. South Atlantic Bight. Envir. Biol. Fish. 29:135–143.

Essig, R. J., and C. F. Cole.
1986. Methods of estimating larval fish mortality from daily increments in otoliths. Trans. Amer. Fish. Soc. 115:34–40.

FAO (Food and Agriculture Organization).
2004. Fishery statistics: capture production, 2002. FAO Yearbook, Fish. Stat. 94/1, 654 p.

Fiedler, P. C.
1992. Seasonal climatologies and variability of eastern tropical Pacific surface waters. NOAA Tech. Rep. NMFS 109, 65 p.
2002. The annual cycle and biological effects of the Costa Rica Dome. Deep-Sea Res. I, 49:321–338.
Forsbergh, E. D.
1963. Some relationships of metorological, hydrographic, and biological variables in the Gulf of Panama. Inter-Am. Trop. Tuna Comm. Bull. 7:1–109.
1969. On the climatology, oceanography and fisheries of the Panama Bight. Inter-Am. Trop. Tuna Comm. Bull. 14:45–385.
Fortier, L. and W. C. Leggett.
1985. A drift study of larval fish survival. Mar. Ecol. Prog. Ser. 25:245–257.
Glynn, P. W., J. L. Mate, A. C. Baker, and M. O. Calderon.
2001. Coral bleaching and mortality in Panama and Ecuador during the 1997–1998 El Nino-Southern Oscillation event: Spatial/temporal patterns and comparisons with the 1982–1983 event. Bull. Mar. Sci. 69:79–109.
González Armas, R.
2002. Aggregation of fish larvae in El Bajo Espiritu Santo in the Gulf of California, their changes in the patterns of distribution and the oceanographic processes that influence them. [In Spanish]. Ph D. diss, 216 p. Centro de Investigaciones del Noroeste S. C. La Paz, Baja California South.
Govoni, J. J., A. J. Chester, D. E. Hoss, and P. B. Ortner.
1985. An observation of episodic feeding and growth of larval *Leiostomus xanthurus* in the northern Gulf of Mexico. J. Plankton Res. 7:137–146.
Graves, J. E., M. A. Simovich, and K. M. Schaefer.
1988. Electrophoretic identification of early juvenile yellowfin tuna, *Thunnus albacares*. Fish. Bull. 86:835–838.
Grimes, C. B.
2001. Fishery production and the Mississippi River discharge. Fisheries 26(8):17–26.
Grimes, C. B., and J. J. Isely.
1996. Influence of size-selective mortality on growth of gulf menhaden and king mackerel larvae. Trans. Am. Fish. Soc. 125:741–752.
Hoff, G. R., and L. A. Fuiman.
1993. Morphometry and composition of red drum otoliths: changes associated with temperature, somatic growth rate, and age. Comp. Biochem. Physiol. 106A:209–219.
Houde, E. D.
1987. Fish early life dynamics and recruitment variability. Am. Fish. Soc. Symp.
1989. Comparative growth, mortality, and energetics of marine fish larvae: temperature and implied latitudinal effects. Fish. Bull. 87:471–495.
Jenkins, G. P., and T. L. O. Davis.
1990. Age, growth rate, and growth trajectory determined from otolith microstructure of southern bluefin tuna *Thunnus maccoyii* larvae. Mar. Ecol. Prog. Ser. 63:93–104.
Jenkins, G. P., J. W. Young, and T. L. O. Davis.
1991. Density dependence of larval growth of a marine fish, the southern bluefin tuna, *Thunnus maccoyii*. Can. J. Fish. Aquat. Sci. 48:1358–1363.
Ji, M., A. Leetmaa, and J. Derber.
1995. An ocean analysis system for seasonal to interannual climate studies. Mon. Wea. Rev. 123:460–481.
Johnson, M. W., J. R. Rooker, D. M. Gatlin III, and G. J. Holt.
2002. Effects of variable ration levels on direct and indirect measures of growth in juvenile red drum (*Sciaenops ocellatus*). J. Exp. Mar. Biol. Ecol. 274:141–157.
Kaji, T., M. Tanaka, M. Oka, H. Takeuchi, S. Ohsumi, K. Teruya, and J. Hirokawa.
1999. Growth and morphological development of laboratory-reared yellowfin tuna *Thunnus albacares* larvae and early juveniles, with special emphasis on the digestive system. Fish. Sci. 65:700–707.
Lang, K. L., C. B. Grimes, and R. F. Shaw.
1994. Variations in the age and growth of yellowfin tuna larvae, *Thunnus albacares*, collected about the Mississippi River plume. Environ. Biol. Fish. 39:259–270.
Large, W. G., and S. Pond.
1981. Open ocean momentum flux measurements in moderate to strong winds. J. Phys. Oceanogr. 11:324–336.
Lauth, R. R., and R. J. Olson.
1996. Distribution and abundance of larval scombridae in relation to the physical environment in the northwestern Panama Bight. Inter-Am. Trop. Tuna Comm. Bull. 21:125–167.
MacKenzie, B. R., T. J. Miller, S. Cyr, and W. C. Leggett.
1994. Evidence for a dome-shaped relationship between turbulence and larval fish ingestion rates. Limnol. Oceanogr. 39:1790–1799.
Margulies, D.
1993. Assessment of the nutritional condition of larval and early juvenile tuna and Spanish mackerel (Pisces: Scombridae) in the Panama Bight. Mar. Biol. 115:317–330.
2001. Preface. Early life history studies of yellowfin tuna, *Thunnus albacares*. Inter-Am. Trop. Tuna Comm. Bull. 22:5–8.
Margulies, D., J. M. Suter, S. L. Hunt,, R. J. Olson, V. P. Scholey, J. B. Wexler, and A. Nakamura.
In press. Spawning and early development of captive yellowfin tuna, *Thunnus albacares*. Fish. Bull.
Margulies, D., J. B. Wexler, K. T. Bentler, J. M. Suter, S. Masuma, N. Tezuka, K. Teruya, M. Oka, M. Kanematsu, and H. Nikaido.
2001. Food selection of yellowfin tuna, *Thunnus albacares*, larvae reared in the laboratory. Inter-Am. Trop. Tuna Comm. Bull. 22:9–51.
Matsumoto, W. M., E. H. Ahlstrom, S. Jones, W. L. Klawe, W. J. Richards, and S. Ueyanagi.
1972. On the clarification of larval tuna identification particularly in the genus *Thunnus*. Fish. Bull. 70:1–12.
McGowan, J. A., and V. J. Fraundorf.
1966. The relationship between size of net used and estimates of zooplankton diversity. Limnol. Oceanogr. 11:456–469.
Miller, T. J., L. B. Crowder, J. A. Rice, and E. A. Marschall.
1988. Larval size and recruitment mechanisms in fishes: toward a conceptual framework. Can. J. Fish. Aquat. Sci. 45:1657–1670.
Nishikawa, Y., M. Honma, S. Ueyanagi, and S. Kikawa.
1985. Average distribution of larvae of oceanic species of scombroid fishes, 1956–1981. Far Seas Fish. Res. Lab., S Ser. 12, 99 p.
Nishikawa, Y., and D. W. Rimmer.
1987. Identification of larval tunas, billfishes and other scombroid fishes (Suborder Scombroidei): an illustrated guide, 20 p. CSIRO Mar. Lab. Rep. 186, Melbourne, Australia.

Olson, R. J., and V. P. Scholey.
1990. Captive tunas in a tropical marine research laboratory: growth of late-larval and early-juvenile black skipjack *Euthynnus lineatus*. Fish. Bull. 88:821–828.
Owen, R. W.
1989. Microscale and finescale patchiness of small plankton in coastal and pelagic environments. J. Mar. Res. 47:197–240.
Owen, R. W., and B. Zeitzschel.
1970. Phytoplankton production: seasonal change in the oceanic eastern tropical Pacific. Mar. Biol. 7:32–36.
Pepin, P.
1988. Predation and starvation of larval fish: a numerical experiment of size-and growth-dependent survival. Biol. Ocean. 6:23–44.
1991. Effect of temperature and size on development, mortality, and survival rates of the pelagic early life history stages of marine fish. Can. J. Fish. Aquat. Sci. 48:503–518.
Peterman, R. M., M. J. Bradford, N. C. H. Lo, and R. D. Methot.
1988. Contribution of early life stages to interannual variability in recruitment of northern anchovy (*Engraulis mordax*). Can. J. Fish. Aquat. Sci. 45:8–16.
Potthoff, T.
1974. Osteological development and variation in young tunas, genus *Thunnus* (Pisces, Scombridae), from the Atlantic Ocean. Fish. Bull. 72:563–588.
Richards, W. J., T. Potthoff, and J. Kim.
1990. Problems identifying tuna larvae species (Pisces: Scombridae: *Thunnus*) from the Gulf of Mexico. Fish. Bull. 88:607–609.
Rochford, D. J.
1962. Hydrology of the Indian Ocean. Part II: the surface waters of the southeast Indian Ocean and the Arafura Sea in the spring and summer. Aust. J. Mar. Freshwater Res. 13:226–251.
Rothschild, B. J., and T. R. Osborn.
1988. Small scale turbulence and plankton contact rates. J. Plankton Res. 10:465–474.
Schaefer, K. M.
1991. Geographic variation in morphometric characters and gill-raker counts of yellowfin tuna *Thunnus albacares* from the Pacific Ocean. Fish. Bull. 89:289–297.
1998. Reproductive biology of yellowfin tuna (*Thunnus albacares*) in the eastern Pacific Ocean. Inter-Am. Trop. Tuna Comm. Bull. 21:201–272.
2001. Reproductive biology of tunas. *In* Fish physiology, Vol. 19, Tuna: physiology, ecology, and evolution (B. A. Block, and E. D. Stevens, eds.), p. 225–270. Academic Press, San Diego, CA.
Scholey, V. P.
1993. Effects of temperature and food concentration on growth and survival of late-larval and early-juvenile black skipjack, *Euthynnus lineatus*. M.Sci. thesis, 56 p. Univ. Washington, Seattle, WA.
Shima, M., and K. M. Bailey.
1994. Comparative analysis of ichthyoplankton sampling gear for early life stages of walleye pollock (*Theragra chalcogramma*). Fish. Oceanogr. 3:50–59.
Smayda, T. J.
1963. A quantitative analysis of the phytoplankton of the Gulf of Panama I. Results of the regional phytoplankton surveys during July and November, 1957 and March, 1958. Inter-Am. Trop. Tuna Comm. Bull. 7:191–253.
1966. A quantitative analysis of the phytoplankton of the Gulf of Panama III. General ecological condtions, and the phytoplankton dynamics at 8°45′N, 79°23′W from November 1954 to May 1957. Inter-Am. Trop. Tuna Comm. Bull. 11:353–612.
Smith, P. E., and S. L. Richardson.
1977. Standard techniques for pelagic fish egg and larva surveys. FAO Fish. Tech. Paper, 175, 100 p. FAO, Rome.
Strutton, P. G., and F. P. Chavez.
2000. Primary productivity in the equatorial Pacific during the 1997–98 El Niño. J. Geophys. Res. 105:26,089–26,101.
Sverdrup, H. U., M. W. Johnson, and R. H. Fleming.
1942. Dynamics of ocean currents. Chapter 13. *In* The oceans their physics, chemistry, and general biology, p. 431–515. Prentice-Hall, Inc., New York, NY.
Takeyama, H., S. Chow, H. Tsuzuki, and T. Matsunaga.
2001. Mitochondrial DNA sequence variation within and between tuna *Thunnus* species and its application to species identification. J. Fish Biol. 58:1646–1657.
Thorrold, S. R.
1993. Post-larval and juvenile scombrids captured in light traps: preliminary results from the central Great Barrier Reef lagoon. Bull. Mar. Sci. 52:631–641.
Ueyanagi, S.
1969. Observations on the distribution of tuna larvae in the Indo-Pacific Ocean with emphasis on the delineation of the spawning areas of albacore, *Thunnus alalunga*. Bull. Far Seas Fish. Res. Lab. 2:177–256.
Ware, D. M., and R. E. Thomson.
1991. Link between long-term variability in upwelling and fish production in the northeast Pacific Ocean. Can. J. Fish Aquat. Sci. 48:2296–2306.
Wexler, J. B.
1993. Validation of daily growth increments and estimation of growth rates of larval and early-juvenile black skipjack, *Euthynnus lineatus*, using otoliths. Inter-Am. Trop. Tuna Comm. Bull. 20:399–440.
Wexler, J. B., D. Margulies, S. Masuma, N. Tezuka, K. Teruya, M. Oka, M. Kanematsu, and H. Nikaido.
2001. Age validation and growth of yellowfin tuna, *Thunnus albacares*, larvae reared in the laboratory. Inter-Am. Trop. Tuna Comm. Bull. 22:52–91.
Wild, A.
1994. A review of the biology and fisheries for yellowfin tuna, *Thunnus albacares*, in the eastern Pacific Ocean. FAO Fish. Tech. Paper 336:52–107. FAO, Rome.
Woodbury, D.
1999. Reduction of growth in otoliths of widow and yellowtail rockfish (*Sebastes entomelas* and *S. flavidus*) during the 1983 El Niño. Fish. Bull. 97:680–689.
Wooster, W. S.
1959. Oceanographic observations in the Panama Bight, "Askoy" Expedition, 1941. Bull. Am. Mus. Nat. Hist. 118:119–151.
Wroblewski, J. S., J. G. Richman, and G. L. Mellor.
1989. Optimal wind conditions for the survival of larval northern anchovy, *Engraulis mordax*—a modeling investigation. Fish. Bull. 87:387–398.
Young, J. W., and T. L. O. Davis.
1990. Feeding ecology of larvae of southern bluefin, albacore and skipjack tunas (Pisces: Scombridae) in the eastern Indian Ocean. Mar. Ecol. Prog. Ser. 61:17–29.
Zar, J. H.
1984. Biostatistical analysis, 2nd ed., 718 p. Prentice-Hall, Englewood Cliffs, NJ.

Annual fecundity, batch fecundity, and oocyte atresia of Atka mackerel (*Pleurogrammus monopterygius*) in Alaskan waters

Susanne F. McDermott (contact author)[1]
Katherine P. Maslenikov[2]
Donald R. Gunderson[2]

Email address for S F. McDermott: Susanne.McDermott@noaa.gov

[1] National Marine Fisheries Service
Alaska Fisheries Science Center
7600 Sand Point Way NE
Seattle, Washington 98115

[2] University of Washington
School of Aquatic and Fisheries Sciences
Box 355020
Seattle, Washington 98195

Abstract—Annual potential fecundity, batch fecundity, and oocyte atresia were estimated for Atka mackerel (*Pleurogrammus monopterygius*) collected in Alaskan waters during 1993–94. Atka mackerel were assumed to be determinate spawners on the basis of decreasing fecundity after batch spawning events. Histological examination of the ovaries indicated that oocytes in the vitellogenic stage and higher had been spawned in the current spawning season. For an average female of 40 cm, potential annual fecundity was estimated to be 41,994 eggs, average batch size (i.e., batch fecundity) was estimated to be 6689 eggs, and there were 6.13 batches per spawning season. Atresia was estimated by examining postspawning specimens and was found to be substantial. The average amount of atresia for a 40-cm fish was estimated to be 11,329 eggs, resulting in an estimated realized fecundity of only 30,664 eggs and 4.64 batches of eggs per spawning season.

Manuscript submitted 22 April 2004 to the Scientific Editor's Office.

Manuscript approved for publication 15 March 2006 by the Scientific Editor.

Fish. Bull. 105:19–29 (2007).

The reproductive biology of Atka mackerel (*Pleurogrammus monopterygius*) is characterized by batch spawning by females and nest-guarding by males. This member of the greenling family (Hexagrammidae) is distributed in Russian and Alaskan waters where it is usually found in dense aggregations and associated with areas of fast currents, such as the passes between the Aleutian Islands (Lowe et al., 2002). Peak spawning occurs from July through October in Alaskan waters (McDermott and Lowe, 1997) and from June through September off Kamchatka (Zolotov, 1993). Batches of adhesive eggs are spawned in rock crevices and are guarded by males until they hatch (Gorbunova, 1962; Zolotov, 1993). Studies with archival tags have indicated that males guard nests for 3–4 months (Nichol and Somerton, 2002). Batches of eggs in different phases of development were found within one nest, indicating a promiscuous mating system (Zolotov and Tokranov, 1989; Zolotov, 1993; Lowe et al., 2003).

Atka mackerel females spawn their annual complement of eggs in several batches over the course of the spawning season. Zolotov (1993) reported that females spawn an average of three batches of eggs per season and that there is at least a two-week hiatus between spawnings in Kamchatkan waters. To estimate the number of batches spawned by a female, it is necessary to estimate annual fecundity and batch fecundity. Annual fecundity is defined as the total number of eggs spawned by a female in a single year and batch fecundity is defined as the numbers of eggs released at one time (Nichol and Acuna, 2001). Direct estimation of annual fecundity is possible if the number of eggs to be spawned that season is fixed or determinate (Hunter et al., 1985). Fish with determinate fecundity are described as showing a well-defined hiatus (or gap) in oocyte-size distribution between the advanced oocytes that will be spawned that year and the immature oocytes that will not develop until the following spawning seasons (Hunter et al., 1985). Species that are characterized by continuous oocyte development and oocyte-size distributions have often been described as indeterminate spawners (Hunter et al., 1985) that have the ability to develop unyolked oocytes continually and add them to the standing stock of advanced-yolked oocytes even after spawning begins. Hunter and Macewicz (2001) stated that potential fecundity can be estimated if three key requirements are met: 1) one can identify a certain standing stock or size range of

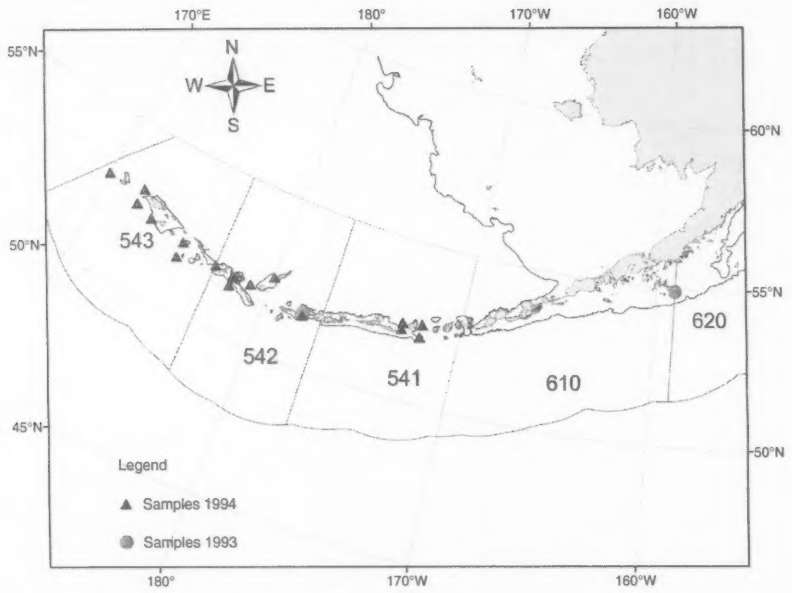

Figure 1

Sampling locations for Atka mackerel (*Pleurogrammus monopterygius*) collected for estimates of annual fecundity and batch fecundity in 1993–94 in the Aleutian Islands, Alaska.

oocytes into which no new oocytes are recruited once spawning begins; 2) females used to estimate potential fecundity have not spawned; and 3) atretic losses are negligible or can be estimated. Recent studies have shown that many fish species reabsorb a substantial number of their oocytes before spawning or at the end of the spawning season—a process known as atresia (Hunter and Macewicz, 1985; Kjesbu et al., 1991; Ma et al., 1998) Atretic losses in Icelandic cod (*Gadus morhua*) and Atlantic herring (*Clupea harengus*) occur mainly during the earlier phase of vitellogenic development, decrease as oocytes mature, and are negligible near the time of spawning (Harðardóttir et al., 2001, Kurita et al., 2003). Scombroid fishes (mackerels and tunas) have been described as having extensive atresia at the end of their spawning season (Hunter and Macewicz, 2001).

Previous studies (Zolotov, 1993) have described Atka mackerel as determinate spawners. However, no study to date has examined the oocyte-size distribution or shown that fecundity decreases after spawning. We examined the oocyte-size distribution for mature oocytes over time. Additionally, all ovaries were examined histologically to identify advanced oocyte stages, presence of postovulatory follicles, and oocyte atresia. We estimated potential annual fecundity and batch fecundity. The number of batches to be spawned was calculated by dividing total fecundity by batch fecundity. Potential fecundity was studied by comparing prespawning individuals with those that had spawned at least one batch of eggs in order to determine if advanced oocytes are added throughout the spawning season. Atresia of mature oocytes was estimated from ovaries of postspawning females to calculate realized fecundity as a measure of oocytes actually spawned per year.

Materials and methods

Data collection

All Atka mackerel examined in this study were either collected by the National Marine Fisheries Service (NMFS) fisheries observers aboard commercial fishing vessels during the commercial Atka mackerel fishery in 1993 or by Alaska Fisheries Science Center (AFSC) scientists during the 1994 NMFS bottom trawl survey of the Aleutian Islands (Table 1, Fig. 1).

During both years, Atka mackerel were subsampled from individual trawl tows. Collections were stratified by fish size; no more than five fish per size group were collected in each NMFS statistical area during a sampling year. The fork length of each fish was measured to the nearest centimeter, and each fish was weighed to the nearest 0.1 kg. In most cases, the stomach was emptied before weighing the fish. The ovaries were excised and placed in labeled cloth bags in 10% formalin solution buffered with sodium acetate (20 g per liter solution). In order to determine maturity stage, and presence of atresia, all ovaries were processed histologically. Four ovarian sections (4-μm thick) were stained

Table 1

Number of fish collected by year, month, and National Marine Fisheries Service (NMFS) statistical area. The number of samples with postovulatory follicles, i.e., in spawning or postspawning condition are shown in parentheses.

		NMFS statistical areas				
Year	Month	541	542	543	620	Total
1993	October		4 (4)		5 (5)	9
1994	June	57				57
	July		49	34 (11)		83
	August			10 (9)		10
Total		57	53	44	5	159

with hematoxilin (Sigma Aldrich, St. Louis, MI) and eosin counterstain (Sigma Aldrich, St. Louis, MI) (H&E). Maturity stages were determined by using categories developed by McDermott and Lowe (1997). Ovaries of prespawning females were defined by the lack of hydrated oocytes in June and the absence of postovulatory follicles once hydrated oocytes were present in July. Presence of atresia was determined according to classifications developed by Hunter and Macewitz (1985).

For the estimation of annual fecundity, only females whose ovaries had not shown any signs of releasing oocytes (i.e., all hydrated oocytes were within their follicles and ovaries contained no postovulatory follicles) were used. Different stages of postovulatory follicles can be distinguished in fish that have spawned multiple batches (McDermott and Lowe, 1997). These different stages indicate that postovulatory follicles persist in ovaries longer than the time period between batch spawning events, minimizing the possibility of incorrectly classifying a partly spent fish as a prespawning fish. Prespawning and partly spent specimens were compared to examine determinate spawning.

Gravimetric method

The gravimetric method was used to count and measure oocytes in weighed samples of Atka mackerel ovarian tissue (Hunter et al., 1985). In our fecundity analysis, small cross-sections were excised from preserved Atka mackerel ovaries. The amount of tissue removed was dependent on the size of eggs present, typically ranging from 0.3 g to 2.5 g. The target sample size was approximately 1000 eggs. The cross-section was divided into wedges in order to ensure a representative sample of ovarian wall tissue in relation to the tissue containing eggs. Ovarian wall tissue weight represents a substantial part of total ovary weight and needed to be represented proportionally in the subsamples. The samples were weighed to the nearest 0.001 g and allowed to sit in water for several hours before handling to reduce exposure to formalin. Ovary tissue was teased apart manually under a dissecting microscope and spread evenly in a 50% solution of glycerol in a dish over a grid partitioned by 1-cm squares. The dissecting microscope was equipped with a Javelin Ultrachip CCTV video camera (model JE-7442, Javelin Electronics, Los Angeles, CA), connected to a computer equipped with BioScan Optimas 4.0 scanning software (Bioscan Inc., Edmonds, WA).

All oocyte stages used in our study were previously described by McDermott and Lowe (1997). It was possible to distinguish the cortical alveoli oocyte stage (stage 3) from the more advanced oocyte stages (stage 4 [oil droplet stage] and stage 5 [vitellogenic stage]) when using the dissecting microscope and camera image to examine whole eggs. Oocytes in stage 4 and above showed a distinct ring around the nucleus, which was attributed to the oil and yolk droplets accumulating in the oocyte. Stage-3 oocytes did not show a distinct ring around the nucleus. However, it was not possible to distinguish oil-droplet oocytes (stage 4) from vitellogenic oocytes or more advanced stages (stage 5+) when examining whole eggs. Because oocyte development is usually attributed to oil-droplet and yolk accumulation, it was initially assumed that oocytes below stage 4 would not be spawned in the current spawning event and therefore would serve as reserve oocytes to be spawned in later spawning seasons. To determine oocyte-size composition, all oocytes stage 4 and above were measured along a vertical axis in each 1-cm square of a grid until 250 eggs had been measured. All eggs in the sample determined to be oocyte stage 4 or above were then counted manually under the dissecting microscope to arrive at an estimate of the number of eggs present per gram of tissue that were oocyte stage 4 and greater.

Location of tissue samples within the ovary

We examined six specimens to determine if location of tissue samples within the ovary affected estimates of fecundity. Two specimens had ovaries in the vitellogenic stage, two had ovaries in the early hydration stage, and two had ovaries in the spawning stage. We took three tissue samples per ovary lobe (six per specimen). The samples were taken from the anterior, center, and posterior location within each lobe of the ovary.

All eggs within the tissue sample that were oocyte stage 4 and above were counted and the first 100 oocytes were measured. Analysis of variance (ANOVA) (S-plus, 7.0 for Windows, Insightful Corp., Seattle, WA) (Venables and Ripley, 2002) was used for this examination with ovary lobe (left or right), position within the ovary, and maturity stage as factors. This analysis was carried out for the mean number of eggs per gram of tissue and mean egg size as response variables. The ANOVA indicated that the tissue sample could be taken from either lobe of the ovaries at any location. All further samples were therefore taken from a central location within either one of the ovary lobes.

Determinate versus indeterminate spawning

Direct estimation of annual fecundity is possible if the number of eggs to be spawned that season is fixed (determinate) and there is a well-defined gap in the oocyte-size distribution between advanced oocytes that will be spawned that year and the immature oocytes. In contrast, indeterminate spawners have the ability to develop unyolked oocytes continually and add them to the standing stock of advanced-yolk oocytes even after spawning begins.

To examine whether Atka mackerel are determinate spawners as previously described (Zolotov, 1993), we measured their oocytes to obtain a size distribution for oocytes over time. Additionally, we compared the potential fecundity of prespawning fish with the potential fecundity of fish that had spawned at least one batch. When all oocytes stage 4 and greater were summed, the tally exceeded the expected number of oocytes to be spawned per year, given the number of eggs in the first batch and the previous estimate of an average of three batches per female (Zolotov, 1993). This total number of oocytes led to the hypothesis that stage-4 oocytes may be developed, but not spawned, in a given year and are part of the standing stock of oocytes to be spawned in the following year. This hypothesis was supported when we found both oil droplet oocytes and atretic advanced-stage oocytes in the spent ovaries of nine specimens collected in 1993 (Fig. 2A).

The specimens from 1994 were consequently divided into two ovary stages:

1 Prespawning-stage ovaries: ovaries with the most advanced oocyte stage of vitellogenic or hydrated oocytes that showed no evidence of having been spawned, i.e., did not have postovulatory follicles (POFs).
2 Spawning-stage ovaries: ovaries that had spawned at least one batch of eggs and therefore contained POFs.

Potential annual fecundity was estimated with the gravimetric method and the total number of oocytes were further divided into stage-4 and stage-5+ oocytes by using the methods described below. The data were log-transformed and linear regressions were fitted by using S-plus. Ovaries of prespawning and spawning fish were compared by testing for differences in intercepts and slopes with S-Plus (Venables and Ripley, 2002).

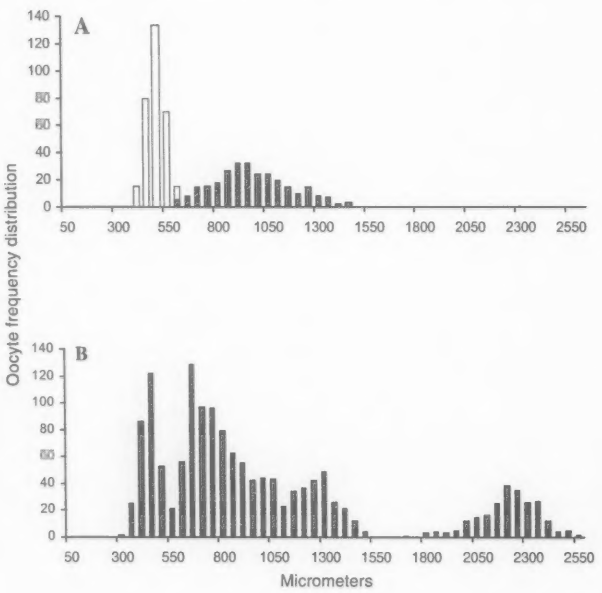

Figure 2

Atka mackerel (*Pleurogrammus monopterygius*) oocyte-size frequency distribution of (**A**) stage-4 (clear bars) and advanced atretic eggs (black bars) typical of a recently spent ovary, measured from whole oocytes (October 1993); (**B**) an ovary collected on 2 August 1994, with a hydrated batch of oocytes ready to be spawned (oocytes larger than 1800 μm are hydrated).

Separation of stage-4 oocytes from more advanced oocytes

To test whether Atka mackerel retain all of their stage-4 oocytes as a standing stock for the next year's fecundity, it became necessary to separate the stage-4 oocytes from the rest of the more developed oocyte stages and then subtract the stage-4+ oocytes from the total oocyte count. It was not possible to distinguish the oil-droplet–stage oocytes from oocytes in the vitellogenic stage or migratory nucleus stage when examining whole oocytes with the dissecting microscope image and the Optimas software. Therefore, we examined nine ovaries that were recently spent, which contained only healthy stage-4 oocytes and atretic hydrated oocytes that could be easily distinguished (Fig. 2A). The average size distribution of stage-4 oocytes was estimated by measuring approximately 250 stage-4 oocytes per ovary. This size distribution could then be applied to the prespawning-stage ovaries, assuming that stage-4 oocyte-size distributions in spent ovaries were the same as those in prespawning-stage ovaries. To test this assumption, the size distribution from prespawning-stage ovaries in histological preparations was compared to the size distribution in postspawning fish by using ANOVA.

In order to deduct the population of stage-4 oocytes from the whole population of stage 5+ oocytes in prespawning-stage ovaries, we determined the size overlap between stage-4 and stage-5 oocytes by examining histological sections from six prespawning-stage ovaries. All oocytes that had been sectioned through the nucleus were measured with a compound microscope and camera system with Optimas software. We determined that all oocytes smaller than 525 μm were stage-4 oocytes and did not overlap in size with stage-5 oocytes in the prespawning-stage ovaries (Fig. 3A). We used the postspawning-stage ovaries that had only stage-4 oocytes and atretic hydrated oocytes to estimate the proportion of stage-4 oocytes that was less then 525 μm. This proportion was then applied to the prespawning-stage ovaries to estimate the number of stage-4 oocytes present.

The total number of stage-4 oocytes in the tissue sample for each prespawning-stage ovary was estimated from

$$\hat{n}_{4i} = \frac{c_i}{\hat{p}} \qquad (1)$$

and

$$\hat{p} = \frac{g_i}{m_i}, \qquad (2)$$

where $\hat{n}_{4i}$ = estimated total number of stage-4 oocytes in a tissue sample of a prespawning specimen i;

c_i = total number of stage-4 oocytes <525 μm in a tissue sample for a prespawning specimen i;

$\hat{p}$ = the estimated proportion of total stage-4 oocytes <525 μm, estimated from ovaries of a postspawning female;

g_i = total number of stage-4 oocytes <525 μm in postspawning-stage ovaries; and

m_i = total number of all stage-4 oocytes in postspawning-stage ovaries.

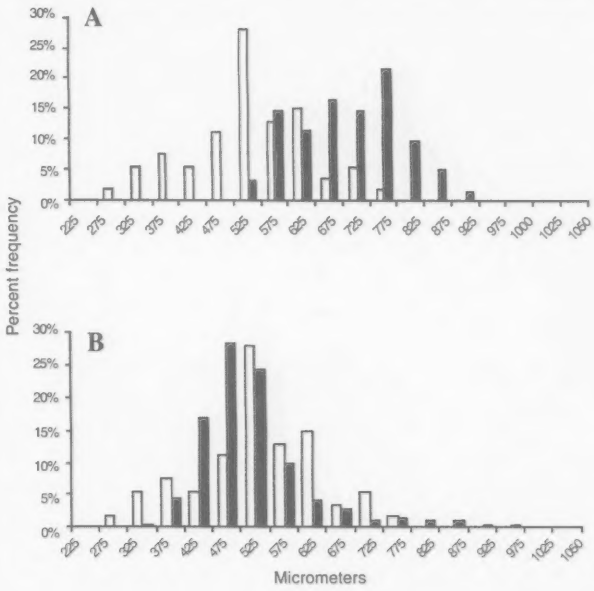

Figure 3

Combined size distributions of (**A**) stage 4 (clear bars) and stage 5 (black bars) oocytes from histological slides of six prespawning Atka mackerel (*Pleurogrammus monopterygius)* specimens (1994); (**B**) stage-4 oocytes from prespawning (clear bars) and postspawning (black bars) fish, measured from histological slides of 1993 and 1994 Atka mackerel specimen.

Estimation of potential annual fecundity and batch fecundity

Potential annual fecundity and batch fecundity were calculated by using prespawning specimens. Two scenarios were examined for potential fecundity:

Scenario 1: potential fecundity$_{total}$ (counting oocytes stage 4 and greater); and

Scenario 2: potential fecundity$_{stage5+}$ (counting only oocytes stage 5+).

The following equation was used:

$$\hat{F}_i = \frac{n_i O_i}{W_i}, \qquad (3)$$

where $\hat{F}_i$ = estimated potential fecundity or batch fecundity for a prespawning specimen i;

n_i = number of oocytes in the tissue sample of a prespawning specimen (for potential fecundity$_{total}$: oocytes of stage 4 and greater; for potential fecundity$_{stage5+}$, oocytes of stage 5+, for batch fecundity, number of hydrated oocytes);

O_i = total ovary weight (g) for a prespawning specimen i; and

W_i = weight of tissue sample (g) for a prespawning specimen i.

Prespawning-stage ovaries that contained oocytes in the early hydration stage (stage 7) or greater were examined to estimate batch fecundity. Atka mackerel appear to hydrate one batch of oocytes at a time and the hydrated oocytes can be clearly separated from less developed oocytes by a gap in oocyte-size distribution (Fig. 2B).

Length-fecundity relationships

Length-fecundity relationships and their 95% confidence intervals were computed for potential annual fecundity ($\hat{F}_i$), batch fecundity ($\hat{B}_i$), and the number of atretic oocytes ($\hat{E}_i$) by using nonlinear regression in S-plus (Venables and Ripley, 2002) with the following model:

$$Y = aL^b \quad (4)$$

where $y = \hat{F}_i, \hat{B}_i, \hat{E}_i$;
a and b = fecundity parameters to be estimated; and
L = fork length.

Oocyte atresia

Occurrence of atresia was divided into high occurrence (more than 10% of oocytes are atretic) and low occurrence (less than 10% of oocytes are atretric) by examining visually all histological slides. Because incidence of atresia was low in prespawning- and spawning-stage ovaries, it was not quantified further.

The occurrence of oocyte atresia in spent oocytes or oocytes that had been spawned was determined by counting the number of atretic oocytes present in the tissue sample of whole oocytes. Atretic eggs were easily distinguished from nonatretic eggs by their shriveled appearance, dark to almost black coloration, and dense texture. In postspawning fish, it appeared that all oocytes in an advanced stage were atretic and that stage-4 or smaller oocytes were healthy (Fig. 2A). When the histological slides of the same specimen were examined for verification of the oocyte stages, it appeared that all atretic oocytes that were counted corresponded to alpha and beta atresia stages (Hunter and Macewicz, 1985). The total number of atretic oocytes for each specimen (E_i) was calculated by multiplying atretic oocytes per gram of tissue by total weight of both ovaries.

Realized annual fecundity

Realized annual fecundity is defined as the number of oocytes actually spawned per fish in a given year. In order to take the occurrence of atresia into account, a predicted realized fecundity-at-length was calculated by subtracting predicted atresia-at-length from the predicted potential fecundity-at-length, by using

$$\hat{R}_l = \hat{F}_l - \hat{E}_l, \quad (5)$$

where $\hat{R}_l$ = estimated realized annual fecundity at length l;
$\hat{F}_l$ = estimated potential annual fecundity at length l; and
$\hat{E}_l$ = estimated number of atretic oocytes at length l.

Variance (Var) of the predictions at length was calculated as the sum of the variances (estimated with S-plus) of the predicted values for potential fecundity-at-length and atresia-at-length:

$$Var(\hat{R}_l) = Var(\hat{F}_l) + Var(\hat{E}_l). \quad (6)$$

Annual number of batches spawned

The potential number of batches spawned for each specimen i was estimated from

$$\hat{D}_i^{pot} = \frac{\hat{F}_i}{\hat{B}_i}, \quad (7)$$

where ($\hat{D}_i^{pot}$) = the potential number of batches spawned for each specimen i;
$\hat{F}_i$ = potential fecundity for specimen i, and
$\hat{B}_i$ = batch fecundity for specimen i.

Batch number for realized fecundity for specimen i was calculated by using the predicted proportion of atretic eggs per length category and applying it to each specimen:

$$\hat{D}_{il}^{real} = \frac{\hat{F}_i(1 - p_l^{atr})}{\hat{B}_i}, \quad (8)$$

where

$$p_l^{atr} = \frac{\hat{E}_l}{\hat{F}_l}, \quad (9)$$

where $\hat{D}_{il}^{real}$ = the batch number per specimen i at length l;
p_l^{atr} = the predicted proportion atretic at length l;
$\hat{E}_l$ = the predicted number of atretic eggs at length l; and
$\hat{F}_l$ = the predicted potential fecundity at length l.

The relationship between batch number and length was examined for both potential and realized fecundity with linear regression (S-plus).

Results

Data collection

Nine samples were collected after spawning events in October 1993 in NMFS statistical areas 542 (n=4) and 620 (n=5) (Table 1, Fig. 1). One hundred-fifty fish were collected from June through August in 1994 in NMFS statistical areas 541 (n=57), 542 (n=49), and 543 (n=44). Most (130) of these fish were in prespawning condition, i.e., contained no postovulatory follicles, and 20 had spawned at least one batch of eggs. Because the fish were collected during the NMFS Aleutian survey, which systematically moves from east to west along the Aleutian archipelago, all specimens in area 541 (Eastern Aleutian Islands) were considered prespawning fish Spawning commenced in late July in area 542 and by the middle of August all fish collected showed signs of spawning.

Location of tissue samples in ovaries

The effect of ovary lobe location or position within the ovary was not significant for either average egg size (P=0.07, 0.43, respectively) or mean number of eggs per gram of ovary tissue (P=0.07, 0.53, respectively). Maturity stage of ovary had a significant effect on both eggs per gram (P<0.0001) and average egg size (P<0.0001).

Separation of oil-droplet–stage oocytes (stage 4) from more advanced oocytes

There was no significant difference in mean egg size for stage-4 oocytes in pre- and postspawning fish (P=0.59)(Fig. 3B). We determined that all oocytes smaller than 525 μm that were measured were stage-4 oocytes (Fig. 3A). The proportion of stage-4 oocytes less than 525 μm ($\bar{p}$) was 0.755 based on samples of postspawning fish in 1993, with g_i = 1592 (the number of stage-4 oocytes that measured smaller than 525 μm), and m_i = 2110 (the total number of stage-4 oocytes measured). This proportion was treated as a constant when estimating the number of oocytes in stage 5 and larger.

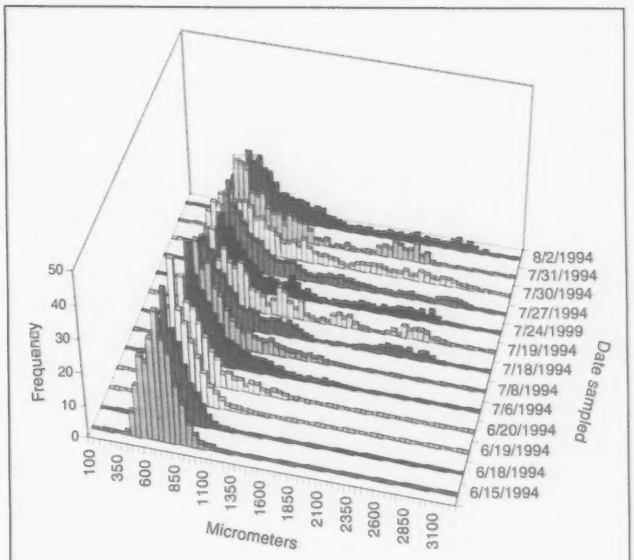

Figure 4

Atka mackerel (*Pleurogrammus monopterygius)* oocyte-size frequency distribution summarized by date for 1994. Oocyte-size frequencies were averaged per day.

Determinate versus indeterminate spawning

With the exception of hydrated eggs, Atka mackerel are characterized by a continuous oocyte-size distribution much like that of an indeterminate spawner (Fig. 4). Atka mackerel ovaries contain several stages of developing oocytes throughout the spawning season.

However, the length-fecundity relationship for the total number of oocytes decreased after the fish had spawned their first batch (Fig. 5A) and there was a significant difference in intercept and slope (P=0.01 and 0.001, respectively). When the length-fecundity relationship for oocytes in stage 5+ was examined, the potential fecundity also decreased after spawning (Fig. 5B), with a significant difference in intercept and slope (P=0.003 and P=0.009, respectively). The numbers of stage-4 oocytes did not appear to differ substantially before and after spawning for fish of comparable size (Fig. 5C) although the slope of the length-fecundity relationship differed significantly (P=0.012). Furthermore, there was no reduction in the number of stage-4 oocytes at comparable fish lengths for the nine spent fish collected late in the spawning season (October) versus prespawning and spawning fish collected in June–August.

Oocyte atresia

Incidence of oocyte atresia in prespawning and spawning fish was found to be low. Only 15 of the 150 ovaries examined showed any signs of atresia. Of these15 ovaries, high occurrence of atresia (more than 10% of oocytes affected) was found in 3, and low occurrence of atresia (less than 10% of oocytes affected) was found in 12. Therefore, atresia in ovaries of pre- and postspawning fish was not quantified further.

Atresia was found to be present in all of the nine ovaries of postspawning fish examined in the study and the number of atretic oocytes corresponded roughly with the number of ooccytes spawned in a batch (batch size). This finding indicates that Atka mackerel may use atresia to regulate reproductive output at the end of the spawning season.

Estimates of annual fecundity and batch fecundity

Length-fecundity parameters (a and b) for predicted fecundities for scenario 1 (oocytes ≥stage 4) and scenario 2 (oocytes ≥stage 5), as well as estimates of batch fecundity and atretic eggs are shown in Table 2 with their respective standard errors. Predicted potential fecundity for both scenarios is shown in Figure 6A.

The length-fecundity relationship for oocytes at stage 5+ is the most realistic because it appears that most stage-4 oocytes will not be spawned in the current season. Predicted potential and realized fecundity for stage 5+ oocytes are illustrated in Figure 6A with their respective confidence intervals. Because the estimates of potential fecundity were treated as data in the length-fecundity regressions, the variance estimates and confidence intervals are conservative. Data and model fit for the relationship of batch fecundity to length is shown in Figure 6B, and the data and model fit for the number of

Table 2

Atka mackerel length-fecundity coefficients derived with the equation $F = a\,L^b$, where F = fecundity and L = fish fork length (cm). SE= standard error of the mean. CI = 95% confidence intervals for predicted values of the mean. n = number of fish in sample.

	Constants					
	a		b			
Fecundity type	Estimate	SE	Estimate	SE	n	Estimate for 40-cm female (±95% CI)
Potential fecundity$_{total}$	0.5601	0.5067	3.0865	0.2409	130	49,321±2535
Potential fecundity$_{stage5+}$	2.3716	2.0913	2.6517	0.2352	130	41,994 ±2061
Number of atretic eggs	0.0013	0.0083	4.3303	1.6502	9	11,329 ±8802
Batch fecundity	0.1157	0.1923	2.9726	0.4536	33	6689 ±577
Realized fecundity$_{total}$						37,992±7873
Realized fecundity$_{stage5+}$						30,664 ±7730
	Mean value		SD			
Batch number potential$_{stage5+}$	6.13		1.35		33	6.13 ±2.64
Batch number potential$_{total}$	7.04		1.52		33	7.04 ±2.98
Batch number realized$_{stage5+}$	4.64		1.03		33	4.64 ±2.01
Batch number realized$_{total}$	5.6		1.15		33	5.33 ±2.25

atretric eggs in the ovary by length category is shown in Figure 6C. Average number of batches corresponding to potential and realized fecundity are shown in Figure 6D.

The average fork length for females during the 1994 NMFS survey was 40 cm (Lowe and Fritz, 1994). Potential fecundity (stage 5+) was estimated to be 41,994 eggs, and realized annual fecundity was estimated to be 30,664 eggs for a 40-cm female (Table 2). Batch fecundity for a 40-cm female was estimated to be 6689 eggs and the number of batches spawned showed no statistically significant relationship with length for both potential (P=0.35) and realized (P=0.75) fecundity (Fig. 6D). The estimated number of batches produced annually per female was calculated by using the grand mean and standard deviation for all specimens combined. The average number of batches of eggs for potential and realized fecundity was estimated at 6.1 and 4.5 batches per year, respectively, with corresponding 95% confidence intervals of ±2.64 and ±2.21 batches. This result would indicate that the average female has the potential to spawn about 6 batches, but may reabsorb 1–2 batches of eggs at the end of the season.

Discussion

The reproductive strategy of Atka mackerel and other hexagrammids has been characterized by low fecundity and large eggs, high parental care, and by larvae hatched at an advanced stage of development (Gorbunova, 1962). Potential fecundity for an average female Atka mackerel of 40 cm was 41,994 eggs for oocytes at stage 5+ and is higher than the estimates for Kamchatkan waters by Gorbunova (1962), who gave a range between 5000 and 31,000 eggs for a 52-cm female. Zolotov (1993) estimated potential fecundity to be 38,700 eggs (vitelline oocytes plus hydrated oocytes in first batch) off Kamchatka, which is also slightly lower than our estimate. Our batch fecundity estimate of 6689 eggs for an average female of 40 cm is similar to Zolotov's (1993) estimate of 6930 for a fish of the same size.

Atka mackerel are characterized by a continuous size distribution of oocytes much like that of indeterminate spawners. However, Atka mackerel have a distinct spawning season (July–October) during which they spawn batches containing a large number of eggs (Zolotov, 1993; McDermott and Lowe, 1997). This spawning pattern differs from that of typical indeterminate spawners that spawn a small number of eggs (in relation to the total number present) almost continuously for many months, as characterized by the northern anchovy (*Engraulis mordax*) (Hunter et al., 1985). Atka mackerel seem to lie somewhere in the middle of determinate versus indeterminate spawning fish. It appears that there is a potential to develop and spawn up to seven batches if all stage-4 oocytes are developed and spawned. Most of the stage-4 oocytes still remaining in the ovary during the spawning phase probably constitute the pool of oocytes to be spawned in the next season. However, those oocytes could be a reserve to be developed and spawned in highly productive years (i.e., during favorable spawning conditions). Estimates of fecundity based on oocytes at stage 5+ may be conservative if some of the stage-4 oocytes are

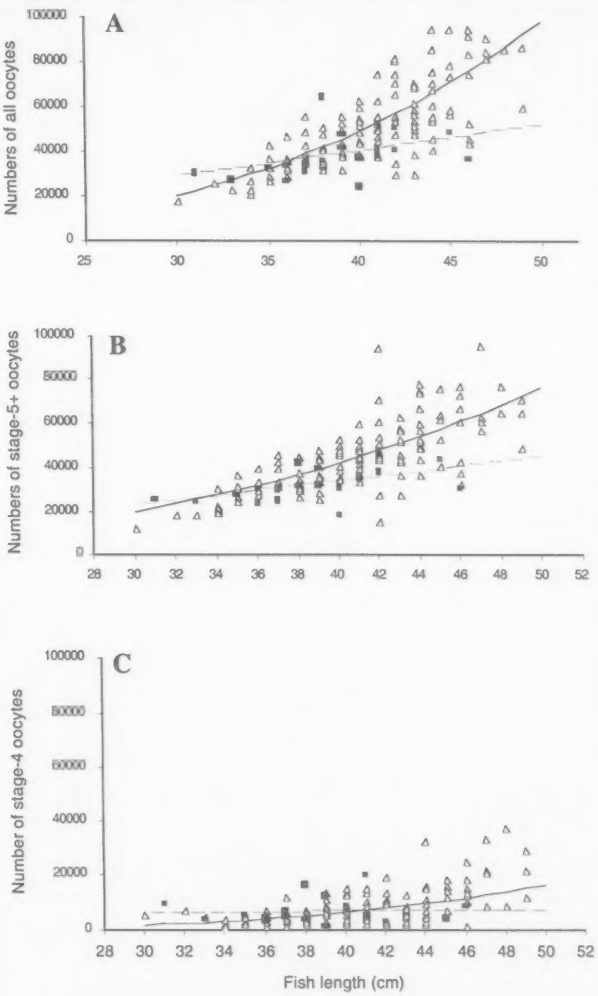

Figure 5

Fecundity of Atka mackerel (*Pleurogrammus monopterygius)* at the prespawning (clear triangles) and spawning (solid squares) phase for (**A**) total number of oocytes at stage 4 and above, (**B**) oocytes at stage 5+, and (**C**) for oocytes at stage 4 only. Regression lines for prespawning and spawning fish are indicated by solid and dashed lines, respectively.

developed and spawned late in the spawning season. However, knowledge of batch size, length of spawning season, and the spawning interval between batches (1–2 weeks) (Gorbunova, 1962; Zolotov, 1993; McDermott and Lowe, 1997), gives us confidence that our estimate of fecundity is realistic. Given that there are 14 days between batches, a 75-day incubation period (Lowe et al., 2003; McDermott, 2003), and that 4.6 batches are spawned annually, the spawning season would be 120 days, which is similar to that observed in the present study.

Conclusions

Prespawning Atka mackerel did not show much atresia during egg development; however high levels of atresia became apparent when ovaries of postspawning fish

were examined. Examination of ovaries of prespawning females alone would lead to the assumption that the potential fecundity is close to the realized fecundity. Atresia in postspawning Atka mackerel has been described in earlier studies (Gorbunova, 1962; Zolotov, 1993), where 400–500 atretic eggs per ovary and the prolonged presence of atretic eggs in the ovaries before reabsorption have been reported. However, this is the first study where atresia from recently spent ovaries has been included in the fecundity analysis in a quantitative manner. When recently spent ovaries were examined, it appeared that atresia had a major effect on potential fecundity and that an average of 1–2 batches were reabsorbed at the end of the spawning period in the ovaries examined. It should be noted that specimens with ovaries in the prespawning phase and specimens with recently spent ovaries were collected in different years. Atresia is likely to be related to feeding ecology, availability of appropriate substrate and environmental conditions for spawning, and could potentially change from year to year. Interannual variability of atresia should be examined in the future.

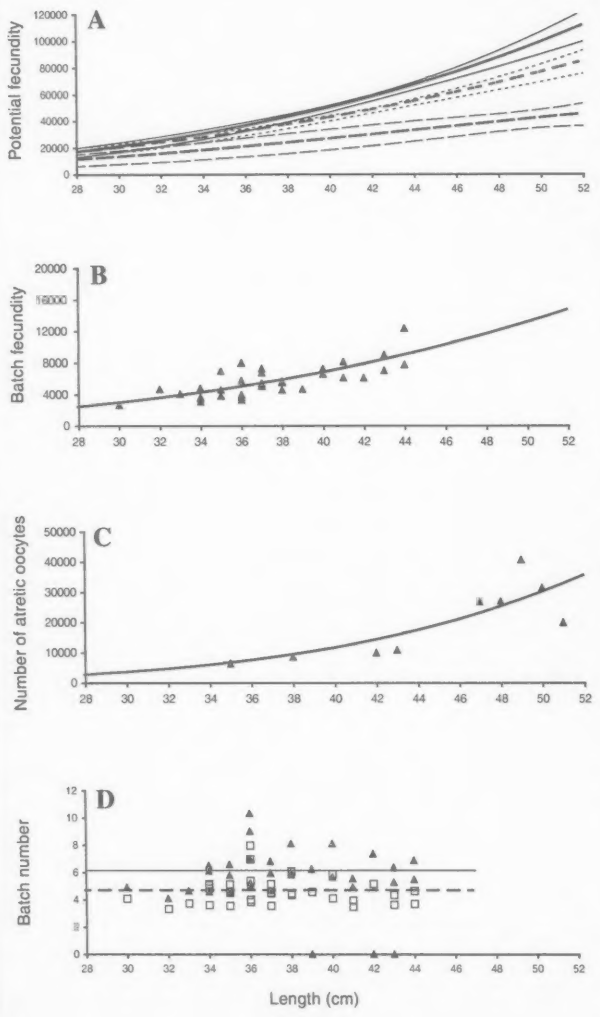

Figure 6

(**A**) Model fit and 95% confidence intervals for potential fecundity of Atka mackerel (*Pleurogrammus monopterygius*) at length for total number of oocytes (solid lines), stage-5+ oocytes (short dashed lines), and realized fecundity (long dashed lines). (**B**) Data and model fit (line) for Atka mackerel batch fecundity by length. (**C**) Data and model fit for number of atretic oocytes in spent ovaries of Atka mackerel by length. (**D**) Number of batches spawned by length for potential fecundity (solid triangles) and realized fecundity (open squares) and the estimated population means (solid line for potential fecundity and dashed line for realized fecundity) for Atka mackerel.

Acknowledgments

We thank G. Thompson and J. Ianelli for their statistical advice and F. Morado for his advice and assistance with histological work. We also thank all the observers and scientists who collected specimens and the commercial fishing industry for providing sampling platforms. G. Stauffer, B. Miller, A. Hollowed, S. Lowe, and S. Hinckley helped greatly by critically reviewing drafts of this paper. This research was supported by the Joint Institute for the Study of the Atmosphere and Ocean (JISAO) under NOAA Cooperative Agreement no. NA67RJ0155 (contribution no. 986).

Literature cited

Gorbunova, N. N.
1962. Spawning and development of greenlings (family Hexagrammidae). *In* Greenlings: taxonomy, biology, interoceanic transplantation (T. S. Rass, ed.), p. 1–103. Tr. Inst. Okeanol., Akad. Nauk. SSSR 59:118–182. In Russian (translated by Isr. Program. Sci. Trans., 1970). [Available from Natl. Tech. Inf. Serv., Springfield, VA, as TT 69-55097 S.]

Harðardóttir, K., O. S. Kjesbu, and G. Marteinsdottir.
2001. Atresia in Icelandic cod (*Gadus morhua* L.) prior to and during spawning. Report of the working group on modern approaches to assess maturity and fecundity of warm- and cold-water fish and squids (O. S. Kjesbu, J. R. Hunter, and P. R. Withames, eds.), 140 p. Institute of Marine Research, Bergen, Norway.

Hunter, J. R., N. C. H. Lo, and R. J. H. Leong.
1985. Batch fecundity in multiple spawning fishes. *In* An egg production method for estimating spawning biomass of pelagic fish: application to the northern anchovy, *Engraulis mordax* (R. Lasker, ed.), p. 67–77. U.S. Dep. Commer., NOAA Tech. Rep. NMFS 36.

Hunter, J. R., and B. J. Macewicz.
1985. Rates of atresia in the ovary of captive and wild northern anchovy, *Engraulis mordax*. Fish. Bull. 83:119–136.
2001. Improving the accuracy and precision of reproductive information used in fisheries. Report of the working group on modern approaches to assess maturity and fecundity of warm-and cold-water fish and squids (O. S. Kjesbu, J. R. Hunter, and P. R. Withames, eds.), 140 p. Institute of Marine Research, Bergen, Norway.

Kjesbu, O. S., J. Klungsøyr, H. Kryvi, P. R. Whitthames, and M. Greer Walker.
1991. Fecundity, atresia, and egg size of captive Atlantic cod (*Gadus morhua*) in relation to proximate body composition. Can. J. Fish. Aquat. Sci. 48: 2333–2343.

Kurita, Y., S. Meier, and O. S. Kjesbu.
2003. Oocyte growth and fecundity regulation by atresia of Atlantic herring (*Clupea harengus*) in relation to body condition throughout the maturation cycle. J. Sea Res. 49:203–219.

Lowe, S. A., and L. Fritz.
1994. Atka mackerel. *In* Stock assessment and evaluation report for the groundfish resources of the Bering Sea/Aleutian Islands regions, 11-1–11-43. North Pacific Fisheries Management Council, P.O. Box 103136, Anchorage, Alaska, 99510.

Lowe, S., J. Ianelli, H. Zenger, and R. Lauth.
2003. Stock assessment of Aleutian Islands Atka mackerel. *In* Stock assessment and evaluation report for the groundfish resources of the Bering Sea/Aleutian Islands regions, p. 711–776. North Pacific Fisheries Management Council, P.O. Box 103136, Anchorage, Alaska 99510.

Lowe, S., J. Ianelli, H. Zenger, and R. Reuter.
2002. Atka mackerel. *In* Stock assessment and evaluation report for the groundfish resources of the Bering Sea/Aleutian Islands regions, p. 609–667. North Pacific Fisheries Management Council, P.O. Box 103136, Anchorage, Alaska 99510.

Ma, Y., O. S Kjesbu, and T. Jørgensen.
1998. Effects of ration on the maturation and fecundity in captive Atlantic herring, (*Clupea harengus*). Can. J. Fish. Aquat. Sci. 55:900–908.

McDermott, S. F.
2003. Estimating abundance of a patchily distributed fish, Atka mackerel, *Pleurogrammus monopterygius*. Ph.D. diss., 149 p. Univ. Washington, Seattle, WA.

McDermott, S. F., and S. A. Lowe.
1997. The reproductive cycle and sexual maturity of Atka mackerel, *Pleurogrammus monopterygius* in Alaska waters. Fish. Bull. 95:321–333.

Nichol D. G., and E. I. Acuna.
2001. Annual batch fecundities of yellowfin sole, *Limanda aspera*, in the eastern Bering Sea. Fish. Bull. 99:108–122.

Nichol, D. G., and D. A. Somerton.
2002. Diurnal vertical migration of the Atka mackerel *Pleurogrammus monopterygius* as shown by archival tags. Mar. Ecol. Prog. Ser. 239:193–207.

Venables, W. N., and B. D. Ripley.
2002. Modern applied statistics with S-plus, 495 p. Springer-Verlag Inc., New York, NY.

Zolotov, O. G.
1993. Notes on the reproductive biology of *Pleurogrammus monopterygius* in Kamchatkan waters. J. Ichthyol. 33:(4):25–37.

Zolotov, O. G., and A. M. Tokranov.
1989. Reproductive ecology of hexagrammidae and cottidae in the Pacific waters of Kamchatka. J. Ichthyol. 3:430–438.

Modification of the biological intercept model to account for ontogenetic effects in laboratory-reared delta smelt (*Hypomesus transpacificus*)*

James A. Hobbs (contact author) [1,2]
William A. Bennett[1,2]
Jessica E. Burton[1]
Bradd Baskerville-Bridges[3]

Email address for J. A. Hobbs: jahobbs@ucdavis.edu

[1] Bodega Marine Laboratory
2099 Westside Road
Bodega Bay, California 94923-0247

[2] John Muir Institute for the Environment
University of California, Davis
One Shields Ave.
Davis, California 95616

[3] Department of Animal Sciences
University of California, Davis
One Shields Ave.
Davis, California 95616

Abstract—We investigated age, growth, and ontogenetic effects on the proportionality of otolith size to fish size in laboratory-reared delta smelt (*Hypomesus transpacificus*) from the San Francisco Bay estuary. Delta smelt larvae were reared from hatching in laboratory mesocosms for 100 days. Otolith increments from known-age fish were enumerated to validate that growth increments were deposited daily and to validate the age of fish at first ring formation. Delta smelt were found to lay down daily ring increments; however, the first increment did not form until six days after hatching. The relationship between otolith size and fish size was not biased by age or growth-rate effects but did exhibit an interruption in linear growth owing to an ontogenetic shift at the postflexon stage. To back-calculate the size-at-age of individual fish, we modified the biological intercept (BI) model to account for ontogenetic changes in the otolith-size–fish-size relationship and compared the results to the time-varying growth model, as well as the modified Fry model. We found the modified BI model estimated more accurately the size-at-age from hatching to 100 days after hatching. Before back-calculating size-at-age with existing models, we recommend a critical evaluation of the effects that age, growth, and ontogeny can have on the otolith-size–fish-size relationship.

Manuscript submitted 24 November 2004 to the Scientific Editor's Office.

Manuscript approved for publication 15 March 2006 by the Scientific Editor.

Fish. Bull. 105:30–38 (2007).

Otolith-based back-calculation models of size-at-age rely on the assumption that the relationship between otolith and somatic growth is a constant proportion. This has often been examined by simply correlating otolith size with fish size for different aged fish. However, correlations of size among similarly growing body parts over time may not equate to proportional growth among these body parts (Cock, 1966). A comprehensive evaluation of the assumption of proportionality requires examining whether somatic variability is independent of age in the otolith-size–fish-size (OS-FS) relationship (Hare and Cowen, 1995). This requires an assessment of the residual variability between otolith size and fish size-on-age to remove the potential influence of age that can bias the OS-FS relationship (Hare and Cowen, 1995). Furthermore, the "growth effect," where slow-growing fish have larger otoliths than fast-growing fish for similar-size fish, and the "ontogenetic effect," where shifts in the OS-FS relationship occur, also need to be addressed before back-calculations. None of these proposed factors necessarily operate in isolation and can occur simultaneously in multiple life stages (Hare and Cowen, 1995; Vigliola et al., 2000; Morita and Matsuishi, 2001). Therefore, before choosing an appropriate model for back-calculating size-at-age, it is necessary to identify the potential mechanisms responsible for variability in the OS-FS relationship.

Back-calculation models differ primarily in their ability to compensate for potential deviations away from a constant proportion between otolith size and fish size. The biological intercept (BI) model (for details on the model see Campana [1990]) compensates for growth effects by incorporating estimates of fish size and otolith size at the origin of the OS-FS proportionality. The time-varying growth (TVG) model adjusts the contribution of small and large increments with regard to body size (see Sirois et al. [1998] for full details), whereas the modified Fry (MF) model directly incorporates the allometric shape of the

* Contribution number 2313 from the Bodega Marine Laboratory, Bodega Bay, California 94923-0247.

relationship into the back-calculation model (for details see Vigliola et al. [2000]). Therefore, although these models can compensate for growth effects when age and ontogenetic effects are linked, they cannot provide accurate estimates when ontogenetic influences act independently of effects caused by growth and age. One means of compensating for ontogenetic shifts in the OS-FS relationship is to use the BI model separately for specific life stages. This model can be useful for providing accurate back-calculations across stage-specific transitions, such as metamorphosis (Jenkins, 1987; Campana, 1990; Otterlei et al., 2002).

We first assess whether the number of ring increments in otoliths accurately reflects absolute age in larvae and juvenile cultured (known-age) delta smelt (*Hypomesus transpacificus*). Second, we evaluate the degree to which age-independent variability occurs in the OS-FS relationship, as well as whether growth rate and ontogenetic effects modify the proportionality of otolith growth to fish growth. Finally, we modify the BI model to account for ontogenetic stage-specific transitions of the OS-FS relationship and compare these results with those from the TVG and MF models to a to assess the performance of our model for size-at-age back-calculations for delta smelt.

The delta smelt is a small osmerid fish endemic to the San Francisco Bay estuary (McAllister, 1963; Moyle, 2002). Historically one of the most common fishes, it was listed as "threatened" under the Federal and State Endangered Species Acts in 1993 (Moyle et al., 1992; USFWS, 1995; Sweetnam, 1999). Recent precipitous declines in the populations have led to a major investigation regarding the cause of such declines. A few of the potential sources include contaminants and exotic species (Bennett and Moyle, 1996; Bennett et al., 2005), both of which may result in reduced growth rates and poor recruitment. Examination of these hypotheses requires accurate estimates of back-calculated size-at-age for a growth-history assessment of the delta smelt (Fujiwara et al., 2005).

Materials and methods

Larval rearing and otolith examination

All known-age delta smelt larvae were reared at the University of California Davis's delta smelt culturing facility located at the U.S. Bureau of Reclamation John F. Skinner fish facility in Byron, California. Newly hatched larvae were raised in 75-L black tanks at 20 larvae/L. Each tank maintained a flow-through system with filtered water from the Sacramento-San Joaquin delta. Ambient water temperatures during the rearing period ranged from 17° to 20°C and salinities from 0 to 1 ppt. The tanks were held in refrigerated cargo containers under 40-W florescent lights for a 12 h light:12 h dark cycle. Larvae up to 30 days after hatching (dah) were fed *Isochyrisis* spp. enriched rotifers. *Nanochloropsis* spp. (green micro-algae) paste was added to create "green" conditions necessary for larval feeding (Baskerville-Bridges[1]; Baskerville-Bridges et al., 2004). Larvae more than 30 dah were fed *Artemia* sp. (brine shrimp) nauplii enriched in Super Selco® (Inve Aquaculture NV, Belgium). Ten larvae up to 10 dah were sacrificed daily with an overdose of MS222 (FINQUEL MS-222 Argent Chemical Labratories, Inc., Redmond, WA) and fixed in 95% ethanol. Fish from 10 dah to 60 dah were sampled every other day and fish from 60 dah to 100 dah were sampled every 5–7 days (Table 1). Samples were collected from bins representing two spawning pairs of fish.

Sagittal otoliths were dissected from larvae and juveniles with fine forceps and dissecting needles. For larvae, care was taken to photograph and analyze only the sagittal otoliths, which were identified by orientation to the notochord. In delta smelt, the sagittal otoliths are located near the notochord, whereas lapilli are located distally and posteriorly in relation to the sagittae. Otoliths were mounted in Crystal Bond thermoplastic glue (Crystalbond™ 509, Ted Pella Inc. Redding, CA) with the sulcus side down. Otoliths from fish 92 dah and older were sanded with 1200-grit wet and dry sandpaper and polished with 0.3-micron alumina and a polishing cloth. Sagittal otolith radii were measured with a light microscope at 400–100× magnification. All otoliths were analyzed with Image Pro 4.0® (Media Cybernetics, Silver Spring, MD). The first increment was determined as the first ring after the nucleus core. Otolith radius was measured with the aid of image analysis, from the core to the dorsal edge, because this direction was consistently the clearest trajectory. All references to otolith size are radial measurements from the core to the dorsal edge. Sagittae were read by two readers without knowledge of fish age. Two readings were made by each reader and reread if age differences exceeded 10%. If age estimates continued to vary, the otolith was removed from the data set.

Statistical analyses

To determine if increment formation occurred on a daily basis, a Student's *t*-test was used to determine the statistical significance of the slope from a linear regression of increment counts on known age. Under the null hypothesis, the slope of increment counts on known age was equal to one. We rejected the null hypothesis if the slope significantly differed from one.

Statistical analyses, similar to those of Hare and Cowen (1995), were used to evaluate age-independent variability in the OS-FS relationship, as well as growth rate and ontogenetic effects. First, regression models (linear and polynomial) of standard length and otolith

[1] Baskerville-Bridges, B. 2001. Progress and development of delta smelt culture: year-end report 2000. Interagency Ecological Program news letter 14:24–29. Department of Water Resources 827 7th St., Room 301, Sacramento, CA 95814.

Table 1

Summary of sample size, number of increment at designated days after hatching, and mean size-at-age.

Date	No. of Larvae sampled	Days after hatching	Mean no. of increments counted	Difference between days after hatching and mean no. of increments counted	Mean standard length (mm)
March 24	10	0	0	0	5.2
March 25	10	1	0	1	5.2
March 29	10	5	0.4	4.6	5.8
March 31	10	7	1.4	5.6	6.1
April 3	10	10	4.2	5.8	6.6
April 7	5	14	7.8	6.2	7.3
April 11	5	18	12.4	5.6	7.4
April 19	5	26	20	6	8.7
April 25	5	32	25.2	6.8	9.6
May 1	5	38	31.8	6.2	9.9
May 11	5	48	42.8	5.2	12.2
May 21	5	58	52.4	5.6	14.6
May 28	5	65	59.8	5.2	16.5
May 31	5	68	61	7	16.2
June 4	5	72	65.8	6.2	17.1
June 8	5	76	69.8	6.2	17.2
June 12	5	80	73.8	6.2	19.4
June 15	5	84	78.2	5.8	19.6
June 24	5	92	84.4	7.6	20.9
July 2	5	100	94	6	23.5

radius were regressed on age and otolith radius and age on standard length. Second, Pearson correlation coefficients of the otolith radius and standard length-on-age residuals were quantified to estimate the amount of age-independent variability. If no age-independent variability existed in the OS-FS relationship, the residuals of otolith radius-on-age and standard length-on-age should be perfectly correlated. The unexplained variability in the correlation between the residuals of the two models can be considered the degree to which age-independent variability can influence the OS-FS relationship. To account for growth rate effects, Pearson correlation coefficients were quantified for the residuals of age-on-length and otolith radius-on-length. Moreover, significant growth effects were detected with a positive correlation. Lastly, the slopes of the OS-FS relationship for each life stage were compared to account for ontogenetic effects. If otolith growth and fish somatic growth are in constant proportion throughout the life stages in question, the slopes between otolith-fish size should not be significantly different (Cock, 1966). The slope of otolith size to fish size was calculated with an allometric model of the form $y = ax^b$, where log transformation results in the formula $\log(y) = \log(a) + b \times \log(x)$ and the parameter b is equal to the slope (Gould, 1966).

Back-calculations

Size-at-age was back-calculated by using three models (Table 2). First, we examined the TVG model. This model accounts for variability in the underlying assumption of constant proportionality of otolith size to fish size by adjusting the contribution of increment widths by a growth factor. Second, we applied the MF model, which accounts for a nonlinear relationship between otolith size and fish size by directly estimating the shape parameters with a simple allometric model. Finally, a modified stage-specific form of the BI model was applied. Although this model depends on a constant proportion between otolith and fish size, we mediated this effect by applying the model to each specific life stage. To account for our stage-specific differences in the OS-FS relationship, we back-calculated size-at-age for the larval stage (5.4 mm SL to 12 mm SL) and juvenile stage (>12 mm SL) with 12 mm SL as the biological intercept. The mean back-calculated size-at-age trajectory was compared to measured standard lengths at time of sampling. We evaluated the fit of each model to the standard length-at-sampling data by comparing the r^2 values, as well as the minimum and maximum percent deviation of the mean back-calculated size-at-age value from the mean length-at-sampling.

Table 2

Summary of the three back-calculation models examined in this study: the time-varying growth (TVG) model (Sirois et al. 1998), modified Fry (MF) model (Vigliola et al. 2000), and the biological intercept (BI) model (Campana 1990). L=standard length; R=otolith radius; L_{0p}=standard length-at-biological intercept; L_i=standard length-at-age i; L_{cpt}=standard length-at-capture; R_{0p}=otolith radius-at-biological intercept; R_i=otolith radius-at-age i; R_{cpt}=otolith radius-at-capture; W=mean otolith increment width during each life stage; W_i=otolith increment width at i; G_e=growth effect; and a=allometric shape parameter.

Back-calculation models	Equation	Reference
Time-varying growth (TVG)	$L_i = L_{0p} + \int(W_i + G_e(W_i - W))(L_{cpt} - L_{0p})(R_{cpt} - R_{0p})^{-1}$	Sirois et al. (1998)
Modified Fry (MF)	$L_i = a + \exp(ln(L_{0p} - a) + ln(L_{cpt} - a) - ln(L_{0p} - a))$ $(ln(R_i) - ln(R_{0p}))(ln(R_{cpt}) - ln(R_{0p}))^{-1})$	Vigliola et al. (2000)
Biological intercept (BI)	$L_i = L_{cpt} + (R_i - R_{cpt})(L_{cpt} - L_{0p})(R_{cpt} - R_{0p})^{-1}$	Campana (1990)

Results

Validation of daily otolith increment formation

The relationship between the number of increments and days after hatching of delta smelt larvae are shown in (Table 1; Fig. 1). The slope of the regression of increment count on known-age was not significantly different from one and thus indicated that increment formation occurred daily. However, the intercept was significantly different from zero ($P<0.001$), indicating that the first increment was not laid at hatching, rather that ring formation began 6 dah. This observation was confirmed by examination of larvae sampled at one and five dah (Table 1).

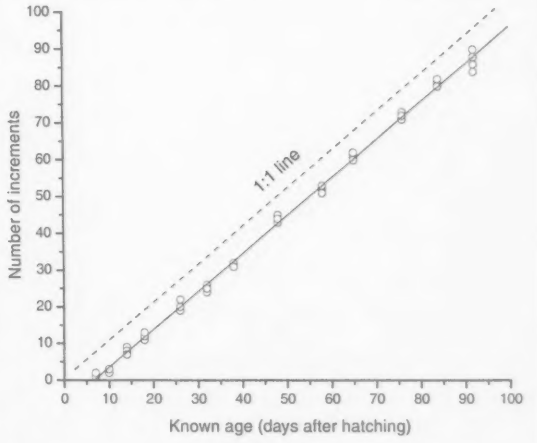

Figure 1

Relationship between the number of increments and the known age for delta smelt (*Hypomesus transpacificicus*). Dotted line is the 1:1 ratio line. Solid line is the linear regression line.

Mean somatic and otolith growth

All somatic otolith-growth relationships were best described by life-stage-specific linear regression models, where larval (0–20 dah, 5–12 mm SL) and juvenile (>20 dah, >12 mm SL) life stages were considered separately. Calculated Akaike information criterion (Sokal and Rohlf, 1973) for the linear models were lower than polynomial models ranging from the 2nd to 9th orders. Somatic growth showed variations in growth over time: fast growth occurred from hatching to 40 dah, followed by a period of slowed growth from 40 dah up to 80 dah. After 80 dah, fish experienced a period of rapid somatic growth associated with the juvenile stage (Fig. 2, A and C). Otolith growth showed a different trend. Otolith growth was slow from hatching to 40 dah, which then increased exponentially from 40 dah to 100 dah, indicating that the relationship between otolith growth and fish growth changes abruptly around 40 dah with the completion of caudal flexing (Fig. 2B). Finally, the relationship between otolith size and fish size was best described by a stage-specific linear regression (Fig. 2D), which accounted for the lack of constant linear proportionality of otolith growth to fish growth. It is important to note that some patterns in the residuals were apparent in the early larval stages. However, we do not consider these slight deviations to have a significant effect on further residual analyses.

Growth and ontogenetic effects and size back-calculations

Correlations of age-independent effects and growth-rate effects are shown in Figure 3, A and B. The strong correlation between standard length-on-age residuals and otolith radius-on-age residuals may indicate that otolith size is proportional to fish size. The age-independent variability in the OS-FS relationship was accounted for by examining the unexplained variability in the residual analysis of otolith and fish size-on-age. Only 11% of the unexplained variability could be associated with age-independent effects. The Pearson correlation coefficient for the residual of standard length-on-age and otolith

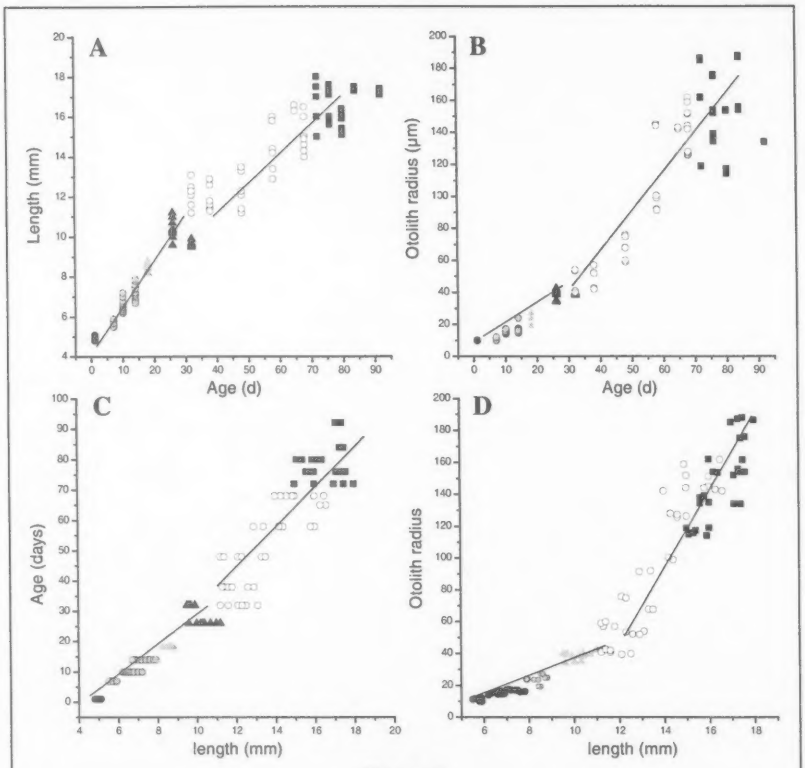

Figure 2

(**A**) Observed standard length of delta smelt (*Hypomesus transpacificicus*) plotted against ages with respective linear regression line; (**B**) observed otolith radius plotted against age sampled with respective linear regression line; (**C**) known-age plotted against observed standard length with linear regression line; (**D**) observed otolith radius plotted against observed standard length with linear regression line. Ontogenetic stages are represented by different symbols: black circles represent yolksac-stage larvae (●), gray circles represent feeding larvae (◍), gray triangles represent finfold-stage larvae (▲), black triangles represent flexion-stage larvae (▲), open circles represent postflexion-stage larvae (○) and black squares represent juvenile-stage fish (■).

Table 3

Comparison of the allometric slope (b) values (log (*otolith radius*) = b×log (*standard length*). P values are from Student's t-statistic.

Life stage	I	II	III	IV	V	VI
I	—					
II	<0.001	—				
III	<0.001	ns	—			
IV	ns	<0.01	<0.001	—		
V	<0.001	ns	ns	<0.001	—	
VI	<0.001	ns	ns	<0.001	ns	—

radius-on-age was 0.885 (P=0.001) (Fig. 3A). Comparison of the residuals of otolith radius-on-length and age-on-length demonstrated that there was no significant growth rate effect on the OS-FS relationship (Fig. 3B). The Pearson correlation coefficient was 0.068 (P=0.244).

A simple log transformation of an allometic model demonstrated ontogenetic differences in the slopes of the OS-FS relationship (Fig. 4). Slopes were significantly reduced for the newly hatched yolksac stage (I) and the larval flexion stage (IV). However, stage-I larvae were the same age; therefore variability due to ontogeny may be difficult to evaluate. Variability in fish length for stage-IV larvae may reflect subtle ontogenetic differences in caudal fin flexing and thus variation in the OS-FS relationship (Table 3).

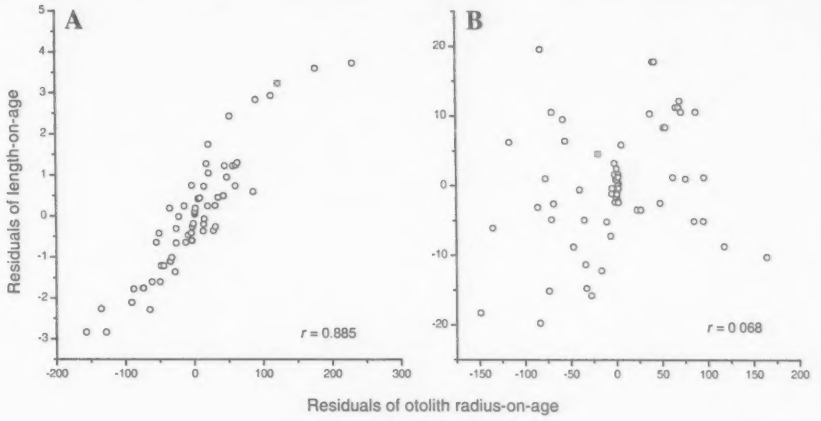

Figure 3

Correlation analysis of residuals evaluating age-independent variability and growth-rate effects in the relationship of otolith size to fish size for young delta smelt (*Hypomesus transpacificus*): (**A**) fish standard length versus otolith radius residuals, (**B**) age versus standard versus otolith radius residuals. Pearson (r) correlation values are shown on graph.

Comparison of the TVG, BI, and MF models

To account for ontogenetic change in the OS-FS relationship, we applied the BI model separately for preflexon and postflexon larvae. Mean back-calculated size-at-age for the TVG model varied from −10.3% to +0.93% of the observed mean-length-at-age and consistently underestimated size from 20 dah to 100 dah. The stage-specific BI model varied from −3.5% to +6.4%, centering closely around zero, and the MF model varied from +2.4% to +13.1% and consistently overestimated size from 15 dah to 100 dah (Table 4; Fig. 5). These results indicate that the ontogenetic stage-specific BI model more accurately describes the observed mean size-at-age trajectories for delta smelt. However, the observed size-at-age was variable from 50 dah to 100 dah, resulting in statistically reasonable fits for all the models, with r^2 values ranging from 0.994 to 0.935 (Table 4).

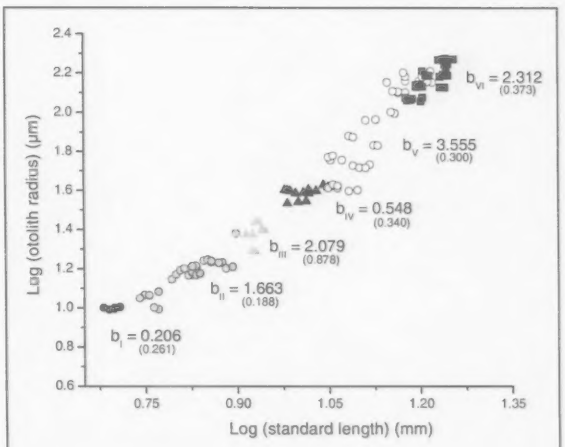
Log (otolith radius) (µm)
Log (standard length) (mm)
b_VI = 2.312 (0.373)
b_V = 3.555 (0.300)
b_IV = 0.548 (0.340)
b_III = 2.079 (0.878)
b_II = 1.663 (0.188)
b_I = 0.206 (0.261)

Figure 4

Simple allometric plot of otolith radius and standard length. Slopes are given from the equation log(*otolith radius*) = log(x) +*b*×log(*standard length*) for each ontogenetic stage, where *b* is the slope and the standard error is in parentheses. Ontogenetic stages are represented as in Figure 2.

Discussion

Validation of daily otolith increment formation

Accurate size-at-age estimates are important for measuring subtle differences in growth during the early life history of fishes because they are used to examine factors affecting recruitment success for many species (Rice et al., 1987; Sirois and Dodson, 2000). However, variability in age estimates can occur. Much of this variability in age estimates depends largely on when the first increment is estimated to have formed (Campana and Neilson, 1985; Campana, 2001). In this study, increment formation in laboratory-reared delta smelt began six dah, about the time of first feeding. Numerous studies of other smelt species have also revealed that

daily increments form at first feeding (Sepulveda, 1994; Hirose and Kawaguchi, 2001). However, for some species of smelt, increment formation does occur at hatching (Ohama, 1990). Otterlei et al. (2002) demonstrated that temperature could further increase age variability by altering the timing of the first increment depending upon when, in the season, a fish was born. Delta smelt spawn from late February through June, potentially resulting in cohorts experiencing temperature differences of more than 10°C at birth (Moyle, 2002). This temperature difference could result in up to a two-fold change in the embryonic development and lead to a 2–3 day difference in the timing of first feeding for delta smelt (first author, unpubl. data).

Table 4

Comparison of growth curves generated from otolith size-at-age data. r^2= coefficient of determination for estimates of size-at-age and known size-at-age for each age group. "% range of mean size-at-capture" represents the variability between estimated size and known mean size at time of sampling.

Model	r^2	% range of mean size at capture
Biological intercept	0.994	−3.5 to +6.4
Modified Fry	0.935	+2.4 to +13.1
Time-varying growth	0.038	−10.3 to +0.90

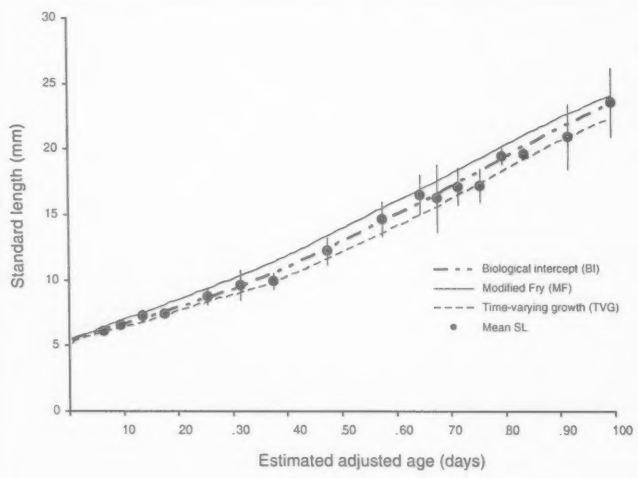

Figure 5

Growth curves back-calculated from delta smelt (*Hypomesus transpacificus*) otoliths. Size-at-age data for laboratory-reared fish are shown as points with ±1 standard deviation. Three models of back-calculation were used to generate growth curves from otoliths: the modified Fry (MF), the stage-specific biological intercept (BI), and the time-varying growth (TVG) model.

Otolith-size–fish-size relationship

The results of this study showed that minimal age-independent variability occurred in the OS-FS relationship and that growth rate effects were negligible (Fig. 3, A and B). Removing the effect of age resulted in a strong correlation between otolith growth and fish growth, indicating that at the preflexion stage, otolith growth was proportional to somatic growth. However, the OS-FS relationship showed a significant interruption in linear growth due to an ontogenetic shift at the postflexion stage, thus demonstrating that the assumption of constant proportionality was violated (Fig. 4). Moreover, this change in proportionality corresponded with the transition from preflexion larvae to postflexion-stage juveniles. Several studies, across broad taxonomic orders have demonstrated similar deviations from proportionality in the OS-FS relationship (e.g., flatfish (*Rhombosolea tapirina* and *Ammotretis rostratus*) [Jenkins, 1987], rainbow smelt (*Osmerus mordax*) [Sirois et al., 1998], and Atlantic cod (*Gadus morhua*) [Otterlei et al., 2002]), which were also associated with life-stage transitions.

Measured growth-rate effects were weak for delta smelt (Fig. 3B) and, thus, are not likely to further explain the age-independent variability in the OS-FS relationship. In contrast, Sirois et al. (1998), found significant growth-rate effects in the OS-FS relationship for rainbow smelt. Furthermore, Hare and Cowen (1995) found both growth-rate effects and ontogenetic shifts in the OS-FS relationship for bluefish larvae (*Pomatomus saltatrix*). These studies highlight the different mechanisms responsible for the variability in the otolith and somatic growth relationship, and, thus, potential violations in the constant assumed proportionality for linear back-calculation models.

Other factors that can influence the OS-FS relationship include temperature and salinity. In the field, delta smelt can experience a broad range of temperatures during their larval stage. The effects of differing temperatures at this life stage on the OS-FS relationship and the influence on otolith back-calculations from field-caught fish is unknown. It is assumed that otolith growth is allometric to fish growth during seasonally variable temperatures. For our study, delta smelt were reared in temperature and salinity controlled conditions, and therefore temperature and salinity were considered to have negligible effects and did not influence the variability in the OS-FS relationship. However, temperature variability can result in different

OS-FS relationships and inaccurate size back-calculations. Indeed, Otterlei et al. (2002) found significant differences in the OS-FS relationships for Atlantic cod reared at different temperatures and therefore temperature effects can result in biased back-calculations if not considered in back-calculation procedures.

Despite the strong correlation between otolith and somatic growth during the preflexion stage, a significant shift in this relationship occurred during caudal fin flexing in the juvenile stage. This morphological transition signals a deviation from constant proportionality in the OS-FS relationship for delta smelt. Therefore, the appropriate choice of a back-calculation model will depend on the form of the relationship between otolith size and fish size. Incorrect assumptions regarding the shape of the OS-FS relationship in various back-calculation models may cause errors in back-calculation of size-at-age and the predictability of growth rates (Hare and Cowen, 1995; Otterli et al., 2002). Campana (1990) suggested the use of a stage-specific form of the BI model to account for the ontogenetic shifts in the OS-FS relationship.

Comparison of the TVG and MF model with the stage-specific BI model

The ontogenetic stage-specific BI model used in our study provided the most parsimonious size-at-age estimates. The TVG consistently underestimated size-at-age, whereas the MF model over-estimated size-at-age for fish greater than 30–40 dah (Fig. 5). Estimated mean size-at-age for the stage-specific BI model was most similar to the observed size-at-age with the minimum and maximum percent deviation of individual size-at-age symmetrically distributed about the mean observed size-at-age. In contrast, the minimum and maximum percent deviation was negative for the TVG model and positive for the MF model (Table 4).

Unlike the stage-specific BI model, the TVG and MF models did not accurately estimate size-at-age because of ontogenetic shifts in the OS-FS relationships. The TVG model was developed to compensate for growth-rate effects in the OS-FS relationship (Sirois et al., 1998). However, for reared delta smelt, growth rate effects in the OS-FS relationship were minimal. When growth-rate effects are negligible, the results of the TVG and the nonstage-specific BI model should be identical (Sirois et al., 1998). This study demonstrates that when ontogenetic shifts occur in the OS-FS relationship independent of growth-rate effects, the TVG model may give poor estimates of size-at-age. Moreover, Vigliola et al. (2000) found the MF model accurately estimated size-at-age for three species of *Diplodus* (seabream), because of the allometric OS-FS relationship. However, for delta smelt, the simple allometric relationship of the MF model consistently resulted in an overestimation of size-at-age because of an ontogenetic shift in the OS-FS relationship.

The transition from the preflexion larval stage to the postflexion juvenile stage created difficulties for accurately estimating size-at-age for both the TVG and MF models. Owing to the unique ontogenetic shift in the OS-FS relationship that delta smelt undergo, the stage-specific BI model more accurately estimated fish size-at-age. However, because of the variability in observed length-at-age, each model described population growth rates with a high degree of certainty (all r^2 values were greater than 0.93). Therefore, we argue that caution should be taken when describing patterns in hatchery-reared growth rates because measured growth rates in our study were significantly reduced in comparison to field growth rates (first author, unpubl. data). Finally, although the intercepts for the stage-specific BI model were derived from the mean population life-stage transition (12 mm SL), the size at life-stage transitions for individuals can be variable, resulting in complex individual biological intercepts that were not taken into consideration.

Conclusions

Criteria for choice of growth back-calculation models

The recent interest in back-calculated size-at-age for individual fish based on otolith increments has resulted in the development of numerous methods to back-calculate size-at-age. The choice of various back-calculation methods can be difficult because assumptions underlying each model may not be evaluated completely. To guide the proper choice of back-calculation models, we recommend a critical examination of the OS-FS relationship. Furthermore, the assessment of ontogenetic variability and growth effects (i.e., Hare and Cowan, 1995) should be evaluated prior to choosing a model. Application of back-calculation techniques requires validation of otolith growth and somatic growth relationships for each species. Therefore, validation may even need to be conducted on a species- or stock-specific basis, and at various levels of environmental variability (see Otterlei et al., 2002). Moreover, accounting for ontogenetic and growth effects on the proportionality of otolith size to fish size will help guide the development and application of appropriate back-calculation models and will lead to accurate estimates of size-at-age for fish recruitment studies. Thus, we conclude that the modified BI model will allow for an accurate estimate of growth histories and reliable information for determining factors influencing delta smelt recruitment.

Acknowledgments

We thank D. Martasian, J. Raum, L. Lewis, and Z. Kane for the work on this project. We also thank the Association of Bay Areas Governments (ABAG), Interagency Ecological Program, and the CALFED Bay-Delta Ecosystem Restoration Program for Funding; the Graduate Group in Ecology at University of California Davis; and S. Morgan and P. Moyle for helpful comments on the manuscript.

Literature cited

Baskerville-Bridges, B., J. C. Lindberg, and S. I. Dorsoshov.
2004. The effect of light intensity, algal concentration, and prey density on the feeding behavior of delta smelt larvae. *In* Proceedings of the symposium early life history of fishes in the San Francisco estuary and watershed (F. Feyrer, ed.), p. 219–228. Am. Fish. Soc., Santa Cruz, CA.

Bennett, W. A.
2005. Critical assessment of the delta smelt population in the San Francisco estuary, California. San Franc. Estuary Watershed Sci. 3:(2) Article 1.

Bennett, W. A., and P. B. Moyle.
1996. Where have all the fishes gone? Interactive factors producing fish declines in the Sacramento-San Joaquin estuary. *In* San Francisco Bay: The ecosystem: further investigations into the natural history of San Francisco Bay and Delta with reference to the influence of man (J. T. Hollibaugh, ed.), p. 519–542. Pacific Division of the American Association for the Advancement of Science, San Fransisco, CA.

Campana, S. E.
1990. How reliable are growth back-calculations based on otoliths? Can. J. Fish. Aquat. Sci. 47:2219–2227.
2001. Accuracy, precision, and quality control in age determination, including a review of the use and abuse of age validation methods. J. Fish Biol. 59:197–242.

Campana, S. E., and J. D. Neilson.
1985. Microstructure of fish otoliths. Can. J. Fish. Aquat. Sci. 42:1014–1032.

Cock, A. G.
1966. Genetical aspects of metrical growth and form in animals. Q. Rev. Biol. 41:131–190.

Fujiwara, M., B. E., Kendall, R. M., Nisbet, and W. A. Bennett.
2005. Analysis of size trajectory data using an energetic-based growth model. Ecology 86:1441–1451.

Gould, S. J.
1966. Allometry and size in ontogeny and phylogeny. Biol. Rev. 41:587–640.

Hare, J. A., and R. K. Cowen.
1995. Effect of age, growth rate, and ontogeny on the otolith size-fish size relationship in bluefish, *Pomatomus saltatrix*, and the implications for back-calculation of size in fish early life history stages. Can. J. Fish. Aquat. Sci. 52:1909–1922.

Hirose, T., and K. Kawaguchi.
2001. Daily otolith increments and growth of reared chika *Hypomesus japonicus* larvae. B. Jpn. Natl. Fish. Res. Inst.:141–144.

Jenkins, G. P.
1987. Age and growth of co-occurring larvae of two flounder species, *Rhombosolea tapirina* and *Ammotretis rostratus*. Mar. Biol. 95:157–165.

McAllister, D. E.
1963. A revision of the smelt family, Osmeridae. National Museum of Canada. Bulletin no. 191. Biological Series, no. 71, 53 p. Ottawa, Dept. of Northern Affairs and National Resources, Ottawa, Canada.

Morita, K., and T. Matsuishi.
2001. A new model of growth back-calculation incorporating age effect based on otoliths. Can. J. Fish. Aquat. Sci. 58:1805–1811.

Moyle, P. B.
2002. Inland fishes of California: revised and expanded, 502 p. Univ. California Press, Berkeley, CA.

Moyle, P. B., B. Herbold, D. E. Stevens, and L. W. Miller.
1992. Life history and status of delta smelt in the Sacramento-San Joaquin estuary, California. Trans. Am. Fish. Soc. 121:67–77.

Ohama, H.
1990. Age determination of Japanese smelt with daily otolith increment. Nippon Suisan Gakkaishi 56:1053–1057.

Otterlei, E., A. Folkvord, and G. Nyhmammer.
2002. Temperature-dependent otolith growth of larval and early juvenile Atlantic cod (*Gadus morhua*). ICES J. of Mar. Sci. 59:401–410.

Rice, J. A., L. B. Crowder, and M. E. Holey.
1987. Exploration of mechanisms regulating larval survival in Lake Michigan [USA] bloater: A recruitment analysis based on characteristics of individual larvae. Trans. Am. Fish. Soc. 116:703–718.

Sepulveda, A.
1994. Daily growth increments in the otoliths of European smelt *Osmerus eperlanus* larvae. Mar. Ecol. Prog. Ser. 108:33–42.

Sirois, P., and J. J. Dodson.
2000. Critical periods and growth-dependent survival of larvae of an estuarine fish, the rainbow smelt *Osmerus mordax*. Mar. Ecol. Prog. Ser. 203:233–245.

Sirois, P., F. Lecomet, and J. J. Dodson.
1998. An otolith-based back-calculation method to account for time-varying growth rate in rainbow smelt (*Osmerus mordax*) larvae. Can. J. Fish. Aquat. Sci. 55:2662–2671.

Sokal, R. R., and J. F. Rohlf,
1973. An introduction to biostatistics, 368 p. W.H. Freeman, San Francisco, CA.

Sweetnam, D. A.
1999. Status of delta smelt in the Sacramento-San Joaquin estuary. Cal. Fish Game 85:22–27.

USFWS (United States Fish and Wildlife Service).
1995. Sacramento-San Joaquin Delta Native Fishes Recovery Plan, 142 p. United States Fish and Wildlife Service, 911 NE 11th Avenue, Portland, Oregon 97232-4181.

Vigliola, L., M. Harmelin-Vivien, and M. G. Meekan.
2000. Comparison of techniques of back-calculation of growth and settlement marks from the otoliths of three species of *Diplodus* from the Mediterranean Sea. Can. J. Fish. Aquat. Sci. 57:1291–1299.

Relationship between abundance of juvenile rockfishes (*Sebastes* spp.) and environmental variables documented off northern California and potential mechanisms for the covariation

Thomas E. Laidig (contact author)
James R. Chess
Daniel F. Howard

Email address for T. E. Laidig: tom.laidig@noaa.gov

National Marine Fisheries Service
Southwest Fisheries Science Center
Fisheries Ecology Division
110 Shaffer Road
Santa Cruz, California 95060

Abstract—We estimated annual abundance of juvenile blue (*Sebastes mystinus*), yellowtail (*S. flavidus*), and black (*S. melanops*) rockfish off northern California over 21 years and evaluated the relationship of abundance to oceanographic variables (sea level anomaly, nearshore temperature, and offshore Ekman transport). Although mean annual abundance was highly variable (0.01–181 fish/minute), trends were similar for the three species. Sea level anomaly and nearshore temperature had the strongest relationship with interannual variation in rockfish abundance, and offshore Ekman transport did not correlate with abundance. Oceanographic events occurring in February and March (i.e., during the larval stage) had the strongest relationship with juvenile abundance, which indicates that year-class strength is determined during the larval stage. Also of note, the annual abundance of juvenile yellowtail rockfish was positively correlated with year-class strength of adult yellowtail rockfish; this finding would indicate the importance of studying juvenile abundance surveys for management purposes.

Manuscript submitted 1 December 2005 to the Scientific Editor's Office.

Manuscript approved for publication 15 March 2006 by the Scientific Editor.

Fish. Bull. 105:39–48 (2007).

Success of annual recruitment of juvenile rockfishes (*Sebastes* spp.) from the pelagic to a demersal phase is highly variable and leads to large fluctuations in year-class strength in the fisheries (Ralston and Howard, 1995). With the abundance of many rockfish stocks at historic low levels, assessment of recruitment is paramount for fishery managers to improve plans for sustainable harvests. Fisheries models (such as the stock synthesis model) often include recruitment data (PFMC[1]). In recent years, larval and juvenile rockfish abundance data have been included in stock assessments for bocaccio (*S. paucispinis*) and cowcod (*S. levis*) (MacCall[2], Butler et al., 2003). If the larval or juvenile abundance data do not accurately reflect the numbers of adults, the models can either over- or underestimate the biomass available to the fishery.

Rockfishes are viviparous, giving birth to larvae that reside in open water for several months before recruiting from the plankton to a more benthic life (Love et al., 2002). The habitat where rockfish initially recruit varies among species and includes floating drift algae (e.g., splitnose rockfish, *S. diploproa* [Shaffer et al., 1995]), soft sediments (e.g., stripetail rockfish, *S. saxicola* [Johnson et al., 2001]), and deeper rocky areas with crevices (e.g., rosy rockfish, *S. rosaceus* [Love et al., 2002]). A major area of recruitment is the nearshore environment, where numerous species of rockfish recruit in the kelp canopy, sand channels, on rocky outcrops, and in midwater among the kelp stipes (Anderson, 1983).

The factors that influence the magnitude of juvenile recruitment of rockfishes are not well known. VenTresca et al.[3] suggested that upwelling was the major factor contributing to the annual variability of juvenile rockfish abundance off Monterey, California. Ralston and Howard (1995) found that the highest survival of blue (*S. mystinus*), and yellowtail rockfish (*S. flavidus*), occurred when sea surface temperature and upwelling were at intermediate levels. Ainley et al.

[1] PFMC (Pacific Fisheries Management Council). 2002. Status of the Pacific Coast groundfish fishery through 2001 and acceptable biological catch for 2002, 26 p. PFMC, 7700 NE Ambassador Place, Suite 200, Portland, Oregon 97220.

[2] MacCall, A. D. 2002. Status of bocaccio off California in 2002. *In* Appendix to the status of the Pacific coast groundfish fishery through 2001 and acceptable biological catches for 2002, 58 p. Pacific Fisheries Management Council, 7700 NE Ambassador Place, Suite 200, Portland, Oregon 97220.

[3] VenTresca, D. A., J. L. Houk, M. J. Paddack, M. L. Gingras, N. L. Crane, and S. D. Short. 1996. Early life-history studies of nearshore rockfishes and lingcod off central California, 1987–92. Cal. Fish Game. Resources Division. Admin. Rep. 96-4, 77 p.

(1993), using seabird diet to assess the abundance of juvenile rockfishes, also reported the greatest abundance of rockfishes in years of intermediate upwelling. Yoklavich et al. (1996) and Johnson et al. (2001) observed that, during years when upwelling was delayed, those rockfishes released later in the year had increased survivorship. In addition, Pastén et al. (2003) observed that monthly tidal cycles were important in estimating the numbers of newly recruited black rockfish (*S. inermis*) in the western Pacific.

In our study, we examined the relationship between the annual abundance of juvenile rockfishes recruiting to the nearshore kelp beds off northern California and three oceanographic variables (sea level anomaly, nearshore temperature, and offshore Ekman transport) over 21 years. Three species of juvenile rockfishes (blue, yellowtail, and black rockfish, [*S. melanops*]) were surveyed. Parturition (the release of larvae from the mother) in these species occurs in the winter and the resulting pelagic larvae and juveniles spend between three to five months in the offshore midwater environment (Love et al., 2002). All juveniles of these species migrate in mid to late spring and early summer from the offshore pelagic environment to nearshore midwater and benthic environments on or next to rocky outcrops, commonly with dense algal growth; this movement we define here as juvenile recruitment (Anderson, 1983).

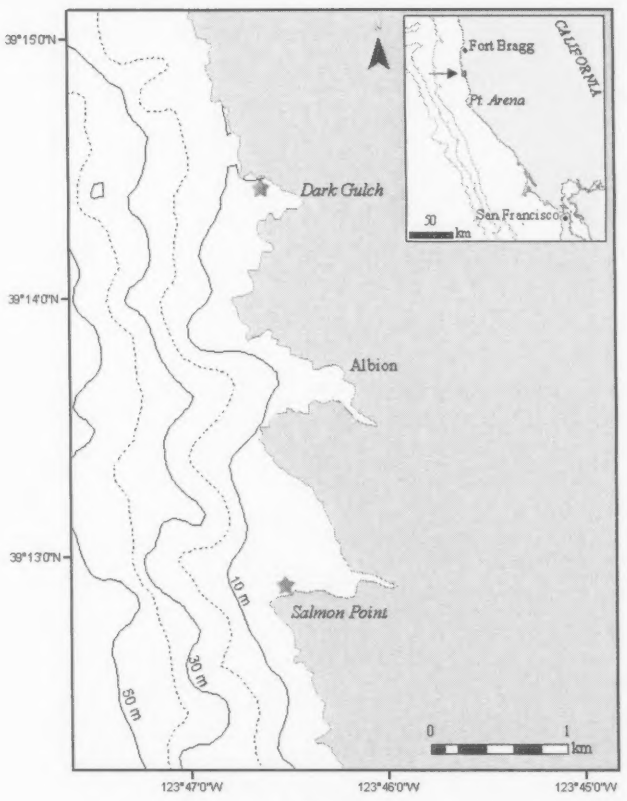

Figure 1

The survey sites in Mendocino County, California. Dark Gulch and Salmon Point kelp beds are represented by the stars.

Materials and methods

Surveys of young-of-the-year (YOY) rockfishes were conducted annually between 1 July and 15 September from 1983 to 2003 within two kelp beds along the northern California coast (Dark Gulch [39°14′N; 123°46′W] and Salmon Point [39°12′N; 123°46′W]) in Mendocino County (Fig. 1). Each kelp bed included high-relief bedrock interspersed with low-relief cobble and sand areas. They were bounded by shoreline on two sides, a sand channel on one side, and deep water on the remaining side, and thus each kelp bed was isolated.

Strip transects were conducted by using SCUBA. Researchers swam in one direction 2 m above the sea floor and counted all juvenile rockfishes within 3 m in any direction for one minute. At the end of each one-minute survey, the numbers of each species were recorded. The researcher would then haphazardly choose another direction to swim and conduct rockfish counts for another minute. Surveys were made throughout the kelp bed at both sites from the surface to 20 m. YOY rockfishes were distinguished from older conspecifics by their size (less than 80 mm standard length in August) and from other rockfish species by body shape and pigment patterns (Anderson, 1983; Love et al., 2002).

Surveys were conducted only when appropriate conditions occurred. First, surveys were conducted between the hours of 0900 and 1700 to standardize light conditions. Second, surveys were made only when underwater visibility was greater than 4 m. Underwater visibility was measured by Secchi disk, transect line, and by estimating the distance at which objects (i.e., fishes and rocks) could be seen. Third, swell height had to be less than 2 m for diver safety and to standardize sea conditions.

An index of annual abundance (index) for each species of juvenile rockfish was computed by pooling all one-minute surveys for a year at each study site, and dividing by the total number of one-minute surveys for that year. We used a paired t-test to compare species-specific indices between the two study sites. Data were log-transformed to equalize the variance among years. We used cross-correlation analysis to examine patterns in the index among species. For no time series (either biological or environmental) was there a significant autocorrelation present. Therefore, our observations complied with the assumption of independence.

We related three oceanographic data sets (sea level anomaly, nearshore temperature, and offshore Ekman transport) to abundance data. Sea level anomaly data were collected from a shore station (with an acoustic gauge measuring in mm) at Arena Cove, CA (38°54'N), and monthly means were obtained from the University of Hawaii Sea Level Center. These data represent a measure of change in sea level height over time and were adjusted for local atmospheric conditions. Sea level anomalies reflect water movement—a positive anomaly being associated with poleward flow and a negative anomaly associated with equatorward flow. Nearshore temperature data were continuously collected at the Dark Gulch site throughout the study. Temperature monitors were located in two areas of the kelp bed, one at 8 m and the other at 15 m water depth. Temperature was recorded hourly and these data were averaged daily, monthly, and seasonally. The offshore Ekman transport data were determined from data gathered by a buoy 20 km offshore of 39°N (Albion, CA). Monthly mean offshore Ekman transport was derived from geostrophic wind stress data determined from atmospheric pressure values at mean sea level (at 6-hour intervals) and obtained from Environmental Research Division, Southwest Fisheries Science Center (NOAA[4]). Offshore Ekman transport was used as a measure of cross-shelf water transport. The offshore flow of surface water causes deep, cold, nutrient-rich water to be brought to the surface to replace the displaced surface waters (the process of upwelling). Monthly and seasonal values were determined for all oceanographic data sets and years, and the seasonal values represented the mean from January to June. The months of July to December were not considered in our analysis because this time period was after the time of juvenile rockfish recruitment to the kelp bed.

The comparison of the abundance index for each species and the oceanographic variables involved numerous statistical tests. Cross-correlation coefficients were computed in pairwise comparisons of the index and the oceanographic data. For each year in the time series, we used both seasonal and monthly means of the oceanographic variables and the annual log-transformed index. We also applied principal components analysis (PCA) to evaluate the relationships among monthly oceanographic variables, and also the relationships among the log-transformed index of the three species. We used canonical correlation analysis (CCA) to explicitly examine the correlations between these oceanographic and rockfish PCAs. PCA develops an ordination space constrained to be a linear combination of the variables (i.e., the eigenvectors). CCA does the same, except the ordination space is constrained to be a linear combination of the other set of variables. The fish data, therefore, are displayed in a space defined by a combination of the oceanographic data (the canonical scores).

Year-specific catch-at-age data for adult yellowtail rockfish were compared with the juvenile yellowtail rockfish abundance index to evaluate the relationship between juvenile rockfish abundance and subsequent landings of adults in the fishery. No age data were available for the adult blue or black rockfishes. Age and catch data of adult yellowtail rockfish commercially caught in trawls from 1997 to 1999 were retrieved from the CALCOM database[5] for the three closest ports to our study sites (Bodega Bay, Fort Bragg, and Eureka, CA). We used expanded age compositions by year class, which were determined from a subset of aged fish for that region. For example, in 1997 there were 10 year-classes in a subset of fish that were aged from Bodega Bay, whereas only six year classes existed in the subset of aged fish for 1998 from Bodega Bay. Year-specific catch-at-age data were determined for each year and port and regressed against the log-transformed index. Significance levels were determined for each port-year combination and for all ports combined.

Results

Over 21 years, 172 dives and 3333 one-minute surveys were completed, averaging 8.2 dives/year and 158.7 one-minute surveys/year (Table 1). The average number of one-minute surveys per dive was 19.4 surveys/dive (calculated by dividing the total number of one-minute surveys by the total number of dives). Total number of dives per year varied from 4 in 1993 to 14 in 1983, and the number of one-minute surveys varied from 80 in 1993 to 330 in 1983. The total number of dives at Dark Gulch was 113, whereas only 59 dives were conducted at Salmon Point. Similarly, nearly twice as many one-minute surveys were completed at Dark Gulch (2165) compared to Salmon Point (1168). This difference was mainly due to sea conditions; Salmon Point sometimes experiences larger ocean swells (because it is less protected), making sampling unsafe.

The abundance index for each species varied among years but was not significantly different (t-test; $n=21$; $P>0.05$) between the two study sites. For this reason, the data from both sites were pooled. The index was highly variable for all species (Fig. 2). For blue rockfish, the index varied from 181 fish/min in 1987 to 0.26 fish/min in 1992. For yellowtail rockfish, the index ranged from 162 fish/min in 1985 to 0.03 fish/min in 1994. Abundance of black rockfish peaked in 1999 at 22 fish/min and was lowest in 1998 at 0.01 fish/min.

[4] NOAA (National Oceanic and Atmospheric Administration). Environmental Research Division. Southwest Fisheries Science Center. NOAA/NMFS/SWFSC, 1352 Lighthouse Ave., Pacific Grove, CA 93950-2097. Website: http://www.pfeg.noaa.gov (accessed 15 March 2006).

[5] CALCOM (California Cooperative Survey). Commercial landings sampling program maintained by California Department of Fish and Game, 350 Harbor Blvd., Belmont, CA 94002; Pacific States Marine Fisheries Commission, 350 Harbor Blvd., Belmont, CA 94002; and Fisheries Ecology Division, SWFSC, NMFS, NOAA, 110 Shaffer Rd., Santa Cruz, CA 95060. Website: 128.114.3.187 (accessed on 15 March 2006).

Table 1

Number of dives and total number of one-minute surveys of juvenile rockfishes by year at each dive site. Data were collected between 1 July and 15 September, 1983–2003.

	Number of dives			Number of 1-minute surveys		
Year	Dark Gulch	Salmon Point	Total	Dark Gulch	Salmon Point	Total
1983	12	2	14	270	60	330
1984	8	3	11	185	99	284
1985	8	4	12	94	35	129
1986	9	2	11	124	30	154
1987	9	3	12	94	18	112
1988	4	3	7	62	38	100
1989	5	3	8	119	68	187
1990	4	2	6	71	33	104
1991	3	3	6	60	60	120
1992	3	3	6	60	60	120
1993	2	2	4	40	40	80
1994	3	3	6	60	60	120
1995	4	3	7	80	40	120
1996	4	1	5	88	22	110
1997	5	3	8	124	71	195
1998	7	2	9	188	40	228
1999	6	5	11	133	89	222
2000	4	3	7	82	84	166
2001	3	3	6	62	63	125
2002	4	4	8	85	87	172
2003	6	2	8	84	41	125
Total	113	59	172	2165	1168	3333
Average	5.4	2.8	dives/year 8.2	103.1	55.6	surveys/year 158.7
Standard deviation	2.6	0.9	2.7	54.7	22.8	63.9

Year-to-year variability was generally synchronous among the three species (Fig. 2). Abundance was below average for the three species in 1983–84, and 1989–98. Above average abundance in all three species occurred in 1985, 1987, 1988, and in 2001. Black rockfish attained relatively greater numbers in 1986, 1999, 2000, and 2003 compared to the other two species. In addition, blue rockfish experienced higher than average abundances in 2001 and 2002 compared to the other species. Generally, the index for black rockfish was lower than for the other two species, but black rockfish abundance was extremely high in 1999, but the abundance of the other two species was below average. Indices for blue and yellowtail rockfish were significantly correlated ($P<0.001$, $r=0.91$), and the index for black rockfish was not significantly correlated with either of the other two species. Using the log-transformed index, we found that blue, yellowtail, and black rockfish were all significantly correlated ($P<0.01$, $r=0.76$) with each other. We used the log-transformed index for the remaining analyses.

In evaluating seasonal oceanographic variables, sea level anomaly and nearshore temperature were significantly and positively correlated ($P<0.05$, $r=0.53$), nearshore temperature and offshore Ekman transport were significantly and negatively correlated ($P<0.05$, $r=-0.69$), and sea level anomaly and offshore Ekman transport were not significantly correlated. There was no significant correlation between the seasonal oceanographic variables and the index for any species.

With PCA, 65% of the variability in the monthly oceanographic ($_O$) data sets was explained by the first eigenvector ($PC1_O$). $PC1_O$ was characterized by the contrast between Ekman transport and the other two variables (Table 2). The second eigenvector ($PC2_O$) explained 30% of the variability and was associated with high sea level anomaly. For the rockfish abundance ($_F$) indices, 77% of the variability was explained in the first eigenvector ($PC1_F$), which was associated with the abundance time series of all three species. The second eigenvector ($PC2_F$) explained 15% of the variability and was associated with the contrast between blue rockfish abundance and the other two species, especially late in the time series. Although $PC3_F$ explained only 8% of the variability in these time series, it was associated

Table 2

Eigenvectors determined from the principal components analysis (PCA) for the monthly oceanographic variables ($_O$) and log-transformed annual juvenile rockfish abundance ($_F$) index by species

	$PC1_O$	$PC2_O$	$PC3_O$
% variance explained	64.5	29.5	6.0
Nearshore temperature	0.68	−0.04	0.73
Sea level anomaly	0.46	0.80	−0.39
Ekman transport	−0.57	0.40	0.56
	$PC1_F$	$PC2_F$	$PC3_F$
% variance explained	77.1	14.6	8.3
Blue rockfish	0.55	0.83	0.13
Yellowtail rockfish	0.60	−0.28	−0.75
Black rockfish	0.58	−0.49	0.64

with the unique pattern in abundance of black rockfish, especially in contrast to yellowtail rockfish.

Correlations varied between the log-transformed abundance indices and the monthly means of the oceanographic variables (Table 3). All three species were significantly and negatively correlated with sea level anomaly during some of the months from January to June. For nearshore monthly temperature, there was a similar pattern of negative correlation with index for all species during January to June. Only blue rockfish were significantly correlated ($P<0.001$, $r=0.58$) with offshore Ekman Transport, and only in February (Table 3). Months of high nearshore temperature or sea level anomaly resulted in low juvenile rockfish abundances. For example, when the abundance index for blue rockfish was compared with sea level anomaly in February (Fig. 3), years of highest abundance of blue rockfish were always years of low sea level anomaly (i.e., 1985, 1987, 1988, 2001, and 2002), but years of low sea level anomaly did not always lead to particularly high rockfish abundance (i.e., 1989). However, years of highest sea level anomaly (e.g., 1983, 1992, and 1998) resulted in the lowest blue rockfish abundance.

The results of the CCA also indicate that low annual abundance was associated with years of high nearshore temperatures and high sea level anomaly. The first canonical correlation was 0.57, which was significantly different from zero ($P<0.0001$), and explained 97 % of the covariance between the two data sets. The remaining two canonical correlations were not significant and explained little of the variability. Blue, yellowtail, and black rockfish were negatively correlated with the first canonical variable for the oceanographic data set (−0.43, −0.45, and −0.55, respectively; Fig. 4). This indicates that fish abundances were low when temperatures and sea level anomalies were high.

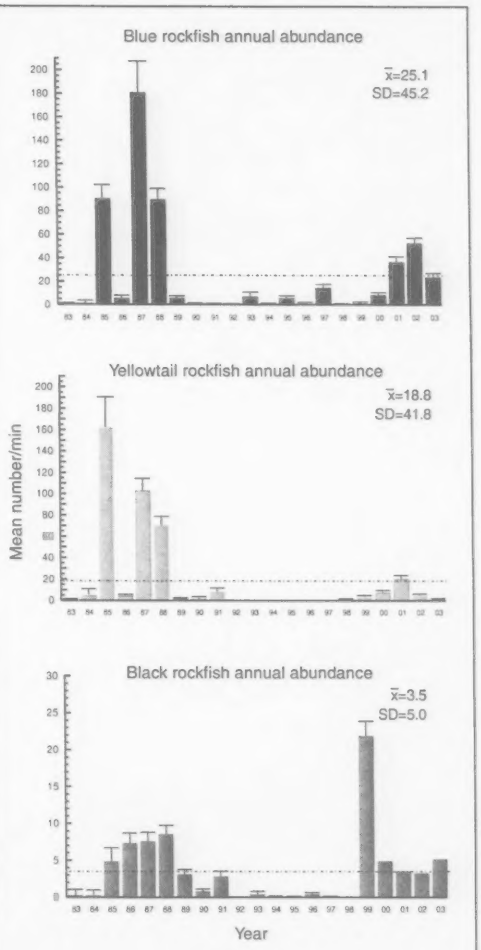

Figure 2

Mean annual juvenile rockfish abundance index for all one-minute surveys in two kelp beds for blue (*Sebastes mystinus*), yellowtail (*S. flavidus*), and black (*S. melanops*) rockfish by year. Note the different scale for black rockfish. Error bar=one standard error. The 21-year mean (represented by a dashed line) and the standard deviation for each species are given on each plot. The sample size for each year is reported in Table 1.

The data for year-class strength of commercially caught adult yellowtail rockfish corresponded with the annual abundance index for juvenile yellowtail rockfish (Table 4), and were significantly correlated for all ports combined for 1997 ($P<0.01$, $n=29$, $r=0.48$) and 1999 ($P<0.04$, $n=31$, $r=0.36$), but not for 1998 ($P<0.1$, $n=21$, $r=0.37$). For 1997, juvenile rockfish abundance was significantly correlated with adult fish numbers at Bodega

Bay ($P<0.02$, R=0.43, Fig. 5A), Ft. Bragg ($P<0.001$, $r=0.62$), and Eureka ($P<0.01$, $r=0.78$). In 1998, Bodega Bay was the only port where adult fish numbers were significantly correlated ($P<0.05$, $r=0.38$, Fig. 5B) with juvenile abundance. In 1999, Eureka was the only port where adult fish numbers were significantly correlated ($P<0.05$, $R=0.35$) with juvenile abundance. From the 1998 adult numbers in Bodega, 1985 was the largest year class of adult yellowtail rockfish, which corresponded to the highest index for juvenile yellowtail rockfish (Fig. 5B).

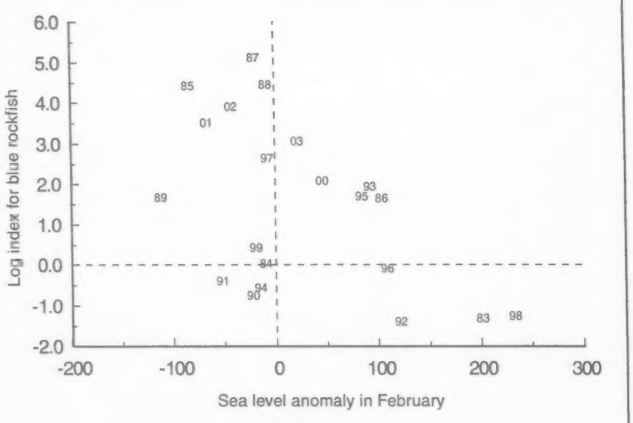

Figure 3

An example of the log-transformed annual abundance index for blue rockfish (*Sebastes mystinus*) and average sea level anomaly in February for each year of the survey (1983–2003). Numbers represent individual years. Dashed lines represent the zero line for both axes.

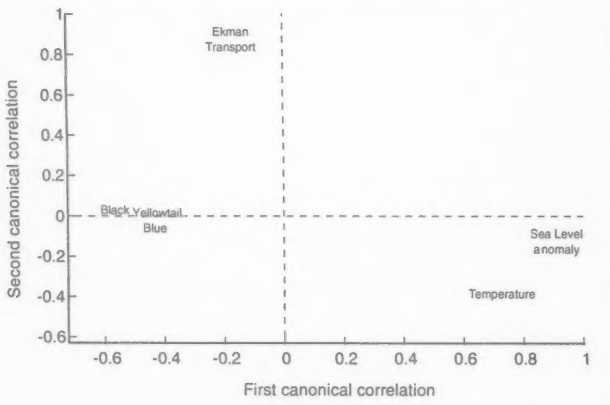

Figure 4

The first and second canonical correlations for the annual abundance index (INDEX) for each rockfish species and the oceanographic factors with the axes defined by the oceanographic data set. Dashed lines represent zero line for both axes.

Discussion

The 21-year time series of juvenile rockfish abundance allowed us to examine long-term change in recruitment of commercially and recreationally important species off the coast of California. The year-to-year variability in recruitment likely relates to variability in year-class strength of the population entering the fisheries. The synchrony in recruitment variability among the three rockfish species indicates that similar environmental processes affect the abundance of all three species. By examining oceanographic variables, we determined that sea level anomaly and nearshore temperatures in February and March were important influences on juvenile rockfish abundance.

Year-to-year variability in young rockfish abundance has been documented in other studies off the west coast of the United States. Yoklavich et al. (1996) found a twenty-fold increase in the abundance of pelagic larval rockfishes off central California in 1993 compared to numbers obtained during a similar time period in 1992. They attributed this difference to increased offshore transport and possibly lower predation rates. Moser et al. (2000) observed large fluctuations in annual larval rockfish abundance off southern California from 1951 to 1998, which was attributed to the reproductive output of each species and oceanographic variables. Mearns et al. (1980) determined that the variability in recruitment of juveniles was the major source of seasonal and annual fluctuations in rockfish catches for stripetail and calico rockfish (*S. dallii*). Matthews (1989) observed that recruitment levels varied between years for three species of rockfishes recruiting to nearshore habitats. Ainley et al. (1993) discovered a three-fold difference in pelagic juvenile rockfish abundance in seabird diets in central California between similar periods in 1985 and 1986, and they attributed this to cross shelf advection of larvae in January and February. Ralston and Ianelli (1998) reported a large variability in juvenile bocaccio abundance over a 13-year period and attributed some of this variability to El Niño events.

Year-class strength was likely established in the period from February through March during the larval stage of the three

Table 3

Correlations between the log-transformed annual juvenile rockfish abundance index by species and the oceanographic variables by month. * = $P<0.05$; ** = $P<0.01$; + = $P<0.1$.

	Jan	Feb	Mar	Apr	May	Jun
Sea level anomaly						
Blue rockfish	−0.36	−0.71**	−0.63**	−0.51*	−0.37+	−0.40+
Yellowtail rockfish	−0.48*	−0.53*	−0.57**	−0.55**	−0.55**	−0.35
Black rockfish	−0.64**	−0.53*	−0.52*	−0.42+	−0.65**	−0.55**
Temperature						
Blue rockfish	−0.22	−0.53*	−0.52*	−0.41+	−0.19	−0.21
Yellowtail rockfish	−0.32	−0.54*	−0.53*	−0.48*	−0.46*	−0.32
Black rockfish	−0.54*	−0.62**	−0.55**	−0.47*	−0.65**	−0.48*
Offshore Ekman transport						
Blue rockfish	0.05	0.58**	0.42+	0.01	−0.02	0.03
Yellowtail rockfish	0.27	0.27	0.39+	0.21	0.17	−0.01
Black rockfish	0.29	0.25	0.19	0.29	0.40+	0.01

Table 4

Correlation coefficients between the log-transformed annual juvenile rockfish abundance index and year-specific adult yellowtail rockfish (*Sebastes flavidus*) commercial landings, by year class, at three ports closest to the study area. * = $P<0.05$; **= $P<0.01$; + = $P<0.1$. Listed in parentheses is the number of year classes determined in each year and the number of adult yellowtail rockfish otoliths that were aged (no. of year classes, number of otoliths aged).

	All ports	Bodega	Bragg	Eureka
1997	0.48 (10, 172)**	0.43 (10,16)*	0.62 (10, 84)**	0.78 (9, 72)**
1998	0.37 (9, 141)+	0.38 (6, 30)*	0.21 (9, 89)	0.32 (7, 22)+
1999	0.36 (12, 198)*	0.32 (9, 84)+	0.25 (11, 37)	0.35 (12, 77)*

species of rockfishes in our study. The abundance of all three species were significantly and negatively correlated with sea level anomaly and nearshore temperature during this time period. Ralston and Howard (1995) also argued that year-class strength was set in the larval period for rockfishes with winter parturition. They analyzed data from midwater trawls in May and June and compared them with data from nearshore surveys in summer. Because there was a strong correlation between the two data sets, they postulated that the year-class was set earlier in the year than May, probably during the larval stage. VenTresca et al.[3] also reported evidence of the establishment of year-class strength in the larval stage. In 1992, they found large concentrations of larval rockfishes in January, but three to four months later very few juveniles appeared in midwater trawls. They surmised that the El Niño conditions of elevated water temperatures and reduced upwelling resulted in poor survival.

Synchrony in juvenile abundance among rockfish species has been observed in other studies. Ralston and Howard (1995) ascertained that trends in abundance for juvenile blue and yellowtail rockfish from midwater trawls were highly correlated over the 10 years of their study. Ammann (2001) discovered a comparable pattern in recruitment of juvenile yellowtail and black rockfish to the kelp bed environment in 1999 and 2000. Stephens et al. (1984) reported that juvenile abundance of both blue and olive rockfish (*S. serranoides*), dropped to virtually zero during the years 1978–81. In our study, blue, yellowtail, and black rockfish covaried over a period of 21 years.

Although offshore Ekman transport, or upwelling, has been suggested as a predictor of year-class strength, we found it to have little correlation with the abundance of juvenile rockfishes from northern California. Maximum upwelling off the central California coast occurs in late spring and summer (Rosenfeld et al., 1994; Yoklavich et al., 1996). This upwelling occurred after the larval period for winter-spawning *Sebastes* spp., and therefore after the timing of year-class determination. Larson et al. (1994) found that larger pelagic juveniles were often close to shore even when upwelling was strong, indicating that later-stage pelagic juveniles were not directly affected by upwelling. If water movement onshore and offshore influences the population size of juvenile rockfishes, perhaps this effect occurs during the early stages.

Temperature and sea level anomaly proved to be important correlates with year-class strength for juvenile rockfishes. Of the three environmental variables examined, nearshore temperature and sea level anomaly were significantly and negatively correlated with the abundance of all three species. Moser et al. (2000) reported a similar relationship, with reduced abundance of larval bocaccio and cowcod during periods of high temperature off southern California. Ralston and Howard (1995) reported a negative correlation between recruited juvenile blue and yellowtail rockfish year-class strength and sea surface temperature in January through March. Stephens et al. (1984) surmised that warm water was the limiting factor in the low recruitment of juvenile blue and olive rockfish during 1978–81 off southern California. Ainley et al. (1993) determined that sea level during February and sea surface temperature in March were negatively correlated with pelagic rockfish abundance for the period of 1973–90 off central California.

Temperature affects the growth rates of rockfishes, which, in turn, affects species abundance. Johnson et al. (2001) determined that growth rates declined during months of high temperatures for juveniles of three rockfish species. However, Boehlert and Yoklavich (1983) found increased growth rates forjuvenile black rockfish with increased temperature in the laboratory, except under starvation conditions. Therefore, reduction in growth rates may be due to lower prey availability during El Niño conditions (Mullin and Conversi, 1989). This lower growth rate of juvenile rockfishes during periods of high temperatures may lead to reduced survival and lower year-class strength.

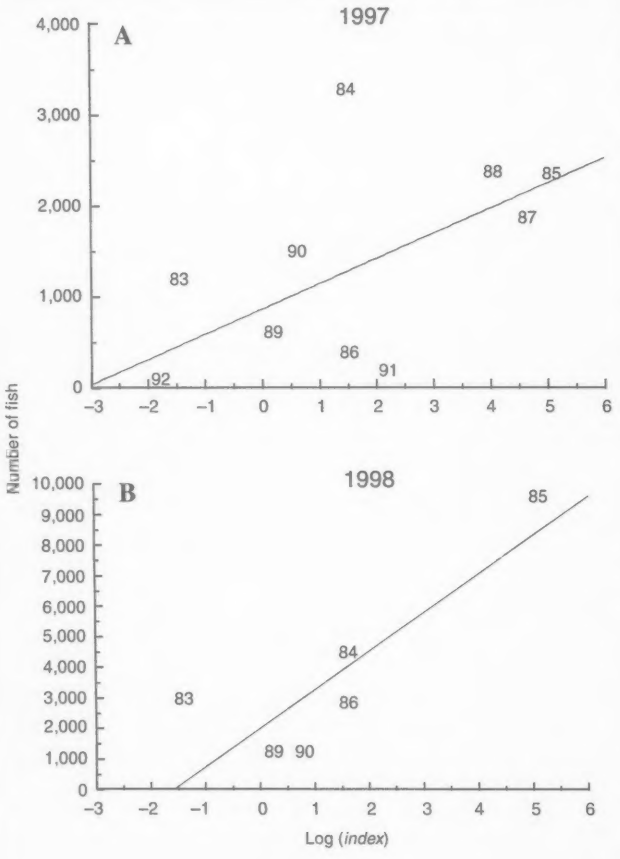

Figure 5

Year-specific catch-at-age data from commercial trawl-caught adult yellowtail rockfish (*Sebastes flavidus*) from Bodega Bay, CA, and the log-transformed annual abundance index for yellowtail rockfish. (**A**) 1997 landings; (**B**) 1998 landings. Numbers represent the year class of aged fish. The solid line represents predicted values from the relationship of the catch-at-age data and the log-transformed index.

Although growth can vary directly with temperature, temperature may also have an indirect effect on rockfish abundance. Strong El Niño events, associated with unusually high water temperatures lasting from a few months to over a year, have occurred off California in 1982–83, 1991–92, and 1997–98 (Fedorov and Philander, 2000; Rebstock, 2001). VenTresca et al. (1995) observed reduced condition factor and gonadal indices for blue rockfish during the 1983 and 1992 El Niños off central California when water temperatures were elevated. These reductions could lead to fewer larvae being produced and hence ultimately to a lower abundance of juveniles. El Niño events can also lead to changes in the strength and timing of the annual phytoplankton bloom, both of which can reduce the distribution and abundance of the zooplankton on which the juvenile rockfishes feed (Lenarz et al., 1995). This reduction in food availability could lead to lower growth or survival of the juvenile rockfishes. Keister et al. (2005) found several warm-water species of euphausiids, chaetognaths, and copepods in Oregon waters during the 1997–98 El Niño. Rebstock (2001) observed that during periods of high temperatures in 1983, 1992, and 1998, the species richness of copepods was lower than a 49-year average. Copepods are a preferred prey item for juvenile rockfishes (Reilly et al., 1992). A change in species richness may reflect a change in species composition to less desirable food sources (e.g., prey is less nutritious or less available to young rockfishes). Although the exact mechanism is not clear, we observed that the three

years of lowest abundance for juvenile rockfishes occurred during El Niño events.

The primary factors that lead to annual fluctuations in abundance were similar for blue, yellowtail, and black rockfish. These three species are found in similar areas at the planktonic stage (Lenarz et al., 1991; Larson et al., 1994). Therefore, it is expected that changes in ocean conditions affect all three species similarly. Nearshore temperature and sea level anomaly had high negative correlations with abundance for all three species, whereas offshore Ekman transport was not correlated with abudance. This finding implies that poor recruitment occurs during years of high temperature and strong, positive sea level anomaly (poleward flow), and vice versa. Our results indicate that recruitment is poor during periods of strong, positive sea -level anomaly and that recruitment is strong only during years of negative sea level anomaly (equatorward flow). However, poor recruitment also occurs in some years with negative sea level anomaly. Therefore, other factors are probably involved in the process and can affect year-class strength in rockfishes. Some of the other factors that have been suggested to have at least some influence on rockfish recruitment include adult spawning biomass (Mason, 1998), increased predation by siphonophores and chaetognaths on larval stages during years of high sea temperature (Yoklavich et al., 1996), turbulence (Ainley et al., 1993), and diet of juvenile rockfishes (Reilly et al., 1992).

Large-scale multiyear oceanographic events (e.g., Pacific Decadal Oscillation and the El Niño-Southern Oscillation indices) also appear to affect juvenile rockfish abundance. Large changes in indices reflect regime shifts in ocean conditions, such as those occurring in 1977, 1989, and 1998 (Hare and Mantua, 2000; Benson and Trites, 2002). Although the mechanisms that affect or cause changes in abundance are unclear, our time series of juvenile rockfish abundance reflects these large-scale shifts in ocean conditions by the generally high recruitment prior to 1989, the much reduced recruitment from 1989 to 1998, and the generally higher recruitment after 1998.

We have continued our juvenile rockfish surveys to present, and have had the opportunity to determine the usefulness of our abundance index as a predictor of rockfish year-class strength. In 2005, average monthly temperature was elevated from January to June (as much as two degrees above average as measured by our temperature monitors). Interestingly, the abundance index of all three species of juvenile rockfishes from our surveys in 2005 was very low. Black and yellowtail rockfish abundances, in particular, were at the third lowest level estimated during what is now a 23-year time-series of recruitment. Therefore, our results demonstrate our ability to predict annual levels of abundance for these species of juvenile rockfishes.

Juvenile yellowtail rockfish abundance in our study reflected adult yellowtail rockfish abundance in the fishery. Mearns et al. (1980) also reported a relationship between juvenile abundance and subsequent adult biomass for stripetail and calico rockfishes by following yearly cohorts from seasonal trawls in southern California over nine years. The high recruitment for bocaccio in 1985 was manifested in the recreational fishery in Monterey Bay, CA in subsequent years (Mason, 1998). Similar trends were observed with large year-classes of chilipepper, *S. goodei*, and yellowtail rockfish (Mason, 1998). Ralston and Ianelli (1998) also found that the abundance of juvenile bocaccio was an indicator of year-class strength in the fishery. Accordingly, the study of juvenile rockfish abundance can help predict good and bad year classes entering a fishery. These data can then be incorporated into fisheries models (see stock assessments for widow rockfish, *S. entomelas*, [He et al.[6]]) to better manage the stocks.

Acknowledgments

We first thank Edmund (Ted) Hobson for his initial conception of this project and his many years of data collection and direction. We also thank all the divers who helped with juvenile rockfish surveys, especially Kelly Silberberg for his many years of dedication to this project. We thank Peter Adams, Steve Ralston, Susan Sogard, Ralph Larson, Mary Yoklavich, and four anonymous reviewers for helpful comments on drafts of this manuscript. Lastly, we thank Craig Syms and Brian Wells for their generous help with statistical matters.

Literature cited

Ainley, D. G., W. J. Sydeman, R. J. Parrish, and W. H. Lenarz.
1993. Oceanic factors influencing distribution of young rockfish (*Sebastes*) in central California: A predator's perspective. Calif. Coop. Oceanic Fish. Invest. Rep. 34:133–139.

Ammann, A.
2001. Evaluation of a standard monitoring unit for the recruitment of fish in central California. M.Sci. thesis, 92 p. Univ. California, Santa Cruz, CA.

Anderson, T. W.
1983. Identification and development of nearshore juvenile rockfishes (genus *Sebastes*) in central California kelp forests. M.Sci. thesis, 216 p. California State Univ., Fresno, CA.

Benson, A. J., and A. W. Trites.
2002. Ecological effects of regime shifts in the Bering Sea and eastern North Pacific Ocean. Fish and Fisheries 3:95–113.

Boehlert, G. W., and M. M. Yoklavich.
1983. Effects of temperature, ration, and fish size on growth of juvenile black rockfish, *Sebastes melanops*. Environ. Biol. Fish. 8:17–28.

[6] He, X., D. E. Pearson, E. J. Dick, J. C. Field, S. Ralston, and A. D. MacCall. 2005. Status of the widow rockfish resource in 2005, 119 p. Pacific Fisheries Management Council, 7700 NE Ambassador Place, Suite 200, Portland, Oregon 97220.

Butler, J. L., L. D. Jacobson, J. T. Barnes, and H. G. Moser.
2003. Biology and population dynamics of cowcod (*Sebastes levis*) in the southern California Bight. Fish. Bull. 101:260–280.

Fedorov, A. V., and S. G. Philander.
2000. Is El Niño changing? Science 288:1997–2002.

Hare, S. R., and N. J. Mantua.
2000. Empirical evidence for North Pacific regime shifts in 1977 and 1989. Prog. Oceanogr. 47:103–145.

Johnson, K. A., M. M. Yoklavich, and G. M. Cailliet.
2001. Recruitment of three species of juvenile rockfish (*Sebastes* spp.) on soft benthic habitat in Monterey Bay, California. Calif. Coop. Oceanic Fish. Invest. Rep. 42:153–166.

Keister, J. E., T. B. Johnson, C. A. Morgan, and W. T. Peterson.
2005. Biological indicators of the timing and direction of warm-water advection during the 1997/1998 El Niño off the central Oregon coast, USA. Mar. Ecol. Prog. Ser. 295:43–48.

Larson, R. J., W. H. Lenarz, and S. Ralston.
1994. The distribution of pelagic juvenile rockfish of the genus *Sebastes* in the upwelling region off central California. Calif. Coop. Oceanic Fish. Invest. Rep. 35:175–221.

Lenarz, W. H., R. J. Larson, and S. Ralston.
1991. Depth distributions of late larvae and pelagic juveniles of some fishes of the California Current. Calif. Coop. Oceanic Fish. Invest. Rep. 32:41–46.

Lenarz, W. H., F. B. Schwing, D. A. VenTresca, F. Chavez, and W. M. Graham.
1995. Explorations of El Niño events and associated biological population dynamics off central California. Calif. Coop. Oceanic Fish. Invest. Rep. 36:106–119

Love, M. S., M. Yoklavich, and L. Thorsteinson.
2002. The rockfishes of the northeast Pacific, 405 p. Univ. California Press, Berkeley, CA.

Mason, J.
1998. Declining rockfish lengths in the Monterey Bay, California, recreational fishery, 1959–94. Mar. Fish. Rev. 60:15–28.

Matthews, K. R.
1989. A comparative study of habitat use by young-of-the-year, subadult, and adult rockfishes on four habitat types in central Puget Sound. Fish. Bull. 88:223–239.

Mearns, A. J., M. J. Allen, M. D. Moore, and M. J. Sherwood.
1980. Distribution, abundance, and recruitment of soft-bottom rockfishes (Scorpaenidae: *Sebastes*) on the southern California mainland shelf. Calif. Coop. Oceanic Fish. Invest. Rep. 21:180–190.

Moser, H. G., R. L. Charter, W. Watson, D. A. Ambrose, J. L. Butler, S. R. Charter, and E. M. Sandknop.
2000. Abundance and distribution of rockfish (*Sebastes*) larvae in the Southern California Bight in relation to environmental conditions and fishery exploitation. Calif. Coop. Oceanic Fish. Invest. Rep. 41:132–147.

Mullin, M. M., and A. Conversi.
1989. Biomasses of euphausiids and smaller zooplankton in the California Current—geographic and interannual comparisons relative to the Pacific whiting, *Merluccius productus*, fishery. Fish. Bull. 87:633–644.

Pastén, G. P., S. Katayama, and M. Omori.
2003. Timing of parturition, planktonic duration, and settlement patterns of the black rockfish, *Sebastes inermis*. Environ. Biol. Fish. 68:229–239.

Ralston, S., and D. F. Howard.
1995. On the development of year-class strength and cohort variability in two northern California rockfishes. Fish. Bull. 93:710–720.

Ralston, S., and J. N. Ianelli.
1998. When lengths are better than ages: the complex case of bocaccio. *In* Fishery stock assessment models: proceedings of the international symposium on fishery stock assessment models for the 21st century (October 8–11, 1997, Anchorage, Alaska) (F. Funk, T. J. Quinn II, J. Heifetz, J. N. Ianelli, J. E. Powers, J. F. Schweigert, P. J. Sullivan, and C.-I. Zhang, eds.), p. 451–468. Lowell Wakefield Fisheries Symposium No. 15. Univ. Alaska Sea Grant College Program AK-SG-98-01, Fairbanks, AK.

Rebstock, G. A.
2001. Long-term stability of species composition in calanoid copepods off southern California. Mar. Ecol. Prog. Ser. 215:213–224.

Reilly, C. A., T. Wyllie Echeverria, and S. Ralston.
1992. Interannual variation and overlap in the diets of pelagic juvenile rockfish (genus:*Sebastes*) off central California. Fish. Bull. 90:505–515.

Rosenfeld, L. K., F. B. Schwing, N. Garfield, and D. E. Tracy.
1994. Bifurcated flow from an upwelling center: a cold water source for Monterey Bay. Continental Shelf Res. 14:931–964.

Shaffer, J. A., D. C. Doty, R. M. Buckley, and J. E. West.
1995. Crustacean community composition and trophic use of the drift vegetation habitat by juvenile splitnose rockfish, *Sebastes diploproa*. Mar. Ecol. Prog. Ser. 123:13–21.

Stephens, J. S. Jr., P. A. Morris, K. Zerba, and M. Love.
1984. Factors affecting fish diversity on a temperate reef: the fish assemblage of Palos Verde Point, 1974–1981. Environ. Biol. Fish. 11:259–275.

VenTresca, D. A., R. H. Parrish, J. L. Houk, M. L. Gingras, S. D. Short, N. L. Crane.
1995. El Niño effects on the somatic and reproductive condition of blue rockfish, *Sebastes mystinus*. Calif. Coop. Oceanic Fish. Invest. Rep. 36:167–174.

Yoklavich, M. M., V. J. Loeb, M. Nishimoto, and B. Daly.
1996. Nearshore assemblages of larval rockfishes and their physical environment off central California during an extended El Niño event, 1991–1993. Fish. Bull. 94: 766–782.

The potential use of time-area closures to reduce catches of bigeye tuna (*Thunnus obesus*) in the purse-seine fishery of the eastern Pacific Ocean

Shelton J. Harley (contact author)

Jenny M. Suter

Inter-American Tropical Tuna Commission
8604 La Jolla Shores Drive
La Jolla, California, 92037–1508
Present address for S. J. Harley: Ministry of Fisheries
PO Box 1020
Wellington, New Zealand
Email address for S. J. Harley: harleys@fish.govt.nz

Abstract—Skipjack (*Katsuwonus pelamis*), yellowfin (*Thunnus albacares*), and bigeye (*Thunnus obesus*) tunas are caught by purse-seine vessels in the eastern Pacific Ocean (EPO). Although there is no evidence to indicate that current levels of fishing-induced mortality will affect the sustainability of skipjack or yellowfin tunas, fishing mortality on juvenile (younger than 5 years of age) bigeye tuna has increased, and overall fishing mortality is greater than that necessary to produce the maximum sustainable yield of this species. We investigated whether time-area closures have the potential to reduce purse-seine bigeye catches without significantly reducing skipjack catches. Using catch and effort data for 1995–2002, we identified regions where the ratio of bigeye to skipjack tuna catches was high and applied simple closed-area models to investigate the possible benefits of time-area closures. We estimated that the most optimistic and operationally feasible 3-month closures, covering the equatorial region of the EPO during the third quarter of the year, could reduce bigeye catches by 11.5%, while reducing skipjack tuna catches by 4.3%. Because this level of bigeye tuna catch reduction is insufficient to address sustainability concerns, and larger and longer closures would reduce catches of this species signficantly, we recommend that future research be directed toward gear technology solutions because these have been successful in many other fisheries. In particular, because over 50% of purse-seine catches of bigeye tuna are taken in sets in which bigeye tuna are the dominant species, methods to allow the determination of the species composition of aggregations around floating objects may be important.

Manuscript submitted 2 April 2004 to the Scientific Editor's Office.

Manuscript approved for publication 5 April 2006 by the Scientific Editor.

Fish. Bull. 105:49–61 (2007).

The Inter-American Tropical Tuna Commission (IATTC) was established by an international convention in 1950 and is responsible for the conservation of tunas and management of fisheries for tunas and other species taken by tuna-fishing vessels in the eastern Pacific Ocean (EPO). Such conservation and management is accomplished by measures imposed by the nations participating in the fishery in response to recommendations by the scientific staff of the IATTC. Currently, the IATTC has adopted two measures to ensure the conservation of bigeye tuna in the EPO (IATTC[1]): catch limits for each longline fleet (based on their 2001 catch levels) and a series of closures for the purse-seine fleet. In this article, we examine the use of the temporary closure of a given area, referred to as a "time-area closure," for management of the purse-seine fishery.

Since the early 1990s, considerable purse-seine fishing effort in the EPO has been directed at tunas associated with floating objects, including man-made fish-aggregating devices (Lennert-Cody and Hall, 2000). The predominant species captured are skipjack (*Katsuwonus pelamis*), bigeye (*Thunnus obesus*), and yellowfin (*Thunnus albacares*) tunas. The floating-object (FOB) fishery has had no noticeable affect on skipjack tuna abundance (Maunder, 2002a) and little effect on yellowfin tuna because the catches of yellowfin tuna from the floating object fishery are small compared to the catches from other purse-seine fisheries (Maunder, 2002b). However, the FOB has led to a considerable increase in fishing mortality on juvenile bigeye tuna (Maunder and Harley, 2002; Harley et al., 2005).

The most recent bigeye tuna stock assessment (IATTC, 2004) has indicated that overall fishing effort should be reduced by at least 38% to allow the stock to produce the maximum sustainable yield (MSY). This assessment is based on a single EPO stock with no net migration between the eastern and western Pacific; however, a "Pacific-wide" assessment has provided a very similar picture of low movement rates for bigeye tuna in the EPO (Hampton et al.[2]).

Since the expansion of the FOB fishery, catches of bigeye tuna from the purse-seine fishery have exceeded those from the longline fishery in some years (Table 1). The bigeye tuna

[1] IATTC (Inter-American Tropical Tuna Commission). 2003. Resolution on the conservation of tuna in the eastern Pacific Ocean, 3 p. Resolution C-03-12, IATTC, 8604 La Jolla Shores Drive, La Jolla, California 92037.

[2] Hampton, J., P. Kleiber, Y. Takeuchi, H. Kurota, and M. Maunder. 2003. Stock assessment of bigeye tuna in the western and central Pacific Ocean, with comparisons to the entire Pacific Ocean, 81 p, SCTB16 BET-1. Sixteenth meeting of the standing committee on tuna and billfish, Mooloolaba, Queensland, Australia; 9–16 July 2003.

Table 1

Annual catches (metric tons) of bigeye (*Thunnus obesus*) and skipjack (*Katsuwonus pelamis*) tuna from purse-seine (PS) fisheries by set type (FOB=floating object associated school, UNA=tuna school unassociated with dolphins, and DOL=tuna school associated with dolphins) and longline fisheries from the eastern Pacific Ocean, east of 150°W, as used in the stock assessments.

	Bigeye tuna						Skipjack tuna					
Year	FOB	UNA	DOL	PS total	Longline total	Annual total	FOB	UNA	DOL	PS total	Longline total	Annual total
1990	3360	1351	0	4711	98,990	103,700	34,980	35,788	867	71,635	42	71,677
1991	1963	1739	38	3740	104,159	107,874	37,655	22,958	786	61,399	33	61,432
1992	1154	4343	0	5497	84,396	89,893	45,556	35,333	869	81,758	24	81,782
1993	6274	4724	134	11,132	72,351	80,420	48,144	34,865	714	83,723	63	83,786
1994	37,901	2624	0	40,525	71,360	100,734	47,992	22,916	516	71,424	69	71,493
1995	45,204	6291	0	51,495	58,076	95,403	81,253	50,715	1032	133,000	74	133,074
1996	66,568	4280	0	70,848	46,771	98,124	74,260	34,635	729	109,624	40	109,664
1997	69,293	1868	48	71,209	52,078	103,693	123,002	29,510	6004	158,516	94	158,610
1998	43,226	5183	91	48,500	45,632	80,787	115,370	25,108	2879	143,357	65	143,422
1999	49,452	6574	0	56,026	32,565	73,176	178,824	84,036	1214	264,074	94	264,168
2000	83,489	3266	0	86,755	46,424	116,579	116,508	81,551	440	198,499	29	211,049
2001	56,753	1273	14	58,040	60,572	103,421	115,571	20,163	1218	136,952	61	144,949
2002	61,230	1166	0	62,396	68,195	103,394	118,485	32,471	2093	153,048	145	157,593

caught in the longline fishery are larger (110–160 cm) and considerably more valuable than the smaller bigeye tuna (50–80 cm) caught mostly by the purse-seine fishery.

Improving the long-term sustainability of the bigeye tuna fisheries could be achieved by reducing the fishing mortality of the smaller individuals that are caught predominantly in the FOB fishery. Annual catches of skipjack tuna from the purse-seine fishery in the EPO are larger and more economically important than those of bigeye tuna (Table 1). Furthermore, there are no concerns regarding sustainability of the skipjack tuna population in the EPO (Maunder, 2002a). Thus, bigeye tuna caught by the FOB fishery are essentially bycatch of the targeted skipjack tuna fishery; thus determining a mechanism by which the catches of bigeye tuna are reduced while minimizing losses in the catches of skipjack tuna is an important management issue.

Hall (1996) argued that to understand and solve bycatch problems it is important to classify the problem by a number of factors (e.g., time, space, and the level of control that fishermen have). With this information, there are many potential tools that can be used by fisheries managers to reduce fishing mortality, e.g., gear regulations, catch limits, closed seasons, and closed areas (Beverton and Holt, 1957). Time and area closures (time-area closures) are recommended as a means to reduce catches of sharks (Baum et al., 2003), protect billfishes from exploitation by the longline fishery (Goodyear, 1999), and protect biodiversity hotspots (Worm et al., 2003). Although time-area closures are not particularly appropriate for fisheries managed under quota systems, they may be beneficial for effort-managed fisheries (Horwood et al., 1998) or fisheries targeting multispecies (Hilborn et al., 2004), such as those for tunas in the EPO.

In this study, we investigated the potential of time-area closures to reduce bigeye tuna catches while minimizing impacts on the catches of skipjack tuna. In contrast to common closure-strategy studies, i.e., those studies devoted to fisheries targeting a single species, we investigated the potential impacts of time-area closures on two species: a large and highly productive skipjack tuna stock, and a considerably smaller and less productive bigeye tuna stock.

We used catch and effort data from the purse-seine fishery to search for potential time-area hotspots for bigeye catches and then applied simple "in-sample" closed-area models to predict the potential impact of closures of these areas. We discuss the likely use of such closures in the light of our findings, alternative management actions that could possibly reduce bigeye tuna catches, and finally, the strengths and weaknesses of the approach used for the closed-area models.

Although yellowfin tuna form an important part of the purse-seine fishery in the EPO, where annual catches are greater than those for bigeye and skipjack tuna combined, we did not consider them in our analysis. Within the EPO purse-seine fishery there are essentially two fleets: one targets yellowfin tuna schools associated with dolphins or schools not associated dolphins and the other targets mainly skipjack tuna associated with floating objects. In our study, we focused on the second fleet and there are many reasons to believe that effort could not be transferred from one fleet to the other, e.g. markets, technological differences (the vessels require different equipment), geographical

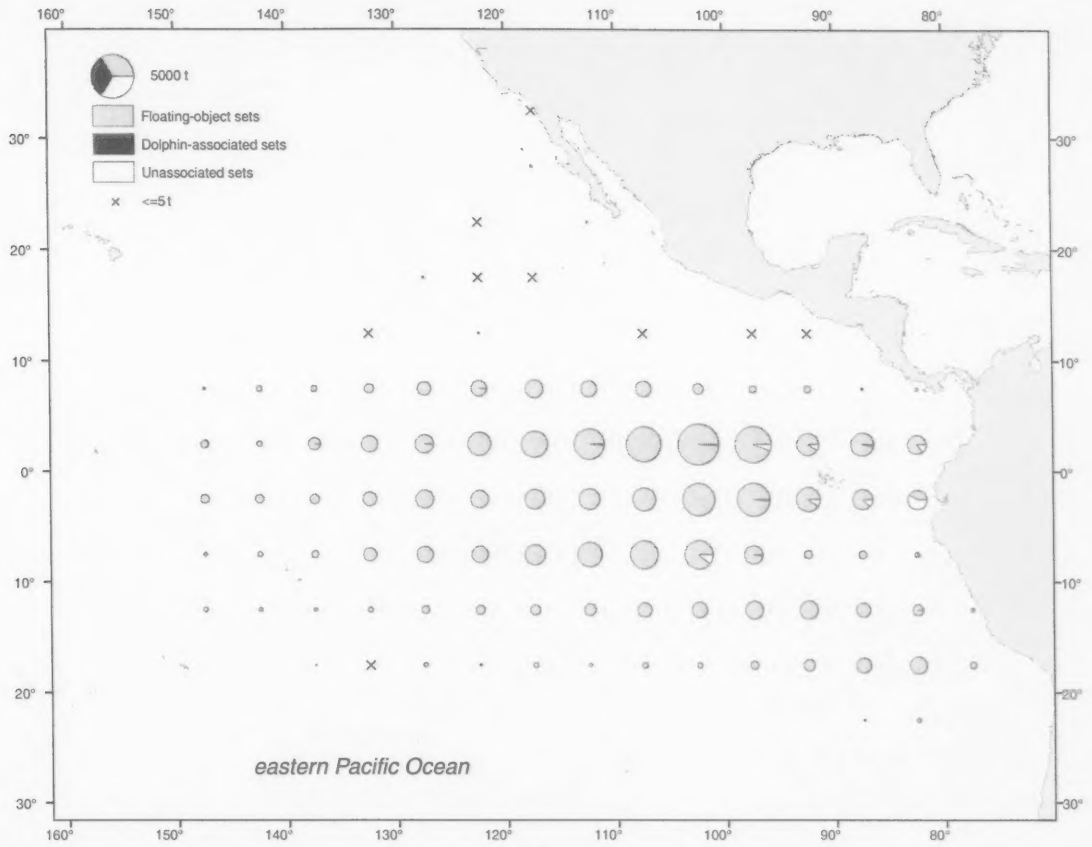

Figure 1

Average annual distribution of the purse-seine catches of bigeye tuna (*Thunnus obesus*), by set type and 5-degree latitude by 5-degree longitude area, in the eastern Pacific Ocean, 1995–2002. The size of the circles is proportional to the catch in each area.

(the fisheries have limited spatial overlap), and restrictions on dolphin mortality limits. In addition, only a small proportion (about 10%) of the purse-seine catches of yellowfin tuna are taken in floating-object sets. Later we discuss extensions to our analysis to include not only yellowfin tuna, but a range of bycatch species taken in the different purse-seine fisheries.

Materials and methods

Data

We used set-by-set catch and effort data from purse-seine vessels that operate in the EPO. The majority of the data was obtained by scientific observers. In the absence of observer data, we used records from the logbooks of the vessels. Data were grouped by 5-degree latitude by 5-degree longitude areas (hereon referred to as 5°×5°areas) by seasonal quarter. The FOB fishery, which is responsible for over 90% of the purse-seine catches of bigeye tuna, was in an expansion phase during 1992–94; therefore we restricted our attention to data for 1995–2002 (Table 1). Because very small amounts of bigeye and skipjack tuna are caught in dolphin-associated (DOL) sets, we excluded these from the analysis and instead focused on sets of tuna associated with floating objects and sets on schools not associated (UNA) with dolphins. For 1995–2002, these two set types were responsible for over 99% of bigeye and skipjack tuna catches from the purse-seine fishery (IATTC, 2004). These two set types were combined in the closed-area model because it was possible to switch effort between those two types of sets. The spatial distribution of catches by set type for bigeye and skipjack tuna are provided in Figures 1 and 2.

Definition of "hotspot"

In defining the spatial and temporal extent of the bigeye catches, we looked for areas where the ratio of bigeye to

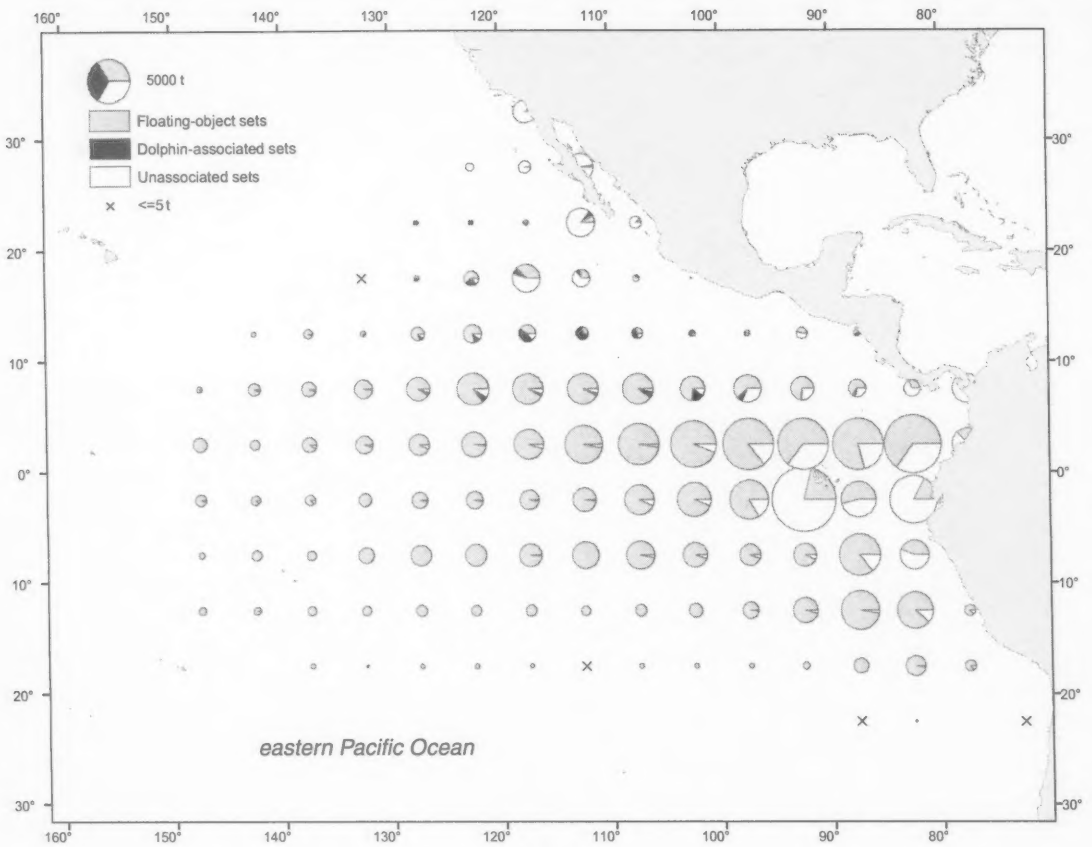

Figure 2

Average annual distribution of the purse-seine catches of skipjack tuna (*Katsuwonus pelamis*), by set type, in the eastern Pacific Ocean, 1995–2002.

skipjack tuna catches was high, rather than just areas of high bigeye tuna catches, because we wanted areas where the losses in skipjack tuna catches would be minimized. We chose 5°×5° areas by quarter of the year as the scale for the individual hotspots.

We defined an index for each time-area strata for each year. The index was a ratio of bigeye tuna catch to skipjack tuna catch that was robust to annual fluctuations in the abundance of either species. We then summed the annual indices over the time period to find areas that consistently resulted in high bigeye to skipjack tuna ratios. The indices were calculated separately for each year so that they were not dominated by data from years with exceptionally high or low catches of either species.

The data used for this and the closed-area analysis were the following:

$B_{i,j,t}$ = bigeye catch in quarter i in area j in year t;
$S_{i,j,t}$ = skipjack catch in quarter i in area j in year t.

We standardized catches within a year on the basis of the median catch of the year.

$$b_{i,j,t} = B_{i,j,t}/\text{median}(B_{\ldots,t});$$
$$s_{i,j,t} = S_{i,j,t}/\text{median}(S_{\ldots,t}).$$

The location of hotspots did not differ noticeably if we standardized by the mean or total catch for each year, rather than the median.

Using the standardized catches, we defined the annual index for a single 5°×5°area by quarter, $\theta_{i,j,t}$ as

$$\theta_{i,j,t} = \begin{cases} 0 & \text{where} \quad b_{i,j,t} = 0 \\ 1 & \text{where} \quad s_{i,j,t} = 0 \\ f(b_{i,j,t}, s_{i,j,t}) & \text{otherwise} \end{cases} \quad (1)$$

$$\text{where } f(b_{i,j,t}s_{i,j,t}) = \frac{b_{i,j,t}/s_{i,j,t} - \min(b_{i,j,t}/s_{i,j,t})}{\max(b_{i,j,t}/s_{i,j,t}) - \min(b_{i,j,t}/s_{i,j,t})}. \quad (2)$$

Note that the index is scaled to be between 0 and 1, and the larger values within this range were associated with greater bigeye-skipjack ratios. To obtain an overview of the hotspots over the 1995–2002 period we summed the annual indices

$$\tilde{\theta}_{i,j} = \sum_{t=1995}^{t=2002} \theta_{i,j}. \quad (3)$$

We defined hotspots as those time-area regions where the summed index was in the top 20% of the values.

Closed-area model

The basic model is summarized in four steps:

1 Choose an area to close in a given time period.
2 Re-allocate effort from the chosen area during the period of the closure to other areas in proportion to the effort in each area. Leave the effort outside the closure period unchanged.
3 Calculate the new catch of each species expected in each area based on the new effort and catch per unit of effort (CPUE) for each species in each area.
4 Compare new annual catches to original catches.

The possible consequences of these assumptions and alternative modeling approaches are detailed in the discussion.

The data used for the closed-area analysis were similar to those used in the hotspot analysis. The definitions of catches remained the same (e.g., $B_{i,j,t}$), although the spatial strata reflected by j differed, depending on the closure considered.

We incorporated effort in terms of the number of sets, $E_{i,j,t}$, and defined the CPUE of bigeye and skipjack tuna in tons per set,

$$U^b_{i,j,t} = \frac{B_{i,j,t}}{E_{i,j,t}} \quad (4)$$

and

$$U^s_{i,j,t} = \frac{S_{i,j,t}}{E_{i,j,t}}. \quad (5)$$

We allocated effort from a time-area closure (i=x and j=y) to the remaining areas in that time period on the basis of proportion of effort in each area ($P_{i,j,t}$) (excluding the closed area) e.g.,

$$P_{i,j,t|i=x,j\neq y} = \frac{E_{i,j,t}}{\sum_{i=x,j\neq y} E_{i,j,t}}. \quad (6)$$

For each time-area closure we determined the new effort allocation, $E_{i,j,t|x,y}$, as

$$E_{i,j,t|x,y} = \begin{cases} 0 & \text{where } i = x \text{ and } j = y \\ E_{i,j,t} + E_{x,y,t} \cdot P_{i,j,t|x,y} & \text{where } i = x \text{ and } j \neq y. \\ E_{i,j,t} & \text{where } i = x \end{cases} \quad (7)$$

The new catch for each time-area closure was estimated as the new effort multiplied by the original CPUE:

$$B_{i,j,t/x,y} = E_{i,j,t|x,y} \cdot U^b_{i,j,t} \quad (8)$$

and

$$S_{i,j,t/x,y} = E_{i,j,t|x,y} \cdot U^s_{i,j,t}. \quad (9)$$

because it was assumed that CPUE in an area will not change when additional effort is added with closure.

The summary statistic for each simulated closure was the percentage change in bigeye and skipjack tuna catches, compared to the catches observed in the absence of a closure.

$$\Delta B_{x,y,t} = \frac{\sum_{i,j} B_{i,j,t|x,y} - \sum_{i,j} B_{i,j,t}}{\sum_{i,j} B_{i,j,t}} \times 100 \quad (10)$$

and

$$\Delta S_{x,y,t} = \frac{\sum_{i,j} S_{i,j,t|x,y} - \sum_{i,j} S_{i,j,t}}{\sum_{i,j} S_{i,j,t}} \times 100. \quad (11)$$

We repeated the calculations for the catch and effort data in each year (1995–2002) to consider the potential variability in the effect of a closure due to interannual variation in the spatial distribution of fish and fishing effort.

In addition to the model described above, we also considered a "two set-type" model in which FOB and UNA sets were redistributed separately (i.e., we did not allow switching between set types). Although this model gave very similar results, it was probably less realistic; therefore the results are not presented here.

Simulated closures

We compared the performance of two closed areas for each quarter and year. The first closed area corresponded to the hotspots (those 5°×5° areas for a quarter for which $\tilde{\theta}_{i,j,t}$ was in the top 20%) associated with each quarter. A closure of the hotspots should be optimal in the sense of reducing bigeye tuna catch with minimal impact on skipjack tuna catch but may not be practical from a management perspective because the 5°×5° areas are not continuous. The second closed area approximated the hotspot closure, but it was a more practical, continuous region. It extended from 5°N–10°S, to 90°–120°W. The total area of this closure was the same as the total area of the hotspot regions. We refer to this as the practical closure. In each case, effort during the closure period was redistributed between two areas, one north and one south of the equator, in proportion to the effort in each open area. Summaries of the effort and CPUE data, stratified by the areas that we used in the practical closure analysis, are provided in Table 2.

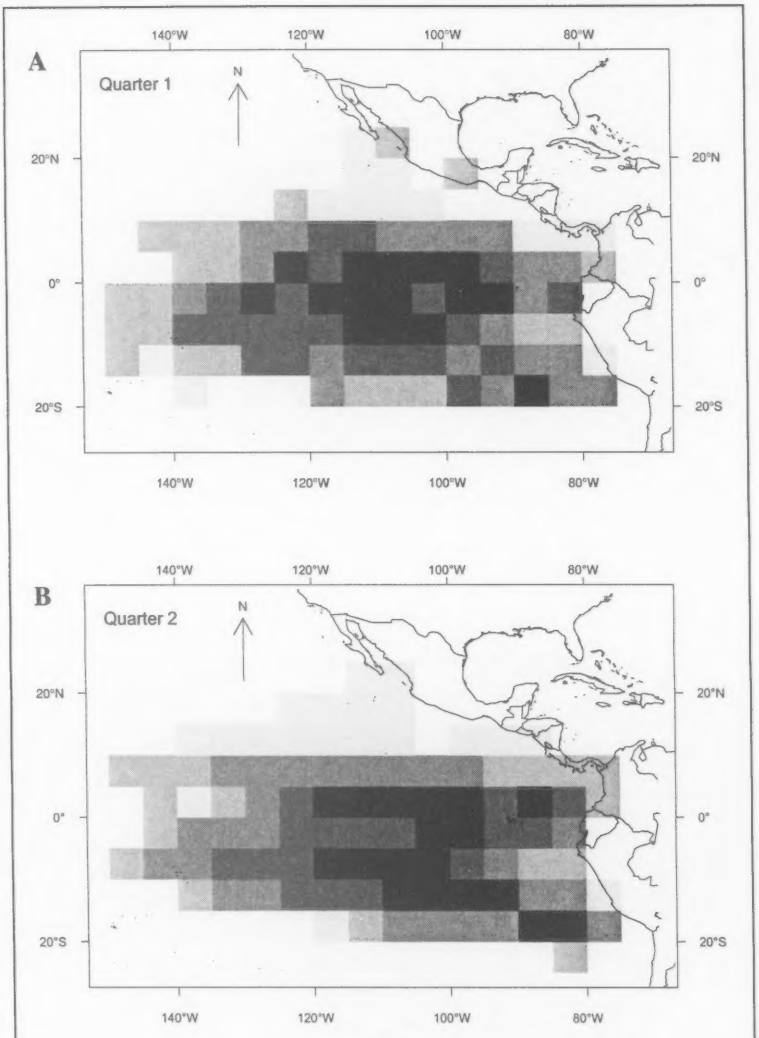

Figure 3

Hotspots of bigeye tuna (*Thunnus obesus*) catches in relation to skipjack tuna (*Katsuwonus pelamis*) catches by seasonal quarter and 5°×5° region for 1995–2002 as measured by our hotspot index (Equations 1–3). Plots **A–D** represent quarters 1–4. Shades are used for different percentiles of the index, and darker regions indicate areas of higher bycatch rates. The black regions represent those time and area strata for which the hotspot index was in the top 20%.

Results

Hotspots

The hotspots were not evenly spread over the year; the third seasonal quarter contained more 5°×5° hotspots (24) than the other quarters (15–18 each) (Fig. 3). During quarters 1 and 4, most of the hotspots were located between 5°N and 10°S, whereas during quarters 2 and 3, the hotspots extended south to 15°S. Over all time-area strata, 90% of the hotspots were west of 90°W and east of 135°W, and over 95% were between 5°N and 15°S—indicating that the hotspots are found within a fairly restricted area.

When we compared the hotspots to the practical closure, 75% of the hotspots were found within the prac-

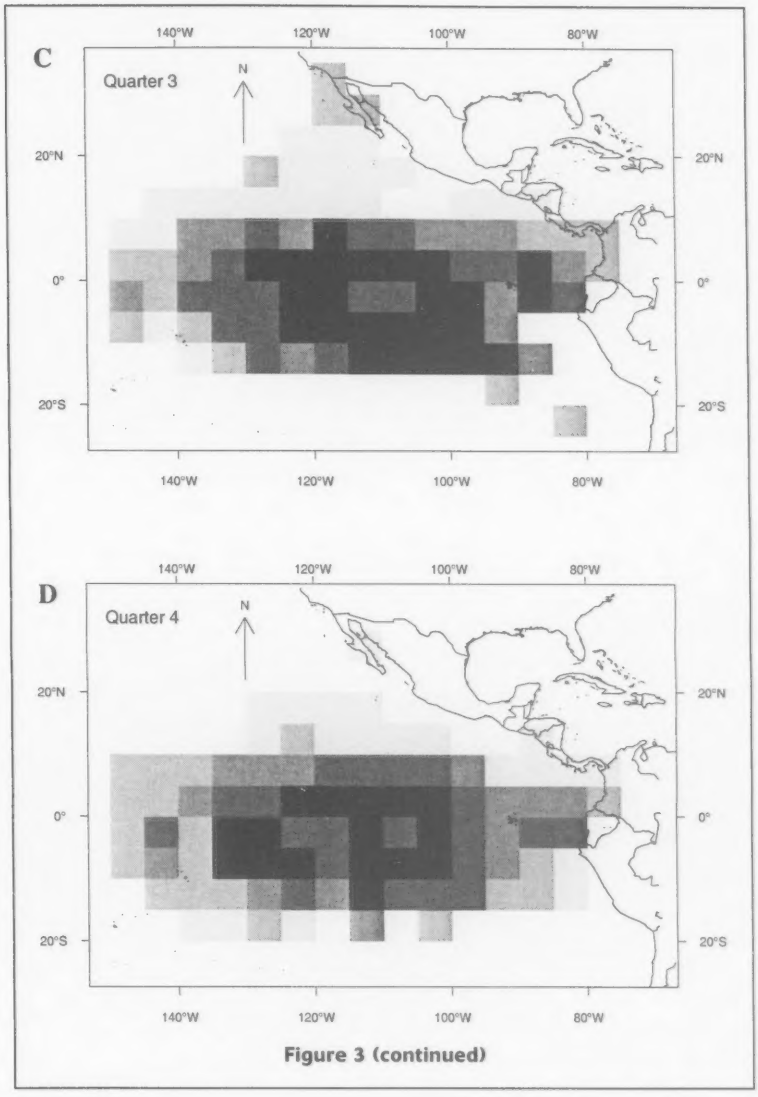

Figure 3 (continued)

tical closure area. Of the remaining 25% of hotspots, most were west of 120°W.

Time-area simulations

Over all years and quarters, the predicted decrease in bigeye tuna catches associated with the hotspot closure ranged from 2.8% to 23.7%, whereas the change in skipjack tuna catches ranged from a 0.9% increase to a 14.1% reduction (Fig. 4). The greatest reductions in bigeye tuna catch were associated with second- and third-quarter closures (mean reduction=14.6%). The mean reductions in skipjack tuna catches did not vary much across quarters (means ranged from 2.8% to 3.7%). For several years, there was little or no predicted reduction in skipjack tuna catch associated with a hotspot closure. Based on the median of the ratios, the greatest contrast between bigeye and skipjack tuna catch reductions was associated with a third quarter closure; the average percentage reduction in bigeye tuna catch was 14.6%, versus 2.8% for skipjack tuna. The performance of second-quarter closures was similar to that of third-quarter closures, but the former was much more variable across years.

The performance of the practical closure was generally similar to that of the hotspot closure. Over all years and

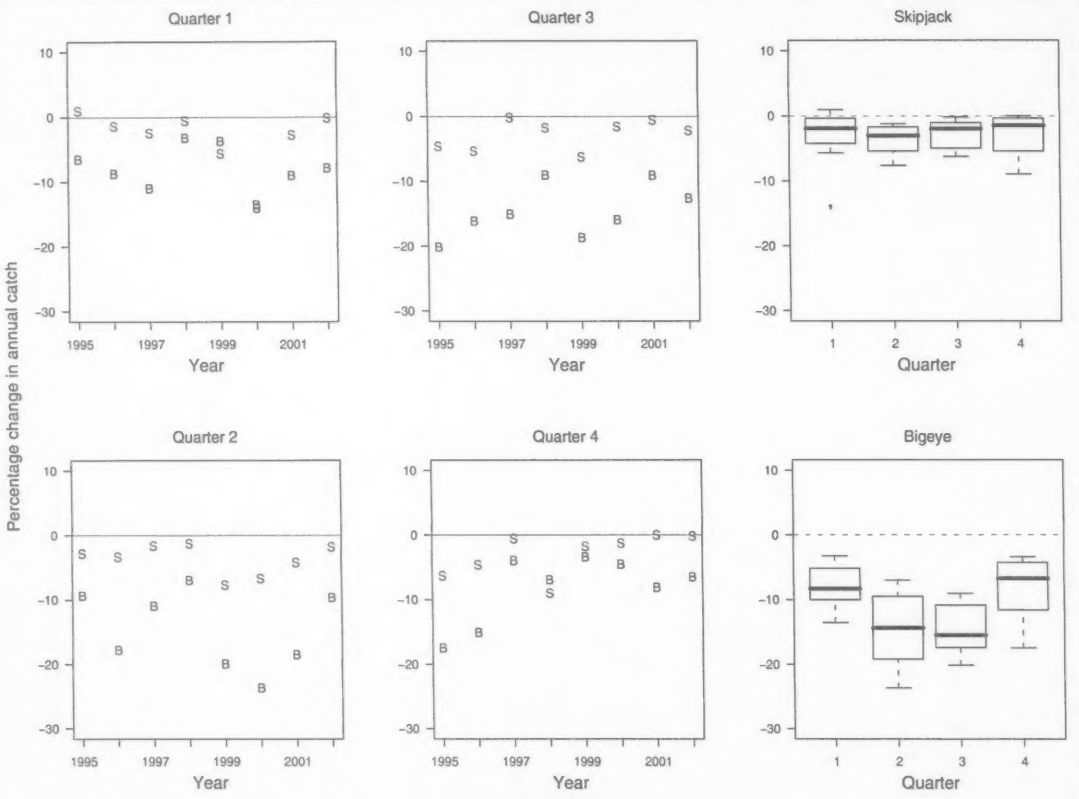

Figure 4

Predicted changes in annual purse-seine catches of bigeye (*Thunnus obesus*) and skipjack (*Katsuwonus pelamis*) tuna associated with a closure of the hotspot areas from Figure 1 for each quarter of the year. The left and middle panels indicate the change in annual catch for bigeye (B) and skipjack (S) tuna estimated to occur in each year of the 1995–2002 period if that area was closed in the 1st, 2nd, 3rd, and 4th quarter, respectively. The plots on the right summarize the predicted changes in bigeye and skipjack tuna catch over the eight years for a closure in each seasonal quarter. The white bar indicates the median change, the dark rectangle indicates the interquartile range (25th–75th percentiles), and the outer lines indicate the extremes. The horizontal dashed line represents zero (i.e., no change in catch).

Table 2

Summary of annual purse-seine effort and catch per unit of effort for bigeye (*Thunnus obesus*) and skipjack (*Katsuwonus pelamis*) tuna by set type (FOB=tuna school associated with floating object(s); UNA=tuna school not unassociated with floating object(s)) for the three areas modeled in the "practical" closure. A "practical" was a more practical, continuous region. It extended from 5°N–10°S, to 90°–120°W. The total area of this closure was the same as the total area of the hotspot regions. The means and standard deviations (SD) were calculated from annual values for 1995–2002.

		Number of sets		Bigeye catch per set		Skipjack catch per set	
Area		FOB	UNA	FOB	UNA	FOB	UNA
Practical closure	Mean	532	229	14.75	0.9	21.64	9.97
	SD	228	295	7	1.27	9.9	8.61
North	Mean	474	882	4.4	0.1	19.42	5.65
	SD	301	517	2.53	0.12	10.19	4.17
South	Mean	404	296	10.43	0.44	17.43	5.48
	SD	377	278	6.35	0.53	7.4	5.14

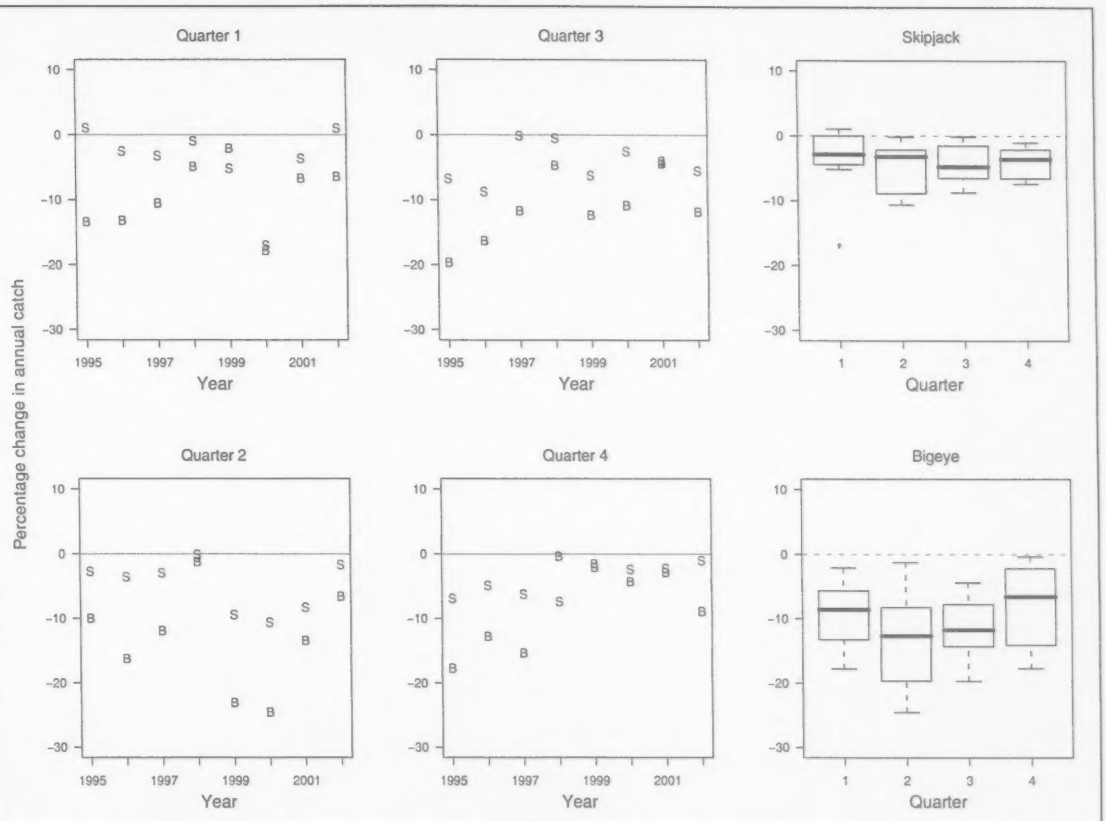

Figure 5

Predicted changes in annual purse-seine catches of bigeye (*Thunnus obesus*) and skipjack (*Katsuwonus pelamis*) tuna associated with a closure of the area between 5°N–10°S and 90°–120°W for each quarter of the year. See Figure 4 for further description of the panels.

quarters, the predicted reductions in bigeye tuna catches associated with the practical closure ranged from 0.3% to 24.5% (777 metric tons [t] to 20,206 t), and the change in skipjack tuna catches ranged from a 1.1% increase to a 17.0% reduction (1204 t to 32,773 t) (Fig. 5). The extreme values of skipjack tuna catch were associated with first-quarter closures. As with the hotspot closure, the greatest reductions in bigeye tuna catch were associated with second- and third-quarter closures (average reductions of 13.4% and 11.5%, respectively, across years) and again the mean reduction in skipjack tuna catches did not vary greatly across quarters (mean reductions ranging from 3.8% to 4.9%). Based on the median of the ratios, the greatest contrast between bigeye and skipjack tuna reductions was associated with a second-quarter closure; the average percentage reduction in bigeye tuna catches was 13.4%, versus 4.9% for skipjack tuna catches.

Overall, the hotspot closure predicted slightly greater reductions in bigeye tuna catches and slightly lesser reductions in skipjack tuna catches than did the practical closure, but the difference in the median of the ratios (5.0 times for the hotspot closure and 3.8 times for the practical closure) is probably not significant. Results for both closures may indicate that a closure during the second or third quarters is optimal. Because the predicted variability in performance was less for a third-quarter closure than a second-quarter closure (in both analyses), the former was preferred as a management tool.

Discussion

Time-area closures are one of a number of fisheries management options (Hilborn et al., 2004). In our study we investigated, using simulations that use historical catch and effort data, whether time-area closures could be a useful tool to reduce bigeye tuna catches in the purse-seine fishery without leading to large reductions in the catches of skipjack tuna.

In the remainder of this article we discuss our findings in terms of the recent stock assessment recommendations for reductions in fishing effort—more specifically whether reductions predicted in our study would be sufficient to reach management objectives. We also discuss alternative measures for reducing bigeye tuna catches in the purse-seine fisheries of the EPO and describe potential improvements for our time-area closure modeling approach that may lead to a more accurate analysis of the likely performance of closures that may be considered in the future.

Predicting performance of time-area closures

Following Hall (1996), we looked for time-area strata in which there were high bigeye tuna to skipjack tuna ratios. These areas were relatively confined geographically and did not vary greatly by quarter. For this reason, the hotspot and practical closures predicted similar results.

Simulation of a practical closure (and one that able to be implemented) indicated that moderate average reductions in bigeye tuna catch (11.5%) could be achieved with lesser average reductions in skipjack tuna catches (4.9%). When we considered these reductions in terms of total catch by weight, the annual bigeye tuna catch reductions ranged up to 20,206 t (average 5722 t) and up to 32,773 t (average 6,807 t) for skipjack tuna.

Based on the current mix of fishing gears in the bigeye tuna fisheries in the EPO, and the estimated maximum sustainable yield (MSY) of about 77,000 t (IATTC, 2004), the purse-seine share of the MSY was around 40,000 t (S. J. Harley, unpubl. data). Considering current purse-seine catches of over 60,000 t, and the 11.5% reduction predicted for the practical closure, we believe that these closures alone are unlikely to yield the required reductions in bigeye tuna catches from the purse-seine fishery.

The closures investigated in our study were based on strata where the ratio of bigeye tuna to skipjack tuna catches was the greatest. For these closures, the reduction in catches (in metric tons) is about the same for bigeye and skipjack tuna, but if a closure is larger or longer, the losses in skipjack catches would quickly outweigh the reductions in bigeye tuna catches. Therefore, although we did not examine larger or longer closures in our study, it is unlikely that these closures could lead to the necessary reductions in bigeye tuna catches without unacceptable losses in skipjack tuna catches.

Table 3

Proportion of the annual floating-object fishery catches of bigeye (*Thunnus obesus*) and skipjack (*Katsuwonus pelamis*) tuna that are caught in sets with or without other species.

	Bigeye tuna		Skipjack tuna	
Year	Without	With	Without	With
1995	0.05	0.95	0.31	0.69
1996	0.06	0.94	0.25	0.75
1997	0.05	0.95	0.25	0.75
1998	0.04	0.96	0.27	0.73
1999	0.02	0.98	0.39	0.61
2000	0.08	0.92	0.38	0.62
2001	0.11	0.89	0.44	0.56
2002	0.08	0.92	0.29	0.71
Average	0.06	0.94	0.32	0.68

The lack of effectiveness of the time-area closures is related to the extent of the interaction between skipjack and bigeye tunas. For the 1995–2002 period, 94% of the bigeye tuna caught by purse-seiners was taken in sets that also caught skipjack tuna (Table 3). This percentage is greater than the proportion of skipjack tuna catch that was taken in association with bigeye tuna (68%). Given this fact, it is not surprising that time-area closures are insufficient.

Management alternatives to reduce catches of bigeye tuna

We have shown that time-area closures alone are unlikely to result in the necessary reductions in fishing mortality for bigeye tuna; therefore alternative or supplementary management actions would be appropriate. In many instances, studies of fish behavior (Wardle, 1983) and gear technology (Larsen and Isaksen, 1993) have led to changes in gear configurations and deployment, resulting in significant reductions of catches of unwanted species. A good example of this type of change is the reduction of dolphin catch from tuna-dolphin aggregations in the EPO (NRC, 1997).

In the 1970s, many thousands of dolphins (mostly *Stenella* sp. and *Delphinus* sp.) were caught and killed by purse-seine vessels that set on dolphins in order to catch the yellowfin tuna that were associated with them (NRC, 1997). Through the introduction of fine-mesh net panels, use of a "back-down" procedure, and the avoidance of areas where oceanographic conditions could lead to net collapse, this mortality was reduced dramatically by the 1990s (NRC, 1997).

It is also possible to exploit behavioral differences among fish species. Through examination of the differential behavior of cod (*Gadus morhua*) and haddock (*Melanogrammus aeglefinus*), it was found that it was possible to configure bottom trawl nets to catch the target species and allow the other species to escape through larger meshes (Cotter et al., 1997). Sorting grids have also been used to allow the escape of unwanted species (Larsen and Isaksen, 1993; Misund and Beltestad[3]; IATTC[4]). Unless studies of bigeye and skipjack tuna be-

[3] Misund, O. A., and A. K. Beltestad. 1994. Size-selection of mackerel and saithe in purse seine. International Council for the Exploration of the Sea Council Meeting, 1994/B:28.

[4] IATTC (Inter-American Tropical Tuna Commission). 1999. Report of the bycatch working group, 25 p. 63rd Meeting of the IATTC; June 8–10, 1999. IATTC, 8604 La Jolla Shore Drive, La Jolla, California 92037.

havior determine a mechanism by which bigeye, but not skipjack tuna, can escape through a sorting grid in a purse-seine net, sorting grids are more likely to be useful for overall reductions in catches of small tunas than as a mechanism for reducing bigeye tuna catches without reducing skipjack tuna catches.

Lennert-Cody and Hall (2000) used a range of statistical models to determine factors (e.g., area, season, characteristics of the floating object and the purse-seine net) that were associated with higher catches of bigeye and skipjack tuna. Unfortunately, many factors were confounded because the fishing practices of the fleet often differ in time and space, making it difficult to determine which gear characteristics may be important. Thus, it appears unlikely that analysis of fishery-collected data will lead to technical measures with the potential to reduce catches of bigeye tuna.

Although it may be difficult to determine important factors relating to bigeye tuna catch rates, fisheries data can be used to examine the nature of the catches of this species. For example, we found that 94% of bigeye tuna are caught in sets that also caught skipjack tuna. We were interested in how the bigeye tuna catches were distributed; were they predominantly from a small number of sets with high catches or from a large number of sets with small catches? Our analysis of this question, based on data for 1995–2002, is presented in Figure 6. It shows than only 5% of bigeye tuna were caught in single-species sets, but that about 50% of bigeye tuna came from sets that contained at least 60% of this species. These sets are responsible for only 7% of the skipjack tuna catch from the floating-object fishery and a smaller proportion of the overall skipjack catch given that about 30% of skipjack tuna catch is still taken from schools unassociated with dolphins (IATTC, 2004).

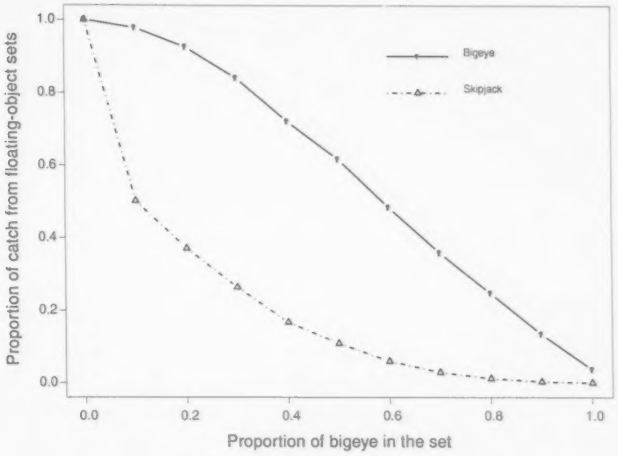

Figure 6

Proportion of bigeye (*Thunnus obesus*) and skipjack (*Katsuwomus pelamis*) tuna taken in sets where at least a given proportion of skipjack tuna were taken, for 1995–2002. For example, just over 60% of bigeye tuna came from sets where 50% or more of the tuna in the set was bigeye tuna, while only 15% of skipjack tuna were taken in these bigeye tuna dominated sets.

The analysis of the catch composition of purse-seine sets described above indicates that if fishing captains can determine, at least roughly, the species composition of an aggregation prior to setting (i.e., which species is dominant), large reductions in bigeye tuna catches could be achieved by not setting on bigeye-tuna–dominated aggregations. Such a measure would have little impact on overall skipjack tuna catches and would not require the fleet to be restricted in its activity by time-area closures.

Schaefer and Fuller (2005) used a range of electronic tags, supplemented with sonar images of fish aggregations around floating objects, to describe differences in the behavior of skipjack and bigeye tunas around floating objects. Exploitation of these differences, combined with the potential ability of fisherman to identify large aggregations of bigeye tuna around floating objects, may lead to the development of fishing practices that can reduce bigeye tuna catches with minimal impact on skipjack tuna catches.

Critical to this approach will be the establishment of incentives 1) to encourage both the identification of the schools and 2) not to set on bigeye-tuna–dominated aggregations. Similar to the dolphin mortality limits currently applied by the IATTC, it could also be possible to have individual vessel limits for bigeye tuna and let fishermen determine how best to modify their fishing operations in order to achieve a given limit. Harley et al.[5] used historical catch-by-vessel data and found that individual vessel limits of about 350 t would be sufficient to reduce purse-seine catches of bigeye tuna in the EPO by 50% in most years. Independent studies of fish behavior, coupled with experimental work investigating modifications in fishing practices and gear, could be fruitful.

Modeling potential effects of time-area closures

We applied simple closed-area models that used historical catch and effort data. Several assumptions are implicit in these models. First, we assumed that the fishing fleet has the flexibility to reallocate effort out-

[5] Harley, S. J., P. K. Tomlinson, and J. M. Suter. 2004. Possible utility of catch limits for individual purse-seine vessels to reduce fishing mortality on bigeye tuna in the eastern Pacific Ocean, 8 p. Inter-American Tropical Tuna Commission, 5th working group on stock assessments, 11–13 May 2004, Document SAR-5-05 BET A. IATTC, 8604 La Jolla Shore Drive, La Jolla, California 92037.

side the closed area. We redistributed effort during the closure to other areas in proportion to historical effort within the same seasonal quarter. Previous studies have chosen not to redistribute effort (Goodyear, 1999), to redistribute effort in proportion to target catch (Worm et al., 2003), or to redistribute effort with the assumption that catch, rather than effort, is a limiting factor (Baum et al., 2003). A good understanding of fleet dynamics is necessary to determine appropriate models for effort redistribution.

Second, we assumed that redistributed effort would yield the same CPUE as previous effort in the area. Redistributed effort assumes that CPUE will remain unchanged when more fish are removed. It is likely that CPUE would decline with abundance as a result of increased effort, therefore it is possible that our analysis overestimates the catches during the closure. Similarly, our model assumes that CPUE is constant within each area, i.e. regardless of where one fishes within the area, one achieves the same CPUE. In reality, it is possible that fishermen could fish close to the edge of the closed area and potentially undermine the effectiveness of a closure.

Related to these first two points is the case of switching between fishing modes. By grouping FOB and UNA sets in our model, we allowed for switching between set types when fishing outside the closed area. Harley et al.[4] showed that the purse-seine vessels that catch the majority of the bigeye tuna, fish almost exclusively on floating-objects (over 90% of the sets). Even with this information, we still believe that the implicit assumption of grouping the two set types is acceptable. We did not consider dolphin-associated sets (that catch almost exclusively yellowfin tuna). We consider it much less likely that effort would be shifted towards dolphin-associated schools for several factors, including politics, market pressure, technological and gear differences, and the inexperience that many skippers who participate in the FOB fishery would have with this alternative mode of fishing.

Finally, we implicitly assumed in our model that fish not caught as a result of the closure could not be caught later in the year. This assumption could lead us to underestimate catches outside of the closure. Thus, we have two potential biases in opposite directions that could affect our conclusions. The best way to quantify these biases would involve a model that integrated population and fisheries dynamics.

A dynamic approach to modeling closed areas could take into account the abundance of fish in different areas and the movement of fish between areas during the year. Modeling the relationship between effort and catches in different areas should include accounting for abundance (e.g., through the use of the catch equation).

Tagging data are necessary to estimate stock parameters, such as residence times within a closed area and fish movement rates between the open and closed areas. In addition to conventional tagging data, information from electronic tagging of bigeye tuna (Schaefer and Fuller, 2002) could provide a basis for describing movement by means of simple movement models (e.g., those of Adam et al. [2003]). Because the vessels catch bigeye and skipjack tunas together, the model must include the movement patterns of both species.

This approach is extremely data demanding, and many of the data for this approach are not yet available. Notwithstanding these problems, future analysis of time-area closures should include consideration of important biological factors such as those described above, as well as socioeconomic data that may be important for predicting fleet dynamics.

Another extension of the modeling approach in our study is to consider additional target and bycatch species. Worm et al. (2003) considered bycatch from the United States swordfish and tuna longline fisheries in the Atlantic when modeling closed areas. With this approach it would be useful to include not only yellowfin tuna and dolphin sets in the model, but also the bycatch species that are taken in the different areas and fisheries.

Conclusions

Time-area closures are one of the many management actions available for the regulation of fisheries. Because of the strong interactions between bigeye and skipjack tunas, we have shown that time-area closures alone are unlikely to be sufficient to address concerns regarding the sustainability of bigeye tuna because it may not be possible to achieve the necessary reductions in bigeye tuna catches without large losses in skipjack tuna catches. We suggest that it will be important to investigate aspects of fish behavior to determine measures that could be used either in conjunction with, or instead of, closures to help reduce mortality on juvenile bigeye tuna while sustaining the important skipjack fishery.

Acknowledgments

We thank R. Allen, W. Bayliff, R. Deriso, and three anonymous reviewers for comments on this manuscript, and M. Hall, C. Lennert-Cody, M. Maunder, and K. Schaefer for useful discussions of closed areas and management options for bigeye tuna.

Literature cited

Adam, M. S., J. Sibert, and D. Itano.
2003. Dynamics of bigeye (*Thunnus obesus*) and yellowfin (*T. albacares*) tuna in Hawaii's pelagic fisheries: analysis of tagging data with a bulk transfer model incorporating size-specific attrition. Fish. Bull. 101: 215–228.

Baum, J. K., D. Kehler, R. A. Myers, B. Worm, S. J. Harley, and P. A. Doherty.
2003. Collapse and conservation of shark populations in the Northwest Atlantic. Science 299:389–392.

Beverton, R. J., and S. J. Holt.
1957. On the dynamics of exploited fish populations. Fish. Invest. London 19:1–533.
Cotter, A. J. R., T. W. Boon, and C. G. Brown.
1997. Statistical aspects of trials of a separator trawl using a twin rig trawler. Fish. Res. 29:25–32.
Goodyear, C. P.
1999. An analysis of the possible utility of time-area closures to minimize billfish bycatch by U.S. pelagic longlines. Fish. Bull. 97:243–255.
Hall, M. A.
1996. On bycatches. Rev. Fish Biol. Fisheries 6:319–352.
Harley, S. J., M. N. Maunder, and R. B. Deriso.
2005. Assessment of bigeye tuna (*Thunnus obesus*) in the eastern Pacific Ocean. Col. Vol. Sci. Pap. ICCAT, 57(2):218–241.
Hilborn, R., K. Stokes, J. J. Maguire, T. Smith, L. W. Botsford, M. Mangel, J. Orensanz, A. Parma, J. Rice, J. Bell, K. L. Cochrane, S. Garcia, S. J. Hall, G. P. Kirkwood, K. Sainsbury, G. Stefansson, and C. Walters.
2004. When can marine reserves improve fisheries management? Ocean Coast. Manag. 47:197–205.
Horwood, J. W., J. H. Nichols, and S. Milligan.
1998. Evaluation of closed areas for fish stock conservation. J. Appl. Ecol. 35:893–903.
IATTC (Inter-American Tropical Tuna Commission).
2004. Tunas and billfishes in the eastern Pacific Ocean in 2003. Fishery Status Report 2, 114 p. IATTC, La Jolla, California.
Larsen, R. B., and B. Isaksen.
1993. Size selectivity of rigid sorting grids in bottom trawls for Atlantic cod (*Gadus morhua*) and haddock (*Melanogrammus aeglefinus*). ICES Mar. Sci. Symp. 196: 178–182.
Lennert-Cody, C. E., and M. A. Hall.
2000. The development of the purse seine fishery on drifting fish aggregating devices in the eastern Pacific Ocean: 1992–1998. *In* Tuna fishing and fish aggregating devices, p. 78–107. [Title translated into English. The paper is in English, but the book is in French]. IFREMER (French Research Institute for Exploitation of the Sea), Issy-les-Moulineaux Cedex, France.
Maunder, M. N.
2002a. Status of skipjack tuna in the eastern Pacific Ocean in 2001 and outlook for 2002. *In* Stock assessment report 3: status of the tuna and billfish stocks in 2001, p. 135–200. IATTC, La Jolla, CA.
2002b. Status of yellowfin tuna in the eastern Pacific Ocean in 2001 and outlook for 2002. *In* Stock assessment report 3: status of the tuna and billfish stocks in 2001, p. 47–134. IATTC, La Jolla, CA.
Maunder, M. N., and S. J. Harley.
2002. Status of bigeye tuna in the eastern Pacific Ocean in 2001 and outlook for 2002. *In* Stock assessment report 3: status of the tuna and billfish stocks in 2001, p. 201–311. IATTC, La Jolla, CA.
NRC (National Research Council).
1997. Dolphins and the tuna industry, 176 p. National Academy Press, Washington D.C.
Schaefer, K. M., and D. W. Fuller.
2002. Movements, behavior, and habitat selection of bigeye tuna (*Thunnus obesus*) in the eastern equatorial Pacific, ascertained through archival tags. Fish. Bull. 100:765–788.
Schaefer, K. M., and D. W. Fuller.
2005. Behavior of bigeye (*Thunnus obesus*) and skipjack (*Katsuwonus pelamis*) tunas within aggregations associated with floating objects in the equatorial eastern Pacific. Mar. Biol. 146:781–792.
Wardle, C. S.
1983. Fish reactions to towed fishing gears. *In* Experimental biology at sea (A. MacDonald, and I. G. Priede, eds.), p. 167–195. Academic Press, New York, NY.
Worm, B., H. K. Lotze, and R. A. Myers.
2003. Predator diversity hotspots in the blue ocean. Proc. Natl. Acad. Sci. USA 100:9884–9888.

Oceanic migration rates of Upper Chesapeake Bay striped bass (*Morone saxatilis*), determined by otolith microchemical analysis*

David H. Secor (contact author)[1]

Philip M. Piccoli[2]

Email for D. H. Secor: secor@cbl.umces.edu

[1] Chesapeake Biological Laboratory
University of Maryland Center for Environmental Science
Solomons, Maryland 20688

[2] University of Maryland
Department of Geology
College Park, Maryland 20742

Abstract—Oceanic incidence and spawning frequency of Chesapeake Bay striped bass (*Morone saxatilis*) were estimated by using microchemical analysis of strontium in otoliths. Otoliths from 40 males and 82 females sampled from Maryland's portion of the Chesapeake Bay were analyzed for seasonal and age-specific patterns in strontium and calcium levels. The proportion of oceanic females increased from 50% to 75% between ages seven to 13; the proportion of oceanic males increased from 20% to ~50% between ages four to 13. Contrary to an earlier model of Chesapeake Bay striped bass migration, results indicated that a substantial number of males undertook oceanic migrations. Further, we observed no mass emigration of females from three to four years of age from the Chesapeake Bay. Seasonal patterns of estuarine habitat use were consistent with annual spawning runs by striped bass of mature age classes, but with noteworthy exceptions for newly mature females. Evidence of an early oceanic presence indicated that Chesapeake Bay yearlings move into coastal regions—a pattern observed also for Hudson River striped bass. Otolith microchemical analyses revealed two types of behaviors (estuarine and oceanic) that confirm migratory behaviors recently determined for other populations of striped bass and diadromous species (e.g., American eels [*Anguilla rostrata*] American shad [*Alosa sapidissima*] and white perch [*Morone Americana*]).

Manuscript submitted 23 July 2004 to the Scientific Editor's Office.

Manuscript approved for publication 17 April 2006 by the Scientific Editor.

Fish. Bull 105:62–73 (2007).

As an estuarine-dependent species, striped bass (*Morone saxatilis*) demonstrate large plasticity in migration patterns (Secor and Piccoli, 1996). Striped bass in Chesapeake Bay are partial migrants; only a fraction of individuals will leave estuarine habitats for oceanic waters (Kohlenstein, 1981). Never the less, Chesapeake Bay striped bass are the major contributors to interjurisdictional ocean fisheries (Merriman, 1941; Wirgin et al., 1993). Rates of contributions by Chesapeake Bay striped bass to those fisheries are determined by lifetime patterns of habitat use, ontogenetic rates of egress from Chesapeake Bay, and regional rates of exploitation and natural mortality (Dorazio et al., 1994). Rates of oceanic residence have been shown to vary by sex and increase with age. Analyzing striped bass tagged in the Potomac River, Kohlenstein (1981) advanced the working hypothesis that young striped bass remain in or near the tributary in which they were spawned for two or three years. At this point a substantial proportion of immature females (ca. 50%) emigrate from the Bay, remaining in ocean waters until sexually mature (age 5–7 years). In contrast, males are mature by age 2 but remain in the Bay throughout their lives. This hypothesis remains untested, although substantial deviation from this proposed pattern is indicated by tagging studies and catch records.

From recaptured striped bass tagged on Chesapeake Bay spawning grounds, Dorazio et al. (1994) estimated that by 800 mm total length (TL), approximately half of the population (males and females combined) used ocean habitats. This length would correspond to an age of seven to 10 years (Secor et al., 1995b). Tagging studies comprise quasilongitudinal analyses, which could provide estimates of age-specific egress rates if tagged and recaptured fish are representative of the population. However, striped bass are moderately long lived and show migration behaviors that vary substantially with sex and age. Therefore, tagging studies often do not comprise sufficient spatial and temporal scales to provide the precise information needed to predict how Chesapeake Bay striped bass contribute to coastal fisheries.

Striped bass longevity exceeds 30 years (Merriman, 1941; Secor et al., 1995b). Life table analysis has indicated that maximum reproductive rate occurs relatively late in life (10–12 years) (Secor, 2002) and that accumulation of adult biomass (reproductive potential) represents an important "storage mechanism" (Warner and Chesson, 1995), improving the

* Contribution 4041 of the University of Maryland Center for Environmental Science, Chesapeake Biological Laboratory, Solomons, Maryland.

odds of recruitment over the lifetime of a fish (Secor, 2000a, 2000b, in press). Life-table–based models (e.g., Goodyear, 1984) depend upon the assumption that annual spawning occurs, which remains unsubstantiated for this species. If spawning frequency declines with age, for instance, then generation time and age-at-maximum reproductive value will be substantially overestimated, which in turn will affect biological reference points (Marshall et al., 2003).

Electron probe micro-analysis (EPMA) of Sr has been developed as a method to reconstruct individual patterns of migration and habitat use by anadromous populations of striped bass (Secor, 1992). In estuarine environments, strontium is often a reliable tracer of salinity; higher marine concentrations (7 ppm) become diluted in estuarine environments by freshwater inputs when freshwater Sr:Ca end-members (where "end-members" are the source of a Sr:Ca ratio) are low (Ingram and Sloan, 1992). Kraus and Secor (2004a) surveyed available data and determined that 83% of estuaries have low freshwater end-members, indicating that the ratio of Sr to Ca should be positively (but not necessarily linearly) related to salinity in most estuaries.

In our study we applied EPMA to examine the fraction of Chesapeake Bay striped bass that migrate to ocean waters and the frequency at which females and males undertake spawning runs. We previously used this method to chart age- and sex-specific patterns of Hudson River striped bass (Secor and Piccoli, 1996; Zlokovitz and Secor, 1999; Secor et al., 2001). Expectations for ontogenetic rates of emigration (i.e., Kohlenstein, 1981) and annual spawning were tested. In addition, we sought evidence for contingent groups (subpopulation groups with similar lifetime migration patterns; Secor, 1999), which we observed previously in Hudson River striped bass.

Material and methods

Samples

Samples collected during spawning runs present the best opportunity to collect a representative sample of mixed age classes, sexes, and migratory behaviors. These samples comprise mostly those ages that have fully recruited to the mature population. We note in our study that this sample incompletely represents migratory behaviors for those females that have not yet become mature and are not participating in the year's spawning run. During the period 15 April–30 May 2000, we obtained samples of 247 male and 122 female striped bass from the upper Chesapeake Bay (N. of 39°00′; n=27), mid-Bay (N. of 37°53W′S. of 39°00′; n=76); Choptank River (n=199), Patuxent River (n=33), and Potomac River (n=28). Capture methods were diverse and included the use of gill- and pound-nets (Maryland Department of Natural Resources monitoring), electro-shocking (National Marine Fisheries Service Northeast Center and University of Maryland scientific collections), and charter boat angling. All fish were measured (fork length [FL] and weight [g]), sex and diet were determined, and otoliths and scales were collected. Fork lengths ranged from 685 to 1110 mm for females and from 320 to 1029 mm for males.

Otolith Sr:Ca measures

To conduct EPMA analyses, otoliths (sagittae) were extracted, soaked in 1% sodium hypochlorite solution, rinsed with deionized water, and embedded within a resin (Secor et al., 1992). Transverse sections, approximately 1 mm thick, were cut through the otolith cores with a metallurgical wafering saw. The sections were mounted on glass slides, polished on wetted 600-grain sandpaper, and polished again on a slurry of 0.3-μm alumina until their surfaces were free of pits and abrasions, which can cause artifacts in microprobe analysis (Kalish, 1990). Annuli were enumerated based upon standard criteria under optical microscopy (Secor et al., 1995b). Before analysis, otoliths were cleaned ultrasonically and carbon-coated in a high-vacuum evaporator.

X-ray intensities for Sr and Ca were quantified by using a JEOL 8900 electron probe microanalyzer (Center for Microscopy and Microanalysis, Univ. Maryland, College Park, MD). Calcite ($CaCO_3$) and strontianite ($SrCO_3$) were used as reference standards and the protocol was checked by using secondary standards containing both Ca and Sr. The details of this analysis can be found elsewhere (Secor and Piccoli, 1996). Detection limits for Sr were approximately 230 ppm (±2 standard errors). Four slides, each containing four otolith sections, were loaded into the specimen chamber of the microanalyzer. After initial calibration to Sr and Ca standards (at programmed settings and intervals), transect assignments were made for up to 16 otolith sections. Transects comprised a series of point measurements from young to old ages across the sectioned otolith. X-ray maps of otolith structure were collected by using wavelength spectrometers.

Sr was expressed as a ratio of Ca (Sr:Ca) because of expected competitive interactions between the isotopic species (Kraus and Secor, 2004a). Further Sr:Ca records were converted to salinity exposure profiles according to the model (Secor et al., 1995a):

$$\text{"}\textit{Salinity inhabitance}\text{"}\ (\textit{sic})\ (\text{psu}) = 40.3\,(1+56.3\,e^{-1523(\text{Sr:Ca})})-1; \qquad r^2=0.94\ ;\ n=54$$

where "salinity inhabitance" (*sic*) is the salinity level (practical salinity units, psu) in the otoliths for the period of time represented for each Sr:Ca datum.

Oceanic incidence of striped bass

For our analysis, a subsample of 122 fish (40 males and 82 females) was drawn from the upper Bay (n=10), mid-Bay (n=46), and Choptank River (n=66). Estimated salinity records for the last year of life (recent

habitat use) were determined from at least five point measurements taken across the last completely-formed annulus (i.e., the last full year of life prior to winter). Opaque zone formation on the otolith occurs just prior to the spawning season (Zlokovitz et al., 2003); therefore measurements were taken between the penultimate and most peripheral (recently formed) opaque zones. We selected the record of maximum salinity, because at least one point in this series can be influenced by the previous year's spawning run, Oceanic habitat use was defined as salinities >29, and individual fish were classified accordingly. Because of unequal sampling among ages, we analyzed four age classes by sex: 4–6, 7–9, 10–12, and 13–18 years of age. Two-way classification tables were constructed to evaluate differences between age classes and sexes in probability of recent oceanic residence.

Life history transects and spawning frequency

Life history transects of salinity exposure, a series of Sr:Ca ratios from the juvenile period to the end of life, were constructed from EPMA measurements from 30 female and 10 male striped bass. This subsample was drawn from the upper Bay (n=2), mid-Bay (n=27), and Choptank River (n=11). To weight seasonal data among ages, time series were selected so that four or five analyzed points were included for each annulus. Data were standardized (Z score= (*transect datum – transect mean*)/*transect standard deviation*) and plotted to examine variations about the transect mean (Sokol and Rohlf, 1981).

Time-series data represented by the life history transects were expected to show autocorrelation across seasonal points and ages. An appropriate method of data analysis that shows interdependence among repeated measures on the same individual is repeated measures multivariate analysis (RM-MANOVA) (Chambers and Miller, 1995). This analysis simultaneously fits several dependent variables to independent factors of interest (SAS, Statistical Analysis System, SAS Institute, Inc., Cary, NC) and evaluates the matrix equation,

$$S_t = \mathrm{Sex}\beta + E,$$

where S_t = salinities at seasonal points; and
t = relative distance between successive opaque zones.

For each fish, S_t is arrayed in n rows, *Sex* contains two treatment levels for each factor (male vs. female) arrayed in n rows, and E is the matrix of model residuals. Degrees of freedom in the analysis depend upon n, which represents the number of individual fish. To avoid the problem of interdependence of seasonal data for combined ages, separate MANOVAs were performed for each age class.

To conduct the RM-MANOVA, it was necessary to have equal numbers of seasonal points (S_t) for each age class. Therefore, narrow annuli that had fewer than three seasonal (interannual) points were omitted from analyses. This excluded analyses of some of the oldest age classes, which typically exhibit narrow annuli (Secor, 1992). For years sampled with more than four or five seasonal points, the extra points were omitted from our analysis. Selection of points to be included was based upon their proximity to the axial distances of the prescribed intervals (either [0, 0.25, 0.5, 0.75] or [0, 0.2, 0.4, 0.6, 0.8]). Individual probe points within transects were separated by 10 to 35 microns.

Results

Demographics

Ages among the sampled Maryland Chesapeake Bay striped bass ranged from three to 18 years and sizes ranged 320 to 1110 mm FL. Females were significantly older and larger than males (ANOVA; P<0.01) and grew at a faster rate. Males were more heavily represented by ages <10 years than females in age-frequency distributions, although fish with ages >15 years were observed for both sexes. Relatively strong year class contributions within the sample occurred for 1982, 1989, 1993, and 1996 and coincided with high young-of-the-year juvenile abundances observed in those years (Secor, 2000a).

Oceanic incidence of striped bass

Female fish, more often than male fish, were classified as having a recent period of oceanic residence based upon the analysis of the last fully formed annulus, but this difference was not significant (χ^2, P>0.1). For individual age classes with sample sizes >5, oceanic incidence ranged from 60% to 75% for females and from 17% to 50% for males (Table 1). There was an indication that the proportion of fish of both sexes with oceanic residence increased with age. Oceanic incidence was observed consistently for >50% of the females. For males, oceanic incidence was 8–32% less than for females within each age class. Error bars, based upon a binomial probability distribution, indicated a fairly well-estimated oceanic classification rate for the age class 10–12 years due to a relatively high sample size. For this age class, oceanic incidence was estimated at 59% and 50% for females and males, respectively. Conversely, use of oceanic habitat for males at ages <10 was poorly estimated because of low sampling size. Indeed, estimated ratios for this group could not be statistically resolved from zero. With increased size, oceanic incidence (sexes combined) tended to increase (Table 1), although there was a decline in the proportion of fish with evidence of oceanic residence from 65.8% for the size class 900–999 mm FL to 46.1% for the size class >1000 mm FL.

Life history transects

Life history transects showed considerable variability (Fig. 1). It is noteworthy that some males exhibited

some degree of oceanic incidence (fish identification [ID] number=98, 198, 260) throughout portions of their lives and many females exhibited a pattern of estuarine use (e.g., ID=197, 263, 271, 272, 280, 281). A single instance of freshwater residency was observed for a fairly long-lived female (ID=271; age=11 years; FL=875 mm). Mean lifetime salinity exposure differed significantly between males and females (Kruskal-Wallis ANOVA; $P=0.01$), with females exhibiting an average 10% higher use of high-salinity habitat during the mature portion (age>6) of their lives (Fig. 2).

The male sample, albeit small ($n=10$), did not exhibit age-dependent patterns in salinity exposure (Fig. 2). In part, high variance in older age classes (8–12) obscured any pattern of salinity exposure at ages <6 years. Females showed a strong and nearly linear trend of increased salinity exposure with age (Fig. 2). Modal salinity increased from a range of 20–25 to a range of 25–30 for ages 2 and 7, respectively. Interestingly, both males and females showed that a polyhaline (salinity>18) habitat was used during the period between age 1 and 2 years. Thus, yearlings may be preferentially using polyhaline regions, followed by a return of some individuals to lower salinity regions (because slightly depressed salinities were observed for ages 2 and 3 compared to age 1 yr in Fig. 2). We have observed a similar pattern in Hudson River striped bass (Zlokovitz et al., 2003). The ontogenetic trend of increased salinity exposure with age in females could be related to maturation (ages 6–8 years)—a pattern observed in two-thirds of female fish (Fig. 3). Males also showed a rise in salinity exposure with age, albeit less consistently (Fig. 4).

Table 1

Degree of oceanic incidence of Chesapeake Bay striped bass collected in 2000. Data is presented for age classes by sex, and for size-class pooled sexes (the latter to permit comparison with results of Dorazio et al., 1994). Lower (LCL) and upper (UCL) confidence limits are presented for oceanic incidence by age class.

	Oceanic incidence (%)	
Age class (yr)	Males (n; LCL–UCL)	Females (n; LCL–UCL)
4–6	20.0 (5; 0–41.3)	—
7–9	25.0 (8; 0–50.2)	55.5 (18; 42.5–68.1)
10–12	50.0 (18; 37.4–62.5)	58.8 (51; 56.8–62.5)
13–18	44.4 (9; 34.0–77.4)	76.9 (13; 60.8–93.6)
	Oceanic incidence (%)	
FL size class (mm)	This study (n)	Dorazio et al. (1994)
300–599	20.0 (8)	<5.0
600–699	—	~8.0
700–799	42.9 (14)	~35.0
800–899	59.0 (44)	~80.0
900–999	65.8 (41)	~90.0
>1000	46.1 (13)	>95.0

Spawning frequency

Life history transects for the sample of ten males and thirty females gave evidence of strong intra-annual patterns in the salinity levels of their habitat (Figs. 3 and 4). Intra-annual trends often showed nadirs at or near the opaque zone of the otolith, a pattern occurring in both males (e.g., ID=124, 196, 327) and females (e.g., ID=192, 297, 298). In some instances, seasonal cycles indicated either less than annual (Fig. 3: ID=320; Fig. 4: ID=298, 300) or greater than annual (Fig. 3: ID=99; Fig. 4: ID=295, 300) cycles in patterns of salinity exposure.

Significant seasonal effects on patterns of salinity exposure were observed for ages 6 and 8 and for pooled ages 6–11 (Table 2), indicating that across individuals there was a seasonal pattern in salinity exposure for mature age classes. The other analysis of five, rather than four, seasonal points of measurement in the otolith did not show strong evidence for seasonality, although pooled age classes 6–11 and 7–11 showed marginal significance at $P=0.06$. In the selection of individuals that contained five seasonal points, sample sizes were substantially reduced. This reduced sample size in turn would have resulted in less statistical sensitivity. Despite high variances among individuals for each seasonal measurement, there was a trend for a seasonal nadir in salinity exposure near the opaque zone on the otolith (seasonal interval=0) (Fig. 5). This trend was especially apparent in males, and in females >6 years.

There was a slight indication of sex-related differences in seasonality of salinity exposure. Significant between-sex differences occurred for S_0 at ages 8 and 11, and all mature age class groupings (Table 2). Significant differences occurred for $S_{0.25}$ at ages 8 and 9 and mature age groupings 7–11 and 8–11; and for $S_{0.5}$ at age 8 and all mature age groupings. Males were found at lower salinities at these seasonal points than were females (Fig. 5).

X-ray maps of Sr within otolith sections showed clear concentric patterns of alternating high and low regions of Sr in association with annuli (Fig. 6). X-ray maps confirmed the cyclical patterns observed in the life history transects (Figs. 3 and 4), but with greater apparent difference between peak and nadir levels of Sr. In one of the X-ray maps (Fig. 6, bottom panel), a high level of Sr occurred within the first annulus).

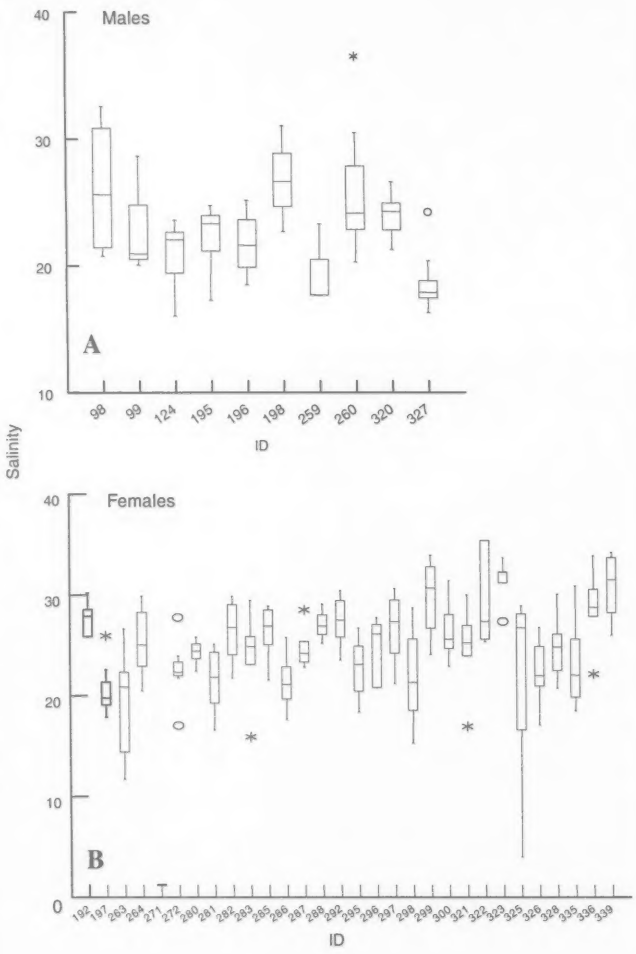

Figure 1

Box and whisker plots of salinity records experienced over a lifetime by individual male (**A**) and (**B**) female Chesapeake Bay striped bass (*Morone saxatilis*) collected in 2000. Median values are given within each box, which represents the first two quartiles of data about the median. Asterisks and circles indicate near and far outliers in relation to the first two quartiles, respectively. Salinity is given in practical salinity units. ID indicates the identification number assigned to each fish.

Discussion

Oceanic incidence of striped bass

Our analysis and that of Dorazio et al. (1994) does not support Kohlenstein's (1981) model of mass egress of female striped bass from Chesapeake Bay after ages two or three. Rather, our life history transects indicated a fairly gradual shift to use of ocean habitats—a shift associated with maturation at ages five to eight (Table 1; Fig. 2). For mature age classes, evidence of oceanic residence was observed for 50–75% of the female sample. Also, in contrast to previous expectations, otolith microanalysis indicated that a large fraction of males leave Chesapeake Bay, albeit at rates <50%.

Mirroring the results of Dorazio et al.'s (1994) tagging experiment, our results showed a trend of increasing oceanic residence with fish size, but found

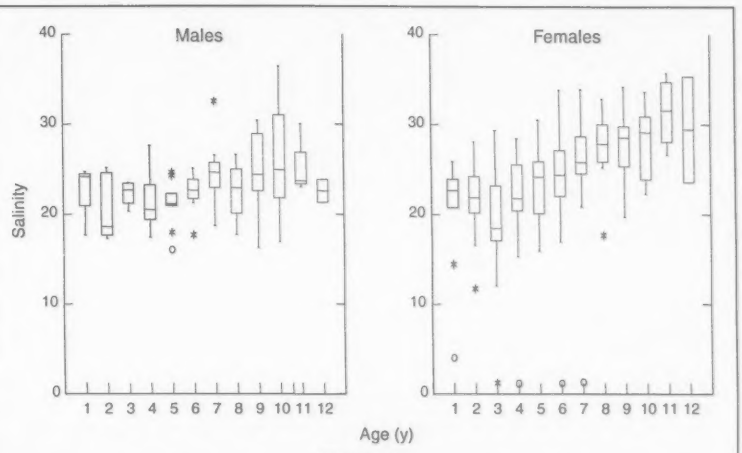

Figure 2

Box whisker plots of age-specific salinities experienced by Chesapeake Bay striped bass (*Morone saxatilis*) collected in 2000. Salinity data for each fish include quarterly seasonal salinity records. Median values are given within each box, which represents the first two quartiles of data about the median. Asterisks and circles indicate near and far outliers in relation to the first two quartiles, respectively. Salinity is given in practical salinity units. ID indicates the identification number assigned to each fish.

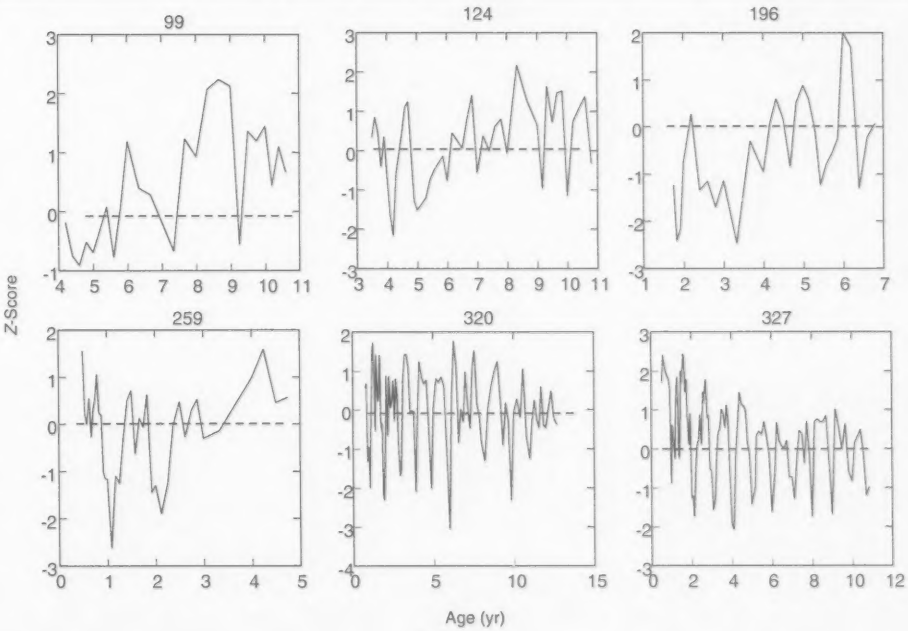

Figure 3

Standardized life history transects for male Chesapeake Bay striped bass (*Morone saxatilis*) collected in 2000. ID, an identification number assigned to each fish, is presented above each panel. *Z*-score indicates standardized salinity records for each fish where Z=(record-mean)/standard deviation. Dashed line demarcates the mean.

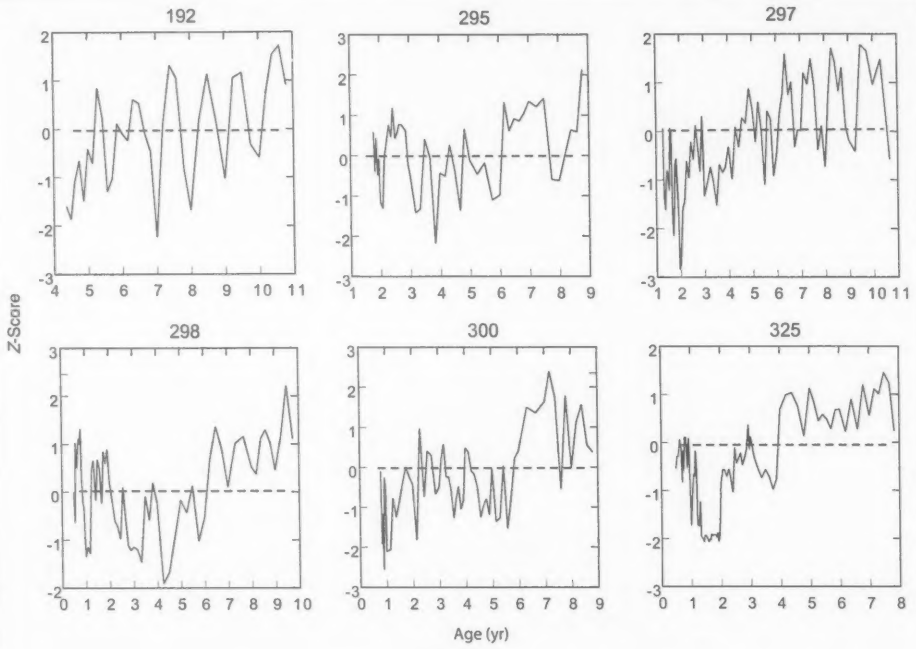

Figure 4

Standardized life history transects for female Chesapeake Bay striped bass (*Morone saxatilis*) collected in 2000. ID, an identification number assigned to each fish, is presented above each panel. *Z*-score indicates standardized salinity records for each fish where *Z*=(record-mean)/standard deviation. Dashed line demarcates the mean.

two important differences. First, we did not observe >90% oceanic incidence at >900 mm TL (877 mm FL) (Table 1). Rather, a substantial fraction of striped bass remained resident in Chesapeake Bay throughout their lives regardless of age or size. At ages >12 years, 25% of the female sample was estimated to have be resident in Chesapeake Bay. As an extreme example, one individual female resided in freshwater during its entire 11-yr lifespan. Secondly, early rates of oceanic migrations at sizes <700 mm TL (<685 mm FL) were substantially higher than rates indicated in the Dorazio et al. (1994) model, which predicted <5% of individuals migrate to ocean waters. Several factors may have contributed to the different results. Dorazio et al. (1994) predicted the degree to which Chesapeake Bay striped bass migrate to coastal regions north of Cape May New Jersey. Thus, their recapture sample represents only a subset of possible coastal fish. This bias would tend to underestimate oceanic residence; yet the Dorazio et al. (1994) estimates tend to be higher for larger mature striped bass. Recapture and reporting rates probably varied between coastal and Chesapeake regions because of more restrictive fishing regulations in Chesapeake Bay that contributed to an overestimate of migrant fish to northern ocean habitats.

In comparing our results to those of past tagging studies, we must also carefully consider limitations to the otolith microchemistry approach. We have sought to overcome some of the past hurdles regarding low sample size and resolution, yet these remain principal concerns. Despite large improvements in microprobe technology, otolith microchemistry remains a very expensive and time-consuming procedure to evaluate population-specific patterns in fish migration. Sample sizes, while larger than in many past projects, remain modest. Also, ages and sizes were not uniformly distributed in the populations sampled because of strong year classes, and this lack of uniform distribution would curtail generalizations across size and age classes. This strong year class phenomenon is common in striped bass, and it is likely that migration patterns in Chesapeake Bay striped bass typically will be influenced by dominant year classes (Merriman, 1941).

A central assumption in using strontium as a tracer of salinity levels is that the ratio of strontium to calcium (Sr:Ca) in the otolith can accurately distinguish between oceanic (salinity >29) and estuarine (salinity <30) habitat use. First, the designation, between oceanic and estuarine water is somewhat arbitary, particularly considering that the mouth of Chesapeake

Table 2

Repeated measures MANOVAs for effects of sex on seasonal salinities experienced by Chesapeake Bay striped bass (*Morone saxatilis*). S_t = salinity at seasonal point t, where t = relative distances between successive opaque zones in otoliths. "Season" is defined by two intervals on the otolith as a proportion of otolith increment width. Univariate F tests (P-values reported) for contrasts between males and females are given for each seasonal point. Differences among seasonal salinities ("Seasonality") within each age were evaluated with a Wilk's statistic (Chambers and Miller, 1995). The interaction between season and sex tested whether sex affected patterns of seasonality in salinity levels in otoliths. NS=not significant.

		Contrast between males and females					
Age (yr)	n	S_0	$S_{0.25}$	$S_{0.5}$	$S_{0.75}$	Seasonality	Season × Sex
1	11	NS	NS	NS	NS	NS	NS
2	19	NS	NS	NS	NS	NS	NS
3	21	NS	NS	NS	NS	NS	NS
4	29	NS	NS	NS	NS	NS	NS
5	33	0.09	NS	NS	NS	NS	NS
6	35	NS	NS	NS	NS	**0.02**	**0.04**
7	32	NS	NS	NS	NS	NS	NS
8	22	**0.02**	**0.01**	**0.04**	NS	**0.04**	NS
9	22	NS	**0.03**	NS	NS	NS	NS
10	20	NS	NS	NS	NS	NS	NS
11	7	**0.04**	NS	0.07	NS	0.07	NS
6–11	138	**0.04**	NS	**0.02**	NS	**0.04**	NS
7–11	103	**0.04**	**0.01**	**0.03**	NS	0.09	NS
8–11	71	**0.03**	**0.002**	**0.01**	NS	NS	NS

		Contrast between males and females						
Age	n	S_0	$S_{0.2}$	$S_{0.4}$	$S_{0.6}$	$S_{0.8}$	Seasonality	Season × Sex
5	31	0.09	NS	NS	NS	NS	NS	NS
6	31	NS	NS	NS	**0.03**	NS	NS	NS
7	22	NS	**0.003**	NS	NS	NS	NS	NS
8	19	**0.02**	0.07	**0.02**	NS	NS	NS	NS
9	13	NS	**0.01**	**0.02**	NS	NS	NS	NS
10	11	NS	NS	**0.02**	NS	NS	NS	NS
11	5	NS	NS	NS	NS	NS	NS	NS
6–11	101	**0.001**	0.007	**0.001**	**0.01**	**0.05**	0.06	NS
7–11	70	**0.001**	**0.001**	**0.001**	NS	NS	0.06	NS
8–11	48	**0.005**	**0.01**	**0.001**	0.08	NS	NS	NS

Bay averages about 25–30 psu during summer and fall months. Still, it was necessary to have a designation for assessing habitat use, and the above designations may have resulted in a liberal estimate of oceanic residence. A second issue is the resolution of the relationship of otolith Sr-Ca ratio to salinity. Resolution level estimated by experimental work of Secor et al. (1995a) was a salinity of 6 psu, which would support the contention that estimates presented here are fairly precise if error is unbiased. Still, the relationship between otolith Sr:Ca and salinity was logistic and very rapid changes in Sr:Ca were predicted to occur with small changes in salinity at salinities between 25 and 35 psu. These rapid changes at high salinities could indicate higher unexplained variability at salinities >24 psu.

Finally, our samples were unequally weighted across subpopulations of striped bass. For instance, no lower Chesapeake Bay subpopulations (those spawning in the James, York, and Rappahannock systems) were represented in our sample). Recent tagging studies have either focused more narrowly on the Potomac River (Kohlenstein, 1981) or have drawn a larger and more representative sample from the Maryland section of Chesapeake Bay (Dorazio et al., 1994). Studies on Virginia subpopulations of striped bass have historically shown low rates of oceanic residence (<5%; Vladykov and Wallace, 1952; Massman and Pacheco, 1961). Kohlenstein (1981) effectively argued that these and other early tagging studies (i.e., Mansueti, 1961) were not appropriately stratified to provide evidence of an increased likelihood of oceanic residence by larger size fish.

In sum, we believe that our otolith microchemistry results indicate higher rates of early oceanic residency in females and overall higher rates of oceanic migrations by males than were observed in previous tag-

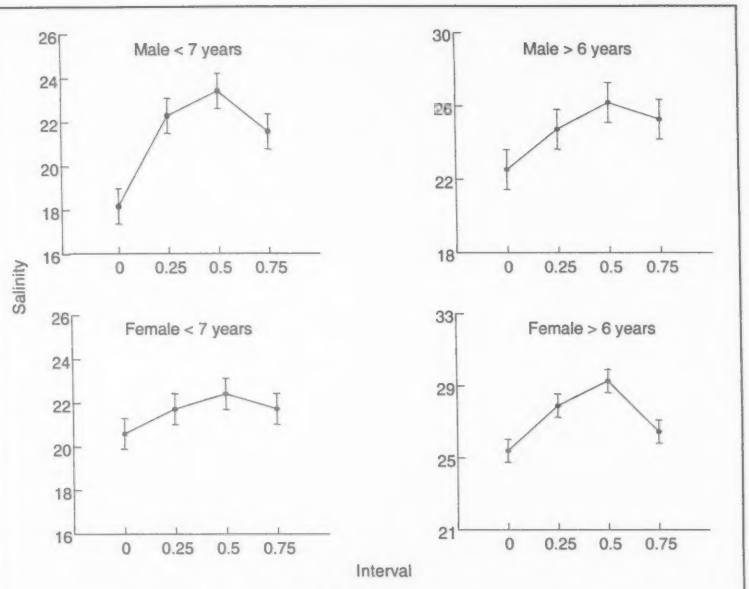

Figure 5

Seasonal patterns in salinity exposure as recorded in the otoliths of Chesapeake Bay striped bass (*Morone saxatilis*) collected in 2000. Mean salinities and standard errors are shown for age classes <7 and >6 years. Seasonal interval indicates the relative distances from the opaque zones in the otolith, which are formed in early spring. Intervals represent the seasons as a proportion of annual otolith increment width.

ging studies (Kohlenstein, 1981; Dorazio et al., 1994). Further, increasing trends in oceanic habitat use with age observed in our study are consistent with the two previous tagging studies. The increased incidence of males in ocean environments shown in our study and previous ones could reflect a true increased likelihood of emigration, perhaps driven by increased striped bass density, or by poorer habitat conditions in Chesapeake Bay. This view would be consistent with the near historically high abundances of Chesapeake Bay striped bass and the increased incidence of summertime hypoxia in Chesapeake Bay during the past two decades (Hagy et al., 2004). However, error due to the otolith microchemistry approach in classifying fish to oceanic or estuarine habitat use must be acknowledged and caution should precede application of the estimates of oceanic residence provided in this study.

Spawning frequency

In general, otolith microchemical analyses gave evidence for the view that most mature striped bass undertake annual spawning runs. For females, immature age classes did not show significant seasonality in changes in salinity, but many mature age classes did. Further, cycles in salinity were largely defined by a nadir that occurs during early spring as evidenced by changes in the chemistry of the opaque zone of the otolith. Thus, evidence of the use of low-salinity habitat was recorded near the opaque zone, consistent with the view of an annual up-estuary migration to low-salinity spawning habitats. Where such nadirs were not observed in the otolith microchemistry, two interpretations are plausible: 1) no spawning migration occurred, or 2) the otolith microchemistry method had insufficient resolution to allow us to detect the spawning migration. The resolution issue relates to two problems. First, the spacing of the microprobe assays could have been such that a spawning run event was missed. Second, spawning-run striped bass occur in low-salinity regions for short periods during which they are not growing and thus incorporating Sr material into their otoliths. In this instance, there would be an insufficient signal for otolith microanalysis of Sr to detect. Despite these likely sources of error, we were still able to detect a dominant annular cycle in otolith Sr for mature age classes of males and females. Therefore, we believe that the otolith microchemistry analysis supports annual spawning for the majority of mature Chesapeake Bay striped bass.

Alternatively, spawning in striped bass may occur less than once a year. Less than an annual spawning, once thought to be specific to relatively few taxa (e.g.,

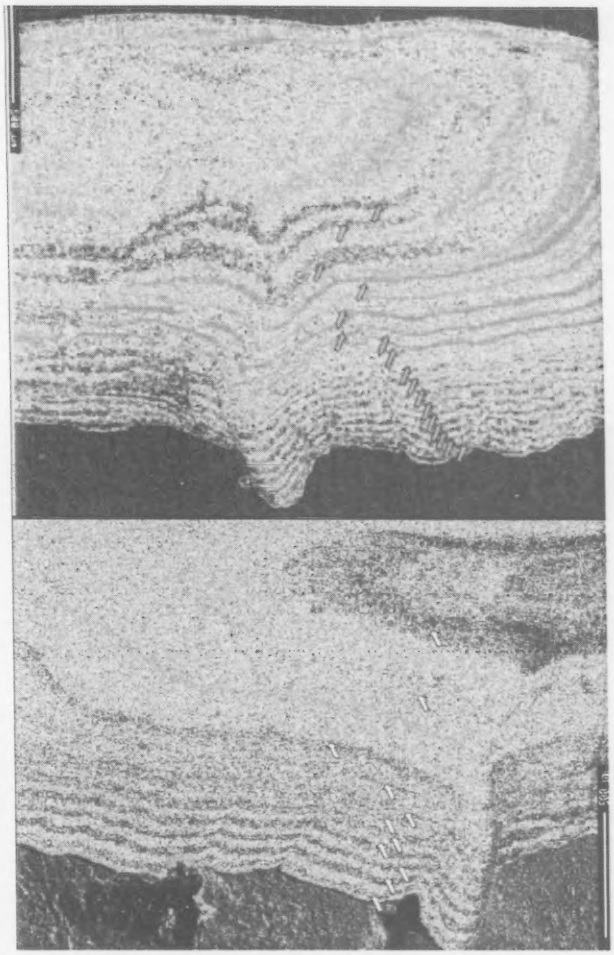

Figure 6

X-ray composition maps of srontium (Sr) seen in otolith for two female striped bass (*Morone saxatilis*) (17 and 11 years old) collected in Chesapeake Bay in 2000. Arrows demarcate annuli. The "warmer" colors (red, orange) represent regions with higher Sr concentrations whereas the "cooler" colors (yellow, green) represent regions with lower Sr concentrations. Composition maps show the coincidence of strontium banding patterns with banding patterns of annuli, indicative of annual anadromous migrations from high to low salinity waters.

sturgeons; Gross et al., 2002) could in fact be common in some longer-lived species (Rideout et al., 2005). For instance, data-archiving electronic tags inserted on Atlantic bluefin tuna (*Thunnus thynnus*) have definitively shown that many adults are found outside spawning habitats for an entire annual spawning season (Block et al., 2005). Further evidence is provided by the reproductive behavior of Atlantic cod (*Gadus morhua*; Jørgensen et al., 2006), a species that does not always spawn each year because of density dependence or other environmental limits on its ability to provision gonads. Interestingly, evidence for this can be observed in two female life history transects in our study of striped bass (Fig. 4: ID=295, 300), where no nadir was observed at age seven following a clear nadir at age six (female striped bass typically mature between five and seven

years of age). We also should expect that, for similar energetic reasons, not every female, which undertakes a springtime up-estuary migration, will actually spawn. Some mature females in a spawning run will not spawn; rather, they will reabsorb final-stage oocytes (first author, personal observ.). Therefore, accurate measurement of spawning frequency depends on both the probability of successful spawning in the field and the frequency of up-estuary migratory runs.

X-ray maps confirmed an annual cycling in otolith strontium, but also showed cycles during the immature period of females, contrary to patterns observed from life history transects. Further, X-ray mapping and life history transects indicated that many yearlings move into oceanic regions—a pattern observed for Hudson River striped bass (Zlokovitz et al., 2003) but not yet described for Chesapeake Bay striped bass. The possibility that young-of-the-year or yearling striped bass are present in ocean environments deserves additional research in the Chesapeake Bay and elsewhere.

Contingent migration behavior

In past research on Hudson River striped bass, we observed modalities in lifetime migration behaviors (Secor et al., 2001); groups of individuals that share similar migration behaviors with some, but not all, members of their population are termed "contingents" (Hjort, 1914[1]; Gilbert 1917[2]; Secor, 1999). In particular, one contingent comprising a small fraction of the Hudson River springtime sample was resident to freshwater and oligohaline regions and was heavily contaminated by polychlorinated biphenyls—an apparent consequence of this lifetime migration behavior (Zlokovitz and Secor, 1996; Ashley et al., 2000). A similar contingent migration behavior has been reported for the Steweiacke River population of striped bass in Nova Scotia (Morris et al., 2003). In contrast, only a single Chesapeake Bay striped bass (of 40 analyzed) exhibited freshwater resident behavior. Small sample sizes could indicate considerable error in estimates of the frequency of this behavior among populations if these estimates are based on research to date, but the fact that three distinct populations exhibited this behavior in our study indicates that contingent migration structuring is common to Chesepeake Bay striped bass.

Contingent migration structure has been observed across diverse taxa, such as American eels (*Anguilla rostrata*), American shad (*Alosa sapidissima*), white perch (*Morone americana*), bluefish (*Pomatomus saltatrix*), and Atlantic bluefin tuna (Secor, 1999, in press; Fromentin and Powers, 2005). Here, a nursery or foraging habitat associated with one contingent migration behavior may make a small contribution in a given year, but over a decade may contribute significantly to spawning stock biomass. Thus, over generation-long time scales, we should expect that minority lifetime migration behaviors can contribute significantly to sustained recruitment. Further research is needed to determine the proximate cause of contingent structure, but based upon research on the sympatric white perch, we advance the hypothesis that Chesapeake Bay striped bass contingent migration structuring results from divergent early growth rates and dispersal behaviors associated with early growth (Kraus and Secor, 2004b).

[1] Hjort, J. 1914. Fluctuations in the great fisheries of northern Europe. Rapports Conseil Permanent International Pour L'exploration de la Mer, 20:1–228. Library, Chesapeake Biological Laboratory, P.O. Box 38, Solomons, MD 20688.

[2] Gilbert, C. H. 1917. Contributions to the life-history of the sockeye salmon. Paper No. 4, report to the Commissioner of Fisheries. British Columbia Fisheries Department, 48 p. + plates. Library, Pacific Biological Station, Fisheries and Oceans Canada, 3190 Hammond Bay Road, Nanaimo, V9R 5K6 British Columbia, Canada.

Acknowledgments

We acknowledge NOAA MARFIN (Marine Fisheries Initiative, Northeast Center) support for this research. S. McGuire assisted with otolith preparation and data analyses. Personnel at Maryland Department of Natural Resources, Horn Point Environmental Laboratory, and the U. S. Fish and Wildlife Service assisted in collection of striped bass. The electron probe microanalyzer was purchased, in part, by a grant from the National Science Foundation (EAR 98-1244).

Literature cited

Ashley, J. T. F, D. H. Secor, E. Zlokovitz, J. E. Baker, and S. Q. Wales.
2000. Linking habitat use of Hudson River striped bass to accumulation of polychorinated biphenyl congeners. Environ. Sci. Techn. 34:1023–1029.

Block, B. A., L. L. H. Teo, A. Walli, A. Boustany, M. J. W. Sokesbury, C. J. Farwell, K. C. Weng, H. Dewar, and T. D. Williams.
2005. Electronic tagging and population structure of Atlantic bluefin tuna. Nature 434:1121–1127.

Chambers, R. C., and T.J. Miller.
1995. Evaluating fish growth by means of otolith increment analysis: Special properties of individual-level longitudinal data. *In* Recent developments in fish otolith research (D. H. Secor, S. E. Campana, and J. M. Dean, eds.), p. 155–175. Belle W. Baruch Library in Marine Sciences Number 19. Univ. South Carolina Press, Columbia, SC.

Dorazio, R. M., K. A. Hattala, C. B. McCollough, and J. E. Skjeveland.
1994. Tag recovery estimates of migration of striped bass from spawning areas of the Chesapeake Bay. Trans. Am. Fish. Soc. 123:950–963.

Fromentin, J. M., and P. E. Powers.
2005. Atlantic bluefin tuna: population dynamics, ecology, fisheries, and management. Fish and Fisheries 6:281–306.

Goodyear, C. P.
1984. Analysis of potential yield per recruit for striped

bass produced in Chesapeake Bay. N. Am. J. Fish. Manage. 4:488–496.

Gross, M. R., J. Repka, C. T. Robertson, D. H. Secor, and W. Van Winkle.
2002. Sturgeon conservation: insights from elasticity analysis. Am. Fish. Soc. Symp. 28:3–10.

Hagy, J. D., W. R. Boynton, C. W. Wood, and K. V. Wood.
2004. Hypoxia in Chesapeake Bay, 1950–2001: long-term changes in relation to nutrient loading and river flow. Estuaries 27:634–658.

Ingram, B. L., and D. Sloan.
1992. Strontium isotopic composition of estuarine sediments as paleosalinity-paleoclimate indicator. Science. 255:68–72.

Jørgensen, C., B. Ernande, O. Fiksen, and U. Dieckmann.
2006. The logic of skipped spawning in fish. Can. J. Fish. Aquat. Sci. 63:200–211.

Kalish, J. M.
1990. Use of otolith microchemistry to distinguish progeny of sympatric anadromous and non-anadromous salmonids. Fish. Bull. 88:657–666.

Kohlenstein, L. C.
1981. On the proportion of the Chesapeake stock of striped bass that migrates into the coastal fishery. Trans. Am. Fish. Soc. 110:168–179.

Kraus, R. T., and D. H. Secor.
2004a. Partitioning of strontium in otoliths of estuarine fishes: experimentation in a model system, white perch *Morone americana* (Gmelin). J. Exp. Mar. Biol. Ecol. 302:85–106.
2004b. The dynamics of white perch (*Morone americana* Gmelin) population contingents in the Patuxent River Estuary, Maryland USA. Mar. Ecol. Prog. Ser. 279:247–259.

Mansueti, R. J.
1961. Age, growth, and movements of the striped bass, *Roccus saxatilis*, taken in size selective fishing gear in Maryland. Chesapeake Sci. 2:9–36.

Marshall, C. T., L. O'Brien, J. Tomkiewicz, G. Marteinsdóttir, M. J. Morgan, F. Saborido-Rey, F. Köster, J. L. Blanchard, D. H. Secor, G. Kraus, P. Wright, N. V. Mukhina, and H. Björnsson.
2003. Developing alternative indices of reproductive potential for use in fisheries management: Case studies for stocks spanning an information gradient. J. Northw. Atl. Fish. Sci. 33161–190.

Massman, W. H., and A. L. Pacheco.
1961. Movements of striped bass tagged in Virginia waters of Chesapeake Bay. Chesapeake Sci. 2:37–44.

Merriman, D.
1941. Studies of the striped bass (*Roccus saxatilis*) of the Atlantic coast. USFWS Fish. Bull. 50:1–77.

Morris, J. A., R. A. Rulifson, and L. H. Toburen.
2003. Life history strategies of striped bass, *Morone saxatilis*, populations inferred from otolith microchemistry. Fish. Res. 62:53–63.

Rideout, R. M., G. A. Rose, and M. P. M. Burton.
2005. Skipped spawning in female iteroparous fishes. Fish and Fisheries 6:50–72.

Secor, D. H.
1992. Application of otolith microchemistry analysis to investigate anadromy in Chesapeake Bay striped bass. Fish. Bull. 90:798–806
1999. Specifying divergent migration patterns in the concept of stock: the contingent hypothesis. Fish. Res. 43: 13–34.
2000a. Longevity and resilience of Chesapeake Bay striped bass. ICES J. Mar. Sci. 57:808–815.
2000b. Spawning in the nick of time? Effect of adult demographics on spawning behavior and recruitment of Chesapeake Bay striped bass. ICES J. Mar. Sci. 57:403–411.
2002. Estuarine dependency and life history evolution in temperate sea basses. Fish. Sci. 68(suppl. 1): 178–181.
In press. The year-class phenomenon and the storage effect in marine fishes. J. Sea Res.

Secor, D. H., J. M. Dean, and E. H. Laban.
1992. Otolith removal and preparation for microstructural examination. Chapter 3 *in* Otolith microstructure examination and analysis (D. Stephenson and S. Campana, eds.), p. 17–59. Special Publication, Can. J. Fish. Aquat. Sci. 117.

Secor, D. H., A. Henderson-Arzapalo, and P. M. Piccoli.
1995a. Can otolith microchemistry chart patterns of migration and habitat utilization in anadromous fishes? J. Exp. Mar. Biol. Ecol. 192:15–33.

Secor, D. H., and P. M. Piccoli.
1996. Age- and sex-dependent migrations of the Hudson River striped bass population determined from otolith microanalysis. Estuaries 19:778–793.

Secor, D. H., J. R. Rooker, E. Zlokovitz, and V. S. Zdanowicz.
2001. Identification of riverine, estuarine, and coastal contingents of Hudson River striped bass based upon otolith elemental fingerprints. Mar. Ecol. Progr. Ser. 211:245–253

Secor, D. H., T. M. Trice, and H. T. Hornick.
1995b. Validation of otolith-based ageing and a comparison of otolith and scale-based ageing in mark-recaptured Chesapeake Bay striped bass, *Morone saxatilis*. Fish. Bull. 93:186–190.

Sokol, R. R., and F. J. Rohlf.
1981. Biometry, 2nd ed., 859 p. W. H. Freeman and Co., New York, NY.

Vladykov, V. D., and D. H. Wallace.
1952. Studies of the striped bass, *Roccus saxatilis* (Walbaum), with special reference to the Chesapeake Bay region during 1936–1938. Bull. Bingham Oceanogr. Coll. 14:132–177.

Warner R. R., and P. L. Chesson.
1995. Coexistence mediated by recruitment fluctuations—a field guide to the storage effect. Am. Naturalist 125:769–787.

Wirgin, I., L. Maceda, J. R. Waldman, and R. N. Crittenden.
1993. Use of mitochondrial DNA polymorphisms to estimate the relative contributions of the Hudson River and Chesapeake Bay striped bass to the mixed fishery on the Atlantic Coast. Trans. Am. Fish. Soc. 122: 669–684.

Zlokovitz, E. R., and D. H. Secor.
1999. Effect of habitat use on PCB body burden in Hudson River striped bass (*Morone saxatilis*). Can. J. Fish. Aquat. Sci. 56 (suppl.1):86–93.

Zlokovitz, E. R., D. H. Secor, and P. M. Piccoli.
2003. Patterns of migration in Hudson River striped bass as determined by otolith microchemistry. Fish. Res. 63:245–259.

Ecotypic variation and predatory behavior among killer whales (*Orcinus orca*) off the eastern Aleutian Islands, Alaska

Craig O. Matkin (contact author)[1]
Lance G. Barrett-Lennard[2]
Harald Yurk[2]
David Ellifrit[3]
Andrew W. Trites[4]

Email address for C. O. Matkin: cmatkin@acsalaska.net

[1] North Gulf Oceanic Society
3430 Main St. B1
Homer, Alaska 99603

[2] Vancouver Aquarium Marine Science Center
University of British Columbia
845 Avison Way
Vancouver, B.C., Canada V6G 3E2

[3] Center for Whale Research
355 Smugglers Cove
Friday Harbor, Washington 98250

[4] Marine Mammal Research Unit, Fisheries Centre
University of British Columbia
Vancouver, B.C., Canada V6T IZ4

Abstract—From 2001 to 2004 in the eastern Aleutian Islands, Alaska, killer whales (*Orcinus orca*) were encountered 250 times during 421 days of surveys that covered a total of 22,491 miles. Three killer whale groups (resident, transient, and offshore) were identified acoustically and genetically. Resident killer whales were found 12 times more frequently than transient killer whales, and offshore killer whales were encountered only once. A minimum of 901 photographically identified resident whales used the region during our study. A total of 165 mammal-eating transient killer whales were identified, and the majority (70%) were encountered during spring (May and June). The diet of transient killer whales in spring was primarily gray whales (*Eschrichtius robustus*), and in summer primarily northern fur seals (*Callorhinus ursinus*). Steller sea lions (*Eumetopias jubatus*) did not appear to be a preferred prey or major prey item during spring and summer. The majority of killer whales in the eastern Aleutian Islands are the resident ecotype, which does not consume marine mammals.

Manuscript submitted 5 December 2005 to the Scientific Editor's Office.

Manuscript approved for publication 18 April 2006 by the Scientific Editor.

Fish. Bull. 105:74–87 (2007).

In 1992, flipper tags from fourteen Steller sea lions (*Eumetopias jubatus*) were found in the stomach of a killer whale (*Orcinus orca*) that had died in Prince William Sound (Heise et al., 2003). This discovery prompted considerable interest and speculation about the role that killer whales may have played in the decline and lack of recovery of Steller sea lions in western Alaska (Barrett-Lennard et al., 1995). Since the late 1970s, Steller sea lions in the Gulf of Alaska and Aleutian Islands have declined by over 80% (Merrick et al., 1987; Trites and Larkin, 1996; Loughlin and York, 2000; Winship and Trites, 2006). Similar sharp declines have also occurred among some populations of harbor seals (*Phoca vitulina*), northern fur seals (*Callorhinus ursinus*), and sea otters (*Enhydra lutris*) (York, 1987; Pitcher, 1990; Trites, 1992; Estes et al., 1998). Whether or not these declines are related to killer whales is currently the subject of considerable scientific debate (Springer et al., 2003; Trites et al., 2006; DeMaster et al., 2006; Mizroch and Rice, 2006).

Most knowledge about killer whales in the North Pacific has been gathered between California and the northern Gulf of Alaska, where three distinct lineages of killer whales have been identified: fish-eating "resident" killer whales, which appear predictably in large groups from Washington to Alaska; marine mammal-eating "transient" killer whales, which appear infrequently and in smaller groups; and "offshore" killer whales, whose feeding habits are poorly known, but are thought to eat fish, including sharks (Matkin et al., 1999a; Barrett-Lennard, 2000; Ford et al., 2000; Saulitis et al., 2000). These groups are genetically and behaviorally distinct, but have overlapping geographic ranges and are considered as ecotypes because of their differences in diet. However, prior to our study, it was not known whether these lineage and ecotype distinctions extended to the northwestern Gulf of Alaska and the

Aleutian archipelago, nor was much known about the extent to which killer whales prey on Steller sea lions and other species of marine mammals in these regions.

The goals of our study were 1) to determine whether the eastern Aleutian Islands are also home to the three lineages and ecotypes of killer whales that have been identified elsewhere in the northeastern Pacific; 2) to derive estimates of killer whale numbers for this region; and 3) to document the behaviour of killer whales foraging on marine mammals. Obtaining such information about killer whale numbers, diets, and hunting behavior is critical for resolving the role that killer whales may have played in the decline and lack of recovery of Steller sea lions and other species of marine mammals in western Alaska.

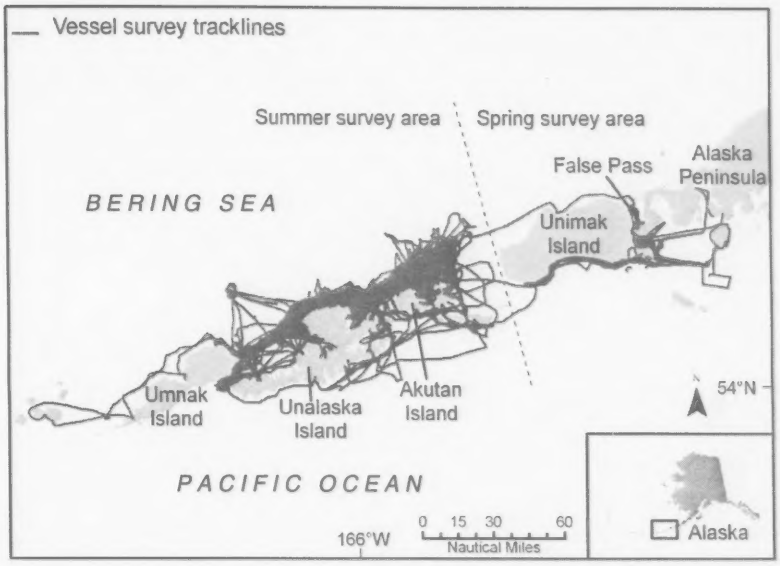

Figure 1

Tracks of the vessels during the surveys for killer whales (*Orcinus orca*) for the years 2001–2004. The vessels tended to return to areas that produced encounters with killer whales. The spring False Pass–Unimak Island surveys are distinguished from the summer Unimak Pass–Umnak Island surveys by the dashed line.

Materials and methods

Following the research method used to collect information on killer whales in other regions (Matkin et al., 1999a; Ford et al., 2000), five types of data were gathered: photo-identification pictures of individuals and groups, acoustic recordings of killer whale calls, skin tissue samples for genetic analysis, prey samples, and accounts of predation. Additionally, we documented the presence of potential marine mammal prey. Analysis of these data allowed the determination of killer whale ecotypes and a description of killer whale feeding habits.

Field methods

Boat-based surveys over a wide geographic range occurred during June–September 2002–2004 from Unimak Pass to Samalga Pass, and surveys over a relatively small range occurred in May and early June 2003–2004 in the False Pass–Unimak Island region. Surveys in the broader region traversed 19,686 nautical miles and were focused in the Bering Sea within twenty miles of the shoreline between Unimak Pass and eastern Umnak Island (Fig. 1). The 2003–2004 False Pass–Unimak surveys traversed 1970 miles in Ikatan Bay and along the Pacific shore of Unimak Island. We operated in areas of suspected high killer whale density according to information provided by local fishermen and researchers from the National Marine Mammal Laboratory (NMML) (Dahlheim, 1997) during previous transect surveys that covered broader regions. We modified our surveys each season to cover the areas that were most productive in providing killer whale encounters.

The research was conducted from aluminum-hull fishing vessels (powered by diesel inboard engines) ranging from 10 to 14 meters in length. Survey effort varied by year with a total of 372 days from 2001 to 2003 from the Unimak Pass to Samalga Pass in summer and a total of 49 survey days in 2003 and 2004 in the False Pass–Unimak Island region in spring (Table 1). All sightings of marine mammals during vessel surveys were recorded and the number of individuals was estimated to determine the relative abundance of potential prey items.

Photographs of the left side of dorsal fins and saddle patches of killer whales were taken with a Nikon F-100 camera (B and H Photo, New York, NY) equipped with either fixed 300-mm lenses or 100–300 zoom lenses and loaded with Fuji Neopan ASA1600 black and white film (B and H Photo New York, NY). These photographs were checked against existing photo-catalogues of Alaskan killer whales (Dahlheim, 1997; Matkin et al., 1999a) and other unpublished photographs. Tissue samples of at least one whale in each group were collected for genetic analysis and biopsy when weather and behavior of the whales permitted close approach. These samples were collected by using lightweight darts and an air-powered rifle (Barrett-Lennard et al., 1996). The outer skin portion of the samples was used for genetic analysis, and the underlying blubber portion was used for

Table 1

Survey effort (in days) and number of encounters with resident and transient killer whales (*Orcinus orca*) in the eastern Aleutians (2001–2004). "Survey days" are the days spent looking for whales; "Miles" are given in nautical miles.

	False Pass–Unimak Island region (single vessel 2003–2004)					Eastern Aleutians (Single vessel 2001, two vessels 2002–04)				
				Encounters					Encounters	
Year	Dates	Survey days	Miles	Resident	Transient	Dates	Survey days	Miles	Resident	Transient
2001		—	—			19 Jun–18 Aug	16	835	13	1
2002		—	—	—		17 Jun–24 Aug	188	6599	57	4
2003	16 May–3 Jun	18	642	0	13	10 Jun–31Aug	108	6321	49	4
2004	4 May–3 Jun	31	1328	0	32	7 Jun–9 Sep	130	6766	70	7
Total		49	1970	0	45		372	20,521	189	16

contaminant analysis, lipid and fatty acid, and stable isotope analysis (see Herman et al., 2005). Genetic analysis involved sequencing the entire mitochondrial control region (see Barrett-Lennard [2000] for details). Acoustic recordings were made when whales were vocalizing and ambient noise levels permitted using an Offshore Acoustics™ (Offshore Acoustics, Nanaimo, British Columbia) hydrophone with a built-in preamplifier and a Sony WM-D6C (B and H Photo, New York, NY) cassette recorder. This system had a frequency response of 10 Hz to 8 KHz (±3 dB).

Single, continuous observation periods with killer whales were termed encounters. During these vessel-based observation periods, the location of the killer whales was plotted at approximately 5-min intervals by using a global positioning system (GPS) linked to a computer with Nobletec™ (Nobletech, Beaverton, OR) navigational software. Time spent in different behavioral states (e.g., feeding, socializing, resting, traveling) was recorded on data sheets. Whales were observed continuously during encounters, and any signs of possible predation were recorded. During behavioral observations, marine mammal kills were confirmed only when marine mammal parts were observed in the mouths of the whales, or when bits of blubber, skin, or viscera, hair were collected, or blood or oil was observed on the surface of the water. Predation on fish was confirmed by observations of fish in the mouths of whales or by collecting and inspecting floating parts. To document the potential marine mammal prey in the region during the period of the study, we recorded the time, location, and number of all marine mammals sighted.

Analytical methods

Photo-identification All photographic negatives were examined over a light table with an 8.0 power Peak™ (B and H Photo, New York, NY) magnification loop. Identifiable individuals were recorded and assigned a unique alphanumeric name in order to be tracked throughout the study. Whales that could not be positively re-identified were not assigned a name. From this photographic database, the actual number and identity of individual killer whales and groups of whales present for each encounter were determined. Because some of the photographs were of poor quality, these photographs were rejected from further analyses; thus not all the whales encountered were identifiable.

Acoustics We inspected acoustic recordings for the presence of discrete calls by listening to tapes and monitoring real-time spectrograms using Cool Edit 2000™ (Syntrillicum Software Corp., Phoenix, AZ) sound manipulation software. Calls were analyzed following the protocol of Ford (1991) and Yurk (2005). Killer whales produce a variety of different types of vocalizations that can be described as clicks, whistles, and calls (Ford, 1989). Calls are the most common type of vocalization, occurring in over 90% of all encounters with vocalizing killer whales. These pulsed vocalizations occur as either signals of a frequently repeated acoustic pattern or as signals of variable acoustic pattern (Ford, 1991). Discrete calls were chosen for this analysis because they retain their recognizable acoustic structure for many years and likely for many generations (Yurk, 2005). Recognized calls were digitized at a 44.1-kHz sampling rate with a 16-bit sample size and further analysed spectrographically using Canary 1.2.4 sound analysis software (Cornell Laboratory of Ornithology, Ithaca, NY). The spectrographic analysis was done by using fast-Fourier transformations (FFT) of time series of the recorded sound pressure waves with sizes of 1024 points for each analyzed time series. The FFT identifies the composing sine waves in sound pressure waves of

acoustic signals and allows spectrographic representations of the sound frequency versus time and pressure. Spectrograms were produced with an 87.5% overlap of the analyzed time series. Resulting spectrograms had a time resolution of 2.9 milliseconds and a frequency resolution of 43 Hz.

We categorized calls by ear and by visual inspection of distinct upper and lower frequency components of the sound spectrum (UFC and LFC, respectively), as described by Miller and Bain (2000) and Yurk et al. (2002). When categorizing the calls as distinct, particular attention was given to 1) the existence and contour shapes of UFCs; 2) LFC contour shapes; 3) LFC segmentation (elements separated by silent intervals); and 4) the component structure (elements within the LFC arising from abrupt shifts in contour and not separated by silent intervals) of the LFCs (Ford, 1991; Yurk, 2005).

The three known ecotypes of killer whales inhabiting waters off British Columbia and southern Alaska (resident, transient, and offshore) are acoustically distinguishable by 1) vocalization rate; 2) the occurrence of different discrete calls; 3) the syllables used in calls; and 4) the production rate and characteristics of echolocation clicks. Transient killer whales, which appear to rely on passive listening to catch their marine mammal prey, vocalize less frequently than resident killer whales (Deecke et al., 2005). Transients rarely use echolocation clicks, in contrast to resident and offshore killer whales (Deecke et al., 2005). All calls of transient killer whales are distinct from the calls of resident whales by 1) an audible quavering of the fundamental sound frequencies (instead of a crisp appearance of these sound frequencies that is typical of calls from resident killer whales), and 2) a distinctively lower amount of different call syllables and a distinct order of these syllables compared to those in calls of resident killer whales (Yurk, 2005). Transient and resident killer whales are distinguishable from offshore killer whales by their use of unique call types (Yurk, 2005). We determined whether the encountered whales fell into discrete acoustic groups and, if so, whether those acoustic groups were similar to any of the acoustic groups observed in British Columbia and southern Alaska. Analysis was completed by Yurk (2005), independent of knowledge of genetic differences and social associations among groups. Call rates were estimated from field estimates of killer whale group sizes for each encounter.

Genetics DNA was extracted from the skin portion of the biopsies using proteinase K digestion, phenol and chloroform purification, and ethanol precipitation using standard procedures (Sambrook et al., 1989)

We obtained mtDNA sequences using the following procedure: 1) the entire D-loop region was PCR-amplified by using custom-designed primers that annealed to the flanking tRNA-Thr and 12s-rRNA regions (Barrett-Lennard, 2000); 2) the PCR product was purified with QIAQuick® spin columns (Qiagen, Valencia, CA) following protocols supplied by Qiagen, Ltd. (Valencia, CA); 3) a sequencing reaction was performed with Fs-Taq® (Applied Biosystems, Foster City, CA) system reagents and protocols supplied by Applied Biosystems, Ltd. (Foster City, CA); and 4) the sequence was resolved on an Applied Biosystems 377 (Applied Biosystems, Foster City, CA) automated DNA sequencer. Because the sequence was too long (950 bases) to be entirely resolved in one direction, sequencing reactions were run from each end of the amplified fragment. We visually checked the output graphs from the automated sequencer and corrected the computer-generated sequences accordingly. We also used the approximately 400-base overlap in the sequences of opposite directions to check for errors. As a final check of accuracy, we overlaid each output graph with a reference graph on a transparent sheet, and scanned the two graphs for differences. We then aligned unique sequences using the program CLUSTAL-W (European Bioinformatics, Cambridge, UK) (Thompson et al., 1994).

Results

Summary of survey effort and encounters with killer whales

On 250 occasions, groups of one or more killer whales were encountered during the surveys that covered a total of 22,491 miles in 421 days in the eastern Aleutians and False Pass–Unimak Island area (Table 1). The majority of survey effort and encounters occurred west of Unimak Pass during summer; surveys in False Pass–Unimak Island area were not initiated until 2003. From approximately half of our encounters with groups of killer whales in both regions, we obtained genetic samples or acoustic recordings (Table 1). Killer whales of the offshore ecotype were encountered only once (in 2003) and both acoustic and genetic samples were obtained during this encounter.

Use of acoustic data, genetic analysis, and group association to infer lineage

Genetic and acoustic analyses revealed the presence of three killer whale populations. As described in more detail below, one population clustered genetically and acoustically with resident killer whales ranging from Puget Sound, Washington to Kenai Fjords, Alaska, and a second population clustered with transient killer whales from the same general area. Accordingly, those two groups were provisionally classified as a resident killer whale group and a transient killer whale group, respectively. The third population clustered genetically with offshore killer whales sampled off British Columbia, and were provisionally classified as an offshore killer whale group. Acoustic comparison was not possible in the case of offshore killer whales because of a scarcity of recordings.

Resident, transient, and offshore killer whales have never been observed interacting socially in the ar-

eas where they were previously identified and studied (Puget Sound to Kenai Fjords), and no interaction was observed in our study between the genetically or acoustically distinguished groups. Therefore, it was possible to infer the population status from the group-association patterns of individuals for which there was no genetic or acoustic data. Animals observed in association with whales of known genetic or acoustic type were assumed to be of that same type. We did not use diet as a criterion for classification to avoid circular reasoning (evidence of dietary differences between populations becomes tautological if diet is used to define populations).

Acoustic analysis During 31 of 39 encounters in which we recorded killer whale vocalizations and did not collect genetic samples, the use of distinct calls, use of echolocation clicks, and the call rate were consistent with attributes of resident killer whale vocalizations from other regions of the Northeast Pacific (Table 2) (Yurk, 2005). All encounters had average call rates of three calls or more per minute, and strings of echolocation clicks were abundant across encounters. During these encounters, 23 structurally distinct calls were identified. Seven calls showed no obvious similarities to calls recorded elsewhere in the northeast Pacific and 15 had structural similarities, sharing some call components with calls used by killer whales that regularly occur in the northern Gulf of Alaska. However, no call from these encounters was identical to any call of the known killer whale call repertoires.

The resident-type killer whales encountered in western Alaska possibly belong to groups that are distinct from the groups of resident killer whales in other regions of Alaska because no call syllables or call patterns (sequence of syllables) between groups were found to match. Resident killer whales learn their distinct call structures in their maternal group, in which they remain for life, and call structures remain stable and group-specific for more than one generation (Ford, 1991; Yurk et al., 2002). However, because we do not know the complete call repertoires of killer whales in western Alaska we cannot be sure that we will not find complete call-type matches in the future.

Table 2

Location and number of encounters that produced recordings of killer whales (*Orcinus orca*) used in our acoustic analyses from 2001 through 2004 in the Eastern Aleutians and False Pass, Alaska.

Year	Location	Number of encounters
2001	Unalaska	3
2002	Unalaska, Akutan Island, Umnak Island	31
2003	False Pass	2
2004	False Pass	3
Total		39

In eight killer whale encounters that did not yield genetic samples (five from False Pass and three from other areas in the eastern Aleutians), vocal activity or average call rate was considerably lower than the three calls per minute that are typical for residents, and was closer to one or less than one call per minute, which is typical for transient killer whales from other areas of the northeast Pacific (Deecke et al., 2005; Saulitis et al., 2005). Furthermore, all recorded calls showed typical characteristics of transient type calls, such as the quavering of the fundamental sound frequencies and the lower number of call syllables compared to those in calls from resident killer whales.

The three encounters that were not from the False Pass region (Table 2) contained three distinct calls that were structurally similar but did not show identical order of syllables or identical syntax to calls used by members of the AT1 transient community. The AT1 transient community is thought to be limited to the Prince William Sound and Kenai Fjords region and to use a distinct call repertoire (Saulitis et al., 2005).

In the recordings made during five encounters in the False Pass region in 2003 and 2004 (Table 2), 14 distinct calls were identified in more than one of the recording sessions. Thirteen of these 14 distinct calls were identified from recordings made during two encounters in 2003. Ten of these 13 calls were also recorded during 3 encounters with killer whales in May 2004 in the same area. Thus, although the majority of calls recorded in 2004 were already identified in 2003, one new distinct call was found. This high number of same distinct-type calls is typical for transient killer whales (Deecke, 2003). Call repertoires of resident killer whales are generally much larger, and this larger repertoire is likely responsible for the detection of several new calls from newly encountered whales in recordings from consecutive years (Ford, 1991; Yurk, 2005). All call types recorded in the False Pass region appeared to be distinct from calls recorded from transient killer whales in other regions of the North Pacific. However, some structural similarity (in the form of matching call components) was found for some of the 14 calls recorded in our study and for the calls recorded from a transient community that inhabits waters along the west coast of North America. These results may indicate that the transient killer whales we encountered in the eastern Aleutians comprise one or more unique populations or communities that show some acoustic similarity with transient killer whales found in other regions of the Pacific.

Genetic analysis A total of 93 skin samples were collected from 2001 through 2004 by using biopsy darting techniques. Separation of ecotypes based on mtDNA haplotype (Barrett-Lennard, 2000) showed that 47 of the 93 samples were of transient-type lineage, 42 were of the resident-type lineage, and 4 were of the offshore-type lineage. Preliminary classifications of lineages based

on morphology and behavior and determined from field observations and photographs were consistent with the genetic analysis. For the 26 encounters that yielded both genetic and acoustic data, the two kinds of data provided identical classifications of lineage.

All 35 killer whales sampled in the False Pass–Unimak Island region had transient haplotypes. Eight of the nine samples collected in the area in 2003 had the GAT1 haplotype, which was first identified in transient killer whales from the northern Gulf of Alaska area in or near Kenai Fjords and Prince William Sound. The remaining sample contained the AT1 haplotype, formerly sequenced only in members of the AT1 transient population of the Prince William Sound area. In 2004, 14 of 26 killer whales sampled in the False Pass–Unimak Island area had the GAT1 haplotype, and the remainder had a GAT2 haplotype, a similar but not identical haplotype known to exist at a low frequency in the Gulf of Alaska transient killer whale population (Barrett-Lennard, 2000). Eleven of the 12 transient whales sampled in the summer months during 2001–2004 in the eastern Aleutians had the GAT1 haplotype, and the remaining one had the GAT2 haplotype.

Ecotypic parameters

Resident killer whales During a majority of our encounters, resident killer whales tended to be found and to travel along or near the 200-meter depth contour (Fig. 2A). This contour corresponds to a steep drop-off from the coastal shelf.

Approximately 92% of the encounters with killer whales during our summer surveys from Unimak Pass to Umnak Island were with whales determined by genetics, acoustics, or group association to be of the resident ecotype; however, this ecotype was not encountered in the spring surveys east of Unimak Pass (Table 1). A minimum of 901 resident whales used the Eastern Aleutians during the study; this count was based on individuals identified from photographs taken from 2001 through 2004. Of these individuals, 143 were seen only once during the study, and the remainder were repeatedly identified. The number of new, previously un-photographed whales observed each year declined from 534 whales in 2002 to 211 whales in 2003, to 156 whales in 2004 (Table 3). The decline in new whale sightings each year may indicate that we have identified the majority of whales that use this area during the summer months; however, there may be hundreds of whales that occasionally use the area but have not been encountered. The study area is likely only a portion of the range of the identified resident whales; several whales were matched with individuals seen in photographs taken in the Pribilof Islands over 200 miles to the west.

The numbers of individuals that could be positively identified in each resident ecotype encounter ranged from 4 to 109. A total of 347 whales were placed in 82 tentative matrilines which consisted of a reproductive female and her offspring of both sexes. These matrilines were determined from repeated association of individuals in both photographs and field observations. This method of determining matrilines was demonstrated effective in other population studies of resident killer whales (Bigg et al., 1990; Matkin et al., 1999b). Most of the matrilines comprised two generations (mother and offspring), although some included a probable grandmother. All matrilines were of consistent composition and maintained their structure over the course of the study, which has been the case in all other resident populations studied to date (Matkin et al., 1999a; Ford et al., 2000). The structure of the population was inferred from 41 groups of one or more matrilines that appeared to be longer-term associations. These groups could be considered as tentative pods (as defined by Bigg et al., 1990). Twenty-one of these groups, containing 266 whales, were sighted frequently enough that basic age and sex classes could be determined. These groups contained 65 adult males (24.4%), 105 females or immature males (39.5%), and 96 juveniles and calves (36.1%). These proportions of males, females and immature males, and juveniles and calves are comparable to those observed in other resident populations in Alaska and British Columbia (Leatherwood et al., 1990).

Table 3

Number of sightings of individual resident killer whales (*Orcinus orca*) in the eastern Aleutians from June to September, 2001 through 2004.

Year	Previously identified whales	New whales identified	Total whales identified
2001	0	38	38
2002	38	496	534
2003	268	211	479
2004	334	156	490
Total		901	

There was no evidence that resident killer whales consumed marine mammals. Whales belonging to the resident ecotype were observed consuming fish only during infrequent observations of predation (halibut were identified from samples, and salmon were probable from visual observations only). Much of the predation by resident killer whales was not visible at the surface and therefore prey samples could not be obtained. Resident whales were the only killer whales observed removing fish from the lines of commercial fishermen and observed following and feeding on fish discards from trawlers.

Transient killer whales A total of 165 individual killer whales were determined to be transients from encounters during 2001–2004 (Table 4). A majority of these whales (114) were photographed during the May–June field work in the False Pass–Unimak Island region in

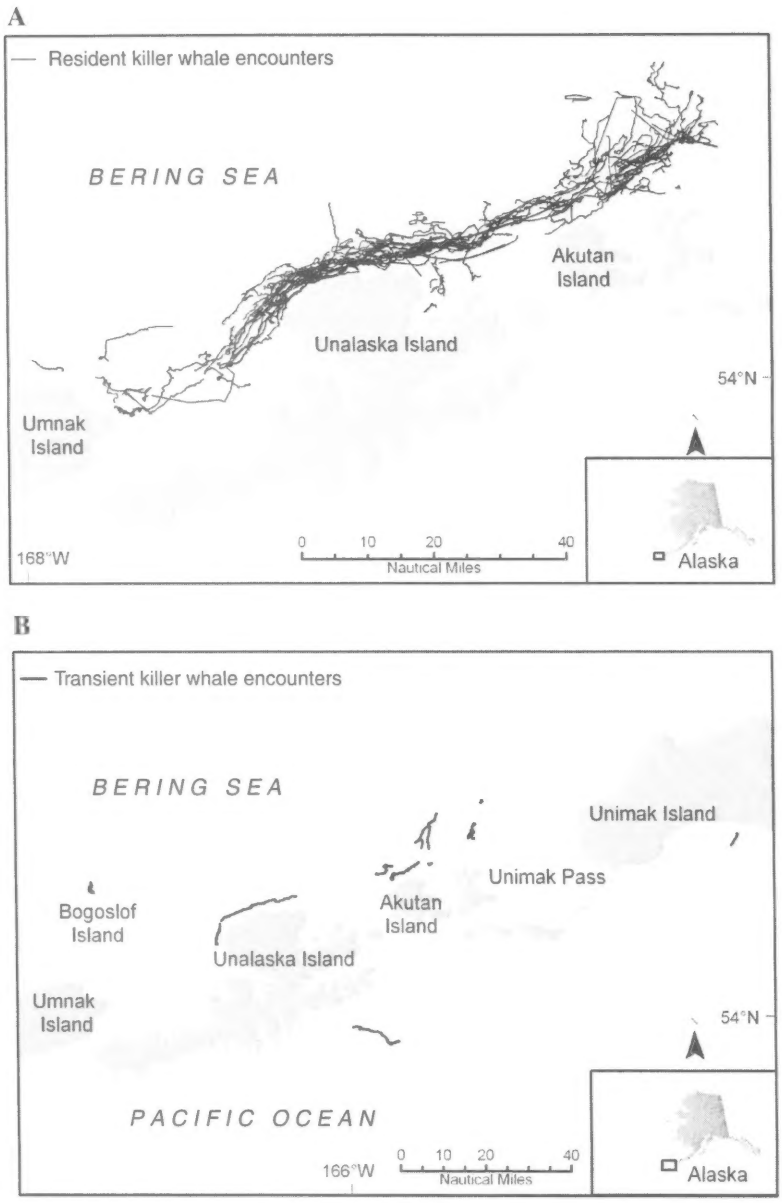

Figure 2

Tracks of the vessels during times that the vessels accompanied groups of killer whales (*Orcinus orca*) 2002–2004. (**A**) tracks of vessels following resident killer whales in the Eastern Aleutians during summer; (**B**) tracks of vessels following transient killer whales in the Eastern Aleutians during summer; (**C**) tracks of transient killer whales near False Pass- Unimak Island during spring.

2003 and 2004 (Fig. 2B). The remaining 51 individuals were photographed during the summer field season when encounters with transient killer whales were relatively infrequent in the eastern Aleutians from Unimak Pass west to Umnak Island (Fig. 2C). There were only six transient whales (less than 4% of the total identified)

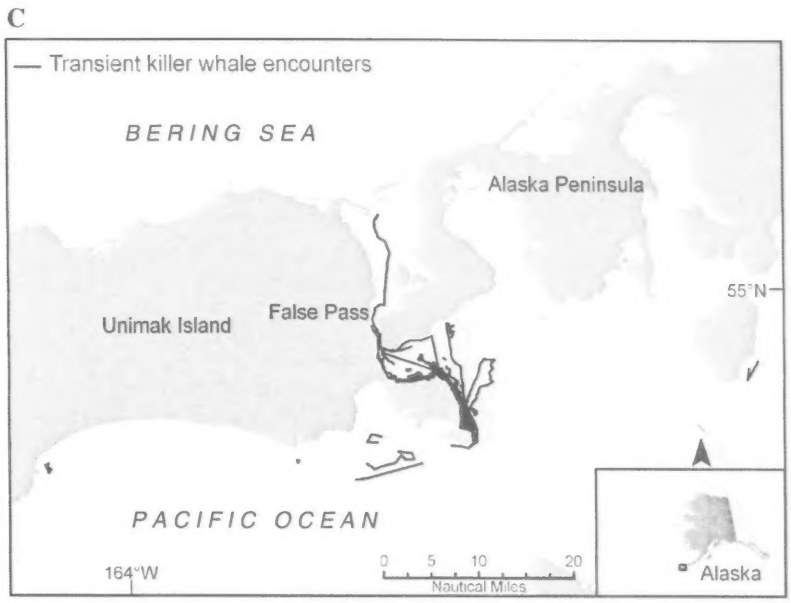

Figure 2 (continued)

Table 4

Number of individual transient killer whales (*Orcinus orca*) identified by region and by year. And the overlap of individuals between regions.

	Regions				
	False Pass (May–June)		Eastern Aleutians (July–September)		
Year	Total whales	New whales	Total whales	New whales	Overlap of individuals between regions
2001	—	—	5	5	—
2002	—	—	18	18	—
2003	84	84	25	18	2
2004	75	30	22	16	4
Total		114		51	6

that were common to both regions and time periods, although the regions are geographically adjacent (Figs. 1 and 2). In the second year, 2004, in False Pass–Unimak Island, 74 whales were identified and 45 (60%) had been photographed the previous year. In the Unimak Pass–Umnak Island surveys in both 2003 and 2004, only about 28% of the whales identified had been previously photographed in the region.

Offshore killer whales Only one encounter, which occurred in the eastern Aleutians (10 July 2003), was with killer whales identified by genetic and acoustic data as the offshore ecotype. We photographed 54 offshore killer whales in this encounter, although not all whales present were photographed. A total of 44 of these offshore whales had been previously photographed off British Columbia, Washington State, and Kenai Fjords, Alaska, and 10 had not been previously photographed (Ellis[1]).

Description of the marine mammal prey base

Although we did not measure the actual abundance of potential marine mammal prey, we recorded sightings of all marine mammals and calculated average group

[1] Ellis, G. 2005. Unpubl. data. Fisheries and Oceans Canada, Pacific Biological Station, 3190 Hammond Bay Road, Nanaimo, British Columbia, Canada V9T 6A7.

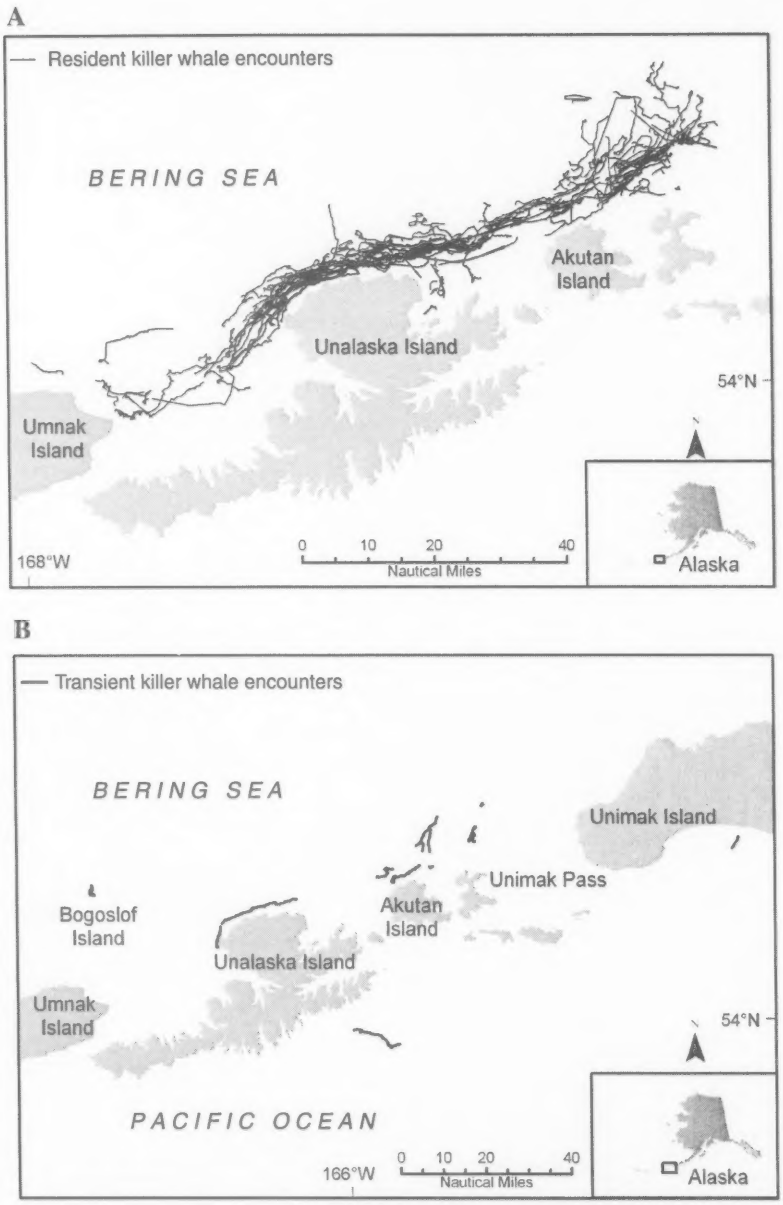

Figure 2

Tracks of the vessels during times that the vessels accompanied groups of killer whales (*Orcinus orca*) 2002–2004. (**A**) tracks of vessels following resident killer whales in the Eastern Aleutians during summer; (**B**) tracks of vessels following transient killer whales in the Eastern Aleutians during summer; (**C**) tracks of transient killer whales near False Pass- Unimak Island during spring.

2003 and 2004 (Fig. 2B). The remaining 51 individuals were photographed during the summer field season when encounters with transient killer whales were relatively infrequent in the eastern Aleutians from Unimak Pass west to Umnak Island (Fig. 2C). There were only six transient whales (less than 4% of the total identified)

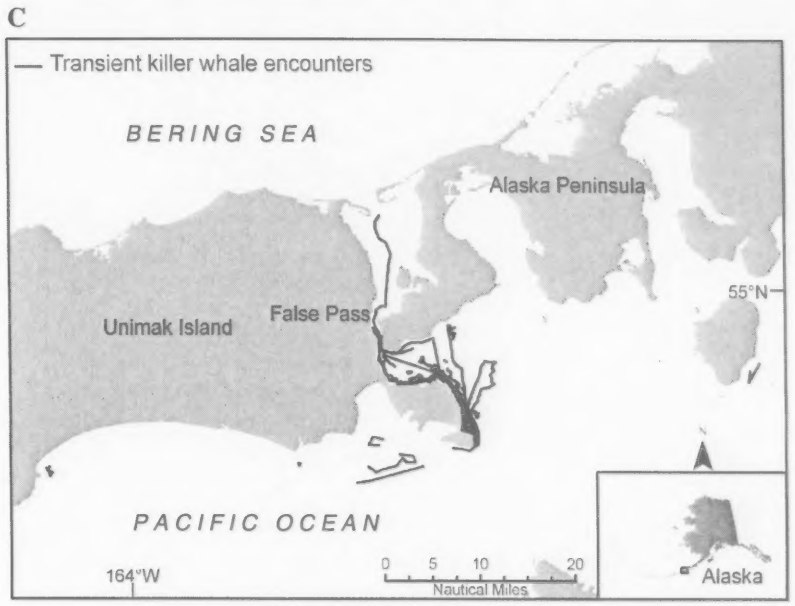

Figure 2 (continued)

Table 4

Number of individual transient killer whales (*Orcinus orca*) identified by region and by year. And the overlap of individuals between regions.

	Regions				
	False Pass (May–June)		Eastern Aleutians (July–September)		
Year	Total whales	New whales	Total whales	New whales	Overlap of individuals between regions
2001	—	—	5	5	—
2002	—	—	18	18	—
2003	84	84	25	18	2
2004	75	30	22	16	4
Total		114		51	6

that were common to both regions and time periods, although the regions are geographically adjacent (Figs. 1 and 2). In the second year, 2004, in False Pass–Unimak Island, 74 whales were identified and 45 (60%) had been photographed the previous year. In the Unimak Pass–Umnak Island surveys in both 2003 and 2004, only about 28% of the whales identified had been previously photographed in the region.

Offshore killer whales Only one encounter, which occurred in the eastern Aleutians (10 July 2003), was with killer whales identified by genetic and acoustic data as the offshore ecotype. We photographed 54 offshore killer whales in this encounter, although not all whales present were photographed. A total of 44 of these offshore whales had been previously photographed off British Columbia, Washington State, and Kenai Fjords, Alaska, and 10 had not been previously photographed (Ellis[1]).

Description of the marine mammal prey base

Although we did not measure the actual abundance of potential marine mammal prey, we recorded sightings of all marine mammals and calculated average group

[1] Ellis, G. 2005. Unpubl. data. Fisheries and Oceans Canada, Pacific Biological Station, 3190 Hammond Bay Road, Nanaimo, British Columbia, Canada V9T 6A7.

Table 5

Number of sightings, harassments, and observed kills of known marine mammal prey species of killer whales (*Orcinus orca*).

Prey species	Prey species				
	Total no. of sightings	Average group size	No. of harassments	No. of observed kills	No. observed to have escaped
Gray whale (May–June only)	18[1]	1.4	19	18	1
Dall's porpoise	521	3.9	3	0	3
Steller sea lion	153	53.4	1	1	0
Humpback whale	834	4.1	0	1	0
Northern fur seal	388	4.2	5	4	1
Minke whale	42	1.2	2	2	0
Harbor porpoise	18	4.9	0	0	0
Harbor seal	82	9.6	0	0	0
Sea otter	94	3.7	0	0	0
California sea lion	2	1.0	0	0	0
Fin whale	15	2.2	0	0	0
Sperm whale	7	1.6	0	0	0
Baird's beaked whale	10	9.4	0	0	0
Total			31	26	5

[1] This number comprises only live whales; most kills were already dead when observed and were not included in these sightings.

size as an indication of the relative availability of potential prey (Table 5). During the 346 survey days in the eastern Aleutians in June–September 2002–2004, the largest number of pinniped sightings was of northern fur seals (375 sightings), which were frequently encountered as single individuals resting at the surface, or were observed on the rookery at Bogoslof Island. Steller sea lions (124 sightings) were counted during our repeated monitoring of rookeries and haulouts in the region, resulting in a relatively large average group size (53.4 sea lions) but were encountered only occasionally off the rookeries. Other pinnipeds included harbor seals (73 sightings), which were primarily observed hauled out in small groups of less than 30 individuals, and two sightings of individual California sea lions (*Zalophus californianus*). Sea otters were observed on 81 occasions. The most frequently encountered cetacean was the humpback whale (*Megaptera novaeangliae*; 834 sightings), followed by Dall's porpoise (*Phocoenoides dalli*; 521 sightings). Less frequently observed species were minke whales (*Baleanoptera* acutorostrata; 42 sightings), fin whales (*Baleanoptera physalus*; 15 sightings), sperm whales (*Physeter macrocephalus*; 7 sightings), and Bairds beaked whales (*Berardius bairdii*; 10 sightings).

During 49 survey days in the False Pass–Unimak Island region in May and early June 2003-2004, Steller sea lions were the most frequently ncountered pinniped (29 sightings), although some fur seals (13 sightings) and harbor seals (9 sightings) were also observed. Sea otters were also present (13 sightings). The most frequently encountered cetaceans were gray whales (18 sightings) and harbor porpoises (*Phocoena phocoena*; 18 sightings). Other cetaceans sighted in this region were minke whales (3 sightings) and humpback whales (1 sighting).

Predation on marine mammals

Predation on or harassment of marine mammals was observed on 31 occasions and was attributed solely to the transient killer whale ecotype. Attacks that did not yield proof of a kill (i.e., tissue, blood, or prey in the mouth) were considered harassments. Gray whales (*Eschrichtius robustus*) were the most frequently taken species (Table 5), with 19 apparent harassments, of which 18 resulted in kills, observed in False Pass in 2003 and 2004 (May to early June). In all but one case, the gray whale was already dead and was being consumed when we found the whale. The only other predatory event during this period was a single harassment of Steller sea lions that were hauled out. During the summer season in the eastern Aleutians (Unimak Pass–Umnak Island), northern fur seals were the most frequently harassed prey; four of the five observed harassments resulted in kills. Other species included Dall's porpoises (harassed on three different occasions), two minke whales (harassed and killed), one Steller sea lion (harassed and killed), and one humpback whale (harassed).

Discussion

Our analysis indicates that the three killer whale ecotypes in the eastern North Pacific also are found in the

eastern Aleutian Islands. All killer whales examined by acoustic or genetic analysis could be placed unequivocally in the resident, transient, or offshore lineage.

Resident killer whales

A vast majority of the whales observed in the eastern Aleutians during summer were determined to be of the resident ecotype. Our minimum estimate of 901 whales is as high as any density of resident killer whales in any region of the eastern North Pacific studied to date (Matkin et al., 1999a; Ford et al., 2000).

Our data indicate that the eastern Aleutian resident killer whales comprise a distinct population, but evidence is equivocal at this time. No repeated associations have been recorded between eastern Aleutian residents and those photographed off Kodiak Island north and eastward, despite extensive field effort and examination of photographic databases for matches. However, at least one group of resident killer whales has been photographed in both regions (Durban[2]). Acoustic analysis indicates that resident whales sampled in the eastern Aleutians have call repertoires distinct from other well-known resident populations described from Kenai Fjords through Washington State. However, on the basis of structural similarities among calls from these regions, it can not be ruled out that some social contact occurs or that these whales share a recent common ancestry. The structure of some call syllables appears to change quickly in a climate of diminishing social contact (Deecke et al., 2000), whereas the overall syllable type and the syntax of syllables in calls remains stable for a longer period of time (Ford, 1991; Yurk, 2005). Genetic samples taken in the eastern Aleutians revealed only the NR haplotype, whereas those from Kodiak Island waters and in Kenai Fjords yielded a mixture of NR and southern resident haplotypes (SR haplotypes) (Barrett-Lennard, 2000). An examination of nuclear alleles is needed to clarify the relationship between eastern Aleutian residents and other resident killer whales in other regions of the North Pacific.

Offshore killer whales

Only one group of whales was determined to be of the offshore ecotype, with 54 individuals identified in a single encounter. Most (44) of the individuals identified in that encounter had been identified in other regions, including southern British Columbia and Kenai Fjords, Alaska, indicating that there is a single wide-ranging population in the eastern North Pacific. This ecotype is not known to consume marine mammals and the only reported stomach contents are salmonid bones, crab shell, sculpin, and eelgrass (Heise et al., 2003).

Transient killer whales

Transient killer whales, as determined in our analyses, were the only whales observed consuming marine mammals and were not seen feeding on fish or engaging in behaviors associated with fish-feeding in other areas (Ford and Ellis, 1999; Saulitis et al., 2000). This observation supports findings in other regions that indicate transient killer whales are a distinct ecotype specializing in marine mammal prey and comprise a subset of the total whales found in any region (Matkin et al., 1999b; Ford et al., 2000). Most of the 165 transient individuals identified in our study were present only in spring and early summer when gray whales were migrating. We documented only 51 different transient individuals in late summer, at which time their appearance was sporadic and they seemed to leave the region for periods of weeks or longer.

Transient killer whales in the eastern Aleutians display a unique call repertoire that is distinct from from the repertoire of transient killer whales in other regions. Therefore, the eastern Aleutian group may represent a separate population. Other than three whales photographed near the Barren Islands by NMML in 2001 (Durban[2]), and resighted east of Unalaska Island in 2002; no other transient whales from this area have been photographed north and east of the Shumagin Islands. The results of mitochondrial DNA analysis are equivocal because the three haplotypes we identified all occur in waters of the northern Gulf of Alaska. Again, extensive examination of nuclear alleles and comparison with those from other regions will be needed to clarify population structure.

For example, more detailed genetic analysis of eastern Aleutian transient killer whales exhibiting the AT1 haplotype has shown that they have dissimilar nuclear alleles from those of the threatened AT1 population of Prince William Sound and Kenai Fjords (Barrett-Lennard[3]). This finding indicates that the similarity of their haplotypes reflects historical lineage sorting rather than a recent descent from a common maternal ancestor. Because haplotypes reflect maternal lineages, the co-occurrence of two haplotypes in the transient whale aggregations encountered in the False Pass–Unimak Island area during spring supports the idea that distinct matrilines that may not associate at other times of year join to form these aggregations.

The small overlap (3.6% of the individuals) between transient killer whales encountered west of Unimak Pass in summer and transient killer whales observed in spring in the False Pass–Unimak Islands area indicates there is further seasonal and spatial structuring in the population. The large percentage of new transient killer whales encountered in each year of summer studies, compared to the lower percentage of resighted individu-

[2] Durban, J. 2005. Unpubl. data. National Marine Mammal Lab, National Marine Fisheries Service, 7600 Sand Point Way NE, Seattle, WA 98115.

[3] Barrett-Lennard L. 2005. Unpubl. data. Vancouver Aquarium, 845 Aviso Rd, Vancouver, BC, Canada.V6G 3E2

als in the spring, indicates that a smaller percentage of the summer whales have been identified. A survey of nearshore waters from the Gulf of Alaska to the Aleutian Islands revealed that the highest densities of transient killer whales were from the Shumagin Islands through the eastern Aleutian Islands, and an estimated abundance of 226 (CV=0.45) transient killer whales were present west of the Shumagin Islands in summer (Zerbini et al., 2006).

Transient killer whales near False Pass in May were concentrated on the Pacific Ocean side of Unimak Island and in Ikatan Bay, where gray whales pass along a shallow shelf and water depth rarely exceeds 70 meters (Fig. 1). Reports from mariners and pilots have indicated that other areas around Unimak Island and along the Bering Sea coast (e.g., Cape Lutke and the coastline near Nelson Lagoon) may also be points of interception of gray whales by killer whales. Our own surveys (Fig. 2B) indicate that transient killer whales inhabit a wide area around Unimak Island and the tip of the Alaska Peninsula, where we recorded kills of gray whales at Deer Island (110 km northeast of False Pass) and Cape Lutke (140 km southwest of False Pass).

Despite uncertainties regarding the range of transient killer whales, it is evident that they are numerous, concentrated, and consistently present in the spring from Unimak Pass eastward. Gray whales have been previously reported as killer whale prey (Matkin and Saulitis, 1994); however, the extent to which transient killer whales were focused on gray whale predation during May–June around Unimak Island has not been previously described. Although subsequent surveys in these areas during summer (C. O. Matkin, unpubl. data; Durban[2].) have identified some of the same whales as those identified in the spring, most of the whales do not remain in these nearshore waters. It is not known whether these transient whales move offshore and disperse, follow the gray whales into the Bering Sea, or move into other unstudied regions.

The distribution of most, if not all, transient killer whales that we identified undoubtedly extends well beyond our survey area. Technical advances in satellite and radio tagging procedures that could be applied to killer whales would aid considerably in understanding the movements and range of transients in this region. Without a better understanding of the range of these whales, it is impossible to fully assess their impact on prey populations.

Northern fur seals appear to be an important prey for killer whales from late June to September west of Unimak Pass. This finding is based on observed kills compared to kills of other species. A substantial number of the fur seals sighted in summer were likely associated with the recently established and expanding fur seal rookery on Bogoslof Island. This population increased rapidly from 898 pups in 1992 to 5096 pups in 1999 (Angliss and Lodge, 2004). Additionally, peak numbers of migrating fur seals pass through Unimak Pass into the Bering Sea in June on their way to the Pribilof Islands and then migrate back to the Pacific in peak numbers during October–November (Bigg, 1990).

Northern fur seals have long been indicated as an important prey for killer whales in the Pribilof Region (Hanna, 1923; Zenkovich, 1938; Tomilin, 1957). However, their importance as prey in the eastern Aleutians has not been previously documented and may have developed with the growth of the Bogoslof rookery. This geographic region presents an opportunity to examine the effects of killer whale predation on an apparently stable or increasing population of fur seals—a species that is declining in other areas.

Minke whales made up a substantial proportion of summer predation despite the relative low frequency with which they were sighted, and the apparent difficulty that killer whales have in capturing this fast swimming species in open water (Ford et al., 2005). Minke whales appear to be a minor part of the diet of killer whales from Washington State to northern southeastern Alaska (Ford et al., 2005).

We observed the harassment of a humpback whale by killer whales once; during the attack, other humpback whales rapidly converged on the attackers and appeared to drive the killer whales away. No injuries were apparent. Harassments of humpbacks have been reported in other regions of Alaska (Saulitis et al., 2000), but did not result in a kill or apparent injury. Photographs of scars indicate that most killer whale attacks on baleen whales target young animals, probably calves on their first migration from low-latitude breeding and calving areas to high-latitude feeding grounds (Mehta[4]).

Although none of the attacks that we observed on Dall's porpoises resulted in confirmed kills, Dall's porpoises could be a significant prey as has been indicated in other regions (Ford et al., 1998; Saulitis et al., 2000); however, more observations are needed. Harbor seals were conspicuously absent from our prey observations despite also being an important prey in other regions of Alaska (Saulitis et al., 2000; Matkin et al., in press). Harbor seals are found in relatively low numbers in the eastern Aleutians.

Although Steller sea lions were observed as prey on one occasion and were harassed on another, they did not appear to be a primary target of the transient killer whales we observed during our spring and summer surveys. Whether or not they are an important prey during other seasons (fall and winter) is not known and will require additional study or the application of other methods to be fully assessed.

Although our study was limited by a small sample size in the summer, it provided significant information on the distribution of transient killer whale prey and the importance of fur seals in the killer whale diet during summer west of Unimak Pass and the importance of grey whales in killer whale diet during spring from Unimak Pass east. An increase in sample size of ob-

[4] Mehta, A. 2005. Unpubl. data. Woods Hole Oceanographic Institute, Woods Hole, MA 02543-1050.

served kills is therefore important to develop greater confidence and detail in estimating the composition of killer whale diets.

Our seasonal bias towards spring and summer leaves uncertainty about killer whale diets during fall and winter. In this regard, analytical techniques that include identification of fatty acids, stable isotopes, and contaminants may prove useful when coupled with field observations to obtain a more complete picture of the feeding habits of killer whales during these seasons (Herman et al., 2005).

Conclusions

Our work underscores the importance of determining lineages and ecotypes of killer whales before making assumptions regarding feeding habits and potential impact of killer whales on prey populations. Although there may be well over 100 marine mammal-eating transient killer whales that aggregate in False Pass–Unimak Island region to feed on gray whales in spring, the majority of the killer whales present in summer are fish-eating residents. In the summer, marine-mammal–eating transients are far less abundant than in spring.

Our study indicates that the diet of transient killer whales off the eastern Aleutian Islands contrasts with the diets of transient killer whales in other parts of the North Pacific. In British Columbia, for example, transient killer whale diet is composed primarily of harbor seals (Ford et al., 1998), whereas both harbor seals and harbor porpoise are the primary prey of killer whales in northern Glacier Bay and Icy Strait region of southeastern Alaska (Matkin et al., 2005). Further north, in Prince William Sound and Kenai Fjords, the dominant prey of the AT1 transient killer whales are harbor seals and Dall's porpoises (Saulitis et al., 2000). Only in the Gulf of Alaska (Kenai Fjords) has predation by some Gulf of Alaska transient killer whales apparently focused on sea lions (Matkin et al., 2005).

Killer whale feeding behavior needs to be examined on a region-by-region basis, as well as seasonally. Experience in other regions of the North Pacific has shown that estimated population sizes, life history parameters, and dietary information can be obtained with a concerted long-term research effort. Our study has demonstrated that the eastern Aleutians also support the presence of three killer whale ecotypes, as has been previously described along the Pacific Coast of North America. It also has developed minimum estimates of the numbers of transient and resident killer whales that use the region and has provided information that may indicate that grey whales and northern fur seals are important prey items in this region at certain times and in certain areas. Steller sea lions were not a primary prey during our spring and summer surveys. Whether or not killer whales are impeding population recovery of Steller sea lions in the eastern Aleutian Islands cannot be answered decisively, nor can the effect that killer whales may be having on other species in this region as yet be ascertained. Answers to these and other questions are expected to become clearer as the observational database for killer whales is expanded and the data for regions within the North Pacific are compared.

Acknowledgments

Financial support was provided by the Cooperative Institute for Arctic Research (CIFAR), the National Marine Mammal Laboratory, the National Oceanic and Atmospheric Administration, the Steller Sea Lion Research Initiative (SSLRI), the North Pacific Universities Marine Mammal Research Consortium (NPUMMRC), the North Pacific Marine Science Foundation, and the Alaska Sea Life Center (ASLC). Field biologists included P. Nielson, T. Markowitz, D. Power, and L. Mazzuca and vessel operations were directed by M. Brittain. Vessel operators were B. Schauff, P. Thompson, B. Laukitis, D. Graves, T. Peterson, A. Bartlett, and G. Marshall. Assistance in the field was provided by L.A. Holmes, R. Brewer, V. Vergara, T. Ciosek, G. Calef, C. Bianchini, A. G. MacHutchon, K. Leonard, F. Nicklin, K. Walker, D. Masters, and R. Blancato. Office and logistic support were provided by P. Rosenbaum and J. Rose.

Literature cited

Angliss, R. P., and K. L. Lodge.
2004. Alaska marine mammal stock assessments, 2003. NOAA Technical Memo. NMFS-AFSC-144, 237 p.

Barrett-Lennard, L. G.
2000. Population structure and mating patterns of killer whales (*Orcinus orca*) as revealed by DNA analysis. Ph.D. diss., 92 p. Univ. British Columbia, Vancouver, B.C., Canada.

Barrett-Lennard, L. G., K. A. Heise, E. Saulitis, G. Ellis, and C. Matkin
1995. The impact of killer whale predation on Steller sea lion populations in British Columbia and Alaska. Report of the Marine Mammal Research Consortium, Univ. British Columbia, 6248 Biological Sciences Road, Vancouver, BC, V6T-1Z4, Canada.

Barrett-Lennard, L. G., T. G. Smith, and G. M. Ellis.
1996. A cetacean biopsy system using lightweight pneumatic darts, and its effect on the behavior of killer whales. Mar. Mamm. Sci. 12:14–27.

Bigg, M. A.
1990. Migration of northern fur seals (*Callorhinus ursinus*) off western North America. Canadian Technical Report of Fisheries and Aquatic Sciences no. 1764, 64 p.

Bigg, M. A., P. F. Olesiuk, G. M. Ellis, J. K. B. Ford, and K. C. Balcomb III.
1990. Social organization and geneaology of resident killer whales (*Orcinus orca*) in the coastal waters of British Columbia and Washington State. Report of the International Whaling Commission. (special issue) 12:386–406.

Dahlheim, M. E.
1997. A Photographic catalog of killer whales, *Orcinus orca*, from the central Gulf of Alaska to the southeastern Bering Sea. NOAA Tech. Rep. NMFS-131, 54 p.

Deecke, V. B.
2003. The vocal behaviour of transient killer whales (*Orcinus orca*) communicating with costly calls. Ph.D. diss. 138 p. Univ. St. Andrews, St. Andrews, Scotland.

Deecke, V. B., J. K. B. Ford, P. J. B. Slater.
2005. The vocal behavior of mammal-eating killer whales: communicating with costly calls. Anim. Behav. 69(2):395–405.

Deecke, V. B., J. K. B. Ford, and P. Spong.
2000. Dialect change in resident killer whales: implications for vocal learning and cultural transmission. Anim. Behav. 60(5):629–638.

DeMaster, D. P., A. W. Trites, P. Clapham, S. Mizroch, P. Wade, R. J. Small, and J. Ver Hoef.
2006. The sequential megafaunal collapse hypothesis: testing with existing data. Prog. Ocean. 68:329–342

Estes, J. A., M. T. Tinker, T. M. Williams, and D. F. Doak.
1998. Killer whale predation on sea otters links oceanic and nearshore ecosystems. Science 282:473–476.

Ford, J. K. B.
1991. Vocal traditions among resident killer whales (*Orcinus orca*) in coastal waters of British Columbia. Can. J. Zool. 69:1454–1483.
1989. Acoustic behaviour of resident killer whales (*Orcinus orca*) off Vancouver Island, British Columbia. Can J. Zool. 67:727–745.

Ford, J. K. B., G. M. Ellis, D. R. Matkin, K. C. Balcomb, D. Briggs, and A. B. Morton.
2005. Killer whale attacks on minke whales: prey capture and antipredator tactics. Mar. Mamm. Sci. 21: 603–618.

Ford, J. K. B., and G. M. Ellis.
1999. Transients: Mammal-hunting killer whales, 96 p. Univ. British Columbia Press, Vancouver, Canada.

Ford, J. K. B., G. M. Ellis, and K. C. Balcomb.
2000. Killer whales, 2nd ed., 104 p. Univ. British Columbia Press, Vancouver, Canada.

Ford J. K. B., G. M. Ellis, L. G. Barrett-Lennard, A. B. Morton, and K. C. Balcomb III.
1998. Dietary specialization in two sympatric populations of killer whales (*Orcinus orca*) in coastal British Columbia and adjacent waters. Can. J. Zool. 76:1456–1471.

Hanna, G. D.
1923. Rare mammals of the Pribilof Islands, Alaska. J. Mammal. 4:209–215.

Heise, K., L. G. Barrett-Lennard, E. Saulitis, C. Matkin, and D. Bain.
2003. Examining the evidence for killer whale predation on Steller sea lions in British Columbia and Alaska. Aquat. Mamm. 29:325–334.

Herman, D. P., D. G. Burrows, P. R. Wade, J. W. Durban, C. O. Matkin, R. G. LeDuc, L. G. Barrett-Lennard, and M. M. Krahn.
2005. Feeding ecology of eastern North Pacific killer whales *Orcinus orca* from fatty acid, stable isotope, and organochlorine analyses of blubber biopsies. Mar Ecol. Prog. Ser. 302:275–291.

Leatherwood, S., C. O. Matkin, J. D. Hall, and G. M. Ellis.
1990. Killer whales, *Orcinus orca*, photo-identified in Prince William Sound, Alaska, 1976 through 1987. Can. Field Nat. 104:362–371

Loughlin, T. R., and A. E. York.
2000. An accounting of the sources of Steller sea lion mortality. Mar. Fish. Rev. 62(4):40–45.

Matkin, C. O., G. M. Ellis, P. Olesiuk, and E. L. Saulitis.
1999a. Association patterns and genealogies of resident killer whales (*Orcinus orca*) in Prince William Sound, Alaska. Fish. Bull. 97:900–919.

Matkin, C. O., G. M. Ellis, E. L. Saulitis, L. G. Barrett-Lennard, and D. Matkin.
1999b. Killer whales of zouthern Alaska. North Gulf Oceanic Society, Homer, AK.

Matkin, C. O., and E. Saulitis.
1994. Killer whale (*Orcinus orca*): biology and m,anagement in Alaska. U.S. Mar. Mamm. Comm., Washington D.C., 80 p. [Contract T75135023.]

Matkin, C. O., E. Saulitis, D. Maldini, J. Maniscalco, and L. Mazzuca.
2005. Steller sea lion predation by killer whales in Kenai Fjords/Prince William Sound, Alaska. *In* Synopsis of research on Steller sea lions: 2001–2005 (T. R. Loughlin, S. K. Atkinson, and D. G. Calkins, eds.), p. 212–226. Alaska Sea Life Center's Steller Sea Lion Research Program, Seward, AK.

Matkin, D. R., J. M. Straley, and C. M. Gabriele.
In press. Killer whale feeding ecology and non-predatory interactions with other marine mammals. *In* Proceedings of the fourth Glacier Bay science symposium, 2004 (J. F. Piatt, and S. M. Gende, eds.). U.S. Geological Survey, Information and Technology Report USGS/BRD/ITR-2005, Washington, D.C.

Merrick, R. L., T. R. Loughlin, and D. G. Calkins.
1987. Decline in abundance of the northern sea lion, *Eumetopias jubatus*, in 1956–86. Fish. Bull. 85:351–365.

Miller, P. J. O., and D. E. Bain.
2000. Within-pod variation in the sound production of a pod of killer whales, *Orcinus orca*. Anim. Behav. 60(5):617–628.

Mizroch, S. A., and D. W. Rice.
2006. Have North Pacific killer whales switched prey species in response to depletion of the great whale populations? Mar. Ecol. Prog. Ser. 310:235–246.

Pitcher, K. W.
1990. Major decline in number of harbor seals, *Phoca vitulina richardsi*, on Tugidak Island, Gulf of Alaska. Mar. Mamm. Sci. 6:121–134.

Sambrook, J., E. F. Fritsch, and T. Maniatis.
1989. Molecular cloning: a laboratory manual. 3rd ed. Cold Spring Harbor, NY.

Saulitis, E., C. O. Matkin, and F. H. Fay.
2005. Vocal repertoire and acoustic behavior of the isolated AT1 killer whale subpopulation in southern Alaska. Can. J. Zool. 83:1015–1029.

Saulitis, E. L., C. O.Matkin, K. Heise, L. Barrett Lennard, and G. M. Ellis.
2000. Foraging strategies of sympatric killer whale (*Orcinus orca*) populations in Prince William Sound, Alaska. Mar. Mamm. Sci. 6:94–109.

Springer, A. M., J. A. Estes, G. B van Vliet, T. M. Williams, D. F. Doak, E. M. Danner, K. A. Forney, and B. Pfister.
2003. Sequential megafaunal collapse in the North Pacific Ocean: an ongoing legacy of industrial whaling? Publ. Nat. Acad. Sci. 100:12,223–12,228.

Thompson, J. D., D. G. Higgins, and J. Gibson.
1994. Clustal W: improving the sensitivity of progressive multiple sequence alignment through sequence weight-

ing position specific gap penalties and weight matrix choice. Nucl. Acids Res. 22:4673–4680

Tomilin, A. G.
1957. Cetacea. Vol. 9 *of* Mammals of the U.S.S.R. and adjacent countries (V. G. Heptner, ed.), 756 p. Izd. Akad. Nauk SSSR, Moscow. [Translated from Russian by Israel Prog. Sci Transl., 1967.]

Trites, A. W.
1992. Northern fur seals: why have they declined? Aquat. Mamm. 18:3–18.

Trites, A. W., V. B. Deecke, E. J. Gregr, J. K. B. Ford, and P. F. Olesiuk.
2006. Killer whales, whaling and sequential megafaunal collapse in the North Pacific: a comparative analysis of the dynamics of marine mammals in Alaska and British Columbia following commercial whaling. Mar. Mamm. Sci. 22.

Trites, A. W., and P. A. Larkin.
1996. Changes in the abundance of Steller sea lions (*Eumetopias jubatus*) in Alaska from 1956 to 1992: How many were there? Aquat. Mamm. 153–166.

Winship, A. J., and A. W. Trites.
2006. Risk of extirpation of Steller sea lions in the Gulf of Alaska and Aleutian Islands: a population viability analysis based on alternative hypotheses for why sea lions declined in western Alaska. Mar. Mamm. Sci. 22:124–155

York, A. E.
1987. Northern fur seal, *Callorhinus ursinus*, eastern Pacific population (Pribilof Islands, Alaska, and San Miguel Island, California). *In* Status, biology, and ecology of fur seals (J. P. Croxall, and R. L. Gentry, eds.), p. 9–21. NOAA Tech. Rept. NMFS 51.

Yurk, H.
2005. Vocal culture and social stability in resident killer whales (*Orcinus orca*) of the northeastern Pacific. Ph. D. diss., 126 p. Univ. British Columbia, Vancouver, British Columbia, Canada.

Yurk, H., L. G. Barrett-Lennard, J. K. B Ford, C. O. Matkin.
2002. Cultural transmission within maternal lineages: vocal clans in resident killer whales in southern Alaska. Anim. Behav. 63(6):1103–1119.

Zenkovich, B. A.
1938. On the grampus or killer whale (*Grampus orca* Lin.). Priroda 4:109–112. [Translated from Russian by L. G. Robbins. U.S. Geological Survey S(570).

Zerbini, A. N., J. M. Waite, J. W. Durban, R. LeDuc, M. E. Dahlheim, and P. R. Wade.
2006. Estimating abundance of killer whales in the nearshore waters of the Gulf of Alaska and Aleutian Islands using line transect sampling. Mar. Biol. DOI 10.1007/s0027006-0347-8.

Removing observational noise from fisheries-independent time series data using ARIMA models

William T. Stockhausen (contact author)

Michael J. Fogarty

Email address for W. T. Stockhausen: William.Stockhausen@noaa.gov

National Ocean and Atmospheric Administration
National Marine Fisheries Service
Northeast Fisheries Science Center
166 Water Street
Woods Hole, MA 02543

Present address for corresponding author: National Marine Fisheries Service
Alaska Fisheries Science Center
7600 Sand Point Way NE
Seattle, Washington 98115

Abstract—Abundance indices derived from fishery-independent surveys typically exhibit much higher interannual variability than is consistent with the within-survey variance or the life history of a species. This extra variability is essentially observation noise (i.e. measurement error); it probably reflects environmentally driven factors that affect catchability over time. Unfortunately, high observation noise reduces the ability to detect important changes in the underlying population abundance. In our study, a noise-reduction technique for uncorrelated observation noise that is based on autoregressive integrated moving average (ARIMA) time series modeling is investigated. The approach is applied to 18 time series of finfish abundance, which were derived from trawl survey data from the U.S. northeast continental shelf. Although the *a priori* assumption of a random-walk-plus-uncorrelated-noise model generally yielded a smoothed result that is pleasing to the eye, we recommend that the most appropriate ARIMA model be identified for the observed time series if the smoothed time series will be used for further analysis of the population dynamics of a species.

Manuscript submitted 12 November 2004 to the Scientific Editor's Office.

Manuscript approved for publication 18 April 2006 by the Scientific Editor.

Fish. Bull. 107:88–101 (2007).

Time series of species abundance from fishery-independent surveys, such as bottom trawl or acoustic surveys, are important in monitoring temporal change in the abundance of marine populations. For commercially important species, catch and effort data from the commercial fishery may be available, allowing estimation of temporal trends of the stock population by means of stock assessment models (e.g., virtual population analysis). However, such records are not available for many species, especially those with little commercial (but perhaps significant ecological) value. Fishery-independent surveys may thus constitute the only source of information for assessing temporal changes in the abundance of these species (Pennington, 1985; Helser and Hayes, 1995).

Annual estimates of abundance derived from fisheries-independent surveys are typically regarded as providing a relative measure of population abundance (i.e., they are indices of abundance, not true estimates of total population size) (Grosslein, 1969; Clark, 1979). Thus, the expected value of the abundance index (e.g., mean catch-per-tow for trawl surveys) is regarded as proportional to the size of the actual population, although the constant of proportionality (the catchability) is unknown. As such, relative changes in an abundance index should reflect similar relative changes in the actual population, and trends in the time series of such an index should reflect similar trends in the corresponding population.

Unfortunately, abundance indices derived from large-scale fishery-independent surveys typically exhibit interannual variability much higher than one would expect from within-survey variance (Byrne et al., 1981; Pennington, 1985). Part of the variability in such indices is presumably due to the variability in the underlying population—a variability that is caused by population-dynamic processes such as recruitment. However, part of the variability is due to observation noise that arises from both within-survey sampling variability because of the heterogeneous distribution of many fish stocks (Byrne et al., 1981), and because of environmentally driven factors that affect catchability over time (Byrne et al., 1981; Collie and Sissenwine, 1983). Low signal-to-noise ratios in abundance indices that are due to high observation noise reduce chances of detecting important changes or trends in actual population abundance. Variability due to within-survey sampling can be reduced (before the fact) by adding more stations to a survey, but additional stations will not reduce variability caused by changes in catchability.

Time series modeling using autoregressive integrated moving average (ARIMA; Box and Jenkins, 1976) models provides an approach to re-

moving observation noise from abundance estimates. ARIMA models are frequently used in economic forecasting (Enders, 2004) and are becoming more common in fisheries research. Recent applications of ARIMA models to other fisheries problems include forecasting monthly landings in the Mediterranean (Lloret et al., 2000), testing theories of population dynamics (Becerra-Munoz et al., 1999), and modeling nutrient dynamics in an upwelling system (Nogueira et al., 1998).

In the context of reducing the influence of observational noise in time series data, Cleveland and Tiao (1976) first developed a noise-reduction and smoothing algorithm for processes that could be described by an ARIMA time series model. Their approach requires that the ARIMA model for the unobserved, underlying process be known. This known model, in turn, uniquely determines the ARIMA model for the observed time series contaminated by observation noise and allows one to estimate the variance of the observation noise. Unfortunately, although the ARIMA model for an unobserved, underlying process may be known in some instances (from theory, perhaps), in many cases the model for the unobserved process will be unknown.

Box et al. (1978) extended Cleveland and Tiao's (1976) ideas and developed a noise-reduction algorithm based on the ARIMA model for the observed time series. However, the ARIMA model for the observed time series merely constrains, but does not determine, the model for the unobserved, underlying process; it provides only an upper bound for the observation error variance. Consequently, this approach generally requires an external estimate of the observation error variance to determine the appropriate level of noise reduction.

Pennington (1985) first applied these ARIMA-based time series modeling techniques to smoothing abundance indices derived from trawl survey data. He assumed that an observed abundance time series reflected a combination of the underlying population abundance and independent, uncorrelated, and multiplicative observation noise (the latter arising perhaps from environmentally driven changes in catchability). He further assumed that both the (log-transformed) observed time series and unobserved population process could be represented by ARIMA models. Pennington (1985) then developed an alternative algorithm to that of Box et al. (1978); his derivation allowed particular simplification in the case where the underlying population process could be modeled as a random walk. In this simple case, the resulting noise reduction filter is an exponentially-weighted average of the observed time series for the endpoint of the time series (Pennington, 1985). More importantly, the observation error variance can be easily estimated from the ARIMA model parameters and an external estimate is unnecessary. Thus, for the case where a random walk model for the underlying process is valid, the appropriate level of smoothing is objectively determined.

As a demonstration, Pennington (1985) applied his noise reduction algorithm to groundfish trawl survey data for haddock (*Melanogrammus aeglefinus*) from the northeastern Atlantic coast of the United States. He found that the variances of the smoothed indices were "considerably lower" than those of the originals. However, this demonstration used an ARIMA model derived from a much longer time series that had been generated from a stock assessment based on commercial catch data. Pennington (1985) assumed that this model represented the underlying population and therefore did not develop models based on the observed time series. Although this assumption was perfectly reasonable, given that such alternative data (the stock assessment) were available, it cannot be applied to situations when only survey data are available to fishery analysts.

The ARIMA model Pennington (1985) derived from stock assessment results was a random walk model; therefore the appropriate level of noise reduction for the corresponding survey data could be objectively determined from the model parameters. Pennington's (1985) method was later used to apply random walk models to survey data (Fogarty et al.[1]; Pennington, 1986; Anonymous, 1988, 1993). Pennington (1986) found that random walk models were appropriate for the survey time series considered in his study. However, random walk models were assumed *a priori* in the remaining three references (Fogarty et al.[1]; Anonymous, 1988, 1993) to generate smoothed abundance trajectories; because less than 25 observations for each time series were considered in these references, reliable identification of the model structure for each time series was considered problematic and random walk models were used as "null" models.

When it is an appropriate description of the underlying process, a random walk model yields an objective determination of the degree of noise reduction appropriate to an observed time series. However, an *a priori* adoption of this model should be viewed with some skepticism. Additionally, if a random walk model is not an appropriate description of the underlying process, the resulting smoothed time series may seem reasonable, but the result no longer has support as the unobserved, underlying process. In this circumstance, we regard the effect of the ARIMA algorithm as merely smoothing, and not necessarily as noise reducing.

As such, we feel that the utility of ARIMA-based approaches to noise reduction for abundance indices derived from survey data has not been adequately explored to date. In addition, substantially longer time series (e.g., 40 observations) are now available with which to test this concept. In our study, we test the utility of the ARIMA time series noise reduction approach propounded by Pennington (1985), using time series of abundance indices from fishery-independent trawl survey data for nine finfish species (Table 1) during two seasons on Georges Bank. We first review the original methods developed by Cleveland and Tiao

[1] Fogarty, M. J., J. S. Idoine, F. P. Almeida, and M. Pennington. 1986. Modeling trends in abundance based on research vessel surveys. ICES CM (council meeting) 1986/G, p. 92. ICES, Copenhagen, Denmark.

Table 1

Time series of abundance indices for the following finfish species on Georges Bank were derived from a fisheries-independent trawl survey and used to test the ARIMA-based smoothing algorithm.

Common name	Scientific name	Type
Winter skate	*Leucoraja ocellata*	Elasmobranch
Little skate	*Leucoraja erinacea*	Elasmobranch
Silver hake	*Merluccius bilinearis*	Groundfish
Atlantic cod	*Gadus morhua*	Groundfish
Haddock	*Melanogrammus aeglefinus*	Groundfish
Winter flounder	*Pseudopleurenectes americanus*	Flatfish
Yellowtail flounder	*Limanda ferruginea*	Flatfish
Atlantic herring	*Clupea harengus*	Pelagic schooling fish
Atlantic mackerel	*Scomber scombrus*	Pelagic schooling fish

(1976) and Box et al. (1978). Framing the problem in terms of power spectra, we also offer some additional new insights into this noise reduction approach. Next, we apply the ARIMA-based noise reduction approach to the time series data and present the results. We have implemented Box et al.'s (1978) algorithm, not Pennington's (1985). Finally, we discuss our perceptions of the utility of this approach in light of our results and overall experience with it.

Materials and methods

General characteristics of ARIMA models

In this section, we first briefly review ARIMA models for stochastic processes. Then we review the approach of Box et al. (1978) for obtaining maximum likelihood estimates for an underlying ARIMA time series from a time series of observations with independent and identically distributed (IID) observation noise.

ARIMA models are parsimonious models that can adequately represent many stochastic time series (Box and Jenkins, 1976). Stochastic time series that can be represented by ARIMA models are essentially the output of a linear filter applied to an input time series of white noise (Box and Jenkins, 1976). We will refer to such time series as ARIMA processes.

For a zero-mean stochastic time series $\{z_t\}$ that can be expressed as an ARIMA model, we denote the model (using the notation of Box and Jenkins, 1976) as

$$\varphi(B)z_t = \alpha(B)a_t, \tag{1}$$

where z_t = the value of the time series at time t;
$\varphi(B)$ = the generalized autoregressive (AR) operator;
$\alpha(B)$ = the moving average (MA) operator;
B = the backward shift operator; and
a_t = IID normally distributed random variables with mean zero and variance σ_a^2.

The backward shift operator B has the property that $B\,z_t = z_{t-1}$; hence $B^m\,z_t = z_{t-m}$. The operators $\varphi(B)$ and $\alpha(B)$ are polynomials in B of order $p+d$ and q (respectively) such that

$$\varphi(B) = 1 - \sum_{j=1}^{p+d} \varphi_j B^j$$
$$\alpha(B) = 1 - \sum_{j=1}^{q} \alpha_j B^j. \tag{2}$$

Furthermore, $\varphi(B)$ can be factored such that $\varphi(B) = \phi(B)(1-B)^d$, where the (ordinary) AR operator $\phi(B)$ has a form similar to $\varphi(B)$ but is of order p. The operator $(1-B)^d$ represents d sequential applications of the backward difference operator $1-B$ such that the original time series $\{z_t\}$ is self-differenced d times before application of the AR operator $\phi(B)$.

As a shorthand, an ARIMA model that consists of an AR operator of order p, d backward difference operations, and a MA operator of order q is abbreviated as (p,d,q). A $(p,0,0)$ model is referred to as an AR model of order p, or AR(p) in shorthand notation, and a $(0,0,q)$ model is referred to as a MA model of order q (MA(q) in shorthand). A $(p,0,q)$ model is referred to as an autoregressive-moving average model (ARMA(p,q) in shorthand) and a (0,d,q) model is referred to as an integrated moving average model (IMA(d,q) in shorthand). Finally, a random walk model is (0,1,0), while a random-walk-plus-uncorrelated-observation noise (RWPUN) model is (0,1,1).

In general, ARIMA models represent nonstationary time series. However, the time series that results from applying the backward difference operator d times to a (p,d,q) ARIMA process is a stationary ARMA(p,q) process. Typical constraints imposed on ARIMA models are that, when B is regarded as a complex variable, the polynomial in B representing the generalized autoregressive operator has zeros on or outside the unit circle ($|B|=1$), whereas the polynomials representing the ordinary autoregressive operator and the moving

average operator have zeros outside the unit circle. Additionally, the white noise variance, σ_a^2, must be finite. These constraints ensure that a model is invertible and stationary (or, if not stationary, that at least it is of a suitable form).

One final property of ARIMA models is of interest here. The power spectrum for an ARMA (p,q) process represented by equation 1 is given by

$$p_z(f) = \tfrac{1}{2}\sigma_a^2 \frac{\left|\alpha(e^{-i2\pi f})\right|^2}{\left|\varphi(e^{-i2\pi f})\right|^2} = \tfrac{1}{2}\sigma_a^2 \frac{\alpha(B)\alpha(F)}{\varphi(B)\varphi(F)} \qquad (3)$$

$$\text{where } B = e^{-i2\pi f}; 0 \le f \le \tfrac{1}{2},$$

and the forward shift operator, $F=B^{-1}$, has the opposite effect to B (i.e., $F^m z_t = z_{t+m}$).

ARIMA models of time series with observation noise

Suppose, then, that $y_1, y_2, \ldots, y_T$ represent a time series of observations at times $t = 1,2, \ldots T$ such that

$$y_t = z_t + e_t, \qquad (4)$$

where the z_t's represent the unobserved, underlying process and the e_t's are IID normal variables with variance σ_e^2 (i.e., e~N$(0,\sigma_e^2)$) that are also independent of the z_t's (i.e., $< e_j z_k >=0$ for all j,k). The goal is to estimate the unobserved time series $\{z_t\}$ by using the observed time series $\{y_t\}$. For the analysis of fishery-independent time series, it seems reasonable to assume that only the ARIMA model for the observed time series $\{y_t\}$ is known (it can be estimated using standard techniques). In particular, this assumption means that the model for $\{z_t\}$ is unknown within constraints implied by the observation equation. However, to develop the approach used here it is helpful to start as though the model for the unobserved process $\{z_t\}$ were known.

Thus, we assume that the time series $\{z_t\}$ can be represented by an ARIMA (p,d,q) process:

$$\varphi(B) z_t = \alpha(B) c_t, \qquad (5)$$

where the c_t's are IID and c_t~N$(0,\sigma_c^2)$. Substituting in $y_t - e_t$ for z_t and rearranging, one obtains

$$\varphi(B) y_t = \alpha(B) c_t + \varphi(B) e_t, \qquad (6)$$

which can be expressed as an ARIMA model for $\{y_t\}$ of the form

$$\varphi(B) y_t = \eta(B) d_t, \qquad (7)$$

where the d_t's are IID, d_t~N$(0,\sigma_d^2)$ and the MA operator is $\eta(B)$. Thus, the generalized AR operator for the observed $\{y_t\}$ is identical to that for the unobserved $\{z_t\}$. Furthermore, because $\alpha(B)$ has order q and $\varphi(B)$ has order $p+d$, $\eta(B)$ must be of order $\max(p+d,q)$. This requirement for $\eta(B)$ constrains the order of potential ARIMA models that could describe the observed process: if $p+d \le q$ then the observed process is also a (p,d,q) process, otherwise it is a $(p,d,p+d)$ process.

In the more realistic situation where $\{y_t\}$ is observed, we can determine the generalized AR operator $\varphi(B)$ and MA operator $\eta(B)$ for the observed process. Its ARIMA model will be order (P,D,Q), say, where the minimum possible value for Q is $P+D$. The model for the corresponding unobserved, underlying process $\{z_t\}$ will have order $(p=P,\ d=D,\ q \le \max(P+D,Q))$ and its associated generalized AR operator will also be $\varphi(B)$. Furthermore, recognizing that c_t and e_t are independently distributed, it can be shown that the moving average operator for the unobserved process, $\alpha(B)$, is additionally constrained by the ARIMA model for the observed process such that the following relationship must be satisfied:

$$\sigma_c^2 \alpha(B)\alpha(F) = \sigma_d^2 \eta(B)\eta(F) - \sigma_e^2 \varphi(B)\varphi(F). \qquad (8)$$

In this equation, σ_e^2, $\eta(B)$,and $\varphi(B)$ are known from the ARIMA model for the observed process, whereas σ_e^2, σ_c^2, and $\alpha(B)$ are unknown.

In general, many combinations of σ_e^2, σ_c^2, and $\alpha(B)$ will satisfy the equality. Defining an "acceptable model" for the unobserved process as one that, given the model for the observed process, $\alpha(B)$ satisfies the previous equation and its zeros are on or outside the unit circle, Box et al. (1978) show that 1) for every given model of an observed process, at least one acceptable model for the unobserved process exists; 2) for a given model of an observed process, the possible values of σ_e^2 are bounded; and 3) for a given model, every σ_e^2 between 0 and the upper bound (K^*, say) determines a unique acceptable model. The upper bound on the observation error variance, K^*, is determined from the constraint that, for a model of the unobserved process to be acceptable, $\sigma_c^2 \alpha(B)\alpha(F) \ge 0$ everywhere on the unit circle (i.e., the power spectrum of the corresponding MA process is non-negative definite). Then, from equation 8, K^* is given by

$$K^* = \min_{|B|=1} \left\{ \frac{\sigma_d^2 \eta(B)\eta(F)}{\varphi(B)\varphi(F)} \right\} \qquad (9)$$

and is completely determined by the ARIMA model for the observed process. When $\sigma_e^2 = K^*$, the variance of the added white noise is maximal, as will be the smoothing of the observed time series.

It is instructive to interpret Equations 8 and 9 in terms of constraints on the power spectra of $\{z_t\}$, $\{y_t\}$, and $\{e_t\}$, although this interpretation is strictly correct only when $\{z_t\}$ and $\{y_t\}$ are stationary. Let $p_z(f)$, $p_y(f)$, $p_e(f)$ denote the power spectra for $\{z_t\}$, $\{y_t\}$, and $\{e_t\}$, respectively. Recalling the definition of the power spectrum (Eq. 3), Equation 8 on the unit circle can be easily recast (multiply both sides by $2/\{\varphi(B)\varphi(F)\}$) as

$$p_z(f) = p_y(f) - p_e(f) \tag{10}$$

because the power spectrum for white noise is constant with frequency: $p_e(F)=2\sigma_e^2$. Because power spectra are nonnegative definite and $p_e(f)$ does not depend on f, the maximum possible observation noise variance K^* corresponds to the minimum of $p_y(f)$ over f (see Fig. 1). Thus, Equation 9 can be recast as

$$K^* = \min_{0 \le f \le 1/2} \left\{ p_y(f) \right\} / 2. \tag{11}$$

Note also that Equation 10 can be recast again as

$$p_z(f) = \left(1 - \frac{p_e(f)}{p_y(f)} \right) p_y(f) = \omega^*(f) p_y(f), \tag{12}$$

where $\omega^*(f)$ represents the term in parentheses. It will be seen below that $\omega^*(f)$ is identical to the polynomial of smoothing weights (Eq. 14) on the unit circle.

Returning to the estimation problem now, knowledge of σ_e^2, then, together with the ARIMA model for the observed process, is sufficient to estimate $\{z_t\}$ (Box et al., 1978). When t is not close to the endpoints of the time series, the smoothed (maximum likelihood) estimate of z_t, which we denote as $E(z_t|y)$, is a symmetric moving average filter of $\{y_t\}$ (Cleveland and Tiao, 1976; Box et al., 1978):

$$E(z_t|y) = \omega(B) y_t, \tag{13}$$

such that

$$\omega(B) = \frac{\sigma_a^2}{\sigma_d^2} \frac{\alpha(B)\alpha(F)}{\eta(B)\eta(F)} = \left[1 - \frac{\sigma_e^2}{\sigma_d^2} \frac{\varphi(B)\varphi(F)}{\eta(B)\eta(F)} \right], \tag{14}$$

where the second equality follows from equation 8. Note that $\omega(B)$ is identical to $\omega^*(f)$ (Eq. 12) on the unit circle ($B=e^{-i2\pi f}$), so that Equations 13 and 14 are also interpretable in terms of relations among power spectra. Equation 13 is equivalent to Equation 2 in Pennington (1985). It turns out (Cleveland and Tiao, 1976) that equation 14 is also valid for t near the endpoints of the time series; thus, one merely uses the ARIMA model for the observed time series to hindcast or forecast additional "observations" as needed. Box et al. (1978) describe a method for calculating the coefficients of $\omega(B)$; because this reference may be difficult to obtain, we repeat their description in the Appendix.

In the case where the model for the underlying process is (0,1,0) (i.e., a random walk model), the model for the observed process is (0,1,1) (i.e., a RWPUN, model). For this case, Pennington (1985) noted that the value of the MA parameter η_1 of the observed process (θ in his notation) is

$$\eta_1 = \frac{\sigma_e^2}{\sigma_d^2}, \tag{15}$$

so that Equation 14 is completely determined by the ARIMA model for the observed process and the observation error variance, σ_e^2, can be estimated.

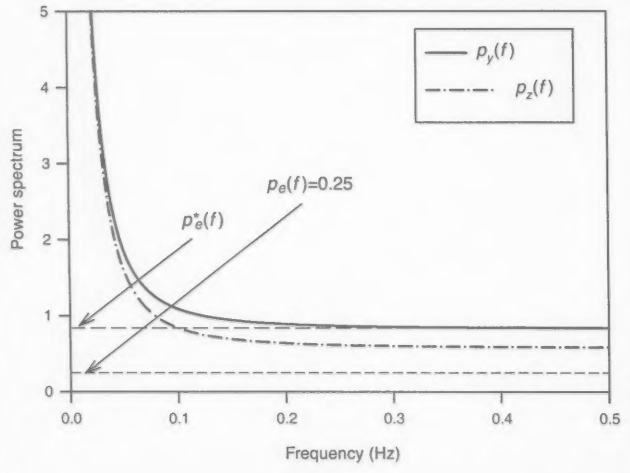

Figure 1

Example power spectra illustrating relationships between $p_y(f)$ (the power spectrum of the observed time series), $p_e(f)$ (the power spectrum of the white observational noise, a constant), and $p_z(f)$ (the power spectrum of the unobserved, underlying time series). In this example, $p_e(f) = 0.25$ so that $p_z(f)$ has the same basic shape as $p_y(f)$, but is shifted downwards at all frequencies by 0.25. $p^*_e(f)$ represents the maximum possible level, consistent with $p_y(f)$ (and the ARIMA model for the observed time series $\{y_t\}$), for the power spectrum of the assumed observational noise. Note that in this case, maximal smoothing (i.e., taking $p_e(f) = p^*_e(f)$) eliminates all high frequency energy and would result in over-smoothing.

Application of the noise reduction algorithm to bottom trawl survey data

We applied Box et al.'s (1978) noise reduction algorithm to 18 time series of abundance indices for finfish (nine species×two seasons; species are listed in Table 1) on Georges Bank in the northwest Atlantic. Time series for the fall survey spanned 40 years (1963–2002), and the spring time series spanned 36 years (1968–2003).

Stratified random bottom trawl surveys have been conducted annually on the northeastern continental shelf of the United States from Cape Hatteras to the Gulf of Maine in the fall since 1963 and in the spring since 1968 by the National Marine Fisheries Service (NMFS), Northeast Fisheries Science Center (NEFSC) (Azarovitz, 1981; Anonymous, 1988; Reid

et al., 1999). We derived annual time series of estimated total abundance during the spring and fall seasons for nine finfish species from trawl survey catch records for the Georges Bank area. Reported catches (biomass) from strata encompassing Georges Bank were expanded on a per-tow basis by using species and length-specific corrections for catchability and coefficients from Edwards (1968) and Harley and Myers (2001). Annual stratified mean (expanded) catch-per-tow was then calculated for each species for both seasonal surveys. Finally, annual total population abundance was calculated by applying a swept area factor to the stratified mean catch-per-tow. Abundance indices corresponding to fall surveys spanned 1963–2002, and those corresponding to spring surveys spanned 1968–2003. Following Pennington (1985), we assumed that changes in catchability induced a lognormal error structure on the observed time series. However, because some time series (notably those for the schooling pelagic fish herring and mackerel) included zeroes, a $\ln(x)$ transformation was not applicable to all series. Thus, before further analysis, all time series were $\ln(x+1)$ transformed.

For each resulting time series, we used SAS (vers. 8, SAS Institute, Cary, NC) to identify candidate ARIMA models, to estimate parameters for these models, and to extend the time series by using forecasts and hindcasts before applying the smoothing algorithm. Candidate model structures for each time series were based on examination of empirical autocorrelation, partial autocorrelation, and inverse autocorrelation functions for the series (Box and Jenkins, 1976). When these functions indicated that the series was nonstationary, we applied the backward difference operator $(1-B)$ to the series and examined the correlation functions for the new (differenced) series. In addition, because of its special significance in terms of interpretation, we always tried a RWUPN model as a candidate. Once candidate models were identified, we estimated coefficients for each model and calculated the associated Akaike information criterion (AIC; Akaike, 1973). AIC provides an objective criterion based on information theory for selecting the "best" approximating model from among a group of good candidate models (i.e., the criterion selects the model with the minimum AIC).

We examined the residuals and the empirical autocorrelation, inverse autocorrelation, and partial autocorrelation functions of the residual time series for significant deviation from white noise. When significant deviation was indicated, we dropped the model from further consideration. We also dropped models with orders (P,D,Q) that were inconsistent with the assumption of additive (after log transformation) observation noise $(Q \geq P+D)$. Following this screening procedure, we were left with a group of "good" alternative models. We then selected the ARIMA model with the smallest AIC from among the remaining candidates as the "best" model to smooth the data.

We developed a MATLAB (vers. 6.5, The Mathworks Inc., Natick, MA) program to perform the noise reduction for each time series based on an extended version of the series and its associated ARIMA model. To allow smoothed estimates to be calculated near the ends of each time series, we extended each time series before smoothing to 40 years before its start by hindcasting with the selected ARIMA model and to 40 years past its end by forecasting with the model. Using the MATLAB program, we then calculated K^*, the maximal smoothing weights $\omega(B)$ corresponding to $\sigma_e^2 = K^*$, and the smoothed estimates $E(z_t|y)$, following the approach of Box et al. (1978) outlined previously.

Results

The abundance indices we derived from fishery-independent bottom trawl surveys for nine finfish species during two seasons displayed a wide variety of trends, as well as a high degree of apparent interannual variability. This variability may be associated with environmentally driven, high-frequency changes in catchability, but we regarded it here as observation noise (Figs. 2 and 3). For example, springtime winter skate (*Leucoraja ocellata*) biomass appeared to increase by a factor of six during the early 1980s from a lower (but highly variable) mean level of ~140,000 t, to which it subsequently returned in the early 1990s (Fig. 2A). Yellowtail flounder (*Limanda ferruginea*), in contrast, declined by a factor of 10 during the 1970s and early 1980s from a high at the beginning of the time series and then began to rebound in the latter 1980s (Fig. 2G). Most recently, yellowtail flounder appear close to regaining their earlier peak abundance.

The 18 ARIMA models corresponding to the $\ln(x+1)$-transformed abundance indices formed a diverse set (Tables 2 and 3). Half the time series were found to be nonstationary; however, one application of backward differencing $(d=1)$ sufficed to achieve stationarity in all nine instances. Interestingly, the ARIMA models for all nine of these time series were consistent with RWPUN models (i.e., [0,1,1] models). For all the models, autoregressive orders (p) ranged between 0 and 3, and moving average orders (q) ranged from 1 to 5. The spring and fall models for little skate (*L. erinacea*) had the highest AR order, and the spring model for silver hake (*Merluccius bilinearis*) had the highest MA order. Only the models for little skate, Atlantic herring (*Clupea harengus*), and yellowtail flounder exhibited the same ARIMA order for both the spring and fall. And although none of the models reflected pure AR processes $(q=0$, an impossibility given the observation noise assumption), two were found to be pure MA processes (winter flounder and Atlantic mackerel [*Scomber scombrus*], both in spring). All nine IMA processes were RWPUN processes (i.e., (0,1,1)).

The effect of ARIMA-based noise reduction on these 18 sets of indices was fairly variable in outcome (Figs. 2 and 3). Little or no smoothing occurred for little skate (spring, Fig. 2B), silver hake (spring, Fig. 2D), and haddock (*Melanogrammus aeglefinus*) (fall, Fig. 3F). Moderate smoothing occurred for winter skate (spring, Fig. 2A; fall, Fig. 3A), little skate (fall, Fig. 3B),

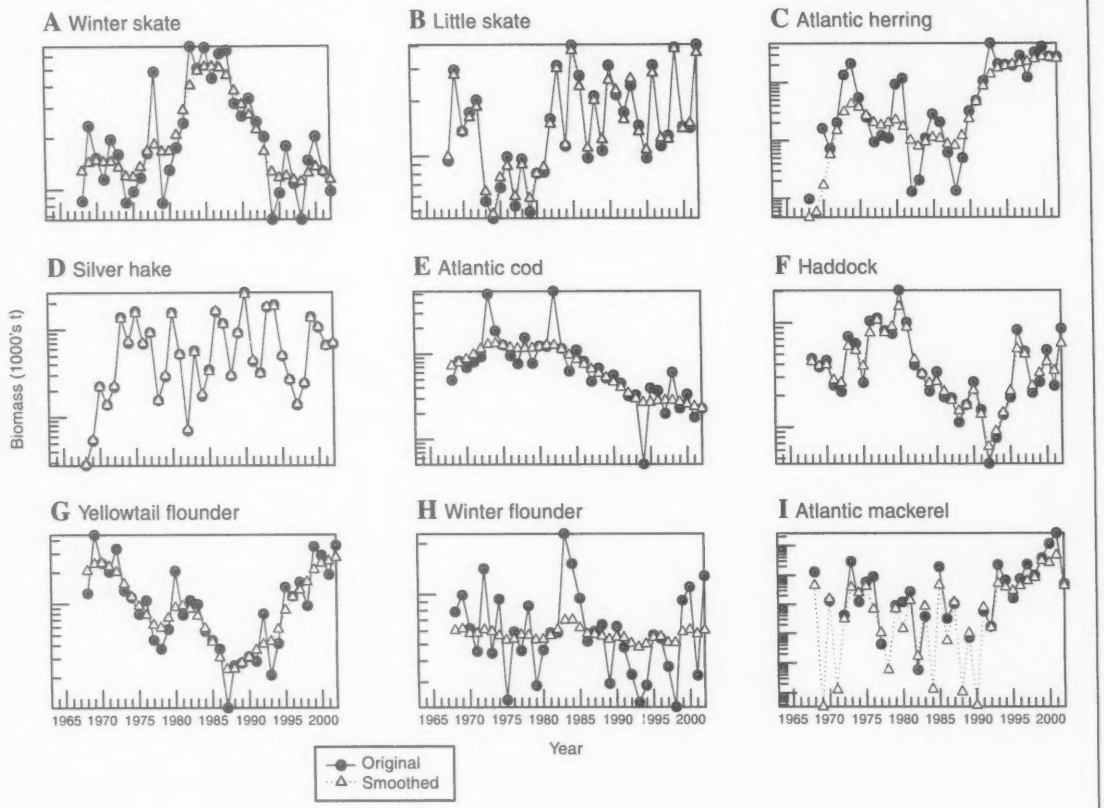

Figure 2

Comparison of original time series of estimated total biomass on Georges Bank from the spring bottom trawl survey (filled circles) and inverse-transformed, ARIMA-smoothed time series (open triangles) for nine finfish species.

Atlantic herring (fall, Fig. 3C), haddock (spring, Fig. 2F), yellowtail flounder (spring, Fig. 2G; fall, Fig. 3G), winter flounder (*Pseudopleuronectes americanus*) (fall, Fig. 3H), and Atlantic mackerel (spring, Fig. 2I). A high degree of smoothing occurred for Atlantic herring (spring, Fig. 2C), silver hake (fall, Fig. 3D), Atlantic cod (*Gadus morhua*) (spring, Fig. 2E; fall, Fig. 3E), winter flounder (spring, Fig. 2H), and Atlantic mackerel (fall, Fig. 3I).

Impressions obtained from visually comparing the original and smoothed time series were consistent with the fraction of innovation variance (K^*/σ_d^2, Tables 2 and 3) in the observed time series ascribed to observation error. Recall that we chose to perform the maximal amount of smoothing possible (i.e., taking $\sigma_f^2=K^*$ in Eq. 13). Our visual classifications fell fairly neatly into the following categories based on K^*/σ_d^2: 1) a low degree of smoothing corresponded to $K^*/\sigma_d^2<0.25$, 2) a moderate degree of smoothing corresponded to $0.25< K^*/\sigma_d^2<0.60$, and 3) a high degree of smoothing corresponded to $0.60\geq K^*/\sigma_d^2$.

In addition, it appeared that the degree of smoothing varied inversely with the order of the moving average component of the ARIMA model for the observed time series. When the order of the moving average component was greater than 2, the degree of overall smoothing was typically small. Substantially more smoothing was evident when the order of the moving average component was 1, because of the equivalence with an exponentially weighted smoother.

The nine time series found to be RWPUN processes provided a means to check whether our choice to perform the maximal amount of smoothing was reasonable. For such time series, the value of the moving average coefficient, η_1, is equal to the ratio of the observation noise variance, σ_e^2, to the innovation variance σ_d^2. Consequently, $\sigma_d^2 \cdot \eta_1 = \sigma_e^2$. For eight of the nine series, the ratio of σ_e^2 to K^* was greater than 80% (Table 4).

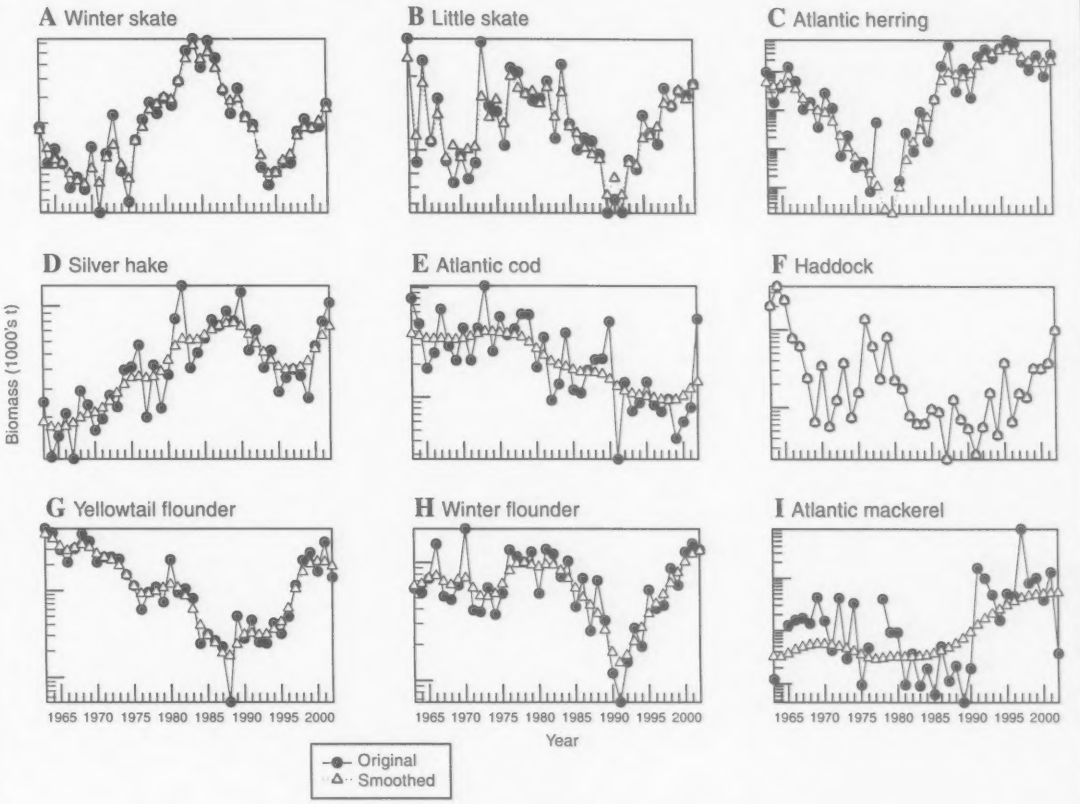

Figure 3

Comparison of original time series of estimated total biomass on Georges Bank from the fall bottom trawl survey (filled circles) and inverse-transformed, ARIMA-smoothed time series open triangles) for nine finfish species.

Discussion

Abundance indices derived from large-scale fishery-independent surveys typically exhibit interannual variability much higher than one would expect from within-survey variance (Pennington, 1985). Although true variability in the underlying population due to population-dynamic processes is reflected in the variability of an index, so too is observational noise arising both from within-survey sampling variability as well as from environmentally driven factors that affect catchability. Low signal-to-noise ratios in abundance indices due to high observational noise reduce one's ability to detect important changes or trends in actual population abundance.

To reduce the impact of white observation noise on time series data, Cleveland and Tiao (1976) developed an approach to noise reduction and smoothing that was based on their knowledge of the ARIMA model (Box and Jenkins, 1976) for an associated unobserved but underlying stochastic process. Box et al. (1978) extended this approach to address the situation where the ARIMA model for the underlying process was unknown, relying instead on an ARIMA model associated with the observed time series. In general, and certainly in regard to fishery-independent survey data, a model structure for the unobserved, underlying process will not be available. Hence, Box et al.'s (1978) approach will be the norm.

In the situation where the observed time series is stationary, we found that a frequency domain interpretation of Box et al.'s (1978) algorithm is particularly enlightening. When the times series is stationary, observation noise increases the power spectral density (PSD) of the observed process over that of the unobserved process by a fixed amount at all frequencies (Fig. 1). Consequently, the PSD of the unobserved process has the same shape as the PSD of the observed process, but with a fixed amount removed at

Table 2

ARIMA smoothing results for $\ln(x+1)$ transformed time series based on spring surveys. Here, σ_d^2 is the innovation variance for the transformed time series and κ^* is the maximum consistent observation noise variance, scaled to σ_d^2 (i.e., K^*/σ_d^2). The degree of smoothing is based on a visual comparison of the original and smoothed time series.

Species	ARIMA model (p,d,q)	σ_d^2	κ^*	Degree of smoothing
Winter skate	(0,1,1)	0.33	0.52	medium
Little skate	(3,0,4)	0.30	0.14	low
Atlantic herring	(0,1,1)	4.90	0.59	high
Silver hake	(0,0,5)	0.85	0.02	low
Atlantic cod	(0,1,1)	0.47	0.71	high
Haddock	(1,0,3)	0.42	0.29	medium
Yellowtail flounder	(0,1,1)	0.45	0.49	medium
Winter flounder	(0,0,1)	0.33	0.89	high
Atlantic mackerel	(0,0,2)	16.9	0.34	medium

Table 3

ARIMA smoothing results for $\ln(x+1)$ transformed time series based on fall surveys. Here, σ_d^2 is the innovation variance for the transformed time series and κ^* is the maximum consistent observation noise variance, scaled to σ_d^2 (i.e., K^*/σ_d^2). The degree of smoothing is based on a visual comparison of the original and smoothed time series.

Species	ARIMA model (p,d,q)	σ_d^2	κ^*	Degree of smoothing
Winter skate	(2,0,3)	0.17	0.31	medium
Little skate	(3,0,4)	0.12	0.38	medium
Atlantic herring	(0,1,1)	4.75	0.48	medium
Silver hake	(0,1,1)	0.22	0.61	high
Atlantic cod	(1,0,1)	0.55	0.77	high
Haddock	(2,0,3)	0.75	<0.01	low
Yellowtail flounder	(0,1,1)	0.40	0.45	medium
Winter flounder	(0,1,1)	0.40	0.50	medium
Atlantic mackerel	(0,1,1)	7.00	0.84	high

Table 4

For time series consistent with random-walk-plus-uncorrelated-noise models, the table provides a comparison between the estimated observation noise variance (σ_e^2) and the maximum noise variance (K^*). The latter was used to smooth all time series.

Season	Species	$\eta_1=\sigma_e^2/\sigma_d^2$	σ_d^2	K^*	σ_e^2/K^*
Fall	Atlantic herring	0.392	4.75	2.28	0.82
	Silver hake	0.566	0.22	0.13	0.93
	Yellowtail flounder	0.342	0.40	0.18	0.76
	Winter flounder	0.420	0.40	0.20	0.84
	Atlantic mackerel	0.832	7.00	5.88	0.99
Spring	Winter skate	0.438	0.33	0.17	0.84
	Atlantic herring	0.541	4.90	2.89	0.92
	Atlantic cod	0.680	0.47	0.33	0.96
	Yellowtail flounder	0.399	0.45	0.22	0.81

all frequencies. Because the unobserved PSD must be nonnegative, the maximum observation noise (and thus the maximum noise reduction and smoothing that may occur) consistent with additive white noise corresponds to the minimum value of the observed process's PSD. Presumed higher values for the observation noise would require that the PSD for the unobserved process be negative over some frequency range. Box et al.'s (1978) algorithm computes the maximum possible observation noise and uses a time domain formula to calculate a smoothed, "unobserved" time series consistent with additive white noise for any noise level up to the maximum.

The ARIMA-based noise reduction approach was first applied to fisheries trawl survey data by Pennington (1985), who developed an alternative algorithm to that of Box et al. (1978) for estimating the smoothed time series. This algorithm was subsequently used in several studies (Pennington, 1985; Fogarty et al.[1]; Pennington, 1986; Anonymous, 1988, 1993) to smooth time series of abundance indices derived from trawl survey data for the northeast coast of the United States. Of these studies, perhaps only Pennington (1986) constitutes a convincing demonstration of the utility of the ARIMA-based approach to time series noise reduction when the ARIMA model for the underlying process is unknown. Pennington's (1985) demonstration relied on an ARIMA model developed for the (usually unobserved) underlying population that was based on stock assessment results for the particular species considered. In contrast, RWPUN models were assumed *a priori* in Fogarty et al.[1] and Anonymous (1988, 1993) because the short time series (<25 observations per series) considered made identification of the underlying ARIMA models problematic. Only in Pennington (1986) was a model used that was fitted to trawl survey data and tested for appropriateness.

However, substantially longer time series are now available to test the ARIMA-based noise reduction concept. Consequently, to revisit the utility of the ARIMA-based approach for smoothing time series data derived from fisheries-independent trawl survey data, we applied Box et al.'s (1978) approach to smoothing to time series of annual abundance indices derived from the NMFS/NEFSC fisheries-independent bottom trawl survey of nine finfish species during two seasons on Georges Bank. Time series for the fall spanned 40 years (1963–2002), and the spring time series spanned 36 years (1968–2003). The species, comprising two elasmobranchs, three groundfish, two flatfish, and two pelagic schooling species, presented a broad range of life history characteristics (Table 1).

The noise reduction results we obtained varied among species and between seasons. Despite smoothing at the maximum level of noise reduction consistent with each model, very little smoothing was obtained for haddock (fall), little skate (spring), and silver hake (spring). The models for these time series had among the highest moving average orders (3–5). Examination of the PSD for each model in the frequency domain revealed very small minima, indicating no scope for noise reduction. Typically, models that had a MA order >2 exhibited substantially less smoothing than models with a MA order ≤2. Models that were of MA order 1 generally resulted in the greatest smoothing. Models that were of MA order 0 did not (and could not) occur.

Of the 18 time series we considered (Tables 2 and 3, Figs. 2 and 3), only half were adequately represented as random-walk-plus-uncorrelated-noise (RWPUN) models. The ARIMA models we developed were varied in structure, ranging from a simple MA(1) model to rather complicated models with multiple parameters. Thus, our results provide evidence against the appropriateness of assuming a particular model structure *a priori* when the objective of the analysis is to identify the underlying dynamic structure of the population. This evidence is further strengthened by the results of Becerra-Munoz et al. (1999), who found only 9 of 52 abundance time series for finfish species from the NMFS/NEFSC bottom trawl survey that corresponded to random walk models.

As an exercise, we also attempted to smooth the nine data sets that were not adequately described as RWPUN models, using this model structure as an *a priori* assumption, even though our analysis indicated that other models were more appropriate. We were not able to estimate convergent models for three species: Atlantic cod (fall), winter flounder (spring), and Atlantic mackerel (spring). For the remaining six time series, the smoothed results appeared to be quite reasonable (Fig. 4), although we obtained little noise reduction when we employed the "correct" ARIMA model. The RWPUN-smoothed time series for haddock (Fig. 4, C and F) were similar to that for spawning biomass derived from virtual population analysis (see Brodziak et al.[2]), but the smoothed time series for silver hake (Fig. 4E) exhibited higher frequency variability than that found for total biomass with a production model (see Brodziak et al.[3]). From the standpoint of estimating the unobserved underlying process, these smoothed results should be viewed with some skepticism: the use of the RWPUN model is rather arbitrary in this situation and it may impose artificial structure on the smoothed results. However, it may be that these time series do not meet one of the key assumptions of the noise reduction method: namely that the observation noise is uncorrelated. The ARIMA models for all six time series had MA orders ≥3, and one effect of correlated observation noise could be to increase the MA

[2] Brodziak, J., M. Traver and L. Col. 2005. Georges Bank haddock. *In* Assessment of 19 northeast groundfish stocks through 2004 (R. K. Mayo, and M. Terceiro, eds.), section 2, p. 30–80. 2005 groundfish assessment review meeting. Northeast Fisheries Science Center, Woods Hole, Massachusetts; 15–19 August 2005. NEFSC Ref. Doc. 05-13. NEFSC, 166 Water Street, Woods Hole, MA 02543.

[3] Brodziak, J. K. T., E. M. Holmes, K. A. Sosebee, and R. K. Mayo. 2001. Assessment of the silver hake resource in the Northwest Atlantic in 2000, 134 p. NEFSC Ref. Doc. 01-03. NEFSC, 166 Water Street, Woods Hole, MA 02543.

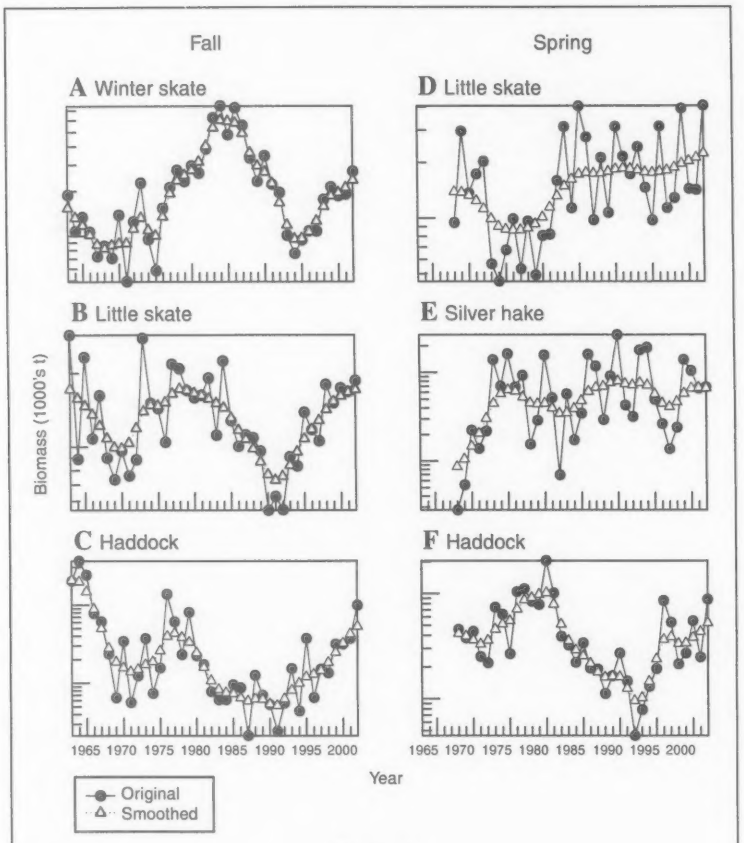

Figure 4

Comparison of original time series of estimated total biomass on Georges Bank from the fall (left column) and spring (right column) bottom trawl survey (filled circles) and inverse-transformed, ARIMA-smoothed time series (open triangles). For these time series, an ARIMA (0,1,1) model (i.e., a random-walk-plus-uncorrelated-noise model) was used, although this was not the model selected in our time series analysis.

order of the observed time series beyond that expected for uncorrelated noise.

Of the nine species considered, only three (little skate, Atlantic herring, and flounder) had models that exhibited the same ARIMA order for both the fall and spring surveys. Taken at face value, this would indicate that the other six species exhibited substantially different dynamical processes during the fall and spring that influenced abundance on Georges Bank. One potential mechanism for this could be differential seasonal migration patterns that result in changes in catchability that have different autocorrelation structures. For example, cod are distributed across the bank during the spring survey, but are found only in deeper waters on the periphery of the bank during the fall where they may be less available to the survey. Assuming that all Georges Bank cod are available to the spring survey, if the fraction of cod available to the survey in the fall is density dependent or is driven by autocorrelated environmental conditions, then the fall survey abundance will exhibit dynamical behavior different from that of the spring survey abundance (note: if this were the case, it would be inappropriate to smooth the fall time series for cod with the ARIMA noise reduction approach applied in our study because, as noted previously, one of the basic assumptions with this approach is that the observation noise is uncorrelated). Other plausible mechanisms can be developed, as well. However, we feel it more likely that the inconsistency in ARIMA order between spring and fall surveys for the same species is an estimation problem and indicates that even a 40-year time series may not be long enough to reduce the variability inher-

ent in ARIMA model estimation to reasonable levels for most species.

Alternative methods, such as locally weighted scatterplot smoothing (LOESS), moving average filters, exponential smoothing filters, Kalman filters, and frequency-domain approaches can be applied to time series to achieve smoother results (e.g., Cleveland and Grosse, 1991; Hamilton, 1994). These approaches typically employ at least one user-determined parameter that can be used to change the amount of smoothing that an algorithm achieves. Generally, one "fiddles" with the adjustable parameters until a "nice," smoothed fit is achieved. However, we think it important to distinguish between these smoothing algorithms and the ARIMA-based noise reduction algorithms. It is quite possible to smooth out real fluctuations in the underlying population process. The principal advantage that we see for the ARIMA-based noise reduction algorithms (used with an appropriate model) over alternative methods is that the former provide a more objective approach to determining an appropriate level of smoothing. As noted previously, Pennington (1985) showed that when a RWPUN model is appropriate, the ARIMA smoothing approach is completely determined by the ARIMA model for the observed time series because it is possible to determine the observation noise variance from the model parameters. In the more general case, Box et al.'s (1978) algorithm at least yields a maximum value for the variance of the observational noise and thus sets an upper limit to the amount of noise reduction and smoothing that can be achieved. For trawl survey data, our results from nine time series where RWPUN models were appropriate (and we can consequently estimate the actual observation noise variance) indicate that smoothing at ~90% of the maximum possible noise reduction level is not an unreasonable default percentage (Table 4).

One drawback to the greater application of ARIMA-based noise reduction methods to time series data is the lack of an integrated software package that allows a user 1) to quickly evaluate an appropriate ARIMA model for a given time series, and 2) to calculate the smoothed time series. We used SAS for the first step and MATLAB for the second, but we found this arrangement rather awkward and burdensome. However, econometrically oriented software packages such as ForecastPro[4] or AutoBox[5] that automate model selection may substantially simplify the first step even if they don't address the second step.

On the whole, ARIMA-based time series models appear to provide the basis for a more objective approach to reducing observation noise in time series data, including time series of fishery abundance indices derived from trawl survey data, than do more conventional smoothing approaches. In the absence of additional information regarding the level of observation noise, we recommend smoothing trawl survey data at 90% of the maximum possible noise reduction level. We also suggest that development of an integrated software package for implementing ARIMA-based noise reduction will facilitate future use of this method.

Finally, if a smoothed time series is desired (e.g., for graphical presentation only), then use of a RWPUN model in lieu of a model-fitting exercise will generally yield a curve pleasing to the eye. Alternatively, other methods such as LOESS could be employed to generate the smoothed results. However, if the resulting time series is to be used for further analysis of the dynamical behavior of the fish stock, we strongly recommend that a model-fitting approach be used to identify the most appropriate ARIMA model for the observed time series, from which the time series for the unobserved, underlying process can be computed. Otherwise, real fluctuations in the underlying process may be oversmoothed, resulting in an apparent dynamical behavior that displays little variability. This oversmoothing, in turn, may lead to erroneous conclusions being drawn regarding, for example, the resiliency of a stock to exploitation or environmental change, and to perhaps concomitant errors being propagated in advice provided to fishery managers.

[4] Business Forecast Systems, Inc. 2006. Website: http://www.forecastpro.com/products/fpfamily/index.html (accessed on 29 March 2006).

[5] Automatic Forecasting Systems. 2003. Website: http://www.autobox.com/autoboxdesc.htm (accessed on 29 March 29 2006).

Acknowledgments

We would like to thank M. Pennington for his insightful comments on an early version of this manuscript. The comments and suggestions from two anonymous reviewers were also very helpful and are much appreciated. This work was supported by the National Research Council, which provided funding support for one of us (Stockhausen) as a postdoctoral fellow at the Northeast Fisheries Science Center.

Literature cited

Akaike, H.
1973. Information theory as an extension of the maximum likelihood principal. *In* Second international symposium on information theory (B. N. Petrov, and F. Csaki, eds.), 267–281. Akademiai Kiado, Budapest, Hungary.

Anonymous.
1988. An evaluation of the bottom trawl survey program of the Northeast Fisheries Center. NOAA Tech. Memo. NMFS-F/NEC-52, 83 p. Northeast Fish. Center, 166 Water St., Woods Hole, MA 02543.
1993. Status of fishery resources off the northeastern United States for 1993. NOAA Tech. Memo. NMFS-F/NEC-101, 140 p. Northeast Fish. Center, 166 Water St., Woods Hole, MA 02543.

Azarovitz, T. R.
1981. A brief historical review of the Woods Hole Laboratory trawl survey time series. *In* Bottom trawl surveys (W. G. Doubleday, and D. Rivard, eds.), 62–67. Can. Spec. Pub. Fish. Aquat. Sci., vol. 58.

Becerra-Munoz, S., D. B. Hayes, and W. W. Taylor.
1999. Stationarity and rate of damping of modeled indices of fish abundance in relation to their exploitation status in the Northwest Atlantic Ocean. Ecol. Mod. 117:225–238.

Box, G. E. P., S. C. Hillmer, and G. C. Tiao.
1978. Analysis of seasonal time series. *In* Seasonal analysis of economic time series (A. Zellner, ed.), 309–334. U.S. Dep. Comm., Washington, DC.

Box, G. E. P., and G. M. Jenkins.
1976. Time series analysis: forecasting and control, 575 p. Holden-Day, Oakland, CA.

Byrne, C. J., T. R. Azarovitz, and M. P. Sissenwine.
1981. Factors affecting variability of research trawl surveys. Can. Spec. Pub. Fish. Aquat. Sci. 58:238–273.

Clark, S. H.
1979. Application of bottom trawl survey data to fish stock assessment. Fisheries 4:9–15.

Cleveland, W. S., and E. Grosse.
1991. Computational methods for local regression. Stats. and Comp. 1:47–62.

Cleveland, W. P., and G. C. Tiao.
1976. Decomposition of season time series: a model for the Census X-11 program. J. Am. Stat. Assoc. 71:581–587.

Collie, J. S., and M. P. Sissenwine.
1983. Estimating population size from relative abundance data measured with error. Can. J. Fish. Aquat. Sci. 40:1971–1983.

Edwards, R. L.
1968. Fishery resources of the North Atlantic area. *In* The future of the fishing industry in the United States (D. W. Gilbert, ed.), p. 52–60. Univ. Washington, Seattle, WA.

Enders, W.
2004. Applied econometric time series, 460 p. John Wiley and Sons, Inc., Hoboken, NJ.

Grosslein, M. D.
1969. Groundfish survey program of BCF Woods Hole. Comm. Fish. Rev. 31:22–30.

Hamilton, J.
1994. Time series analysis, 820 p. Princeton Univ. Press, Princeton, NJ.

Harley, S. H., and R. A. Myers.
2001. Hierarchical Bayesian models of length-specific catchability of research trawl surveys. Can. J. Fish. Aquat. Sci. 58:1569–1584.

Helser, T. E., and D. B. Hayes.
1995. Providing quantitative management advice from stock abundance indices based on research surveys. Fish. Bull. 93:290–298.

Lloret, J., J. Lleonart, and I. Sole.
2000. Time series modeling of landings in northwest Mediterranean Sea. ICES J. Mar. Sci. 57:171–184.

Nogueira, E., F. F. Perez, and A. F. Rios.
1998. Modelling nutrients and chlorophyll a time series in an estuarine upwelling ecosystem (Ria de Vigo: NW Spain) using the Box-Jenkins approach. Estuar. Coast. Shelf Sci. 46:267–286.

Pennington, M.
1985. Estimating the relative abundance of fish from a series of trawl surveys. Biometrics 41:197–202.
1986. Some statistical techniques for estimating abundance indices from trawl surveys. Fish. Bull. 84: 519–525.

Reid, R. N., F. P. Almeida, and C. A. Zetlin.
1999. Fishery-independent surveys, data sources, and methods. NOAA Tech. Memo. NMFS-NE-122. Northeast Fish. Sci. Center, 166 Water St., Woods Hole, MA 02543.

Appendix

For the convenience of the reader, we summarize here Box et al.'s (1978) algorithm to calculate the coefficients of the smoothing polynomial $\omega(B)$. Recall from Equation 14 that

$$\omega(B)=\left[1-\frac{\sigma_e^2}{\sigma_d^2}\frac{\varphi(B)\varphi(F)}{\eta(B)\eta(F)}\right], \tag{A.1}$$

where $\varphi(B)$ is a polynomial of order $P+D$ and $\eta(B)$ is a polynomial of order Q. Because $Q \geq P+D$, one can write

$$\begin{aligned}\varphi(B)&=1-\varphi_1B^1-\varphi_2B^2\ldots-\varphi_QB^Q;\\ \eta(B)&=1-\eta_1B^1-\eta_2B^2\ldots-\eta_QB^Q,\end{aligned} \tag{A.2}$$

where $\varphi_j = 0$ for $j>P+D$.

First, define

$$C(B)\equiv\frac{\varphi(B)}{\eta(B)};\ C(B)=1+C_1B^1+C_2B^2+\ldots. \tag{A.3}$$

One can solve for the coefficients of C using an iterative process by recognizing that the coefficients of each power of B in the following expression must be zero:

$$0=\varphi(B)-\eta(B)C(B).$$

Consequently, one obtains

$$C_1=\eta_1-\varphi_1;\ C_j=\eta_j-\varphi_j+\sum_{i=1}^{j-1}C_{j-i}\eta_i, j=2,\ldots Q \tag{A.4}$$

and higher order coefficients of C (i.e., for $j>Q$) can be computed recursively using the relation

$$C_j=\sum_{i=1}^{Q}C_{j-i}\eta_i. \tag{A.5}$$

Next, define

$$\begin{aligned}X(B,F)&\equiv C(B)\frac{\varphi(F)}{\eta(F)}\\ \text{where } X(B,F)&=X_0+\sum_{j=1}^{\infty}X_j(B^j+F^j).\end{aligned} \tag{A.6}$$

From this definition, one obtains

$$X(B,F)\eta(F)\equiv C(B)\varphi(F). \tag{A.7}$$

The largest degree of F on the righthand side of this equation is Q. By matching coefficients of F^j on both sides of the equation, Box et al. (1978) found, for $j=0,1,...Q$, that

$$\boldsymbol{\eta X} = \boldsymbol{C\varphi}, \tag{A.8}$$

where $\mathbf{X}$, φ are $Q+1$ column vectors $\mathbf{X}^T=(X_0, X_1,..., X_Q)$, $\varphi^T=(1, -\varphi_1,..., -\varphi_Q)$ and η, $\mathbf{C}$ are $(Q+1)x(Q+1)$ matrices such that

$$\mathbf{C}=\begin{bmatrix} 1 & C_1 & . & . & C_Q \\ & . & . & & . \\ & & . & . & . \\ & & & . & C_1 \\ \mathbf{0} & & & & 1 \end{bmatrix} \tag{A.9}$$

$$\boldsymbol{\eta}=\begin{bmatrix} 1 & -\eta_1 & . & . & -\eta_Q \\ -\eta_1 & . & . & -\eta_Q & \\ & . & . & . & \\ & -\eta_Q & & & \\ -\eta_Q & & & & \mathbf{0} \end{bmatrix}+\begin{bmatrix} 0 & 0 & & & \mathbf{0} \\ 0 & 1 & & & \\ . & \eta_1 & . & & \\ . & & & & \\ 0 & -\eta_{Q-1} & . & -\eta_1 & 1 \end{bmatrix}.$$

Thus, Equations A.8 and A.9 define a set of $Q+1$ equations in $Q+1$ unknowns (X_0, X_1,..., X_Q) which can be solved for by matrix inversion such that

$$\boldsymbol{X} = \boldsymbol{\eta}^{-1}\boldsymbol{C\varphi}. \tag{A.10}$$

For $j>Q$, the X_j's are computed recursively by using the relation

$$X_j = \sum_{i=1}^{Q} X_{j-1}\eta_i. \tag{A.11}$$

Finally, the coefficients of $\omega(B)$ are given by

$$\omega_0 = 1-\frac{\sigma_e^2}{\sigma_d^2}X_0;\ \omega_j = -\frac{\sigma_e^2}{\sigma_d^2}X_j, j=1,\ldots. \tag{A.12}$$

Abstract—The eastern Steller sea lion (*Eumetopias jubatus*) population comprises animals that breed along the west coast of North America between California and southeastern Alaska. There are currently 13 major rookeries (>50 pups): five in southeastern Alaska, three in British Columbia, two in Oregon, and three in California. Overall abundance has increased at an average annual rate of 3.1% since the 1970s. These increases can largely be attributed to population recovery from predator-control kills and commercial harvests, and abundance is now probably as high as it has been in the last century. The number of rookeries has remained fairly constant (n=11 to 13) over the past 80 years, but there has been a northward shift in distribution of both rookeries and numbers of animals. Based on the number of pups counted in a population-wide survey in 2002, total pup production was estimated to be about 11,000 (82% in southeastern Alaska and British Columbia), representing a total population size as approximately 46,000–58,000 animals.

Abundance and distribution of the eastern North Pacific Steller sea lion (*Eumetopias jubatus*) population

Kenneth W. Pitcher[1]

Peter F. Olesiuk[2]

Robin F. Brown[3]

Mark S. Lowry[4]

Steven J. Jeffries[5]

John L. Sease[6]

Wayne L. Perryman[4]

Charles E. Stinchcomb[4]

Lloyd F. Lowry[7]

Email address for K. W. Pitcher: ken_pitcher@fishgame.state.ak.us

[1] Division of Wildlife Conservation
Alaska Department of Fish and Game
525 West 67th Avenue
Anchorage, Alaska 99518

[2] Pacific Biological Station
Department of Fisheries and Oceans Canada
Nanaimo, BC V9T 6N7, Canada

[3] Marine Mammals Research Program
Oregon Department of Fish and Wildlife
7118 NE Vandenberg Avenue
Corvallis, Oregon 97330

[4] Southwest Fisheries Science Center
National Marine Fisheries Service, NOAA
8604 La Jolla Shores Drive
La Jolla, California 92037

[5] Marine Mammal Investigations
Washington Department of Fish and Wildlife
7801 Phillips Road SW
Lakewood, Washington 98498

[6] National Marine Mammal Laboratory
National Marine Fisheries Service, NOAA
7600 Sand Point Way, NE
Seattle, Washington 98115

[7] 73-4388 Pa'iaha Street
Kailua-Kona, Hawaii 96740

The Steller sea lion (*Eumetopias jubatus*) is the largest of the Otariidae and inhabits the North Pacific Rim from California to Japan. Individuals breeding at rookeries[1] located along the west coast of North America from California northward through southeastern Alaska (Fig. 1) to 144°W longitude form a distinct population segment, generally referred to as the eastern population. Historically, exchange of reproductive females with the Steller sea lion population to the north and west of 144°W longitude has been extremely low as shown by genetic studies (Bickham et al., 1996) and resightings of marked animals (Raum-Suryan et al., 2002). This indicates that population changes have been driven by birth and death rates within each population because immigration and emigration of breeding females among populations were too infrequent to affect population dynamics. More recent genetic analyses have confirmed the ancient divergence of the eastern and western populations. However, two new rookeries (White Sisters and Graves Rocks, Fig. 1) at the northern end of the range of the eastern population appear to have been colonized by females from both populations (O'Corry-Crowe et al., 2005). The number of western female immigrants to the eastern population has been small (in the 100s) to date, has not had a major impact on the growth dynamics of the overall eastern population and has been limited to the extreme northern range of the eastern population. However, the presence of breeding female immigrants from the western population within the range of the eastern population indicates that our prior assumption that population dynamics of the eastern population was completely driven by internal rates of reproduction and survival was incorrect for the past several years.

[1] For purposes of this paper, rookeries are arbitrarily defined as traditional, terrestrial sites where >50 pups are born annually. Other terrestrial sites used by sea lions are referred to as haulouts. Small numbers of pups are also born on haulouts, but probably constitute <1% of the total <100 in the eastern population.

Manuscript submitted 28 March 2006 to the Scientific Editor.

Manuscript approved for publication 21 June 2006 by the Scientific Editor.

Fish. Bull. 107:102–115 (2007).

In recent years, attention has focused on the western Alaskan population because of a precipitous decline since the 1970s (Loughlin et al., 1992; Trites and Larkin; 1996) resulting in an "endangered" classification under the U.S. Endangered Species Act. The eastern population is currently classified as "threatened." Abundance from southern Oregon through southeastern Alaska has generally shown an increasing trend (Calkins et al., 1999; Brown et al.[2]; DFO, 2003), whereas numbers in southcentral California have declined substantially (Le Boeuf et al.[3]; Hastings and Sydeman, 2002). This is the first detailed population-wide status evaluation of abundance, trend, and distribution with a historical perspective for the eastern population. We also present the results of the first population-wide census of pup production conducted in 2002 and apply life-table analysis to estimate total population size.

In our study, we reviewed records of Steller sea lion abundance, with particular emphasis on data collected at rookeries. Some counts date back to the early 1900s, but early surveys were not systematic and methods lacked standardization, and some of the counts may have been affected by culling and hunting activities. Although these earlier survey methods preclude formal statistical analyses, the historical data provide a general sense of gross changes in abundance and distribution. Systematic surveys began in most regions along the west coast in the 1970s, but counting techniques varied among the researchers and agencies conducting the surveys, and surveys were not coordinated between jurisdictions. Nevertheless, these time series indicate changes in relative abundance within each geopolitical region. In recent years, there has been an effort to compare and calibrate counting techniques, especially for pups (Snyder et al., 2001; P. F. Olesiuk, unpubl. data), and to synthesize survey results (Loughlin et al., 1992).

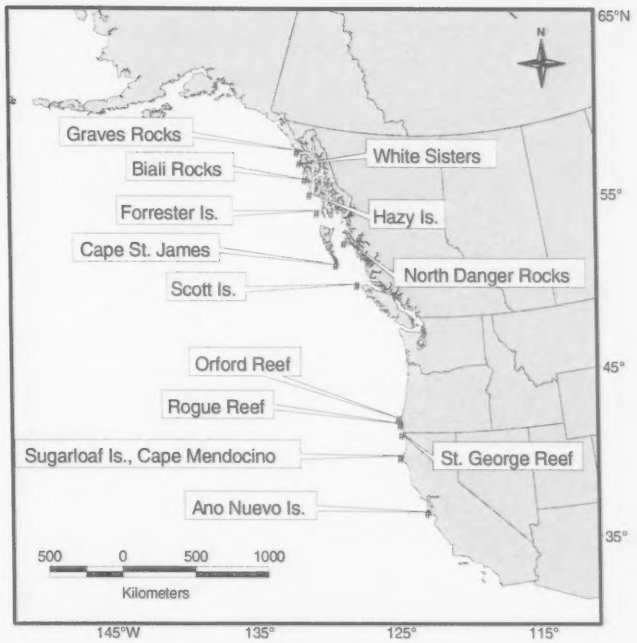

Figure 1

Geographic range of the eastern Steller sea lion (*Eumetopias jubatus*) population showing locations of major (>50 pups born) breeding rookeries.

Materials and methods

Count data used to estimate population trends between the late 1970s and 2004 were of two types: 1) counts of pups obtained between late June and early July (at the end of the pupping season) when most pups are <1 month of age, and 2) counts of juveniles and adults ≥1 year of age (i.e., nonpups) obtained from mid June to early July (mid to late in the breeding season). Steller sea lions normally give birth between late May and early July and breed between late May and mid July, although timing of these events varies somewhat geographically (Pitcher et al., 2001). Counts of pups are the preferred index to population size for many species of pinnipeds (Berkson and DeMaster, 1985). For the Steller sea lion, the vast majority of births occur at traditional rookeries, and because pups are confined to land for the first month of life, surveys of rookeries at the end of the pupping season provide a nearly complete estimate of annual pup production.

Pups are more difficult to count than nonpups because of their small size and dark color. This disadvantage is especially pronounced for counts made at oblique angles from aircraft circling rookeries or from vessels adjacent to the sites. From the mid 1970s to the late 1990s, pups were usually counted by placing people on rookeries, herding nonpups into the water, and tallying the number of pups while walking through the rookery (Calkins and Pitcher, 1982). However, the methods of obtaining such counts are disruptive to sea lions (Lewis, 1987), and counts may not be possible where rookeries are protected in parks or ecological and nature reserves. More recently, vertical 126-mm format aerial photography has been shown to be as accurate and far less disruptive (Snyder et al., 2001) for counting pups. Depending on the physical size,

[2] Brown, R. F., S. D. Riemer, and B. E. Wright. 2002. Population status and food habits of Steller sea lions in Oregon. Report from Oregon Dept. of Fish and Wildlife to Oregon State Univ. Contract F0225A-01, 17 p. Oregon Department of Fish and Wildlife, Marine Mammal Research Program, 7118 NE Vandenberg Ave., Corvallis, OR 97330.

[3] Le Boeuf, B. J., K. Ono, and J. Reiter. 1991. History of the Steller sea lion population at Año Nuevo Island, 1961–1991. NOAA Admin. Report NMFS-SWFSC LJ-91-45C, 9 p.

substrate, and topography of rookeries, high-quality oblique 35-mm photographs can sometimes provide counts of pups with an acceptable accuracy (P. F. Olesiuk, unpubl. data). In 2002, vertical 126-mm format photography was used at all rookeries within the range of the eastern population to obtain the first estimate of total pup production (pup numbers at some rookeries had been reported previously but not for all rookeries in a single year). We have included additional counts of pups made at some sites between 2003 and 2005 for trend analyses within geographic subareas. However, only counts from the complete population-wide survey in 2002 were used to estimate total population abundance in order to provide an estimate for a single point in time.

Few reliable counts of pups were available before the 1970s, but counts of non-pups on rookeries have dated back to the early 1990s. Non-pups are easier to count, and there tends to be a high degree of correlation for counts of non-pups between oblique 35-mm format and vertical 126-mm format images (Fritz and Stincomb, 2005). However, some Steller sea lions, particularly juveniles, range widely (Raum-Suryan et al., 2002); therefore counts at haulouts within a particular geographic area may not necessarily represent the number of animals supported by local rookeries, although breeding animals show a higher degree of site fidelity. The number and proportion of various sex and age classes of non-pups that are hauled out varies with season, time of day, and (in some cases) with tide (Winthrow, 1982; Calkins et al., 1999).

Table 1

Counts of pups and nonpups for each rookery and for all haulout sites combined by region for the population-wide survey of the eastern Steller sea lion (*Eumetopias jubatus*) population in 2002. Pup counts were made from vertical 126-mm format images, and nonpup counts from either vertical 126-mm format images or oblique 35-mm photographs. Nonpup counts included counts of pups at the indicated number of major sites (used by >50 animals on a regular basis during the breeding season), as well as counts of pups at numerous minor sites and counts of a few scattered animals.

Site	Pups	Nonpups
Southeastern Alaska		
Graves Rocks	98	1001
White Sisters	403	1156
Biali Rocks	59	625
Hazy Islands	1257	2050
Forrester Island	3060	3699
Haulout sites (20 major sites)	9	6752
Southeastern Alaska total	4886 (49%)	15,283 (43%)
British Columbia		
North Danger Rocks	207	592
Cape St. James	655	982
Scott Islands	2451	3865
Haulout sites (24 major sites)	5	6681
British Columbia total	3318 (33%)	12,120 (34%)
Washington		
Haulout sites (2 major sites)	0 (0%)	651 (2%)
Oregon		
Orford Reef	382	1178
Rogue Reef	746	1264
Haulout sites (7 major sites)	8	1727
Oregon total	1136 (11%)	4169 (12%)
California		
Saint George Reef	367	716
Sugarloaf Island-Cape Mendocino	150	588
Año Nuevo Island	189	255
Haulout sites (6 major sites)	7	1543
California total	713 (7%)	3102 (9%)
Eastern population	10,053	35,325

Counts from the 2002 population-wide survey (Table 1) indicated a fairly tight relationship between the number of pups and nonpups counted on rookeries (Fig. 2). A similar pattern was noted for rookeries in British Columbia and the relationship persisted over the three decades concurrent pup and nonpup counts were available (P. F. Olesiuk, unpubl. data). The historical counts of nonpups (or total animals where pups and nonpups were not distinguished) on rookeries thus likely provide a general index of the size of the breeding population associated with each rookery.

Systematic surveys have been conducted to monitor trends of the eastern Steller sea lion population, but methods and schedules have varied depending on the agency conducting the surveys. In southeastern Alaska, the Alaska Department of Fish and Game periodically conducted ground counts of pups on rookeries from 1979 through 1998, and used vertical 126-mm format photography to count pups since 1998. In British Columbia, the Department of Fisheries and Oceans has conducted province-wide aerial surveys of rookeries and haulout sites at 2–5 year intervals since the early 1970s, using oblique 35-mm format photography to count both pups and nonpups. In 1998 and 2002, both pups and nonpups were counted at British Columbia rookeries with the use of vertical 126-mm format photography. There are no Steller sea lion rookeries in Washington, but the Washington

Department of Fish and Wildlife has conducted numerous aerial surveys of haulout sites during the breeding season using oblique 35-mm format photography since 1978. In Oregon, the Oregon Department of Fish and Wildlife has conducted state-wide aerial surveys of nonpups on rookeries and haulouts using oblique 35-mm format photography on a nearly annual basis since the mid-1970s and has periodically obtained ground, or more recently vertical 126-mm format or high-resolution digital 35-mm format, pup counts. In California, the National Marine Fisheries Service, Southwest Fisheries Science Center, conducted statewide surveys during early July beginning in 1996 using vertical 126-mm format photography to count pups and nonpups at all rookeries and haulout sites. Time series of counts that were obtained with assorted methods were also available for some rookeries in California dating back to the 1970s. Although these surveys provide reliable information on changes in relative abundance within each region or at a particular rookery, they are difficult to synthesize into a population-wide assessment because of uncoordinated survey schedules and methods. Given the consistency within, but inconsistency between, these geo-political jurisdictions, we assessed trends in abundance by region (southeastern Alaska, British Columbia, Washington, Oregon, and California). Counts for each region were converted to natural logarithms and then regressed on year to determine average annual population growth rates.

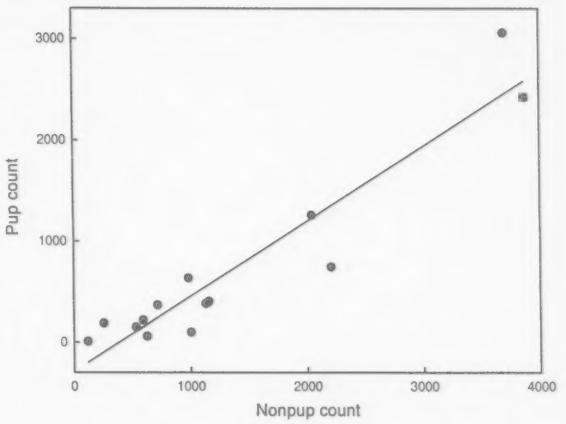

Figure 2

Relationship between number of pup and nonpup Steller sea lions (*Eumetopias jubatus*) counted on rookeries during the population-wide survey in 2002 (r^2=0.90; n=14; P<0.001).

We estimated the total population size in 2002 from the predicted ratio of pups to nonpups in the population (Calkins and Pitcher, 1982; Trites and Larkin, 1996). From life tables for a stable sea lion population in the Gulf of Alaska, Calkins and Pitcher (1982) estimated total population size to be about 4.5 times the number of pups born. In order to apply this approach to the eastern population, which was not stable but increasing (see "Results" section), we conducted sensitivity analyses to determine how this multiplier varies with population growth rate (λ) by incrementally changing each of the life history parameters that affect it, namely juvenile mortality rates, adult mortality rates, age at maturation, and fecundity rates (Lotka, 1907; Cole, 1954) .

We also reviewed historical records of Steller sea lion abundance in an attempt to relate current population size with abundance prior to the initiation of standardized surveys. Although these records provide insights into relative population levels, caution must be used because the older counts were obtained by a variety of methods and the seasonal timing of counts was inconsistent. In most cases the counts were made by professional biologists or naturalists hired by government agencies to conduct sea lion investigations, and special trips were made to rookeries to obtain first-hand counts; therefore it is unlikely numbers were grossly inaccurate. Because of the *ad hoc* nature of these counts, it was difficult to synthesize them into even a regional estimate of abundance, or to conduct statistical analyses; therefore these counts were generally examined on a rookery-by-rookery basis (Appendix).

Results

Southeastern Alaska

Counts of Steller sea lion pups in southeastern Alaska increased from 2219 in 1979 to 5510 in 2005 (Fig. 3A), representing an average annual rate of increase of 3.2% (r^2=0.91; n=10; P<0.001). Prior to the early 1980s, the only rookery in southeastern Alaska was the Forrester Island complex. Only 50–100 animals were recorded when the site was first noted in the 1920s, and 350 animals were recorded when the site was revisited in 1945, and there was no mention of pupping in either case (Rowley, 1929; Imler and Sarber, 1947). Thus, although count data are extremely limited, it appears that Steller sea lion abundance was probably quite low in southeastern Alaska during the first half of the 20th century. Counts are not available, but the Forrester Island rookery must have grown dramatically through the 1950s and 1960s (Fig. 4A). By the time the first aerial survey was conducted in 1961, Forrester Island had grown to about one-third its current size in terms of both the numbers of pups and nonpups (Bigg, 1985). However, increases at Forrester Island appear to have slowed since the late 1970s, showing only a slight increase in pup production (0.6% per year; r^2=0.40; n=13; P=0.021) and no discernible increase in the number of nonpups (r^2=0.22; n=12; P=0.125).

With the slowing of growth on Forrester Island, several new rookeries were established in southeastern Alaska (Calkins et al., 1999) (Appendix I). Hazy Islands were a substantial haulout in the 1950s (Mathisen and Lopp, 1963), but pup counts increased after they were first observed in 1979 (13% per year, r^2=0.76; n=11; P<0.001). White Sisters developed into a rookery in the early 1990s and counts of pups also increased rapidly (16% per year, r^2=0.87; n=10; P<0.001). In recent years, Graves Rocks and Biali Rocks appear to be developing into rookeries; 175 and 100 pups were counted respectively at the two sites in 2005. Growth of these four new rookeries accounted for about 48% of the increase in total pup production in southeastern Alaska during the 1980s, and for about 74% of the total increase since 1990.

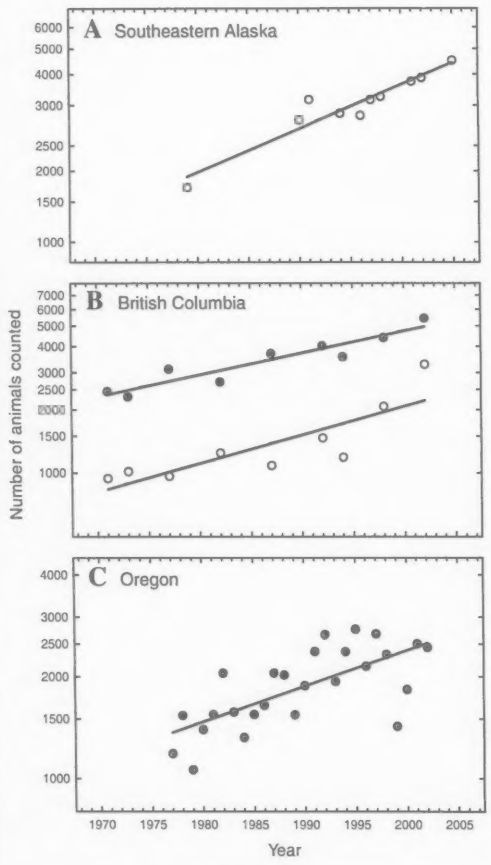

Figure 3

Recent trends in counts of Steller sea lion (*Eumetopias jubatus*) pups (○) and nonpups (●) on rookeries in (**A**) Southeastern Alaska, (**B**) British Columbia, and (**C**) Oregon. These areas combined account for over 90% of pup production in the eastern population. Survey techniques were standardized within each region, but differed among regions. The slopes are all statistically significant (P<0.001), and none differed significantly from the overall rate of increase of 3.1%.

In addition to the five rookeries, sea lions use about 20 major haulout sites (>50 animals) and several smaller sites in southeastern Alaska on a regular basis during the breeding season, as well as numerous other sites during the nonbreeding season. During the 2002 survey, a total of 6752 nonpups were counted at haulout sites and another 8531 nonpups were counted at rookeries (Table 1).

British Columbia

There are currently three Steller sea lion rookeries in British Columbia: the Scott Island complex (Triangle, Beresford-Maggot, and Sartine Islands), Cape St. James, and North Danger Rocks. Counts of pups from oblique 35-mm format photographs increased from 941 in 1971 to 3276 in 2002 (Fig. 3B), representing an average annual rate of increase of 3.2% (r^2=0.71; n=9; P=0.005), similar to the overall rate observed in southeastern Alaska. However, piecewise regressions provide a better fit to the time series of pup counts, indicating that most of this increase has occurred since the 1980's (r^2=0.85; n=9; P=0.002). Significant increases in pup production (P<0.005) were evident at all three rookeries (Appendix), but mean rates varied among sites (3.7% at Scott Islands, 2.0% at Cape St. James, and 2.7% on North Danger Rocks). Numbers of nonpups on rookeries also increased significantly (r^2=0.89; n=9; P<0.001), paralleling the increases in pup production (Fig. 3B).

Counts on rookeries in British Columbia date back to 1913 (Newcombe and Newcombe, 1914) and indicate breeding populations were historically large (Fig. 4B). Extensive sea lion reduction programs were conducted in British Columbia from 1912 through 1966, and attempts were made to commercially harvest sea lions during the 1960s. One major rookery, the Sea Otter Group, was eradicated by intensive control efforts during the 1920s and 1930s. The site was visited each year toward the end of the pupping season and all pups and as many nonpups as possible were killed, and by about 1940 it was no longer used as a rookery. Predator-control kills and commercial harvests in British Columbia continued into the 1960s and impacted all rookeries, and the breeding population was reduced to about 30% of peak levels by the late 1960s (Bigg, 1985). It appears that numbers at Scott Islands have fully recovered from these kills, but numbers at the two other rookeries are still below historical peak levels (Appendix).

Sea lions also currently use 24 major haulout sites (>50 animals) in British Columbia on a regular basis during the breeding season, up from 18 sites when systematic province-wide surveys were initiated in the early 1970s (Bigg, 1985). Numbers of animals counted on these sites increased at rate of 4.0% since the early 1970s (r^2=0.82; n=9; P<0.001), which is not significantly different from

the rate of growth observed on rookeries. During the 2002 survey, 6681 nonpups were counted on haulout sites, and another 5439 on rookeries (Table 1).

Washington

There are no rookeries in Washington, but Steller sea lions are found along the coast throughout the year. Four haulouts, including two major sites (>50 animals), are regularly used during the breeding season. Since 1989, surveys have been conducted almost annually, and numbers of sea lions counted have increased at an average annual rate of 9.2% (r^2=0.38; n=37; P<0.001). These animals are assumed to be immature animals and nonbreeding adults associated with rookeries from other areas. Juvenile sea lions branded as pups on Forrester Island in southeastern Alaska (Raum-Suryan et al., 2002) and on Rogue Reef in Oregon (R. F. Brown, unpubl. data) have been observed in Washington.

Older records indicate that current abundance on the Washington coast is reduced from historical levels (Fig. 4C). Between 2000 and 3000 Steller sea lions were reported to be present during August and September of 1914, 1915, and 1916 on Jagged Island (Kenyon and Scheffer, 1959), compared with a maximum statewide breeding season count of 847 during 1978–2001. Washington State Department of Fisheries offered a bounty of $8.00 for sea lions between 1944–48, but in 1949 this was reduced to $3.00 and limited to inside waters because aerial patrols indicated that the main coastal haulouts at Jagged Island and Split Rock had been reduced from 600 sea lions in the 1930s to fewer than 100 by 1949 (Scheffer, 1950). Only sporadic counts were available for individual sites during the 1950s and 1960s, but they indicate that few sea lions (<100 animals) were present during the breeding season and that total abundance did not exceed 500 during any season by the 1950s (Scheffer, 1950; Kenyon and Scheffer, 1959).

Oregon

Steller sea lions breed and pup at two rookeries, located at Rogue Reef and Orford Reef, and occupy seven major haulout sites in Oregon during the breeding season. The total number of nonpup sea lions on rookeries increased from 1186 in 1977 to 2442 in 2002 (Fig. 3C), representing an average annual rate of increase of 2.5% (r^2=0.49; n=26; P<0.001). Although not as well documented, pup numbers also appear to have increased. In 1990, 492 and 298 pups were observed during ground counts at Rouge Reef and Orford Reef respectively, compared with 746 and 382 pups on 126 mm format images in 2002 (2.3% average annual rate of increase). During the 2002 population-wide survey, an additional 1727 nonpups were counted at haulout sites in Oregon (Table 2).

Historical data on Steller sea lion abundance in Oregon are few (Fig. 4D). Pearson and Verts (1970) counted 862 animals (including some pups) during a state-wide aerial survey in June 1968, somewhat lower than the 1977 nonpup count of 1461 animals. The largest rookery was Orford Reef, where 475 animals, including pups, were counted. Interestingly, only 125 animals were reported at Rogue Reef, which is currently the largest rookery in Oregon, and Pearson and Verts (1970) suggested that it was no longer used as a rookery. Earlier counts are lacking, but the population was presumably substantially larger in the 1920s because about 4000 sea lions were

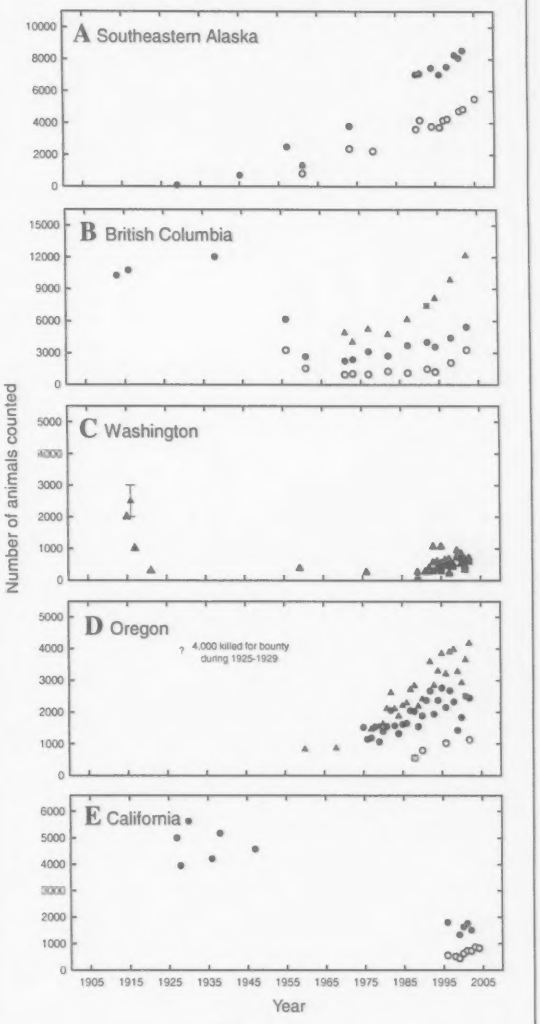

Figure 4

Historical counts over the last century of Steller sea lion (*Eumetopias jubatus*) pups (○), non-pups on rookeries (●), and total nonpups on rookeries and haulouts (▲) for (**A**) Southeastern Alaska, (**B**) British Columbia, (**C**) Washington, (**D**) Oregon, and (**E**) California.

Table 2

Results of life-table sensitivity analyses showing the potential change in ratio of total population size to pups for a population increasing at 3.1% per annum. The vital rates in Calkins and Pitcher's (1982) life tables[1] for a stable population of Steller sea lions (*Eumetopias jubatus*) were incrementally adjusted until a population growth rate, λ, of 3.1% was attained. The corresponding stable sex- and age-distributions were calculated by using Cole's (1954) finite approximations of Lotka's (1907) population equations.

Parameter that changed	Relative change	Population growth rate (λ)	Pup multiplier
Δ Mortality all ages	−15%	3.1%	5.0
Δ Juvenile mortality	−27%	3.1%	5.2
Δ Adult mortality	−33%	3.1%	4.7
Δ Fecundity	+32%	3.1%	4.2
Δ Age at maturation	−1.6 years	3.1%	4.2

[1] Calkins, D. G., and K. W. Pitcher. 1982. Population assessment, ecology and trophic relationships of Steller sea lions in the Gulf of Alaska. *In* Environmental assessment of the Alaskan continental shelf. p. 447–546. U.S. Department of Commerce and U.S. Department of Interior, Final Report of Principal Investigators 19:1–565.

killed for bounty on the Oregon coast during 1925–29 (Pearson and Verts, 1970), although some of these may have been nonbreeding animals associated with rookeries in California, British Columbia, and Alaska.

California

Steller sea lions historically have used six rookeries in California (San Miguel Island, Año Nuevo Island, the Farallon Islands, Seal Rocks off San Francisco, Sugarloaf Island-Cape Mendocino, and Saint George Reef). San Miguel Island and Seal Rocks are no longer used by Steller sea lions and only a few pups have been born on the Farallon Islands each year since the 1980s. There may have also been several additional small rookeries south of Año Nuevo (Bonnot, 1928; Rowley, 1929).

Statewide surveys, with the use of vertical 126-mm format aerial photography, were implemented in California in 1996. From 1996 through 2004 there was no discernible statewide trend for nonpups on rookeries (r^2=0.408; n=7; P=0.123), however, pup production increased at an average annual rate of 8% (r^2=0.68; n=8; P=0.012).

Although there has been a long and intermittent time series of counts for rookeries in California over the last 75 years (Bonnot, 1928, 1929; Bonnot and Ripley, 1948; Bartholomew and Boolootian, 1960; Orr and Poulter, 1967; LeBoeuf et al., 1991; Stewart et al., 1993), caution is warranted when attempting to evaluate population trends from the older data because they are drawn from a variety of sources where different survey methods were used. Statewide, total counts of nonpups at the six rookeries during the first half of the 20th century were on the order of 3900–5600. The 2004 count at these same six sites was 1578 nonpups and 818 pups—indicating that, perhaps, only about a third as many animals are currently present in the state (Fig. 4E). Population trends differed markedly among sites (Appendix).

Historically, Steller sea lions extended south to the Channel Islands in southern California, and San Miguel Island was considered to have been the southernmost rookery (Bonnot, 1928, 1929). It appears that Steller sea lion were once more abundant than California sea lions (*Zalophus californianus*) in that area (Bartholomew, 1967). Steller sea lions were reported to breed there in small numbers; Bonnot (1929) counted 50 pups in 1928. Abundance of nonpups in the Channel Islands peaked at about 2000 in the late 1930s (Appendix), although hunting and harassment could have resulted in fewer animals being present during the surveys (Bonnot and Ripley, 1948; Stewart et al., 1993). Numbers subsequently declined—the main declines occurring between the late 1930s and 1950s (Bartholomew and Boolootian, 1960; Bartholomew, 1967). No births have been recorded since 1982 and no adults have been seen since 1983 (Stewart et al., 1993).

In central California, Steller sea lion abundance at Año Nuevo and the Farallon Islands is currently only about 20% of the levels reported between the 1920s and 1960s (Appendix). Steller sea lions had deserted the rookery at Seal Rocks near the entrance to San Francisco Bay by the late 1920s, purportedly as a result of persistent harassment by fishermen (Rowley, 1929). During the 1920s, Año Nuevo Island and the Farallon Islands were identified as the most important rookeries in California, with 625 and 400 pups counted at each site, respectively, in 1922 (Bonnot, 1929). On Año Nuevo, numbers remained at high levels until the early 1960s, then declined thru the mid-1990s (Orr and Poulter, 1967; Le Boeuf et al., 1991) (Appendix). Since 1996, both pup production (r^2=0.035; n=8; P=0.656), and nonpup numbers (r^2=0.018; n=8, P=0.755) have been stable. Fewer counts are available for the Farallon Islands, but the pattern appears to be similar (Appendix); abundance was at high levels from the 1920s to early 1960s and then declined sharply during the 1960s or early 1970s (Hastings and Sydeman, 2002). Pup production on the Farallons has been low since at least 1974 (Appendix). An average of only nine pups was counted between 1996 and 2004 and the site presently does not meet our criteria for a rookery (>50 pups). Nonpup numbers were stable (r^2=0.173;

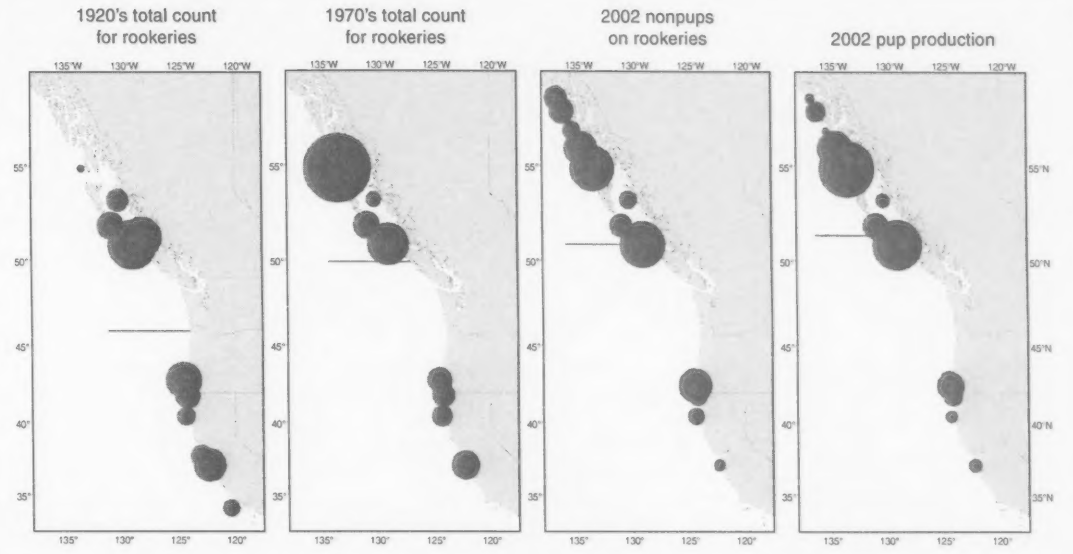

Figure 5

Map showing the shift in distribution and relative importance of rookeries in the eastern Steller sea lion (*Eumetopias jubatus*) population. Circles represent the proportion associated with each rookery of the total estimated abundance in the 1920s (1913–17 for British Columbia) and 1970s; and the proportion of nonpups and pups associated with each rookery during the 2002 range-wide survey. The horizontal lines indicate the center of the distribution (the latitude of each rookery weighted by the number of animals on it). For the 1920s, rookery counts in California represent minimum abundance because pups were not always included. Historic counts were unavailable for Oregon; therefore the minimum abundance was taken as the number killed for bounty during 1925–29. Because Oregon lies near the estimated center of the breeding distribution, the center of distribution is insensitive to the numbers assumed on Oregon rookeries (halving or doubling the Oregon figures shifts the center by less than 0.5° of latitude).

n=15; P=0.123) at low levels (Appendix) between 1974 and 2004.

Steller sea lions have been counted only sporadically at the Sugarloaf-Cape Mendocino and Saint George Reef rookeries in northern California until recent years (Appendix). Numbers of nonpups have been relatively stable since 1996 at both Sugarloaf-Cape Mendocino (r^2=0.106; n=8; P=0.431) and Saint George Reef (r^2=0.128; n=9; P=0.345). A comparison of counts made during the 1927–47 period with recent counts (Appendix) indicates that current abundance is probably only slightly reduced from historical levels. The Sugarloaf-Cape Mendocino rookery is small; counts of pups increased from 62 in 1996 to 131 in 2004, representing an average annual increase of 13% (r^2=0.725; n=8; P=0.007). For the Saint George Reef rookery, located near the California-Oregon border, counts of pups increased from 243 in 1996 to 444 in 2004, representing an average annual rate of 10% (r^2=0.70; n=8; P=0.009). Over the same period, counts of nonpups showed no discernible trend (r^2=0.11; n=12; P=0.431).

Steller sea lions use about six major (>50 animals) haulout sites along the California coast between Saint George Reef and Año Nuevo Island, as well as numerous smaller sites, during the breeding season. In 2002, a total of 1543 nonpups were counted at haulouts, in addition to the 1559 nonpups counted on rookeries. At least 12 former Steller sea lion haulout sites and perhaps a few rookeries between the Channel Islands and Año Nuevo Island (Bartholomew and Boolootian, 1960; Bonnot, 1928; Bonnot and Ripley, 1948; Rowley, 1929) have been abandoned.

Overall trend for the eastern North Pacific Steller sea lion population

The eastern North Pacific Steller sea lion population has exhibited significant and similar annual rates of growth in all three regions that support the largest rookeries: 3.2% in southeastern Alaska, 3.2% in British Columbia, and 2.5% in Oregon (Fig. 3). Combining the trend trajectories for these three regions, which currently account for over 90% of total pup production in the eastern population, overall abundance is estimated to have increased by about 215% over the last 25 years, representing an annual rate of increase of 3.1%. The time series for California is shorter; however pup production increased significantly at 7% per year between 1996 and 2004.

With the exception of the southernmost rookery at Año Nuevo Island and the (former) Farallon Islands rookery, both greatly reduced from historical levels, pup production has increased consistently throughout the range of the eastern population over the past 25+ years.

The total population-wide pup count in 2002 was 10,053 pups, of which 49% were found in southeastern Alaska, 33% in British Columbia, 11% in Oregon, and 7% in California (Table 1). This represents minimum pup production because some pups may have died and disappeared from rookeries prior to the survey, or were born after the census. Following Trites and Larkin (1996), we applied an arbitrary adjustment of 10% to account for pups that had been missed during our survey, giving a pup production estimate of 11,060. Using life tables, Calkins and Pitcher (1982) estimated the ratio of total animals to pups in a stationary population would be about 4.5:1. Our sensitivity analyses indicated that for a population increasing at 3.1%, the ratio could be as low as 4.2:1 if the growth were due to increased fecundity, or as high as 5.2:1 if the growth was due to reduced juvenile mortality (Table 2). The eastern population is thus estimated to have numbered about 46,000–58,000 animals in 2002. During the 2002 survey, we actually counted 45,378 animals (10,053 pups and 35,325 nonpups) on rookeries and at haulouts. This count represents an absolute minimum population size because not every site was surveyed and some animals were absent from rookeries and haulouts during the surveys and therefore were not counted.

The general sparseness and lack of standardization of the pre-1970 counts prevents a rigorous comparison of current and historical population levels; however several clear patterns emerge (Appendix). In southeastern Alaska abundance was apparently quite low during the first half of the 20th century, but numbers have increased consistently since that time. We have no explanation for the low numbers during the early 1900s because we are not aware of large-scale hunting or predator control efforts. Numbers were high in British Columbia in the early 1900s but were then reduced by about 70% by predator control and hunting. They have since recovered to levels approximately two-thirds of those of the early 1900s. Numbers on haulouts in Washington State were severely reduced by bounty hunting in the early to mid-1900s. Although there has been substantial recovery, peak numbers still appear to be only about half of levels of 1915. There are no count data available for Oregon prior to 1968, but the fact that about 4000 sea lions were killed for bounty during 1925–29 would indicate a sizable population at that time. There has been a substantial recovery since the 1968 surveys. The California population was apparently large during the early 1900s. Sites in southern California began declining in the late 1930s and that portion of the range was abandoned by the 1980s. Numbers in central California remained high into the 1960s, then declined to low levels, and stabilized during the 1990s. In northern California numbers were likely reduced during the mid 1900s, but now appear to be approaching levels of the early 1900s. Overall, the eastern population currently appears to be similar in size to historical levels of the early 1900s; the large population increase in southeastern Alaska balances out the declines in the southern portion of the range.

Although the number of rookeries used by the eastern Steller sea lion population has remained relatively constant (range 10–13), their distribution has shifted (Fig. 5). In the 2002 survey, the breeding population was centered (the latitude of each rookery weighted by the number of animals on it) at about 51.5°N (central British Columbia coast). Just over half of the rookeries (7 of 13) and births (57%) occurred north of that latitude, with the northernmost rookery at 58.2°N. For the 2002 population-wide survey, the pattern was similar for both pups and total numbers (pups and nonpups), suggesting they both provided an index of breeding distribution. In comparison, during the 1970s the breeding population was centered at roughly 49.9°N (central Vancouver Island), with the northernmost rookery at 54.8°N, representing a northward shift of 0.5° of latitude or 65 km per decade. In the 1920s, the breeding population was probably centered somewhere around 46.0°N (Washington-Oregon border); only two small rookeries accounted for about 13% of total abundance situated north of 51.5°N (the current center of pupping). At the southern end of their range, the declines of Steller sea lions appear to have begun in southern California (San Miguel) between the late 1930s and 1950s, and were followed by declines in central California between 1960 and 1990; however the two northernmost sites in California exhibited relative stability. Conversely, at the northern end of their range, Steller sea lions probably began breeding in significant numbers in southern southeastern Alaska (Forrester Island) in the late 1940s or 1950s and extended their breeding range to central southeastern Alaska (Hazy Islands) in the early 1980s, and northern southeastern Alaska (White Sisters) in the 1990s. Overall, the southern end of the breeding range contracted by about 3° latitude (330 km), and the northern limit was extended by about 5° latitude (550 km).

Discussion

The population increases observed in recent years over most of the range of eastern North Pacific Steller sea lion population almost certainly represent recovery from the impacts of prior predator-control programs, harvesting, and indiscriminate killing that took place prior to protection under the Canadian Fisheries Act of 1970 and implementation of the U.S. Marine Mammal Protection Act in 1972. The overall annual rate of increase of 3.1% was widespread (from Oregon to southeastern Alaska) and has been underway for at least 25 years, and there is no evidence of it slowing with increasing sea lion densities. The consistent, long-term observed rate of increase of 3.1% throughout most of the range of the eastern population is well below the theoretical maximum intrinsic rate of increase for pinnipeds

(Wade, 1998; Harkonen et al., 2002). This annual rate of increase indicates that either some factor or factors are still limiting the growth rate of this population or that the growth potential of this otariid is less than the theoretical maximum, which was derived from phocid population growth rates. We have observed Steller sea lions that have been shot or entangled in marine debris, and this undocumented mortality could be preventing the population from increasing at a higher rate. In addition, the Steller sea lion tends to have a longer period of maternal investment and a lower reproductive rate than most phocids (Pitcher et al., 1998), both of which may limit the growth potential of populations.

Although the three geographic regions supporting the largest rookeries all increased at about the same rate, individual rookeries often exhibited different population growth rates or temporal changes in growth rates. At the northern end of the range, Forrester Island accounted for essentially all of the population growth until the 1970s; however the observed rate of change has slowed since the 1980s. At the same time, some of the rookeries to the south of Forrester Island in British Columbia and to the north of it in central-northern southeastern Alaska have exhibited higher-than-average growth rates since the 1980s. The mechanism causing these geographic patterns is unknown, but could involve 1) dispersal of breeding animals between rookeries, 2) differences in local conditions that affect reproduction and survival, or 3) a shift in distribution of prey resources. Some dispersal of breeding females from their natal rookeries has been shown to occur. Six of 31 females that were marked as pups on the Forrester Island rookery were subsequently observed to have given birth on other rookeries (Raum-Suryan et al., 2002). The authors of that study concluded that the Steller sea lion generally conformed to the metapopulation concept as depicted by Hanski and Simberloff (1997), in that local breeding populations (rookeries) and movements among these local populations have the potential of affecting local dynamics.

For our assessment of long-term historic population trends, we relied mainly on counts of non-pups (or occasionally pups and nonpups combined) on rookeries, as few reliable pup counts were available prior to the 1970s. The 2002 population-wide survey (Fig. 2) and the last 30 years of counts in British Columbia indicated there is a relationship between the numbers of nonpups and pups on rookeries. However, departures from this relationship can occur, especially where existing rookeries are being abandoned or new rookeries are being formed. For example, the Farallon Islands, which no longer meet our definition of a rookery, now serves largely as a haulout site (Le Boeuf et al., 1991). The historical rookery on the Sea Otter Group in British Columbia, the only rookery known to have been extirpated by control efforts, is also still used during the breeding season as a haulout by nonbreeding animals. Conversely, in southeastern Alaska, the new rookeries were established at sites previously used as major haulouts by nonbreeding animals. The lack of accurate pup counts may, thus, have influenced our historical interpretation of historical data and our depiction of the exact breeding range, but there is a general consensus that the breeding range has shifted. Pup production in southern California has disappeared and in central California has dropped to less than one-fifth of what it was in the 1920s. Few, if any, pups were born in southeastern Alaska in the early 1900s, whereas this area now accounts for nearly half of total pup production in the eastern North Pacific population.

Control programs and harvesting clearly depleted the eastern Steller sea lion population and may have contributed to its redistribution, but the kills cannot fully explain the shift in the distribution. For example, while control efforts were underway in British Columbia during the 1950s and 1960s, animals may have taken refuge just north of the British Columbia-Alaska border at Forrester Island, or animals breeding on Forrester Island may have benefited from reduced competition as a result of the reductions on British Columbia rookeries. However, the northward expansion of the breeding range in southeastern Alaska continued through the 1980s and 1990s, even though killing of sea lions in British Columbia ceased in the 1960s. At the southern end of their range, sea lions were apparently very abundant in California before the 1860s, but were depleted during the 1870s because of intense hunts of sea lions for oil and hides (Bonnot, 1929). The last organized kills were made in 1909, although hunting, especially of bulls for trimmings (genitals, lips with whiskers, and gall bladders) continued into the 1930s. Nevertheless, the population declines in southern California began in the late 1930s, and in central California began in the late 1960s and early 1970s, well after major kills by humans had ended (Hastings and Sydeman, 2002).

The reason for the northward shift in the overall breeding distribution is unknown, and different factors may have been in play at the southern and northern ends of the range. In the south, competition with increasing populations of other pinnipeds may have been a factor in range constriction (Stewart et al., 1993). In particular, the number of California sea lions breeding in California increased from at most a few thousand in the 1920s (Bonnot, 1928) to about 240,000 in 2000 (Lowry and Maravilla-Chavez, 2005). It is likely that California sea lions and Steller sea lions compete with each other because 1) their ranges overlap, 2) they share the same haulout sites, and 3) they probably consume many of the same prey species. On San Miguel Island and the Farallon Islands, where Steller sea lions used to predominate (Bartholomew and Boolootian, 1960; Ripley et al., 1962; Stewart et al., 1993), the declines in Steller sea lions coincided with large increases in numbers of California sea lions (Stewart et al., 1993; Hasting and Sydeman, 2002).

For unknown reasons, southeastern Alaska represents the only area throughout the range of the eastern North Pacific population where new Steller sea lion rookeries have been established. Steller sea lion rookeries are normally located on remote, offshore islands or reefs and require adequate areas above high water levels where young pups can survive most weather conditions. There

must also be adequate prey on a consistent basis within the foraging range of lactating females. Perhaps the limited availability of such sites has restricted the establishment of new rookeries at other locations.

Changes in the ocean environment, particularly towards warmer water temperatures (Field et al., 2006), have also been proposed as a factor that has favored the California sea lion and other pinnipeds over the Steller sea lion in the southern part of their range (Bartholomew and Boolootian, 1960). Environmental conditions can affect sea lion populations directly or indirectly. Temperature could directly affect the survival of animals and such effects would be expected to be most evident at the latitudinal extremes of the range. The ocean environment can also act indirectly by affecting marine food webs, and thus the quantity and quality of prey available to sea lions. Unfortunately, with historical survey data being so scant, and with sea lions having been artificially reduced below natural levels, one can only speculate about the long-term effects of environmental conditions on the eastern Steller sea lion population, but conditions currently appear to be favorable through much of their range.

A somewhat similar change in Steller sea lion distribution and the establishment of new rookeries have been noted along the Asian coast. There the southern range limit has moved northward by 500–900 km over the past 50 years and several new rookeries have been established (Burkanov and Loughlin, in press).

Based on the population-wide survey in 2002, pup production for the eastern population is currently estimated to be about 11,000, and total abundance on the order of 46,000–58,000. It should be emphasized that this should be regarded as a "general" estimate because several factors can affect the accuracy of pup counts and correction factors. Following Trites and Larkin (1996), we added 10% to pup counts to estimate pup production (i.e., actual number of births), which seems reasonable, but the adjustment is subjective and arbitrary, and in reality the adjustment probably varies from site-to-site and year-to-year. The sex and age structure of populations, and hence the ratio of pups to nonpups, may differ between populations and change with population status in ways we do not understand. We attempted to delineate the possible range of changes in the correction factors by using sensitivity analyses, which showed the multiplier could either decrease if population productivity is controlled by fecundity or age at maturation, or increase if population productivity is controlled by mortality. Assessments for the western North Pacific population have indicate that the population declines were primarily due to poor juvenile survival (York, 1994), and if this is in fact the main determinant of population growth, the pup multiplier and estimated abundance of the eastern population may lie toward the high end of our range.

During the 2002 population-wide survey, a surprisingly large number of nonpups were observed (75–100% of the number expected based on our life table analysis). Because one would expect appreciable numbers of juveniles and adults to be dispersed at sea and missed during surveys, the actual size of the eastern population may be near the upper end of our estimated range. On the other hand, 2002 may merely have been an exceptional year for pup production, although the more recent pup counts available for California (2003 and 2004) and southeastern Alaska (2005) indicate that pup numbers have continued to increase. The apparent surplus of nonpups observed during the 2002 survey could also be indicative of the presence of nonbreeding animals associated with the western population in our survey area. Studies (where sea lions have been branded) have shown there is some overlap in the nonbreeding range of the two populations (Raum-Suryan et al., 2002), although there is no reason to expect a higher degree of movement from west to east. Moreover, the observed ratios of total counts to pup counts was uniformly high over the entire range of the eastern population (4.1 in southeastern Alaska, 4.7 in British Columbia, 4.7 in Oregon, and 5.4 in California), and if anything decreased slightly towards the north where one would expect the greatest overlap with the western population. The high nonpup to pup ratios indicate that high survival rather than high fecundity may be the primary mechanism responsible for population growth.

Steller sea lions in the eastern population currently breed at 13 major rookeries (>50 pups born), and the highest concentration of breeding animals is in southeastern Alaska, northern British Columbia, and near the Oregon-California border. Currently there is a large gap (993 km) between the Scott Islands rookery off northwestern Vancouver Island and the Orford and Rogue Reef rookeries in southern Oregon. There are no records of rookeries along this coastline, and natives hunting sea lions along the Washington coast had no knowledge of rookeries in that state (Scheffer, 1950). However, it would not be surprising to see new rookeries founded or re-established at haulout sites along this gap, as has occurred in southeastern Alaska, if the eastern population continues to increase in the northern part of its range. Nonbreeding animals use approximately 59 major haulout sites (>50 animals during) during the breeding season, plus numerous smaller sites and many seasonal haulout sites. The major haulouts are widely distributed from Cape Fairweather (58.8°N, 137.9°W) to Año Nuevo Island (37.1°N, 122.3°W), providing Steller sea lions with access to coastline spanning about 22° of latitude or 2400 km.

During the 1970s the eastern population represented only about 10% of the total number of Steller sea lions along the North American coast. With the large decline in the western population in conjunction with the increase in the east, this percentage has changed dramatically; about 55% of pup production in North America now occurs in the eastern population. We anticipate that continued monitoring and comparisons of the growing eastern population with the western population will provide insight into factors that ultimately regulate Steller sea lion populations, and we hope this synthesis for the eastern population will contribute toward better coordination of surveys and standardization of counting methods over the distribution range of the species.

Acknowledgments

We thank S. Riemer and B. Wright of the Oregon Department of Fish & Wildlife for their extensive contributions to survey work, counting, and database management. D. McAllister of the Alaska Department of Fish and Game conducted many of the surveys in southeastern Alaska. We thank K. Raum-Suryan for drafting Figure 1. R. DeLong and R. Small reviewed and provided useful comments on an earlier draft of this manuscript. We appreciate the timely comments and suggestions provided by three anonymous reviewers and by the editorial staff of Fishery Bulletin. Surveys in the U. S. were conducted under research permits from the Office of Protected Resources of the National Marine Fisheries Service and in Canada with authorization of Fisheries and Oceans Canada. Surveys in Oregon were conducted under special use permits granted by the U.S. Fish & Wildlife Service, Oregon Coastal Refuge Complex, and surveys at protected sites in B.C. were authorized by the Ecological Reserves Unit of B.C. Parks and Parks Canada.

Literature cited

Bartholomew, G. A.
1967. Seal and sea lion populations of the Channel Islands. *In* Proceedings of the symposium on the biology of the California Channel Islands (R. N. Philbrick, ed.), p. 229–244. Santa Barbara Botanical Garden, Santa Barbara, CA.

Bartholomew, G. A., and R. A. Boolootian.
1960. Numbers and population structure of pinnipeds on the California Channel Islands. J. Mammal. 41:366–375.

Berkson, J. M., and D. P. DeMaster.
1985. Use of pup counts in indexing population changes in pinnipeds. Can. J. Fish. Aquat. Sci. 42: 873–879.

Bickham, J. W., J. C. Patton, and T. R. Loughlin.
1996. High variability for control-region sequences in a marine mammal: implications for conservation and biogeography of Steller sea lions (*Eumetopias jubatus*). J. Mammal. 77:95–108.

Bigg, M. A.
1985. Status of Steller sea lion (*Eumetopias jubatus*) and California sea lion (*Zalophus californianus*) in British Columbia. Can. Spec. Pub. Fish. Aquat. Sci. 77:1–20.

Bonnot, P.
1928. The sea lions of California. Calif. Fish and Game. 14:1–16.
1929. Report on the seals and sea lions of California. California Division of Fish and Game. Fish. Bull. No. 14, 61 p.

Bonnot, P., and W. E. Ripley.
1948. The California sea lion census for 1947. Calif. Fish and Game 34:89–92.

Burkanov, V. N., and T. R. Loughlin.
In press. Distribution and abundance of Steller sea lions on the Asian coast, 1720s–2005. Mar. Fish. Rev.

Calkins, D. G., D. C. McAllister, K. W. Pitcher, and G. W. Pendleton.
1999. Steller sea lion status and trend in Southeast Alaska: 1979–1997. Mar. Mamm. Sci. 152:462–477.

Cole, L. C.
1954. The population consequences of life history phenomena. Quarterly Rev. Biol. 29:103–137.

DFO (Department of Fisheries and Oceans, Canada).
2003. Steller sea lion (*Eumetopias jubatus*). DFO, Can. Sci. Advis. Sec. Stock Status Rep. 2003/037, 9 p.

Field, D. B., T. R. Baumgartner, C. D. Charles, V. Ferreira-Bartina, and M. D. Ohman.
2006. Planktonic foraminfera of the California Current reflect 20th century warming. Science 311:63–66.

Fritz, L. W., and C. Stinchcomb.
2005. Aerial, ship, and land-based surveys of Steller sea lions (*Eumetopias jubatus*) in the wetern stock in Alaska, June and July 2003 and 2004. NOAA Tech. Memo. NMFS-AFSC-153, 56 p.

Hanski, I., and D. Simberloff.
1997. The metapopulation approach, its history, conceptual domain and application to conservation. *In* Metapopulation biology: ecology, genetics and evolution (Hanski and M. Gilpin, eds.), p. 5–26. Academic Press, London, England.

Harkonen, T., K. C. Harding, and M. Heide-Jorgensen.
2002. Rates of increase in age-structured populations: a lesson from the European harbour seal. Can. J. Zool. 80:1498–1510.

Hastings, K. K., and W. J. Sydeman.
2002. Population status, seasonal variation in abundance, and long-term population trends of Steller sea lions (*Eumetopias jubatus*) at the South Farallon Islands, California. Fish. Bull. 100:51–62.

Imler, R. H., and H. R. Sarber.
1947. Harbor seals and sea lions in Alaska. U.S. Fish Wildl. Serv., Spec. Sci. Rep. 28, 23 p.

Kenyon, K. W., and V. B. Scheffer.
1959. Wildlife surveys along the northwest coast of Washington. Murrelet 42:29–37.

Lewis, J. P.
1987. An evaluation of a census-related disturbance of Steller sea lions. M.S. thesis, 89 p. Univ. Alaska, Fairbanks, Alaska.

Lotka, A. J.
1907. Relation between birth rates and death rates. Science 26: 21–22.

Loughlin, T. R., A. S. Perlov, and V. A. Vladimirov.
1992. Range-wide survey and estimation of total number of Steller sea lions in 1989. Mar. Mamm. Sci. 8:220–239.

Lowry, M. S., and O. Maravilla-Chavez.
2005. Recent abundance of California sea lions in western Baja California, Mexico and the United States. *In* Proceedings 6th California Islands symposium, Ventura, California, U.S., December 1–3, 2003, p. 485–497. National Park Service Tech Publ. CHIS-05-01, Institute for Wildlife Studies, Arcata, CA.

Mathisen, O. A., and R. J. Lopp.
1963. Photographic census of the Steller sea lion herds in Alaska, 1956–58. U.S. Fish Wildl. Serv., Spec. Sci. Rep. Fish. No. 424, 20 p.

Newcombe, C. F., and W. A. Newcombe.
1914. Sea lions on the coast of British Columbia. Ann. Rep. British Columbia Comm. Fish for 1913, p. 131–145.

O'Corry-Crowe, G., T. Gelatt, K. Pitcher, and B. Taylor.
2005. Crossing significant boundaries: evidence of mixed-stock origins of new Steller sea lion, *Eumetopias jubatus*, rookeries in Southeast Alaska (Abstract). *In*

The 16th biennial conference on the biology of marine mammals (book of abstracts); December 12–16, 2005, San Diego, California, 330 p. Society for Marine Mammology.

Orr, R. T., and T. C. Poulter.
1967. Some observations on reproduction, growth, and social behavior in the Steller sea lion. Proc. Calif. Acad. Sci. 32:377–404.

Pearson, J. P., and J. P. Verts.
1970. Abundance and distribution of harbor seals and northern sea lions in Oregon. Murrelet 51:1–5.

Pitcher, K. W., V. N. Burkanov, D. G. Calkins, B. J. Le Boeuf, E. G. Mamaev, R. L. Merrick, G. W. Pendleton.
2001. Spatial and temporal variation in the timing of births of Steller sea lions. J. Mammal. 82:1047–1053.

Pitcher, K. W., D. G. Calkins, and G. W. Pendleton.
1998. Reproductive performance of female Steller sea lions: an energetics-based reproductive strategy? Can. J. Zool. 76:2075–2083.

Raum-Suryan, K. L., K. W. Pitcher, D. G. Calkins, J. L. Sease, and T. R. Loughlin.
2002. Dispersal, rookery fidelity, and metapopulation structure of Steller sea lions (*Eumetopias jubatus*) in an increasing and a decreasing population in Alaska. Mar. Mamm. Sci. 18:746–764.

Ripley, W. E., K. W. Cox, and J. L. Baxter.
1962. California sea lion census for 1958, 1960 and 1961. Calif. Fish. Game 48:228–231.

Rowley, J.
1929. Life history of the sea-lions on the California coast. J. Mammal. 10:1–39.

Scheffer, V. B.
1950. Mammals of the Olympic National Park and vicinity. Northwest Fauna no. 2, p. 192–225.

Snyder, G. M., K. W. Pitcher, W. L. Perryman, and M. S. Lynn.
2001. Counting Steller sea lion pups in Alaska: an evaluation of medium-format, color, aerial photography. Mar. Mamm. Sci. 17:136–146.

Stewart, B. S., P. K. Yokum, R. L. DeLong, and G. A. Antonelis.
1993. Trends in abundance and status of pinnipeds on the southern California Channel Islands. *In* Third California Islands symposium: recent advances in research on the California islands (E. Hochberg, ed.), p. 501–516. Santa Barbara Museum of Natural History, Santa Barbara, CA.

Trites, A. W., and P. A. Larkin.
1996. Changes in the abundance of Steller sea lions (*Eumetopias jubatus*) in Alaska from 1956 to 1992: how many were there? Aquat. Mamm. 22:153–166.

Wade, P. R.
1998. Calculating limits to the allowable human-cause mortality of cetaceans and pinnipeds. Mar. Mamm. Sci. 14:1–37.

Withrow, D. E.
1982. Using aerial surveys, ground truth methodology, and haulout behavior to census Steller sea lions, *Eumetopias jubatus*. M.S. thesis, 102 p. Univ. Washington, Seattle, WA.

York, A. E.
1994. The population dynamics of northern sea lions, 1975–1985. Mar. Mamm. Sci. 10:38–51.

Appendix

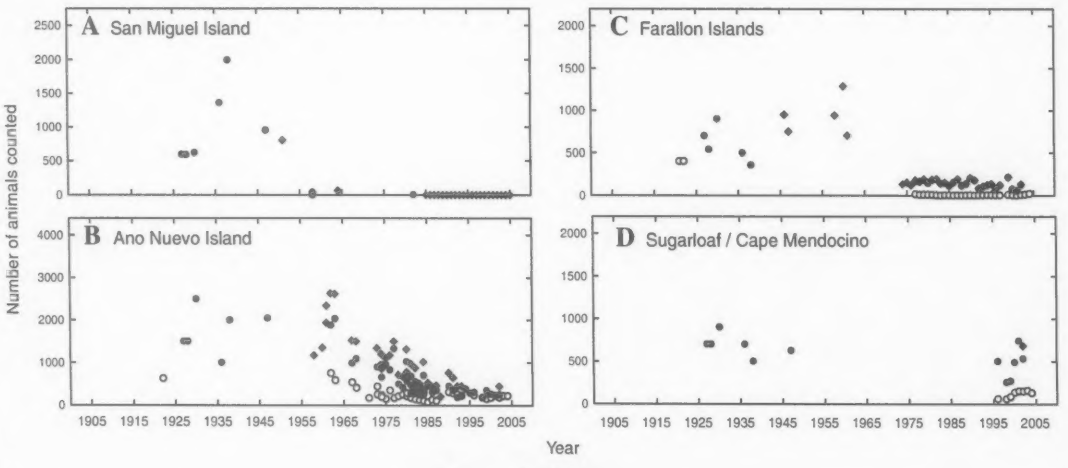
A San Miguel Island
B Ano Nuevo Island
C Farallon Islands
D Sugarloaf / Cape Mendocino
Number of animals counted
Year
1905 1915 1925 1935 1945 1955 1965 1975 1985 1995 2005

Appendix Figure

Historic counts made over the last century of Steller sea lion (*Eumetopias jubatus*) pups (○), nonpups (●), and total number of animals (♦) at each breeding rookery within the range of the eastern Steller sea lion population.

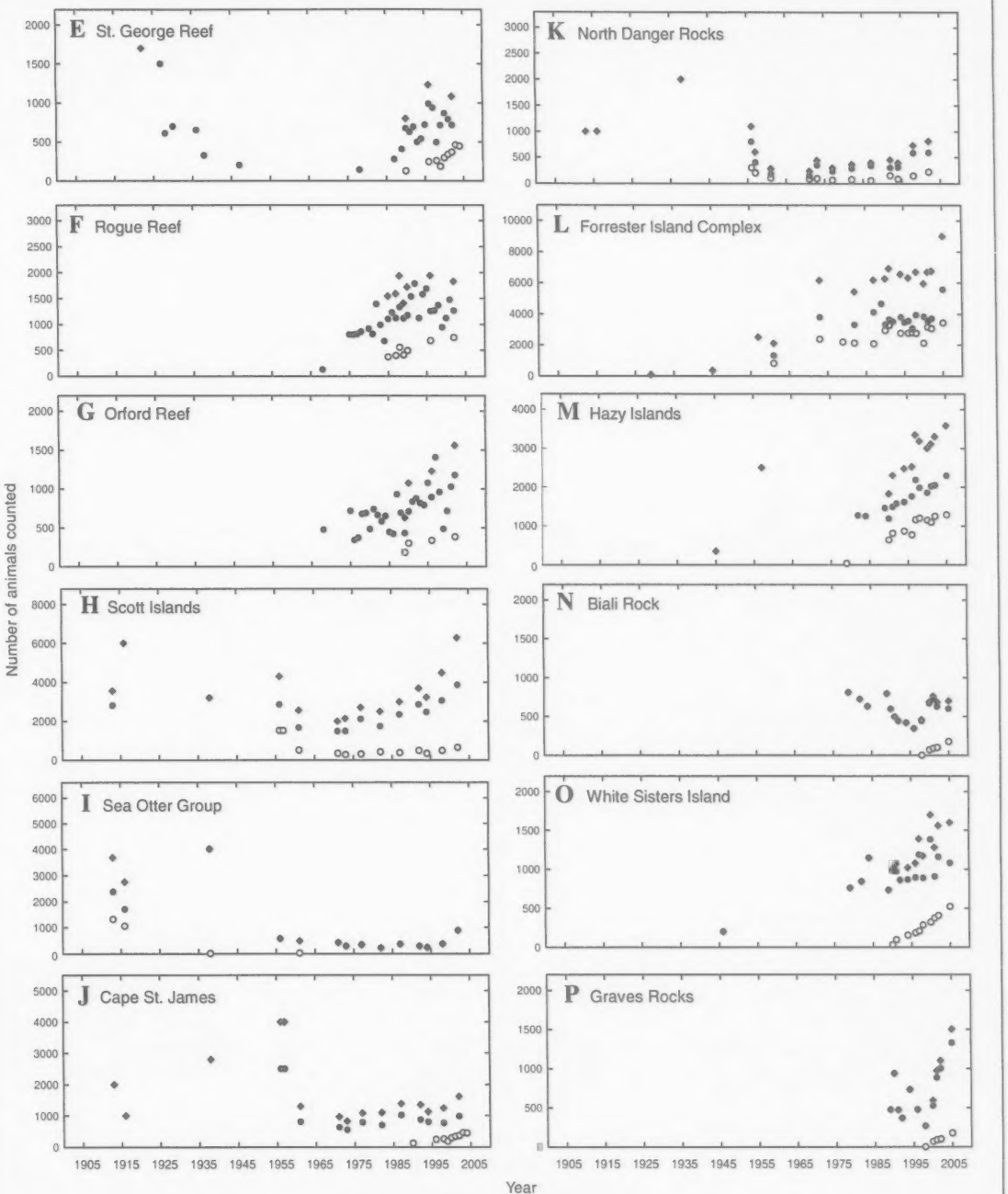

Appendix Figure (continued)

Abstract—For most fisheries applications, the shape of a length-frequency distribution is much more important than its mean length or variance. This makes it difficult to evaluate at which point a sample size is adequate. By estimating the coefficient of variation of the counts in each length class and taking a weighted mean of these, a measure of precision was obtained that takes the precision in all length classes into account. The precision estimates were closely associated with the ratio of the sample size to the number of size classes in each sample. As a rule-of-thumb, a minimum sample size of 10 times the number of length classes in the sample is suggested because the precision deteriorates rapidly for smaller sample sizes. In absence of such a rule-of-thumb, samplers have previously under-estimated the required sample size for samples with large fish, while over-sampling small fish of the same species.

Manuscript submitted 17 May 2006 to the Scientific Editor's Office.

Manuscript approved for publication 22 June 2006 by the Scientific Editor.

Fish. Bull. 106:116–120 (2007).

Precision estimates and suggested sample sizes for length-frequency data

Hans D. Gerritsen (contact author)[1]

David McGrath[2]

Email address (for H. D. Gerritsen): hans.gerritsen@marine.ie

[1] Fisheries Science Service, Marine Institute
Rinville, Oranmore
County Galway, Ireland

[2] Commercial Fisheries Research Group
Galway-Mayo Institute of Technology
Dublin Road
Galway, Ireland.

Length measurements are fundamental to many aspects of fisheries science. However, there is little formal guidance on the appropriate size of a length sample. Such guidance is of particular relevance when the number of fish available exceeds the number that can be measured at a reasonable cost, and a subsample needs to taken. Clearly, the required precision of a length sample depends on the purpose of sampling. In order to identify modes of individual year classes for a length-based assessment, the precision of the sample needs to be quite high. Sample sizes of more than 1000 are necessary to identify more than half the modes in a typical length distribution (Erzini, 1990). A sample size of at least 100 adult fish was recommended for age-based stock assessment purposes (Anderson and Neumann, 1996), although the authors did not mention how they arrived at this number.

Regardless of the type of assessment that is used, the shape of the length-frequency distribution is of interest, rather than simple summary statistics such as the mean or the variance. For this reason, it has proved difficult to quantify what constitutes a representative or adequately precise length distribution. Some studies have attempted to find minimum or optimum sample sizes by comparing samples to an expected distribution (e.g., Muller[1]; Gomez-Buckley et al.[2]; Vokoun et al., 2001). However, the true distribution is usually unknown, and dissimilarity from the expected distribution does not necessarily indicate an imprecise sample. In addition, these methods provide only indirect measures of precision that are difficult to evaluate objectively.

Thompson (1987) used the precision of a sample explicitly to establish an appropriate sample size. Thompson proved that a sample size of 510 is sufficient to be 95% confident that all estimated proportions in a multinomial distribution are no more than 5% from the true proportion. However, Thompson based this figure (n=51) on a worst-case scenario, which, in the present case, is a length-frequency distribution that is evenly apportioned over three size classes. Because this is not the typical shape of a length-frequency distribution used in fisheries science, Thompson's measure of precision is too conservative for the vast majority of cases.

For most fisheries applications, it would be more useful to define the

[1] Müller, H. 1996. Minimum sample sizes for length distributions of the catch estimated by an empirical approach. ICES CM 1996/J12, 18 p.

[2] Gomez-Buckley, M., L. Conquest, S. Zitzer, and B. Miller. 1999. Use of statistical bootstrapping for sample size determination to estimate length-frequency distributions for pacific albacore tuna (*Thunnus alalunga*). Final report to National Marine Fisheries Services, FRI UW 9902, 7 p. Website: http://www.fish.washington.edu/research/publications/pdfs/9902.pdf (accessed 31 March 2006).

precision of a length-frequency sample as the mean precision over the entire size range. However, it appears that this approach has not been used to establish an optimum sample size. Such mean precision estimates over the entire size range might be used to obtain a rule-of-thumb for sample sizes that are required in order to obtain a certain precision level of the catch at each location. In the present study we aim 1) to determine a rule-of-thumb for obtaining an appropriate sample size when the number of fish available in a particular sample exceeds the number that can be measured at a reasonable cost, and 2) to examine the sample sizes that have been taken in the past, in absence of such guidance.

Materials and methods

Data were used from the Irish Groundfish survey, which was carried out on RV *Celtic Explorer* in the waters around Ireland during October and November 2005. The catch was sorted into species and, if appropriate, into size grades, each of which were treated as a separate length sample. Length measurements were taken from all fish and squid species that were caught. If the number of individuals in a sample was large, a subsample was taken by repeatedly transfering the sample from each fish box into two other boxes and discarding one of these. This method ensures that the entire catch is represented uniformly in the subsample. At the time of the survey, the samplers did not have any particular guidance on the appropriate size for a subsample; they used their own judgment to decide on the sample size.

The precision of the number of observations in each length class of a random sample can be estimated by assuming a multinomial distribution (Smith and Maguire, 1983). If the precision in each length class is expressed in the form of a coefficient of variation (CV), an overall measure of precision can be obtained by weighting each CV by the number of fish in each length class. This mean weighted CV (MWCV) provides a description of the precision over the entire range of size classes in a length frequency distribution.

Under the assumption of a multinomial distribution, the standard deviation (σ_i) of the number of fish in a sample that are length category i can be estimated by

$$\sigma_i = \sqrt{np_i(1-p_i)}, \quad (1)$$

where n = the total number of fish in the sample; and
p_i = the proportion of the sample that is length i.

The coefficient of variation (CV) of the number of fish at length i, is given by

$$CV_i = \frac{\sigma_i}{np_i} \quad (2)$$

and the mean weighted coefficient of variation (MWCV) is given by

$$MWCV = \sum p_i CV_i = \frac{\sum \sigma_i}{n}. \quad (3)$$

The highest possible value of the MWCV results from a length-frequency distribution that is evenly distributed over a large number of size classes. The number of fish at each length class are then Poisson distributed with a standard deviation that equals the square root of the number at length (Zar, 1999). The theoretical maximum MWCV is therefore given by

$$MWCV = (n/c)^{-0.5}, \quad (4)$$

where c = the number of size classes in the sample.

The minimum MWCV is zero and would result from a distribution where all observations fall within a single length category. Therefore, the MWCV estimates will always lie between zero and the curve described by Equation 4.

Results

During the 2005 survey, a total of 2332 length samples were taken for 80 different species of fish and squid. In most cases, the sample size was limited by the number of individuals in the catch. However, 596 samples were deemed too large to measure all individuals and subsamples were taken. The median subsample size was just under a quarter of the total catch (by weight), whereas 90% of the subsamples were smaller than half of the total catch. The four most common species that were subsampled were poor cod (*Trisopterus minutus*), blue whiting (*Micromesistius poutassou*), haddock (*Melanogrammus aeglefinus*), and Norway pout (*Trisopterus esmarkii*).

The estimated MWCV of the subsamples was closely associated with the ratio of the number of individuals measured to the number of length classes in the sample (Fig. 1). The MWCV appeared to follow an exponential curve that was close to the maximum MWCV given by Equation 4. The MWCV decreased very rapidly with increasing sample size up to sample sizes of around 10 times the number of length classes in the sample, after which the sample size would need to be increased considerably for a moderate further improvement in precision. If the sample size is taken as 10 times the number of length classes in the distribution, an MWCV of around 0.25 can be expected; a sample size of 48 times the number of length classes would result in an MWCV of 0.10 and a sample size of 155 times the number of length classes would be necessary to reduce the MWCV to 0.05.

The mean sample size in the subsamples taken on the survey was just under nine times the number of length classes per sample, resulting in a mean MWCV of 0.33. However, there was quite a large spread in the sample sizes (Fig. 1); therefore some samples were measured with very low precision, whereas others had

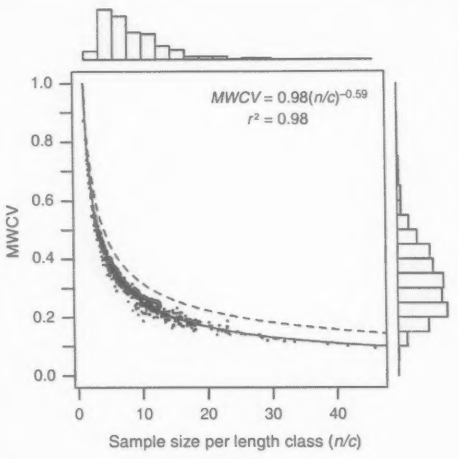

Figure 1

The mean weighted coefficient of variation (MWCV) for 596 subsamples was closely related to the sample size (n) divided by the number of per length classes in the sample (c). A good fit was obtained for the power function indicated by the solid line; its parameters are given at the top of the plot. The dashed line indicates the theoretical maximum MWCV (Eq. 4.). The histograms show the distribution of the samples on both axes.

excessively large sample sizes. The range of sample sizes was between 2.2 and 24.7 times the number of length classes (2.5% and 97.5% quantiles), resulting in a range of MWCVs between 0.14 and 0.61. With a minor increase in effort, the sample size might be increased to 10 per length class for each subsample, resulting in an MWCV of around 0.25 for all samples. Considering that the precision deteriorates very rapidly for sample sizes of less than 10 per length class, a minimum sample size of 10 times the number length classes in the sample is suggested as a rule-of-thumb in the present case.

The previous analysis shows that, in order to obtain the same level of precision for all subsamples, the sample size should be directly proportional to the number of size classes. In absence of specific guidance on the sample size during the 2005 survey, the chosen sample size was only weakly correlated to the number of length classes in the sample of poor cod and haddock, whereas no significant correlation was found for blue whiting and Norway pout (Fig. 2). The same figure also shows that the MWCV in subsamples tended to increase with the mean length of the fish in the sample. This increase indicates that samples with a large mean size tended to be sampled with lower precision than samples of smaller fish of the same species.

Discussion

Length distributions that result from combining a number of different samples exhibit greater variation than predicted under the multinomial model given in Equation 1 (Smith and Maguire, 1983). Fish populations are usually not uniformly mixed; therefore individual samples are not random samples from the population (Pennington et al., 2002). The simple multinomial model does not take account of the between-sample variability and will therefore underestimate the total variance. However, Equation 1 does provide an unbiased estimate of the variability within each sample, which is the variability that would occur if one could repeatedly take a random sample at the same location and time and measure these without error. This is the variability that is of interest when deciding whether the sample size is large enough to estimate the length distribution from a particular haul with a certain precision. Therefore, the MWCV is a suitable measure for this exercise.

In order to obtain a precise population estimate, it is important to maximize the number of sampling locations because of the considerable between-sample variability that is usually present (Pennington et al., 2002). Pennington et al. (2002) suggested maximizing the number of sampling locations at the expense of the number of fish measured. However, the number of hauls is often limited by practical considerations, and length measurements can be obtained quickly and cheaply. Therefore, it seems prudent to sample enough fish from each haul to obtain a length distribution that is representative of that catch at that particular location. Detailed information on the length distribution at each station can be valuable for exploratory data analysis, such as investigating the spatial structure in the data. Nevertheless, this level of sampling may not be strictly necessary for a precise population estimate of the length-frequency distribution for an age- or length-based assessment.

The samples in Figure 1 included a large range of species and size categories of fish, but the variability in the MWCV was small after taking account the sample sizes. This small amount of variability indicates that the MWCV is not very sensitive to the exact shape of the distribution and can be predicted with high precision, at least within the range of distributions encountered on the survey. A minimum sample size of 10 times the number of length classes in the sample appears to be a reasonable compromise between effort and precision in the present case.

The current analysis has focused on subsampling during surveys; however the same principles can be applied to any process of collecting data for which the shape of the distribution is of interest. The desired precision level for these cases will depend on a number of factors. For certain species that are of little commercial or scientific interest, but which may span across a large number of length classes, the suggested sample size of 10 per length class may be excessive. Likewise, as the MWCV is directly proportional to the number of length

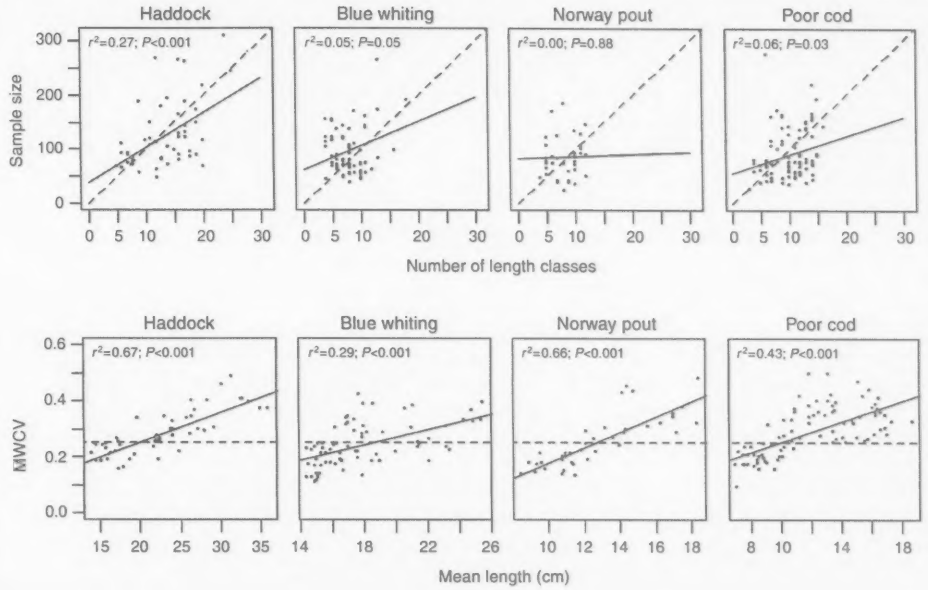

Figure 2

The sample sizes of subsamples taken on the survey were correlated with the number of length classes in the samples of haddock (*Melanogrammus aeglefinus*) and poor cod (*Trisopterus minutus*), but not significantly so for blue whiting (*Micromesistius poutassou*) and Norway pout (*Trisopterus esmarkii*) (top row). There was considerable variation in the mean weighted coefficient of variation (MWCV), which correlated with the mean length of fish in the samples (bottom row). The solid lines represent linear regressions and the dashed lines indicate the sample sizes and MWCV that would have resulted from a sampling scheme where the sample size was chosen to be 10 times the number of length classes in the distribution. The coefficients of determination, r^2, are given together with their *P*-values.

classes in the sample, the choice of the interval of the length classes will determine the precision. Although increasing the size of length intervals will reduce the MWCV, this action will result in a loss of information which is undesirable. The cost of sampling, the detail required, and the purpose of the data collection need to be considered before the required precision level can be determined for applications other than the present example.

Without formal guidance on the appropriate sample size, the sample sizes chosen were, at best, weakly correlated with the number of size classes in the samples. It appears that the samplers under-estimated the required sample size for samples with large fish, whereas samples of smaller fish of the same species were over-sampled. This tendency to under-estimate the sample size may be related to the fact that the volume of a sample increases with the cube of its mean length; therefore a sample size of large fish may appear to be larger than the same number of small fish. In addition, samples with large fish tend to be spread out over a larger number of size classes, thus requiring higher sample numbers.

In practice, it will be difficult for a sampler to estimate both the number of size classes and the number of fish in a sample. Therefore, the Marine Institute in Ireland is developing a software application that allows samplers to examine the length frequencies of the samples directly after they have been measured. The software estimates the weight of the suggested sample size for each distribution. Because size distributions tend to be similar on consecutive hauls, the sampler can gain an insight into the required weight of an appropriate sample for each species and size category.

The information contained in a length-frequency distribution is largely a function of sample size. The present method allows the amount of information contained in a length-frequency distribtuion to be quantified in terms of precision, allowing samplers to make informed decisions on the sample size that is required to obtain an adequate estimate of the length-frequency distribution of a particular catch.

Acknowledgments

Free R-software has been used for this work and the authors would like to thank the R development core team and all contributors to the R project (http://www.R-project.org). We also thank Colm Lordan and two anonymous reviewers for their valuable comments.

Literature cited

Anderson, R. O., and R. M. Neumann.
1996. Length, weight, and associated structural indices. *In* Fisheries techniques, 2nd ed. (B. R. Murphy and D. W. Willis, eds.), p. 447–482. Am. Fish. Soc., Bethesda, MD.

Erzini, K.
1990. Sample size and grouping of data for length-frequency analysis. Fish. Res. 9:355–366.

Pennington, M., L. M. Burmeister, and V. Hjellvik.
2002. Assessing the precision of frequency distributions estimated from trawl-survey samples. Fish. Bull. 100:74–80.

Smith, S. J., and J. J. Maguire.
1983. Estimating the variance of length composition samples. *In* Sampling commercial catches of marine fish and invertebrates (W. G. Doubleday and D. Rivard, eds.), p. 165–170. Can Spec. Pub. Fish. Aquat. Sci. 66, Ottawa, Canada.

Thompson, S. K.
1987. Sample size for estimating multinomial proportions. Am. Statist. 41:42–46.

Vokoun, J. C., C. F. Rabeni, and J. S. Stanovick.
2001. Sample-size requirements for evaluating population size structure. N. Am. J. Fish. Manage. 21:660–665.

Zar, J. H.
1999. Biostatistical analyis, 4th ed., 663 p. Prentice-Hall, Inc., Englewood cliffs, NJ.

Early marine growth in relation to marine-stage survival rates for Alaska sockeye salmon (*Oncorhynchus nerka*)

Edward V. Farley Jr[1]
James M. Murphy[1]
Milo D. Adkison[2]
Lisa B. Eisner[1]
John H. Helle[1]
Jamal H. Moss[1]
Jennifer Nielsen[3]

Email address for E. V. Farley: Ed.Farley@noaa.gov

[1] NOAA, Auke Bay Laboratory
National Marine Fisheries Service, NOAA
11305 Glacier Highway
Juneau, Alaska 99801

[2] Juneau Center, School of Fisheries and Ocean Sciences,
University of Alaska Fairbanks
11120 Glacier Highway
Juneau, Alaska 99801

[3] U.S. Geological Survey, Alaska Science Center
1011 East Tudor Road
Anchorage, Alaska 99503

Abstract—We tested the hypothesis that larger juvenile sockeye salmon (*Oncorhynchus nerka*) in Bristol Bay, Alaska, have higher marine-stage survival rates than smaller juvenile salmon. We used scales from returning adults (33 years of data) and trawl samples of juveniles (n=3572) collected along the eastern Bering Sea shelf during August through September 2000–02. The size of juvenile sockeye salmon mirrored indices of their marine-stage survival rate (e.g., smaller fish had lower indices of marine-stage survival rate). However, there was no relationship between the size of sockeye salmon after their first year at sea, as estimated from archived scales, and brood-year survival size was relatively uniform over the time series, possibly indicating size-selective mortality on smaller individuals during their marine residence. Variation in size, relative abundance, and marine-stage survival rate of juvenile sockeye salmon is likely related to ocean conditions affecting their early marine migratory pathways along the eastern Bering Sea shelf.

Manuscript submitted 27 March 2006 to the Scientific Editor.

Manuscript approved for publication 5 July by the Scientific Editor.

Fish. Bull. 105:121–130 (2007).

Pacific salmon (*Oncorhynchus* spp.) experience relatively high mortality rates during the first few months at sea (Hartt, 1980), and it is believed that size plays an important role in survival (Parker, 1968; Pearcy, 1992). Size-dependent mortality of juvenile salmon may be concentrated during two specific life-history stages. The first stage is thought to occur just after juvenile salmon enter the marine environment, where smaller individuals are believed to experience higher size-selective predation (Parker, 1968; Willette et al., 1999). The second stage is thought to occur after the first summer at sea, when smaller individuals may not have sufficient energy reserves to survive late fall and winter (Beamish and Mahnken, 2001). Thus, larger individuals likely have a higher probability of survival during both of these stages, and size and growth while salmon reside in the estuary and during their first summer at sea may be important for survival.

Previous studies indicate that scale radius length is proportional to fish body length (Francis, 1990; Ricker, 1992) and, in particular, incremental increases in sockeye salmon (*O. nerka*) scale radius are strongly correlated with somatic growth (Fukuwaka and Kaeriyama, 1997). In our study, scales from adult Bristol Bay sockeye salmon were examined to determine the relationship between size after their first year at sea and survival to adulthood. We compared the time series (1965–97) of brood-year returns per spawner with scale growth measurements taken from adult sockeye salmon returning to the Egegik and Kvichak River systems in Bristol Bay, Alaska.

Juvenile sockeye salmon enter the marine waters of the eastern Bering Sea during May and June (Burgner, 1991) and migrate through Bristol Bay to the Bering Sea and North Pacific during the summer and early fall months (Straty, 1981; Farley et al., 2005). Two differing models of seaward migration are believed to exist for juvenile Bristol Bay sockeye salmon: in some years juvenile sockeye salmon migrate along the coastal waters of the eastern Bering Sea near the Alaska Peninsula, and in other

years their migration is farther offshore (Farley et al., 2005). We also compared the size of juvenile Bristol Bay sockeye salmon collected during late summer and early fall (2000–02) trawl surveys along the eastern Bering Sea shelf with indices of their abundance, marine stage survival rate after our survey, and returns per spawner from these cohorts. Interannual differences in the size and growth rates of juvenile sockeye salmon were also compared to their early marine distribution and ocean conditions. The specific objectives of this study were to determine whether larger, presumably faster growing, juvenile sockeye salmon in fact had higher survival rates than smaller, presumably slower growing individuals, and what aspects of the marine environment might influence these growth rates.

Materials and methods

Data

Our research focused on Bristol Bay sockeye salmon because this region has the largest returns and commercial harvest of sockeye salmon in the world. Scales from adult sockeye salmon, their fork lengths, and data on brood-year return per spawner for the Egegik and Kvichak Rivers in Bristol Bay, Alaska, as well as annual totals of the number of adult Bristol Bay sockeye salmon returns and spawners, were obtained from the Alaska Department of Fish and Game (ADF&G). Salmon scales are collected annually by ADF&G to estimate the age composition of adult sockeye salmon for fishery management. Age was designated by the European notation, i.e., $a.b$, where a = the number of winters spent in freshwater prior to going to sea and b = the number of winters spent in the ocean (Koo, 1962a). Salmon scale collections and brood year return per spawner data were available for the dominant freshwater and ocean age groups of sockeye salmon sampled in the Kvichak River (brood year returns for ages 1.2, 1.3, 2.2, 2.3; 1965–97) and the Egegik River (brood year returns for ages 1.3, 2.2, 2.3; 1965–97).

Scales were selected for measurement by following the procedures described in Ruggerone et al. (2005). Briefly, scales were selected when our age determination matched that previously made by ADF&G, the shape of the scale indicated that the scale was from the "preferred area" (below the dorsal fin and above the lateral line—see Koo, 1962b), and the circuli and annuli were clearly defined and not affected by scale regeneration or significant resorption along the measurement axis. The number of scale samples for each river system and age group are provided in Table 1.

Scales from adult sockeye salmon were digitized following procedures described by Hagen et al.[1] and Ruggerone et al. (2005). The scale measurement axis was determined by a perpendicular line drawn from a line intersecting each end of the first saltwater annulus. Distance (mm) between the focus and the outer edge of the scale was designated as the total scale length. The relationship between total scale length and adult fork length was linear for both the Egegik River (F-test, $P<0.001$; $r^2=0.41$) and Kvichak River (F-test, $P<0.001$; $r^2=0.36$) sockeye salmon samples. For an index of total growth through the first year at sea, we measured the distance from the focus to the outer edge of the first saltwater growth zone for each fish. A time series of annual means of the individual growth during the first year at sea ($MSW1_{i,a,t}$) estimated for each adult freshwater age group (a represents 1 or 2) within a river system (i represents Egegik, Kvichak) was used as an index of size that sockeye salmon would have attained after their first year (t) at sea.

Table 1

The total number of scale samples for sockeye salmon (*Oncorynchus nerka*) for brood years 1965–97 from the Egegik and Kvichak River systems in Bristol Bay, Alaska. Age groups are 1.2, 1.3, 2.2, and 2.3.

	Age group			
River	1.2	1.3	2.2	2.3
Egegik	0	1265	1592	1581
Kvichak	1563	1441	1582	1246

The total number of fish caught and the fork lengths (mm) of juvenile sockeye salmon within each trawl haul were recorded during the Bering-Aleutian Salmon International Survey (BASIS) research cruises along the eastern Bering Sea shelf during fall (August–September) 2000 to 2002 (Fig. 1). The surveys were conducted over a broad area of the shelf and over major oceanographic domains (coastal and middle domains; Kinder and Schumacher, 1981) along the eastern Bering Sea shelf. In addition, the surveys were designed to sample the entire population of juvenile sockeye salmon from Bristol Bay lake systems to reduce the chance of sample variability that could affect one's ability to interpret results from these samples. Recent descriptions of juvenile salmon migration pathways along the eastern Bering Sea shelf (Farley et al., 2005) and genetic stock composition indicate that juvenile sockeye salmon collected during the surveys were primarily from Bristol Bay.

Fish were collected by using a mid water rope trawl (see Farley et al., 2005 for description) rigged to sample the top 15 m of the water column. We attempted to collect scales from juvenile sockeye salmon during all three years of the survey; however, sample sizes of scales (from the preferred location on fish) were too small for statistical analyses because of descaling of the juvenile salmon by our mid-water rope trawl. Data

[1] Hagen, P. T., D. S. Oxman, and B. A. Agler. 2001. Developing and deploying a high resolution imaging approach for scale analysis. Doc. 567, p. 11. North Pacific Anadromous Fish Commission, 889 Pender Street, Vancouver, Canada.

collected during each trawl included the trawl speed obtained with a global positioning system and the height and width of the net opening obtained with a Simrad FS900 (Simrad, Lynnwood, WA) net sounder. The mean date of collection of juvenile sockeye salmon sampled for length differed slightly between years (i.e., 26 August during 2000; 5 September during 2001; 1 September during 2002); lengths were adjusted to account for these differences.

Survival and early marine-stage growth rates inferred from adult scales

For each freshwater age group, we calculated an index of survival rate that normalized the data and removed possible density-dependent effects (i.e., Peterman et al., 1998; Mueter et al., 2002). Specifically, our index of survival rate was the time series of residuals from a Ricker model defined by

$$\ln\left(\frac{R_{i,a,2,t+2}+R_{i,a,3,t+3}}{S_{i,t-(a+1)}}\right) = \alpha_{i,a}-\beta_{i,a}S_{i,t-(a+1)}+\varepsilon_{i,a,t}, \quad (1)$$

where t = the first ocean year for sockeye salmon;
S = the total number of spawners within river system i (i represents Egegik or Kvichak);
R = the total return (catch+spawners) for each freshwater age group a (a represents freshwater age 1 or 2) within river system i;
α and β = model parameters representing the number of recruits per spawner at low numbers of spawners and the level of density dependence (Quinn and Deriso, 1999); and
$\varepsilon_{i,a,t}$ = the normally distributed residuals of the model.

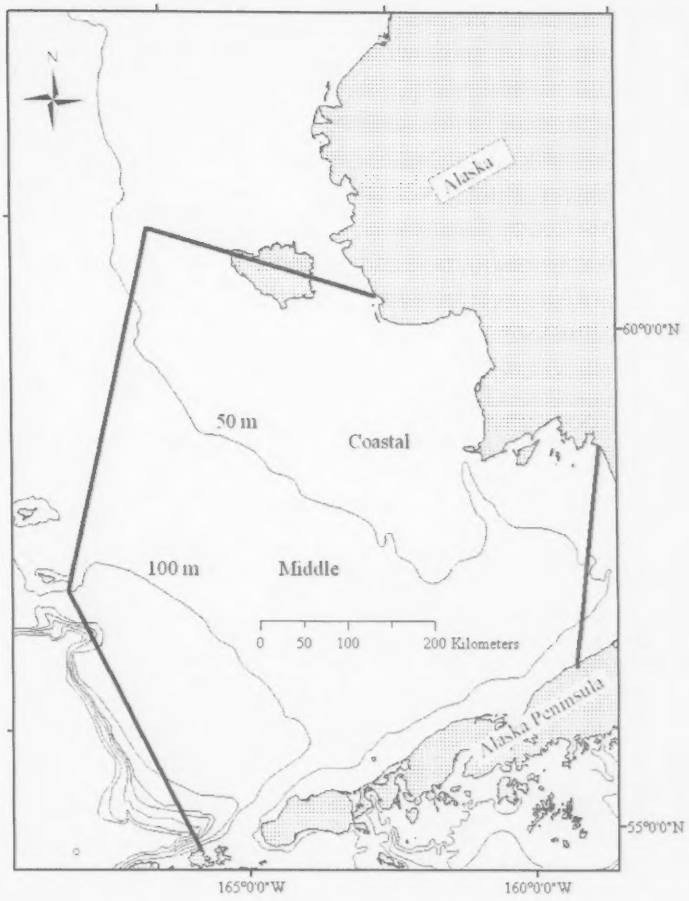

Figure 1

Survey area of the annual August–September (2000–2002) Bering-Aleutian Salmon International Survey (BASIS) within the coastal and middle domains of the eastern Bering Sea.

For our analysis, partitioning salmon brood-year productivity by freshwater age group was necessary to directly compare our index of survival with our time series of $MSW1_{i,a,t}$ growth.

Analysis of covariance (ANCOVA) was used to examine the effect of $MSW1_{i,a,t}$ on our indices of survival (see Fig. 2, A–D for scatter plots of $\varepsilon_{i,a,t}$ and $MSW1_{i,a,t}$ and the addition of river system, age group and year were used as factors in the model. The results indicated that the year factor was highly significant (F-test, $P<0.001$) and that $MSW1_{i,a,t}$ was not significant (F-test, $P=0.18$). It was possible that during some years all fish could have had excellent growth and attained a large size, but the ANCOVA model would have attributed the large size to the highly significant year factor. However, when we removed the year factor from the ANCOVA model, $MSW1_{i,a,t}$ was less significant (F-*test*, $P=0.27$). In addition, the residuals from these models contained significant positive autocorrelation.

Because our data contained significant autocorrelation and showed a time series character, we created univariate time series models (Wei, 1990) for both $MSW1_{i,a,t}$ and $\varepsilon_{i,a,t}$ to determine whether autoregressive or moving average components were present. The univariate models were developed by examining the sample autocorrelation and partial autocorrelation functions for each time series. Time series data were considered white noise processes, i.e., uncorrelated random variables

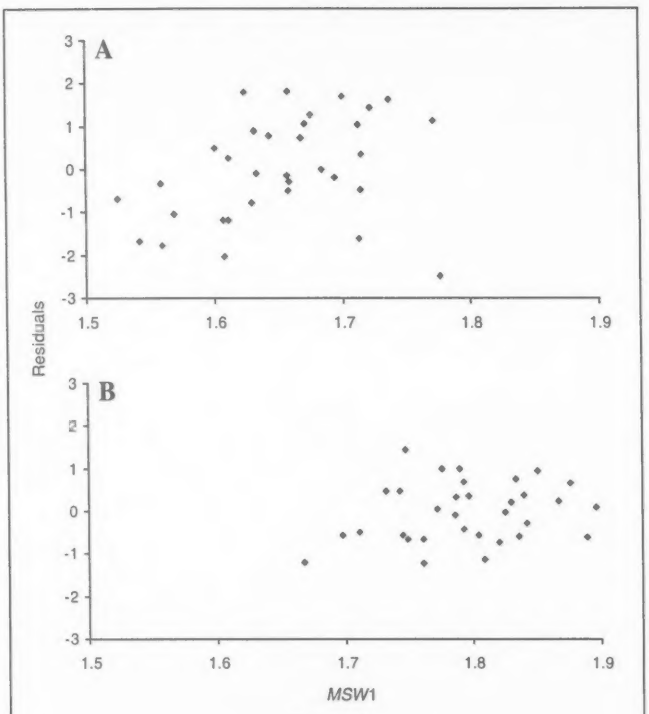

Figure 2

The relationship between the index of marine-stage survival rate (residuals) and growth after the first year at sea (*MSW*1) for Egegik freshwater age groups 1 (**A**) and 2 (**B**) and Kvichak freshwater age groups 1 (**C**) and 2 (**D**) sockeye salmon (*Oncorhynchus nerka*).

with constant mean and variance, when none of the components of the sample autocorrelation and partial autocorrelation functions differed significantly (P=0.01) from zero (Wei, 1990).

Multivariate time series models in the form of linear transfer function (LTF) models (Liu and Hudak, 1992) were developed to describe the relationship between $MSW1_{i,a,t}$ and our index of survival rate for each freshwater age group and river system. All the univariate time series of survival rate indices contained significant positive first-order autoregressive parameters (see Table 2). Therefore, we included the first order autoregressive parameter in the LTF models. The models were defined as

$$\varepsilon_{i,a,t} = c_{i,a} + \lambda_{i,a} MSW1_{i,a,t} + \frac{1}{(1-\phi_{1,i,a}B)} N_{i,a,t} , \qquad (2)$$

where t, i, a are described in Equation 1;

$MSW1$ = the early marine growth index for sockeye salmon during their first year at sea;

ϕ_1 = the autoregressive lag 1 parameter;

B = the symbol for the backshift operator (i.e., $B \times S_t = S_{t-1}$),;

$c_{i,a}$ and $\lambda_{i,a}$ = parameters within the model; and

$N_{i,a,t}$ = a sequence of random errors that are independently and identically distributed with a normal distribution.

Parameters within the univariate and LTF models were deemed significant when their t-value was greater than 2.0 (P<0.05).

Autocorrelation analysis was used to examine whether the model residuals were white noise. Univariate and LTF models were compared by using Schwartz's Bayesian criterion (SBC; Wei, 1990) to determine if the inclusion of *MSW*1 in Equation 2 improved the model fit.

Analyses of data from juveniles collected by trawling

Next, we developed an index of relative survival rate of adult Bristol Bay sockeye salmon for 2000–02, and indices of abundance and marine-stage survival rate of juvenile sockeye salmon collected during 2000–02 to compare with mean lengths of juvenile sockeye salmon collected during those years. Relative survival was defined as the number of returning adult sockeye salmon from brood-year escapements that contributed to the

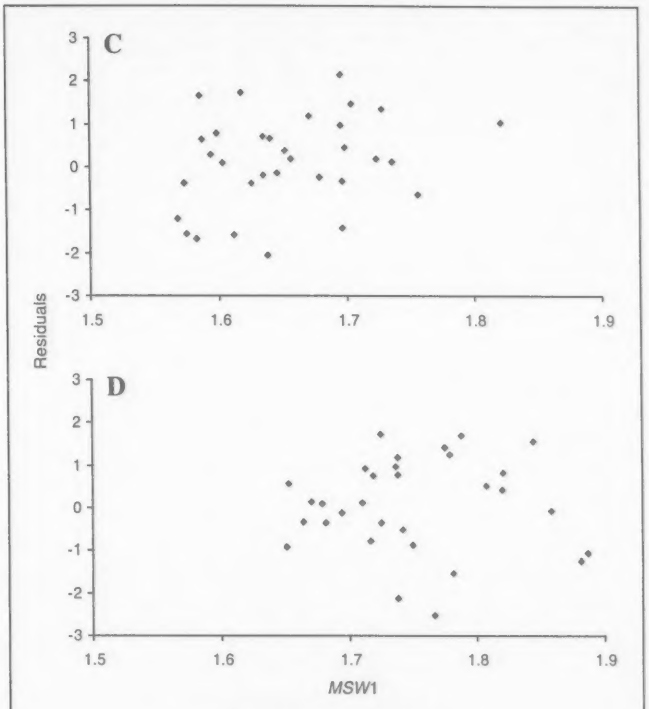

Figure 2 (continued)

Table 2

Univariate (Univ) and linear transfer function (LTF) models indicating the effect of early marine growth index (*MSW1*) on the index of marine stage survival rates for each freshwater age group of sockeye salmon (*Oncorhynchus nerka*) returning to the Egegik and Kvichak rivers. Other variables include the constant (*Const*) and the autoregressive parameter ϕ_1. Model statistics included the number of effective observations (n), the coefficient of determination (r^2), residual standard error (*RSE*), the number of parameters (M), and Schwartz's Bayesian criterion (*SBC*).

								Model coefficients			*t*-value		
River	Age (yr)	Model	n	r^2	RSE	M	SBC	*Const.*	*MSW1*	ϕ_1	*Const.*	*MSW1*	ϕ_1
Egegik	1	Univ	32	0.34	0.958	2	4.19	0.13	—	0.48	0.40	—	3.37
		LTF	32	0.41	0.908	3	4.22	−10.38	6.36	0.30	−2.22	2.25	2.07
	2	Univ	32	0.17	0.630	2	−22.64	0.02	—	0.42	0.10	—	2.64
		LTF	32	0.25	0.601	3	−22.19	−6.61	3.69	0.41	−1.74	1.75	2.59
Kvichak	1	Univ	32	0.29	1.075	2	11.56	−0.15	—	0.54	−0.36	—	3.60
		LTF	32	0.29	1.074	3	14.97	1.06	−0.73	0.54	0.21	−0.24	3.62
	2	Univ	32	0.35	0.986	2	6.00	−0.32	—	0.64	−0.64	—	3.99
		LTF	32	0.35	0.985	3	9.43	0.71	−0.59	0.64	0.18	−0.26	3.98

juvenile sockeye salmon in the trawl samples taken during years 2000, 2001, and 2002. For instance, juvenile sockeye salmon contributing to the early marine population during 2000 comprised age-2.0 fish from the 1997 and age-1.0 fish from the 1998 brood-year escapements, and these fish would have returned as adults during 2002 and 2003. Relative marine-stage survival rate (RS) was thus calculated as

$$RS_t = \frac{\sum_{a=1}^{2}(R_{a,2,t+2} + R_{a,3,t+3})}{(S_{t-2} + S_{t-3})/2}, \quad (3)$$

where t = the year juvenile sockeye salmon were sampled (t=2000, 2001, 2002);
a = the freshwater age (1.0 or 2.0);
R = is the total number of returning adult sockeye salmon to Bristol Bay after year t; and
S = the total number of spawners in Bristol Bay that contributed to the juvenile salmon population during year t.

For instance, freshwater juvenile sockeye salmon (ages 1.0 and 2.0) sampled during 2000 came from cohorts spawning during 1998 (age 1.0) and 1999 (age 2.0) and returned to Bristol Bay during 2002 as adult salmon at age 1.2 and 2.2 in 2002 and at age 1.3 and 2.3 in 2003. The numbers of returning adult and spawning Bristol Bay sockeye salmon were estimated from brood-year return information provided by ADF&G.

Annual indices of juvenile sockeye salmon abundance (IA) were defined as

$$IA_t = \left(SA / \overline{ma}\right)\overline{C}_t, \quad (4)$$

where SA = the estimated survey area (189,000 km^2);
$\overline{ma}$ = the mean area sampled by a trawl haul during the survey (distance traveled during the tow multiplied by the width of the net); and
$\overline{C}_t$ = the mean number of juvenile sockeye salmon caught during year t (t=2000, 2001, 2002).

This formula would give the abundance of juvenile sockeye salmon in the survey area if we assumed that catchability with our midwater trawl was 1, (i.e., all fish in front of the net were caught). Because this is unlikely, we treat our estimates as an index rather than as actual abundance. In fact, our juvenile sockeye salmon abundance indices were less than the resultant adult returns in some years, indicating that catchability of the net was much less than 1. One study (Shuntov et al., 1993) where larger surface trawl gear was used to sample juvenile salmon indicated that catchability of juvenile salmon was 0.3. We therefore divided our abundance indices by 0.3, although we still considered these values to be indices.

An index of juvenile sockeye salmon marine-stage survival rate (IMS) was estimated by

$$IMS_t = \frac{\sum_{a=1}^{2}(R_{a,2,t+2} + R_{a,3,t+3})}{IA_t} \times 100, \quad (5)$$

where R is defined above in Equation 3, IA_t is defined in Equation 4, t is the year juvenile sockeye salmon were sampled (t=2000, 2001, 2002), and a is freshwater age (age 1.0 or 2.0).

These survival rate indices were correlated with the mean length of juvenile fish collected during the corresponding first year at sea. Because the mean date for juvenile sockeye salmon sampled for length differed among years, we adjusted fish lengths to provide a standardized length using September 1 as the standard date. Adjusted mean fish lengths were calculated by assuming three different daily growth rates: 1) 0 mm/day, representing no daily growth at sea; 2) 0.3 mm/day, the lower end of published growth-rate ranges for juvenile Pacific salmon; and 3) 1.7 mm/day, representing the upper end of the ranges (see Fisher and Pearcy, 1988, 1990; Fukuwaka and Kaeriyama, 1994; Orsi et al., 2000 for daily growth-rate ranges for juvenile Pacific salmon).

Results

Analyses of adult scale data

Examination of the autocorrelation and partial autocorrelation functions for Kvichak River freshwater age groups 1 and 2 and the Egegik River freshwater age-group-1 MSW1 univariate time series indicated that these time series had a constant mean and variance. For the Egegik River freshwater age-group-2 MSW1 growth index, the sample autocorrelation and partial autocorrelation functions indicated that a lag-1 autoregressive parameter was appropriate and the estimate of the parameter was significant (t-test, P<0.01). Coefficients of variation were less than 4% for the MSW1 growth-rate indices for each freshwater age group, and thus confirmed the univariate model results that these time series varied little over time. By comparison, the coefficients of variation for the time series of returns per spawner for each freshwater age group were between 70% and 135%.

The MSW1 growth index was not significantly related to survival in any of the LTF models except for Egegik freshwater age group 1 (Table 2). Parsimonious univariate models were reasonable explanations of survival for both river systems and age groups, having values of SBC nearly as low as the "best" models. The sample autocorrelation and partial autocorrelation functions indicated that a lag-1 autoregressive parameter was appropriate for the all of the univariate survival rate time series models. The estimates of the lag-1 autoregressive parameter were positive for all of the univariate models.

Analyses of data from juveniles collected by trawling

The distribution of juvenile sockeye salmon along the eastern Bering Sea varied among years (Fig. 3). During 2000 and 2001, 75% of the total catch of juvenile sockeye salmon occurred south of 56°N, within the middle domain and south within the stratified waters near the

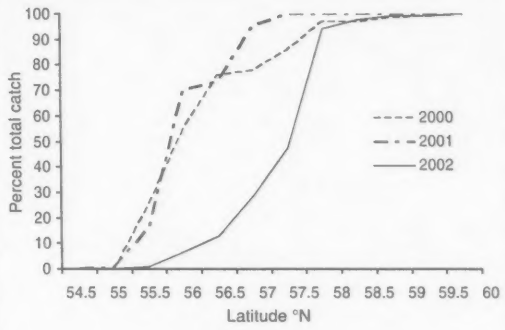

Figure 3

The percentage of total catch of juvenile sockeye salmon (*Oncorhynchus nerka*) in relation to latitude (°N) along the eastern Bering Sea shelf during August–September 2000, 2001, and 2002.

coastal domain along the Alaska Peninsula. During 2002, 75% of the total catch of juvenile sockeye salmon occurred north of 57°N, with 50% of the total catch occurring north of 58°N within the shallow stratified waters near the northern coastal domain.

Average fork length of juvenile sockeye salmon was significantly smaller during 2001 than during 2000 and 2002 for growth rates greater than 0.3 mm/day (*t*-test; $P<0.01$) and not significantly different from 2000 (*t*-test; $P=0.05$) for growth rates equal to 0 mm/day (Table 3). The rank order of juvenile sockeye salmon fork lengths was the same for all growth rates, and the largest fish taken in 2002 and the smallest, in 2001. For all three growth rates, average fork length was significantly larger during 2002 than during 2000 and 2001 (*t*-test; $P<0.01$).

The marine-stage survival rate and abundance in the indices mirrored the observed variation in fish fork length; they were highest during 2002 and at or near their lowest during 2001 (Table 4). In addition, the nearshore distribution of juvenile sockeye salmon (2001; Fig. 3) appeared to coincide with lower indices of abundance and marine-stage survival rate, whereas fish distributed in the northern area of our survey (2002; Fig. 3) exhibited higher marine-stage survival rate and abundance.

Discussion

Our study indicates that the size of Bristol Bay sockeye salmon after their first year at sea is not directly related to their survival, when size is measured from growth rings on the scales of adults returning to the Egegik and Kvichak rivers. Analyses of the MSW1 growth index indicated that most of the time series had a constant mean and variance. Similar studies where adult scales

Table 3

Average fork length of juvenile sockeye salmon (*Oncorhynchus nerka*) collected along the eastern Bering Sea during 2000, 2001, and 2002. Daily growth rate (mm) was assumed to be 0, 0.30, and 1.7. Statistics include sample size (*n*), average fork lengths, and standard deviation (SD) of the original length data.

		Average fork length (mm)			
Year	*m*	0	0.3	1.7	SD
2000	834	174.77	176.53	184.76	19.99
2001	802	171.91	170.61	164.53	35.55
2002	1936	197.96	197.94	197.83	34.74

Table 4

Indices of abundance (*IA*), marine-stage survival rate (*IMS*), and relative marine-stage survival rate (*RS*) for juvenile sockeye salmon (*Oncorhyncus nerka*) collected along the eastern Bering Sea during 2000, 2001, and 2002.

Year	*IA*	*IMS*	*RS*
2000	130	21%	3.8
2001	137	15%	1.9
2002	180	34%	6.0

from Atlantic (*Salmo salar* L.; Crozier and Kennedy, 1999), coho (*O. kisutch*; Briscoe, 2004), and chum (*O. keta*; Helle, 1979) salmon were used to measure growth (size) of salmon during their first year at sea revealed that the survival rate of a cohort was statistically unrelated to variation in growth (size) of the salmon. The relative uniformity in the size of salmon after their first year at sea and the lack of a relationship between size and survival rate is contrary to the prevailing paradigm that the size achieved by fish after their first summer at sea is important to survival (Beamish and Mahnken, 2001). However, these results do not necessarily invalidate this paradigm; the adult scale samples available for analysis may reflect only those juvenile salmon that had attained sufficient size in order to survive to adulthood, and not those that died at sea (Crozier and Kennedy, 1999).

In support of this possibilty, when we directly measured the fork length of juvenile sockeye salmon (Tables 3 and 4) during late summer and early fall surveys along the eastern Bering Sea shelf (2000–02), smaller fish had lower indices of marine-stage survival rate. This result is consistent with that from other studies of teleost fish, where larger individuals gained a survival advantage over smaller conspecifics during the juvenile life-history stage (Parker, 1968; Healey, 1982; Holtby et

al., 1990; Pearcy, 1992; Sogard, 1997; Mortensen et al., 2000; Beamish and Mahnken, 2001; Moss et al., 2005). This result is also in accord with the critical-size and critical-period hypothesis in which brood-year survival is determined by the number of juvenile salmon that have reached a critical size by the end of their first marine summer (Beamish and Mahnken, 2001; Beamish et al., 2004). The assumption with this hypothesis is that fish that do not reach a critical size after their first summer at sea will die because they are unable to meet minimum metabolic requirements during late fall and winter (Beamish and Mahnken, 2001). Although our results indicate that larger juvenile sockeye salmon have higher relative marine-stage survival rate after their first year at sea, it is difficult to directly address when the mortality would occur because sockeye salmon can spend an average of 2 to 3 years at sea. However, the overwhelming evidence from field and laboratory studies of juvenile stages of teleost fishes seems to indicate that size-selective mortality occurs during winter because larger members of a cohort are better than smaller members at tolerating physical extremes and enduring longer periods without food (Sogard, 1997).

One other test of the critical-size and critical-period hypothesis is that mortality rates after this period should be large in relation to other sources of early marine mortality (Beamish et al., 2004). To interpret our indices of marine-stage survival rate as the actual post-survey marine survival rate requires making a variety of questionable assumptions (e.g., that the vulnerability of juvenile salmon to our gear is known). However, if our estimates are close to correct, they would indicate that marine-stage mortality rates of juvenile sockeye salmon may be greater than 70% (Table 4) after our late-summer–early-fall surveys. These marine-stage mortality rates are substantial and approach late fall and winter mortality rates of greater than 90% found for other Pacific salmon (Beamish et al., 2004).

Lengths of juvenile sockeye salmon differed significantly among years if we assumed daily growth rates of 0.3 mm and greater. Differences in fork length of juvenile sockeye salmon could reflect annual differences in early marine growth rates or may also reflect annual differences in the size of smolt leaving Bristol Bay lake systems. However, limited surveys of sockeye salmon smolt from the Kvichak and Ugashik Rivers during 2000 through 2002 (Egegik River sampling was not undertaken in 2002) by ADF&G indicate that differences in smolt length among years and within age classes and river systems were less than 9%. In addition, the smallest average smolt size among these three years was seen during 2002, the year with the largest juvenile sockeye salmon size. Thus, it is likely that annual differences in length observed during our survey were due to differences in marine growth rates between years.

The annual variability in juvenile sockeye salmon size and in indices of marine-stage survival rates may be linked to the early marine migration of these salmon along the eastern Bering Sea shelf. Although we had only three years of data, size and survival indices of Bristol Bay sockeye salmon were lowest when juvenile sockeye salmon were distributed nearshore along the Alaska Peninsula (i.e., the coastal migration pathway) and highest when they were distributed farther north and offshore. In support of this theory, the coastal migration pathway of juvenile Bristol Bay sockeye salmon observed by Straty (1981) during the late 1960s and early 1970s coincided with a significantly lower production of Bristol Bay sockeye salmon that occurred before the mid 1970s (Adkison et al., 1996).

The annual variability in seaward migration pathways is likely related to ocean conditions on the shelf during spring and summer. Recent studies indicate that sea surface temperatures along the eastern Bering Sea in summer, the period when juvenile sockeye salmon are present on the shelf, is positively correlated with Bristol Bay sockeye salmon survival rates (Mueter et al., 2002). It is possible that the effect of sea surface temperatures on survival rates of juvenile Bristol Bay sockeye salmon is a result of its influence on early marine distribution of juvenile sockeye salmon. For example, during the late 1960s and early 1970s, the nearshore migration of juvenile Bristol Bay sockeye salmon was thought to be a result of sockeye salmon using the warmer nearshore waters rather than the colder sea surface temperatures offshore in order to maximize their growth (Straty, 1981). Depth-averaged sea temperatures from an oceanographic mooring along the eastern Bering Sea middle shelf domain from mid-July to mid-September were consistently warmer during 2001 through 2002 than during 1995 through 1997 (Overland and Stabeno, 2004). Presumably, the warmer sea temperatures during 2001 would have been conducive to offshore migration of juvenile sockeye salmon during that year. Although sea temperatures were warmer during 2001 through 2002, sea temperatures along the shelf were 1° to 2°C cooler from late June to September during 2001 than during 2002 (Overland and Stabeno, 2004). Thus, it may be that warmer sea temperatures during the time juvenile sockeye salmon first are present over the eastern Bering Sea shelf (beginning in June) provide a conduit for rapid offshore migration (and possibly higher survival) and that cooler sea temperatures delay offshore migration.

Our results indicate that after the first summer in the Bering Sea, larger juvenile sockeye salmon may gain a survival advantage over smaller individuals. This result, coupled with previous findings of reduced juvenile-to-adult survival for pink (Moss et al., 2005) and coho (Beamish et al., 2004) salmon that spend their first summer in the coastal waters of the Gulf of Alaska and Strait of Georgia, indicates that reduced growth of Pacific salmon during their first year at sea may lead to substantial salmon mortality, presumably during their first winter at sea. This phenomenon may not be seen if size of the salmon after their first year at sea is inferred from the scale growth increments of returning adults, because these individuals could be a biased sample from the faster-growing portion of the

population (Crozier and Kennedy, 1999). We suggest that annual variability in the size of sockeye salmon may be related to summer sea surface temperatures along the eastern Bering Sea shelf temperatures that appear to influence the spatial distribution and early marine migration pathways of this species.

Acknowledgments

P. Hagen, formally with the Alaska Department of Fish and Game in Juneau, Alaska, was instrumental in aging and creating digital pictures of juvenile sockeye salmon scales. We gratefully appreciate the help of the captains (M. Cavanaugh and S. Brandstitter) and the crew of the FV *Sea Storm* and captain C. Bronson and the crew of the FV *Great Pacific* for their fine efforts and technical assistance in all aspects of the field surveys. We thank A. Wertheimer, G. Kruse, and three anonymous reviewers for suggestions during this study and comments on the manuscript.

Literature cited

Adkison, M. D., R. M. Peterman, M. F. Lapointe, D. M. Gillis, and J. Korman.
1996. Alternative models of climatic effects on sockeye salmon, *Oncorhynchus nerka*, productivity in Bristol Bay, Alaska, and the Fraser River, British Columbia. Fish. Oceanogr. 5:137–152.

Beamish, R. J., and C. Mahnken.
2001. A critical size and period hypothesis to explain natural regulation of salmon abundance and the linkage to climate and climate change. Prog. Oceanogr. 49:423–437.

Beamish, R. J., C. Mahnken, and C. M. Neville.
2004. Evidence that reduced early marine growth is associated with lower marine survival of coho salmon. Trans. Am. Fish. Soc. 133:26–33.

Burgner, R. L.
1991. Life history of sockeye salmon (*Oncorhynchus nerka*). *In* Pacific salmon life histories (C. Groot and L. Margolis, eds.), p. 3–117. Univ. British Columbia Press, Vancouver, Canada.

Briscoe, R. J.
2004. Factors affecting marine growth and survival of Auke Creek, Alaska coho salmon (*Oncorhynchus kisutch*). M.S. thesis, 57 p. Univ. Alaska Fairbanks, Fairbanks, AK.

Crozier, W. W., and J. A. Kennedy.
1999. Relationships between marine growth and marine survival of one sea winter Atlantic salmon, *Salmo salar* L., from the River Bush, Northern Ireland. Fish. Manage. Ecol. 6:89–96.

Farley, E. V., Jr., J. M. Murphy, B. W. Wing, J. H. Moss, and A. Middleton.
2005. Distribution, migration pathways, and size of western Alaska juvenile salmon along the eastern Bering Sea shelf. Alaska Fish. Res. Bull. 11(1):15–26.

Fisher, J. P., and W. G. Pearcy.
1988. Growth of juvenile coho salmon (*Oncorhynchus kisutch*) off Oregon and Washington, USA, in years of differing coastal upwelling. Can. J. Fish. Aquat. Sci. 45:1036–1044.
1990. Spacing of scale circuli versus growth rate in young coho salmon. Fish. Bull. 88:637–643.

Francis, R. I.
1990. Back-calculation of fish length: a critical review. J. Fish Biol. 36:883–902.

Fukuwaka, M., and M. Kaeriyama.
1994. A back-calculation method for estimating individual growth of juvenile chum salmon by scale analysis. Scientific Reports of the Hokkaido Salmon Hatchery 48:1–9.
1997. Scale analyses to estimate somatic growth in sockeye salmon, *Oncorhynchus nerka*. Can. J. Fish. Aquat. Sci. 54:631–636.

Hartt, A. C.
1980. Juvenile salmonids in the oceanic ecosystem: the critical first summer. *In* Salmonid ecosystems of the North Pacific (W. J. McNeil and D. C. Himsworth, eds.), p. 25–57. Oregon State Univ. Press, Corvallis, OR.

Healey, M. C.
1982. Timing and relative intensity of size-selective mortality of juvenile chum salmon (*Oncorhynchus keta*) during early sea life. Can. J. Fish. Aquat. Sci. 39:952–957.

Helle, J. H.
1979. Influence of marine environment on age and size at maturity, growth, and abundance of chum salmon, (*Oncorhynchus keta*) from Olsen Creek, Prince William Sound, Alaska. Ph.D. diss., 118 p. Oregon State Univ., Corvallis, OR.

Holtby, L. B., B. C. Andersen, and R. K. Kadowaki.
1990. Importance of smolt size and early ocean growth to interannual variability in marine survival of coho salmon (*Oncorhynchus kisutch*). Can. J. Fish. Aquat. Sci. 47:2181–2194.

Kinder, T. H., and J. D. Schumacher.
1981. Hydrographic structure over the continental shelf of the southeastern Bering Sea. *In* The eastern Bering Sea shelf: oceanography and resources, vol. 1 (D. W. Hood and J. A. Calder, eds.), p. 31–52. Univ. Washington Press, Seattle, WA.

Koo, T. S. Y.
1962a. Age designation in salmon. *In* Studies of Alaska red salmon (T. S. Y. Koo, ed.), p. 41–48. Publications in Fisheries, New Series 1, Univ. Washington, Seattle, WA.
1962b. Age and growth studies of red salmon scales by graphical means. *In* Studies of Alaska red salmon (T. S. Y. Koo, ed.), p. 49–121. Publications in Fisheries, New Series 1, Univ. Washington, Seattle, WA.

Liu, L., and G. B. Hudak.
1992. Forecasting and time series analysis using the SCA statistical system, 435 p. Scientific Computing Associates Corporation, Oak Brook, IL.

Mortensen, D., A. Wertheimer, S. Taylor, and J. Landingham.
2000. The relation between early marine growth of pink salmon, *Oncorhynchus gorbuscha*, and marine water temperature, secondary production, and survival to adulthood. Fish. Bull. 98:319–335.

Moss, J. H., D. A. Beauchamp, A. D. Cross, K. Myers, E. V. Farley Jr., J. M. Murphy, and J. H. Helle.
2005. Higher marine survival associated with faster growth for pink salmon (*Oncorhynchus gorbuscha*). Trans. Am. Fish. Soc. 134:1313–1322.

Mueter, F. J., D. M. Ware, and R. M. Peterman.
2002. Spatial correlation patterns in coastal environmental variables and survival rates of salmon in the northeast Pacific Ocean. Fish. Oceanogr. 11(4):205–218.
Orsi, J. A., M. V. Sturdevant, J. M. Murphy, D. G. Mortensen, and B. L. Wing.
2000. Seasonal habitat use and early marine ecology of juvenile Pacific salmon in southeastern Alaska. N. Pac. Anad. Fish Comm. Bull. 2:111–122.
Overland, J. E., and P. J. Stabeno.
2004. Is the climate of the Bering Sea warming and affecting the ecosystem? EOS, Trans. Am. Geophys. Union. 85(33):309–312.
Parker, R. R.
1968. Marine mortality schedules of pink salmon of the Bella Coola River, Central British Columbia. J. Fish. Res. Board Can. 25:757–794.
Pearcy, W. G.
1992. Ocean ecology of the North Pacific salmonids, p. 179. Univ. Washington Press, Seattle, WA.
Peterman, R. M., B. J. Pyper, M. F. Lapointe, and M. D. Adkison.
1998. Patterns of covariation in survival rates of British Columbian and Alaskan sockeye salmon (*Oncorhynchus nerka*) stocks. Can. J. Fish. Aquat. Sci. 55:2503–2517.
Quinn, T. J., II, and R. B. Deriso.
1999. Quantitative fish dynamics, 542 p. Oxford Univ. Press, New York, NY.
Ricker, W. E.
1992. Back-calculation of fish lengths based on proportionality between scale and length increments. Can. J. Fish. Aquat. Sci. 49:1018–1026.
Ruggerone, G. T., E. V. Farley Jr., J. Nielsen, and P. Hagen.
2005. Seasonal marine growth of Bristol Bay sockeye salmon (*Oncorhynchus nerka*) in relation to competition with Asian pink salmon (*O. gorbuscha*) and the 1977 ocean regime shift. Fish. Bull. 103:355–370.
Shuntov, V. P., V. I. Radchenko, V. V. Lapko, and Y. N. Poltev.
1993. The distribution of the Pacific salmons in the Sakhalin-Kuril region at a period of anadromous migration (in Russian). J. Ichthy. Moscow 33:348–358.
Sogard, S. M.
1997. Size-selective mortality in the juvenile stage of teleost fishes: a review. Bull. Mar. Sci. 60(3):1129–1157.
Straty, R. R.
1981. Ecology and behavior of juvenile sockeye salmon (*Oncorhynchus nerka*) in Bristol Bay and the eastern Bering Sea. *In* The eastern Bering Sea shelf: oceanography and resources, vol. 2 (D. W. Hood and J. A. Calder, eds.), p. 285–320. Univ. Washington Press, Seattle, WA.
Wei, W. W. S.
1990. Time series analysis: univariate and multivariate methods, 478 p. Addison-Wesley Publ. Company, Redwood City, CA.
Willette, T. M., R. T. Cooney, and K. Hyer.
1999. Predator foraging mode shifts affecting mortality of juvenile fishes during the subartic spring bloom. Can. J. Fish. Aquat. Sci. 56:364–376.

Degeneration of postovulatory follicles in the Iberian sardine *Sardina pilchardus*: structural changes and factors affecting resorption

Konstantinos Ganias[1,2]
Cristina Nunes[2]
Yorgos Stratoudakis[2]

Email for K. Ganias: kganias@bio.auth.gr

[1] School of Biology
Laboratory of Ichthyology
Aristotle University of Thessaloniki
54 124 Thessaloniki, Greece

[2] Instituto Nacional de Investigação Agrária e das Pescas
Instituto de Investigação das Pescas e do Mar
Avenida de Brasilia s/n, 1449-006
Lisbon, Portugal

Abstract—Inaccuracy in the aging of postovulatory follicles (POFs) and in estimating the effect of temperature on the resorption rate of POFs may introduce bias in the determination of the daily spawning age classes with the daily egg production method (DEPM). To explore the above two bias problems with field-collected European pilchard (*Sardina pilchardus*, known regionally as the Iberian sardine), a method was developed in which the time elapsed from spawning (POF age) was estimated from the size of POFs (i.e., from the cross-sectional area in histological sections). The potential effect of the preservative type and embedding material on POF size and the effect of ambient water temperature on POF resorption rate are taken into account with this method. A highly significant log-linear relationship was found between POF area and age; POF area shrank by approximately 50% per day. POFs were also shown to shrink faster at higher temperatures (approximately 3% per degree), but this temperature effect is unlikely to be an important source of bias in the assignment of females to daily spawning classes. The embedding material was also shown to influence the size of POFs, the latter being significantly larger in resin than in paraffin sections. In conclusion, the size of POFs provides an indirect, reliable estimation of the time elapsed from spawning and may thus be used to test both the validity of POF staging criteria for identifying daily classes of spawners and the effect of other factors (such as temperature and laboratory processing) in applications of the DEPM to *S. pilchardus* and other fish species.

Manuscript submitted 12 May 2006 to the Scientific Editor.

Manuscript approved for publication 5 July 2006 by the Scientific Editor.

Fish. Bull. 105:131–139 (2007).

The postovulatory follicle (POF) consists of the follicular layers that remain in the ovary of fish after the release of the ovum during spawning (Saidapur, 1982). Initially, the POF is a distinct structure, but it rapidly deteriorates and becomes undetectable within a few days (Hunter and Goldberg, 1980). The study of POF degeneration is important in fishery studies because it permits the assignment of spawning females to daily classes to provide estimates of the daily fraction of spawning fish in the population (POF method, Hunter and Goldberg, 1980). The most common application of the POF method is in the daily egg production method (DEPM; Parker, 1980), where spawning fraction, together with other adult parameters, are used to estimate daily specific fecundity (Picquelle and Stauffer, 1985) for the fisheries-independent estimation of spawning biomass. A prerequisite for such applications is the existence of an accurate aging key that describes the time course of POF degeneration (Hunter and Macewicz, 1985).

In most DEPMs, the degeneration of POFs is described by a small number of histomorphological stages (see "Materials and methods" section) that are usually assumed to correspond to distinct daily classes (see review by Stratoudakis et al., 2006). However, because the process of POF degeneration is continuous and DEPM samples are usually obtained opportunistically throughout the day, the direct assignment of POF stages to daily classes of spawning fish can be imprecise. Also, morphological stages are often attributed to daily classes without prior validation and thus can lead to biased estimates of the spawning fraction. Validation is best performed in the laboratory by sacrificing female spawning fish at known time intervals after ovulation (e.g., Hunter and Goldberg, 1980; Pérez et al., 1992). Alternatively, in fish with daily spawning synchronicity, such as with the Iberian sardine *Sardina pilchardus* (also known as the European pilchard, FAO, 1985) (Bernal et al., 2001; Zwolinski et al., 2001; Ganias et al., 2003), validation can be performed indirectly through the examination of field samples collected at different hours of the day (Goldberg et al., 1984).

Another source of potential bias in the POF method is the duration of follicular degeneration, which may be temperature-dependent (Hunter and Macewicz, 1985), because the metabolic rates of poikilotherms, like fish, may be directly affected by ambient temperature. As a result, POF degeneration may be faster at higher temperatures and may lead to biased

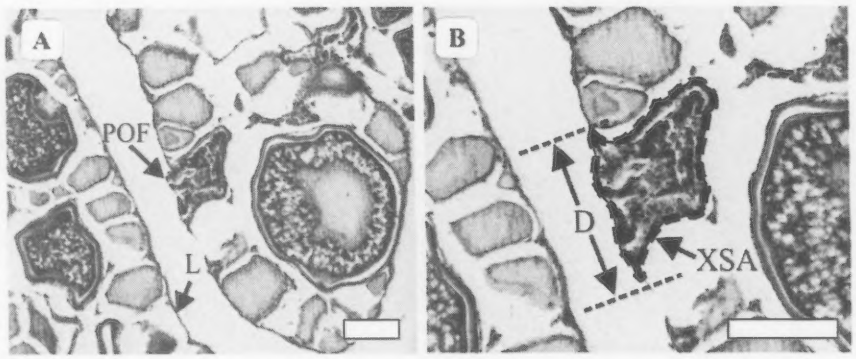

Figure 1

(**A**) Microphotograph of a postovulatory follicle (POF) situated at the epithelium of an ovarian lamella (L) in the Iberian sardine *Sardina pilchardus*; (**B**) the same POF magnified, indicating the perimeter of its cross-sectional area (XSA) and its diameter (D). Scale bar = 0.1 mm.

estimates of the spawning fraction and biomass when spatial variation in ambient water temperature is large within a survey area. This dependence can be assessed under laboratory conditions through inspection of specimens spawning under different temperature regimes (Fitzhugh and Hettler, 1995). Alternatively, the effect of temperature on POF degeneration can be studied in the wild by the examination of individuals caught at variable environmental conditions (Ganias et al., 2003; Roumillat and Brouwer, 2004).

Because of the above unresolved issues of the POF method (that can be species specific), the spawning fraction remains the most poorly estimated DEPM parameter (Hunter and Lo, 1997; Stratoudakis et al., 2006). The main objective of our study was to devise a method whereby one can test indirectly for potential sources of bias in the attribution of stage and age to the POFs of the field-collected sardine *S. pilchardus*. We used the size of POFs (cross-sectional area and diameter) as an index of POF age and, together with other histomorphological characteristics (follicle shape, state of the granulosa layer), we refined existing criteria for determining the stage and age of POFs in sardine. Then, we modeled the size of POFs as a function of POF age, ambient temperature, type of preservative, and type of embedding material. The analysis allowed us to test whether our staging criteria were valid and to examine whether temperature and laboratory processing introduced bias in the process.

Materials and methods

Adult sardines were collected off Portugal and the Gulf of Cadiz in 1997, 1999, and 2005 within the framework of DEPM surveys for the estimation of the spawning biomass of the Atlanto-Iberian sardine stock (ICES, 2004). Sampling was conducted during peak spawning months for sardine (January–March), either on board the RV *Noruega* or from the commercial purse-seine fleet. During the surveys, sea surface temperature (SST) was recorded on an extensive grid representing hydrographic casts that covered the whole sampling area during the ichthyoplankton surveys (ICES, 2004).

Fish gonads were immediately removed after capture and placed in jars either with AFA (65 parts by volume of 50% alcohol, 32 parts formalin, and 13 parts glacial acetic acid) solution [1997, 1999] or with 4% formalin [2005]). In the laboratory, ovaries were embedded either in paraffin (1997, 2005) or in resin (1999), and histological sections (paraffin: 5 μm; resin: 3 μm) were stained with hematoxylin and eosin. Histological slides were examined and scored for maturity, atresia, and presence of POFs. When POFs were detected, slides were scanned in detail to locate the largest follicle situated along the epithelium of the lamellae. These POFs were photographed with a digital camera attached to the microscope at various magnifications so that the whole follicle would fit into the microphotograph (Fig. 1A). The cross-sectional area of the whole POF (all samples) and the distance between the two extremes of the follicle on the lamella (POF diameter, paraffin samples) were measured with UTHSCSA image analysis software (Univ. Texas Health Science Center, San Antonio, Texas) (Fig. 1B). Differences in the dimensional (size, shape) and fine histological (deterioration of the granulosa layer) characteristics were used, together with existing descriptions for *Sardina* populations (Atlantic: Pérez et al., 1992; Mediterranean: Ganias et al., 2003), to describe the pattern of POF resorption.

The evolution in the shape of POFs was assessed through the allometric relationship between diameter (*D*) and cross-sectional area (*XSA*):

$$XSA = a \times D^b , \quad (1)$$

where a and b are parameters.

In case of isometry, (i.e., b=2), shrinkage is supposed to occur evenly in all dimensions, and the shape of the regressing POFs does not undergo significant changes. In any other case (b>2, or b<2), the shape is altered along resorption, and thus its intermediate phases may be used in the staging of POFs.

Existing histological criteria for the staging of sardine POFs were refined and based on two hauls from the 2005 survey that contained more than 90 histological specimens each. Given that individuals in each sample were caught at the same time and temperature, POFs in each daily cohort should have been at the same stage and have had the same age, maximizing the morphological contrast among daily classes. Furthermore, one of these hauls was performed in the evening, just before the average daily spawning hour for the Iberian sardine (20:00; Zwolinski et al., 2001; ICES, 2004) and thus provided information on the final histological state of each daily class of POFs.

After refining the staging criteria and classifying the POFs from all surveys into daily classes, we used the time of capture and daily spawning hour to estimate the exact age of POFs, i.e., the time in hours elapsed between spawning and sampling. The effect of POF age and other factors on POF cross-sectional area were tested with a generalized linear model (GLM) with an overdispersed Poisson distribution and a logarithmic link function. Apart from POF age, the effect of temperature, sampling year, and the one-way interaction of year with age were considered in the model. The significance of the relationship between POF age and size indicated whether our staging and aging criteria were accurate. Furthermore, because the laboratory processing of the ovaries differed from year to year, the year effect and its interaction with age was used to test the effect of preservation medium (AFA, formalin) and embedding material (paraffin, resin) on the size of POFs. Residual inspection plots revealed the adequacy of the fitted model.

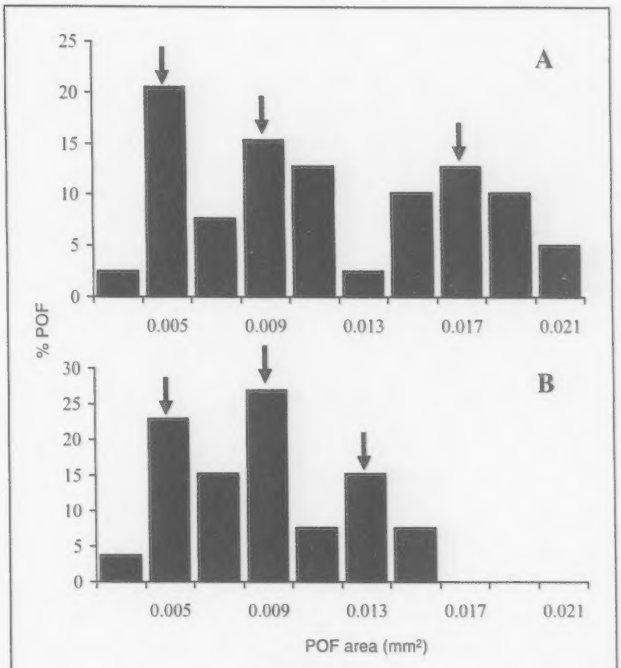

Figure 2

Frequency distribution of postovulatory follicle (POF) cross-sectional areas from two samples of the Iberian sardine *Sardina pilchardus* from the 2005 survey. (**A**) Sample collected at 12:00, n=48; (**B**) sample collected at 17:30, n=32. Arrows indicate POF size modes in each sample.

Results

A total of 249 ovaries with POFs were detected and used in our analysis (1997: 65, 1999: 104, 2005: 80). The two hauls from the 2005 survey that were used for refining POF staging criteria contained many females with POFs at various stages and sizes, facilitating the distinction between successive daily classes of spawners. The frequency distribution of POF cross-sectional areas in the two hauls displayed three size modes, which were considered to correspond to different age classes (Fig. 2). The most advanced size mode in the sample hauled at 12:00 (Fig. 2A) consisted of larger POFs compared to the POFs in the sample hauled at 17:30 (Fig. 2B). Re-examination and comparison of POF size modes in each sample showed that, apart from size, they differed in shape and in the fine histological characteristics of the follicular layers (Fig. 3). In particular, large POFs had an irregular shape and contained a large, convoluted, and thick granulosa layer (Fig. 3A). In the intermediate size mode, the shape of the follicle changed to semirectangular and the granulosa layer tended to lose its convoluted appearance and to form a single layer (Fig. 3B). Finally, in the smaller size mode, all POFs displayed a triangular shape (Fig. 3, C–E). However, more detailed examination showed that these triangular POFs could be further separated into 1) a group of slightly larger POFs with a thin layer of the granulosa (Fig. 3C), and 2) a group of very small POFs that contained only granulosa remnants in the form of residual vacuoles (Fig. 3, D and E).

POF diameter increased significantly with POF cross-sectional area (Fig. 4) and the relationship was not significantly different between the paraffin samples from 1997 and 2005 (P>0.05). The allometric coefficient b of Equation 1 differed significantly from the square

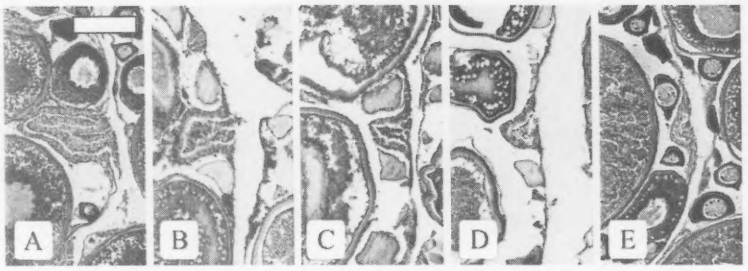

Figure 3

(**A–E**) Microphotographs of postovulatory follicles (POFs) at consecutive phases of deterioration in the Iberian sardine *Sardina pilchardus*, showing the degeneration of POF size and shape, and the state of the granulosa (same scale for all images). Scale bar = 0.1 mm.

($P<0.001$), indicating that POF resorption in the Iberian sardine is not isometric, i.e., the shape of POFs changes throughout degeneration. More specifically, b was estimated to be 1.5 (standard error=0.13), indicating that the diameter of POFs along the lamellar epithelium diminishes at a lower rate than that for the overall POF area. This allometric pattern of POF resorption confirms the shape differences along POF degeneration described above and shown in Figure 3.

The differences in the dimensional characteristics and the morphological state of the granulosa (Table 1) were used to assign POFs from all surveys into four daily classes. The reliability of these aging criteria was confirmed by a very good relationship between POF age and POF size in all years of the study (Table 2; Fig. 5A). The rate of resorption, i.e., the relationship of the slope of the POF cross-sectional area to POF age was not found to differ significantly between the three years, indicating that estimates of resorption rate are not biased either by the preservation medium (AFA or formalin) or by the embedding material (paraffin or resin). In all study years, POFs were shown to shrink exponentially with time in a way that their cross-sectional area decreased daily by almost 50% (Fig. 5A).

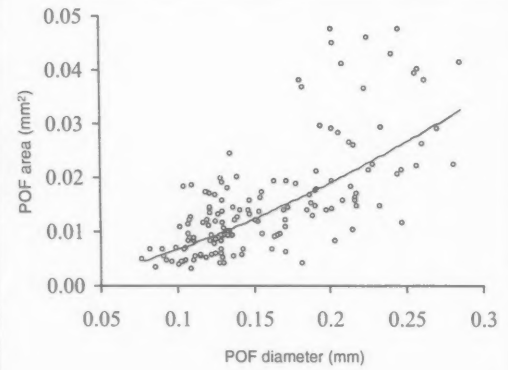

Figure 4

Allometric relationship between postovulatory follicle (POF) diameter and POF cross-sectional area for the Iberian sardine *Sardina pilchardus*.

The relationship of the intercept of the POF cross-sectional area on POF age in the GLM was similar for the two preservation mediums (no significant difference between 1997 and 2005), but differed significantly between the two embedding materials (significant difference between 1999 and the other two years) (Table 2). POF area at any given time was significantly higher for resin (Fig. 5A), indicating that processing in paraffin wax leads to a higher shrinkage of all cellular structures in the gonad. This higher rate of shrinkage was also evident by differences in the histological appearance of POFs between the two embedding materials, especially at earlier phases of degeneration (Fig. 6). The structure of POFs in resin was more compact and the cellular organization of the granulosa was clearly visible (Fig. 6A). On the other hand, in paraffin sections, the cells of the granulosa layer were hardly detectable and the follicular folds were usually detached from the surrounding theca (Fig. 6B).

During the entire survey period, sea surface temperature ranged between 11.6° and 19.3°C, and there were marked interannual differences (2005 being the coldest [mean SST: 14°C ±2.1] and 1997 being the warmest year [mean SST: 16.2°C ±2.2°]). The fitted GLM showed that ambient temperature had a significant effect on the rate of POF degradation (Table 2; Fig. 5B). However, this effect appeared to be limited because an increase of 1°C in ambient temperature accelerated the rate of POF resorption by only 3% (compared to the reduction of POF area by almost 50% per day since spawning; Table 2). This finding indicates that the maximum dif-

Table 1

Summary of dimensional (shape, cross-sectional area) and fine histological (state of the granulosa layer) characteristics of different daily classes of postovulatory follicles (POFs) in the two embedding materials (P=paraffin; R=resin) for the Iberian sardine *Sardina pilchardus*.

Daily POF class	Shape	State of granulosa	Cross-sectional area (mm^2)
<1	Irregular	Thick and looped	0.0164 ±0.0004 (P) 0.0355 ±0.0001 (R)
1–2	Rectangular	One well-formulated layer	0.0093 ±0.0002 (P) 0.0176 ±0.0005 (R)
2–3	Triangular	A thin receding layer	0.0059 ±0.0002 (P) 0.0126 ±0.0003 (R)
>3	Triangular	Resorption almost completed, some residual vacuoles	0.0042 ±0.0002 (P) 0.0072 ±0.0004 (R)

ference in POF duration for the Iberian sardine across the study years could never exceed 0.5 days, thus reducing the concerns in relation to the potential bias introduced by varying ambient temperatures in the estimation of the spawning fraction.

Discussion

The incorrect attribution of age to POFs and the effect of temperature on POF resorption rate constitute major sources of potential bias in the determination of daily spawning classes in routine applications of the DEPM (Stratoudakis et al., 2006). Our method was devised as an indirect way to test the above issues together with the effect of laboratory processing, i.e., type of preservative and embedding material. The method is based on the assumption that in species with diel spawning synchronicity, such as in *S. pilchardus*, daily classes of spawning fish have, at any given time, POFs of similar size. The first task in our analysis was to refine existing staging criteria for the POFs of *Sardina pilchardus*. This task was mainly attempted through analyzing the frequency distribution of POF cross-sectional areas in females caught simultaneously and by inspecting POFs in each size-age mode for differences in the cytomorphological characteristics.

The main cytomorphological changes during the degeneration of POFs in sardine ovaries are the gradual deterioration of the structure of the follicular layers and alterations in the dimensional characteristics (shape and size), accompanied by a decrease in their overall number in the slide. Histo-

Table 2

Summary statistics of the general linear model fitted to the postovulatory follicle cross-sectional area for the sardine *Sardina pilchardus*. All parameter estimates were tabulated at the scale of the linear predictor (the intercept for resin as an increment). SE = standard error.

Variable	Estimate	SE	*t*-value	*P*
Age (hour)	−0.021	0.0004	−46.78	<0.001
Temp (°C)	−0.030	0.012	−2.44	0.016
Intercept (paraffin)	−3.344	0.197	−16.98	<0.001
Intercept (resin)	0.710	0.027	25.90	<0.001

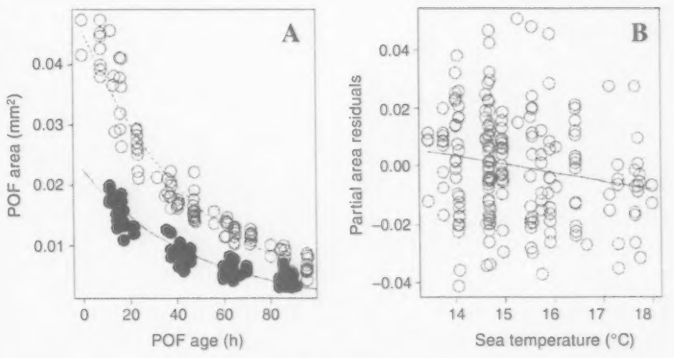

Figure 5

(**A**) Degeneration of the postovulatory follicle (POF) cross-sectional area (POF area) with time elapsed from spawning (POF age) for the Iberian sardine *Sardina pilchardus*; ○=resin ; ●=paraffin. (**B**) Effect of ambient temperature on the sardine POF cross-sectional area.

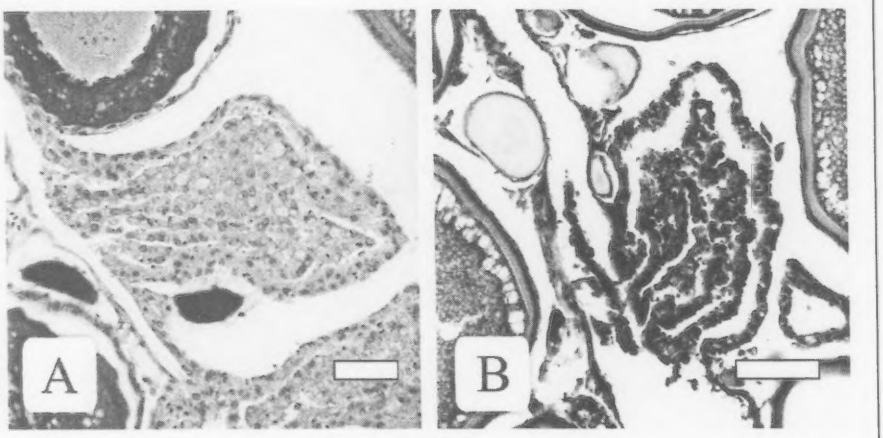

Figure 6

Microphotographs of very early-stage postovulatory follicles from the female Iberian sardine *Sardina pilchardus*, captured during the daily spawning period. Embedding materials used in the experiment were (**A**) resin; (**B**) paraffin.

logical changes in the granulosa seem to follow the general pattern of degeneration described for other populations of sardine (Japanese sardine [*Sardinops melanostictus*]: Murayama et al., 1994; Mediterranean sardine [*S. pilchardus*]: Ganias et al., 2003; Pacific sardine [*Sardinops sagax*]: Goldberg et al., 1984; South African sardine [*S. sagax*]: Akkers et al., 1996) and other fish species (see interspecific comparison in Hunter and Macewicz, 1985). The information provided in our study mostly concerns the changes in the dimensional characteristics of POFs and how these may be used in the aging of these POFs.

The evolution in the shape of POFs is allometric because the POF surface along the lamellar epithelium decreases at a lower rate than the overall area of the follicles. As a result, throughout degeneration, POFs passed consecutively from an irregular to a semirectangular and finally a triangular shape, providing a useful additional morphological criterion for determining the stage of the POF. POFs remain for the whole of their "life" on the epithelium of the lamellae, where they occupy approximately the space of an oocyte at the yolk vesicle stage (early POFs) or of a primary oocyte (late POFs). For an indeterminate spawner like sardine, where recruitment of new spawning batches of oocytes occurs continuously and directly from the oogonia, fast resorption is necessary because the aggregation of old POFs would restrict the space available for the development of new oocytes. On the other hand, late atretic pre-ovulatory follicles separate from the epithelium and concentrate medially in the lamellae—a pattern that has also been observed in other fish species such as striped mullet (*Mugil cephalus*) (McDonough et al., 2005). Late atretic follicles remain in fish ovaries for long periods, which might extend up to the next spawning season (Hunter and Lo, 1997; Miranda et al., 1999). Therefore, their separation from the lamellar epithelium possibly constitutes a mechanism for managing space availability for the newly recruited spawning batches.

The aforementioned morphological phases and the different histological characteristics of the granulosa layer were used, together with follicle size, in the aging of POFs. Four daily classes were identified, implying that full POF resorption in the Iberian sardine exceeded 72 hours. The duration of POF degeneration is variable among fish species, ranging from less than 1 day in the skipjack tuna (*Katsuwonus pelamis*) (Hunter et al., 1986) to more than 7 days in the piau-jejo (*L. taeniatus*) (Santos et al., 2005). However, there are reports of intraspecific variability in the duration of POF resorption, both under laboratory conditions (e.g., Atlantic menhaden, *Brevoortia tyrannus*; Fitzhugh and Hettler, 1995) and in the field (e.g., spotted seatrout [*Cynoscion nebulosus*]: Roumillat and Brouwer, 2004). In some cases the duration of POF resorption is underestimated because late POFs can be confused with late atretic stages (e.g., northern anchovy [*Engraulis mordax*] Hunter and Macewicz, 1980). However, given that surveys for refining the DEPM are undertaken at peak spawning months (Stratoudakis et al., 2006), POFs would so greatly outnumber atretic follicles in fish ovaries that there would be little confusion in distinguishing the two and thus would lead to a very minor bias in the duration of POF resorption. In addition, POFs in *S. pilchardus* are effectively distinguished from all types of atresia, and this distinction has been confirmed by the high degree of consistency in the scoring of postovulatory and atretic follicles by different observers. At

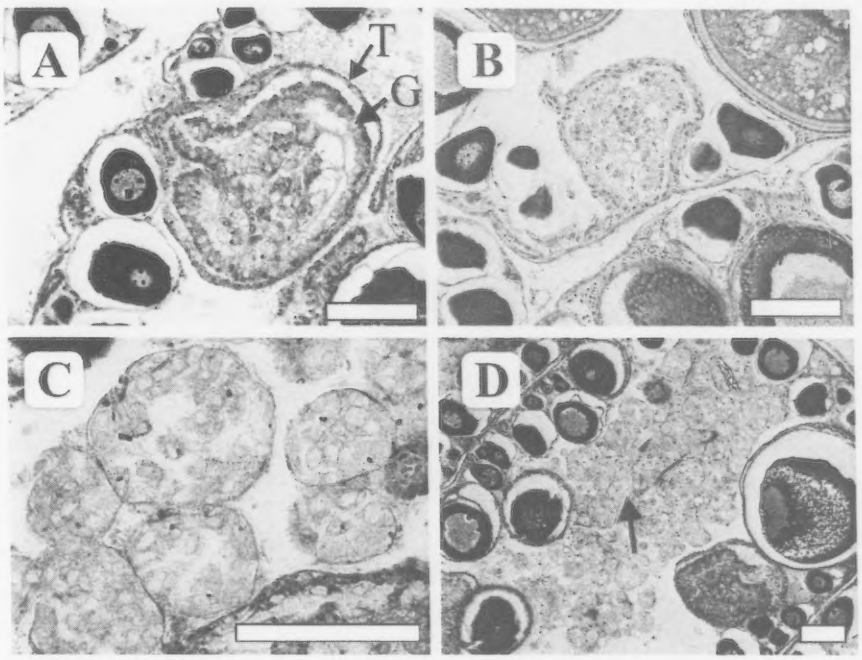

Figure 7

Consecutive stages of oocyte atresia in the Iberian sardine *Sardina pilchardus* from very new (**A**), to intermediate (**B**), to very late (**C**, **D**). T=theca layer; G=granulosa layer; arrow indicates the aggregation of very late atretic oocytes in the central area of an ovarian lamella. Scale bar: 0.1 mm.

all stages, atretic follicles constitute enclosed cellular structures (Fig. 7), whereas POFs always maintain an opening towards the ovarian lumen (Fig. 3). In addition, as previously reported, late atretic oocytes separate from the epithelium of the lamellae (Fig. 7D), whereas POFs remain on the epithelium until full resorption (Fig. 3).

Sardine POFs shrank exponentially with time, reducing to almost half their size daily. Therefore, after the exponential relationship of POF resorption with time is estimated, ages may be estimated by applying the data for the cross-sectional areas of POFs and times of capture to the model. The measurement of POF cross-sectional areas is not very time consuming and could be merged into the routine of histological analysis for DEPM analyses. Finally, the attribution of ages may be finely tuned by inspecting histomorphological characteristics, especially from specimens that lie outside the fitting curve.

Before applying the above aging procedure to fish populations, attention should be drawn to other factors that may affect POF cross-sectional area, such as the laboratory treatment of ovaries and the environmental conditions at sampling, e.g., water temperature. In our study, the use of different preservation media (AFA solution and formalin) did not appear to affect the size of the POFs. On the other hand, the embedding material significantly affected the follicle's size, for POFs in resin were almost double those in paraffin. Resin is known to maintain cellular organization in tissues slightly affected, whereas paraffin causes significant shrinkage (Casotti, 2001; Dorph-Petersen et al., 2001). Besides size, the morphological characteristics of the follicles also differed between the two materials. Although the whole POF structure remained compact in resin, follicular folds in paraffin had shrunk and were detached from the thecal layer, even in young POFs. These differences, in combination to the thinner slices that are achieved with resin, make resin a much better material for detailed histological observations. However, for accuracy in the staging of POFs, both resin and paraffin seem to provide similar results.

Water temperature may affect the rate of POF resorption in teleosts both in the field (Ganias et al., 2003; Roumillat and Brouwer, 2004) and laboratory studies (Fitzhugh and Hettler, 1995). However, this effect has never been precisely quantified and thus temperature

could never be introduced as an auxiliary factor in the aging of POFs. In the present study, temperature had a significant effect on the rate of POF resorption. This effect appeared to be limited because an increase of 1°C in ambient temperature was estimated to accelerate the rate of POF resorption by almost 3%. Nevertheless, the maximum range of 4–5°C that can be observed during sardine DEPM surveys off the Iberian Peninsula corresponds to a 12–15% maximum difference in the rate of resorption and thus to a maximum of 8 hours lag in the degree of POF degeneration. The results of this analysis imply that in each DEPM survey, temperature differences between the subareas of the survey area are not expected to introduce serious bias in the correct classification of POFs and to subsequently affect estimates of their ages. Finally, given that the late daily classes of POFs are usually excluded from the estimation of spawning fraction, the maximum effect between the most extreme temperatures is even less important (<10%).

Tests, such as described in our study, should be performed at least once for each species or population to assess bias in the criteria used to determine POF stages and ages. Moreover, the test would provide comparative information on POF resorption rates, the impact of embedding material, and the effects of temperature and other environmental parameters on the estimates. In routine DEPM analyses, the measurement of POF cross-sectional areas could increase technical work, but not necessarily the precision in the estimates of the spawning fraction because females are again broken down into spawning nights as they were with the histological staging method. However, in cases where such relationships of POF age on POF size are already available, correspondence of POF sizes to spawning nights would be much more realistic than simple histological staging, which strongly depends on the experience of the observer and the quality of the slides.

Acknowledgments

This work was supported by the program PELAGICOS (PLE/13/00) funded by the Portuguese Ministry of Science and the National Sampling Plan for DEPM surveys funded by the European Union. The contribution of K. Ganias was funded by a postdoctoral scholarship in Portugal (FCT-BPD/17488/2004). We thank four anonymous reviewers for helpful recommendations. In particular, we thank all IPIMAR (Instituto de Investigação das Pescas e do Mar) staff that contributed to the collection of DEPM samples and the histological preparations.

Literature cited

Akkers, T. R., Y. C. Melo, and W. Veith.
1996. Gonad development and spawning frequency of the South African pilchard *Sardinops sagax* during the 1993–1994 spawning season. S. Afr. J. Mar. Sci. 17:183–193.

Bernal, M., D. Borchers, L. Valdes, A. Lago de Lanzos, and S. T. Buckland.
2001. A new aging method for eggs of fish species with daily spawning synchronicity. Can. J. Fish. Aquat. Sci. 58:2330–2340.

Casotti, G.
2001. Effects of season on kidney morphology in house sparrows. J. Exp. Biol. 204:1201–1206.

Dorph-Petersen, K., J. Nyengaard, and H. Gundersen.
2001. Tissue shrinkage and unbiased stereological estimation of particle number and size. J. Microsc. 204:232–246.

Fitzhugh, R. G., and F. W. Hettler.
1995. Temperature influence on postovulatory follicle degeneration in Atlantic menhaden, *Brevoortia tyrannus*. Fish. Bull. 93:568–572.

Ganias, K., S. Somarakis, A. Machias, and A. Theodorou.
2003. Evaluation of spawning frequency in a Mediterranean sardine population (*Sardina pilchardus sardina*). Mar. Biol. 142:1169–1179.

Goldberg, S. R., V. Alarcon, and J. Alheit.
1984. Postovulatory follicle histology of the pacific sardine, *Sardinops sagax*, from Peru. Fish. Bull. 82: 443–445.

Hunter, J. R., and S. R. Goldberg.
1980. Spawning incidence and batch fecundity in northern anchovy, *Engraulis mordax*. Fish. Bull. 77:641–652.

Hunter, J. R., and N. C. H. Lo.
1997. The daily egg production method of biomass estimation: some problems and potential improvements. Ozeanografika 2:41–69.

Hunter, J. R., and B. J. Macewicz.
1980. Sexual maturity, batch fecundity, spawning frequency, and temporal pattern of spawning for the northern anchovy, *Engraulis mordax*, during the 1979 spawning season. Calif. Coop. Oceanic Fish. Invest. Rep. 21:139–149.
1985. Measurement of spawning frequency in multiple spawning fishes. *In* an egg production method for estimating spawning biomass of pelagic fish: application to the northern anchovy, *Engraulis mordax* (R. Lasker, ed.), p. 79–93. NOAA Tech. Rep. NMFS 36.

Hunter, J. R., B. J. Macewicz, and H. R. Sibert.
1986. The spawning frequency of skipjack tuna, *Katsuwonus pelamis*, from the South Pacific. Fish. Bull. 84:895–903.

ICES (International Council for the Exploration of the Sea).
2004. The DEPM estimation of spawning-stock biomass for sardine and anchovy. ICES Coop. Res. Rep., 91p.

McDonough, C. J., W. A. Roumillat, and C. A. Wenner.
2005. Sexual differentiation and gonad development in striped mullet (*Mugil cephalus* L.) from South Carolina estuaries. Fish. Bull. 103:601–619.

Miranda, A. C. L., N. Bazzoli, E. Rizzo, and Y. Sato.
1999. Ovarian follicular atresia in two teleost species: a histological and ultrastructural study. Tissue and Cell 31:480–488.

Murayama, T., M. Shirashi, and I. Aoki.
1994. Changes in ovarian development and plasma levels of sex hormones in the wild female Japanese sardine (*Sardinops melanostictus*) during the spawning period. J. Fish Biol. 45:235–245.

Parker, K.
1980. A direct method for estimating northern anchovy, *Engraulis mordax*, spawning biomass. Fish. Bull. 78:541–544.
Pérez, N., I. Figueiredo, and B. J. Macewicz.
1992. The spawning frequency of sardine, *Sardina pilchardus* (Walb.), off the Atlantic Iberian coast. Bol. Inst. Esp. Oceanogr. 8:175–189.
Picquelle, S. J., and G. Stauffer.
1985. Parameter estimation for an egg production method of anchovy biomass assessment. *In* An egg production method for estimating spawning biomass of pelagic fish: application to the northern anchovy, *Engraulis mordax* (R. Lasker, ed.), p. 7–16. NOAA Tech. Rep. NMFS 36.
Roumillat, W. A., and M. C. Brouwer.
2004. Reproductive dynamics of female spotted seatrout (*Cynoscion nebulosus*) in South Carolina. Fish. Bull. 102:473–487.
Saidapur, K. S.
1982. Structure and function of postovulatory follicles (corpora lutea) in the ovaries of nonmammalian vertebrates. Int. Rev. Cytol. 75:243–285.
Santos, B., E. Rizzo, N. Bazzoli, Y. Sato, and L. Moro.
2005. Ovarian regression and apoptosis in the South American teleost *Leporinus taeniatus* Lutken (Characiformes, Anostomidae) from the Sao Francisco Basin. J. Fish Biol. 67:1446–1459.
Stratoudakis, Y., M. Bernal, K. Ganias, and A. Uriarte.
2006. The daily egg production method (DEPM): recent advances, current applications, and future challenges. Fish and Fisheries 7:35–57.
Whitehead, P. J. P., Wongratana, T., and G. J. Nelson.
1985. Clupeid fishes of the world (Suborder Clupeoidei): an annotated and illustrated catalogue of the herrings, sardines, pilchards, sprats, shads, anchovies, and wolfherrings. FAO species catalogue, vol. 7, part 1, 303 p. FAO, Rome.
Zwolinski, J., Y. Stratoudakis, and E. Soares.
2001. Intra-annual variation in the batch fecundity of sardine off Portugal. J. Fish Biol. 58:1633–1645.

Use of genetic data to assess the uncertainty in stock assessments due to the assumed stock structure: the case of albacore (*Thunnus alalunga*) from the Atlantic Ocean

Haritz Arrizabalaga[1] (contact author)
Victoria López-Rodas[2]
Eduardo Costas[2]
Alberto González-Garcés[3]

Email address for H. Arrizabalaga: harri@pas.azti.es

[1] AZTI Tecnalia
Herrera Kaia
Portualdea z/g
20110 Pasaia (Gipuzkoa) Spain

[2] Universidad Complutense
Genética, Facultad de Veterinaria
Avda. Puerta de Hierro s/n
28080 Madrid. Spain

[3] IEO
Cabo Estay, Canido
Apdo 1552
Vigo (Pontevedra), Spain

Stock assessments can be problematic because of uncertainties associated with the data or because of simplified assumptions made when modeling biological processes (Rosenberg and Restrepo, 1995). For example, the common assumption in stock assessments that stocks are homogeneous and discrete (i.e., there is no migration between the stocks) is not necessarily true (Kell et al., 2004a, 2004b).

On the other hand, it is essential that the stock structure assumed during the assessment and management process corresponds to the real population structure of the resource. Otherwise, fishery management becomes inefficient (less productive populations may be overfished and collapse, while more productive populations may be underexploited [Allendorf et al., 1987; Begg et al., 1999]) and may affect biological attributes, such as growth, productivity, or genetic diversity (Ricker, 1981). In spite of this problem, current regulations on several fisheries are based on spatial schemes that do not necessarily reflect the real biological structure of the populations (Pawson and Jennings, 1996; Stephenson, 1999; Ward, 2000). In these cases, the results of stock assessments may be biased and, in general, an important level of uncertainty exists in stock assessments (NRC, 1994; Turner, 1998) due to the assumed stock structure.

An assessment of the magnitude of this uncertainty is important so as to increase confidence in the assessment itself. Moreover, quantifying the uncertainty allows the evaluation of the relative effect of stock structure assumptions with respect to other assumptions about biological, fishery, or modeling parameters in the assessment. Knowing the relative importance of the effect of these underlying assumptions will allow management scientists to prioritize the types of research needed to better ground the stock assessments with real information.

In this note, we suggest a way to assess uncertainty in stock assessments that is due to assumptions of stock structure. The assessment is essentially based on a sensitivity analysis conducted by testing alternative stock structure hypotheses derived from available genetic, fishery, and biological information. The method is illustrated with albacore (*Thunnus alalunga*, Bonn. 1788) in the Atlantic Ocean.

Albacore is a highly migratory species distributed between latitudes 45°N and 45°S. Studies of albacore reproduction in the Atlantic Ocean have shown different spawning periods and areas in both hemispheres (Beardsley, 1969; Koto, 1969). Shiohama (1971) and Uozumi (1996), based on Japanese longline distribution studies, described an adult concentration area in each hemisphere. These findings, along with studies of larval concentration areas (Ueyanagi, 1971), support the existence of two separate populations, one in each hemisphere. Based on these studies, it is assumed within the International Commission for the Conservation of Atlantic Tunas (ICCAT) that there are two albacore management units in the Atlantic, separated by parallel 5°N. However, various authors have suggested the possibility that albacore move between the north and south Atlantic (reviewed in González-Garcés, 1997). Moreover, the continuous spatial distribution of catches around the equator also suggests this possibility (Fig. 1).

Recent studies have shown genetic differences between north and south Atlantic albacore (Takagi et al., 2001; Arrizabalaga et al., 2004), but it is still unclear whether the limit between both populations is at latitude 5°N or somewhere else. In fact, results from Arrizabalaga et al. (2004) are not concordant with the limit at latitude 5°N because a sample from the Gulf of Guinea (1°N, 15–16°W) was genetically more like the sample from the north Atlantic than the one from the south Atlantic. This observation may indicate that either the limit between both stocks may be located farther south than that currently assumed or that

Manuscript submitted 15 June 2005
to the Scientific Editor's Office.

Manuscript approved for publication
14 December 2005 by the Scientific Editor.

Fish. 105:140–146 (2007).

there may be some interchange between individuals of both stocks. An earlier statistical comparison of blood group frequencies in albacore found in the Gulf of Guinea (lat. 0°–9°S, long. 0°–8°W), northwest Atlantic (lat. 23°–31°N, long. 60°–70°W) and middle-north Atlantic (lat. 1–34°N, long. 11°–40°W) in an earlier study (Suzuki, 1962) did not show differences between them, again indicating that the fish present in the Gulf of Guinea may belong to the northern population.

Materials and methods

Taking into account the above findings, we assessed the uncertainty in north and south Atlantic albacore stock assessments by means of a sensitivity analysis. This analysis consisted in assessing both stocks, either under alternative stock boundaries or by assuming certain migration rates between them.

Stock assessment under the assumption of alternative boundaries between stocks

Two alternative boundaries between albacore stocks were considered: at lat. 0°N and lat. 5°S. The catch-at-age within lat. 5°N–0°N and lat. 5°N–5°S was removed from the southern catch-at-age matrix and added to the northern one, by using available catch (ICCAT[1]), size, and growth information (Bard, 1981; Sarralde et al., 2002). For each boundary, abundance and fishing mortality rates were estimated separately for each stock by virtual population analysis (VPA) by using the VPA-2box, vers. 3.0 program (Porch et al., 2001). This program assesses the abundance and mortality of one or two intermixing stocks by fitting age-structured population equations to fishery data. All stock assessment options were maintained as in the ICCAT 2001 report (ICCAT[2]) and variance of estimated parameters was computed by performing 400 nonparametric bootstraps of the abundance indices.

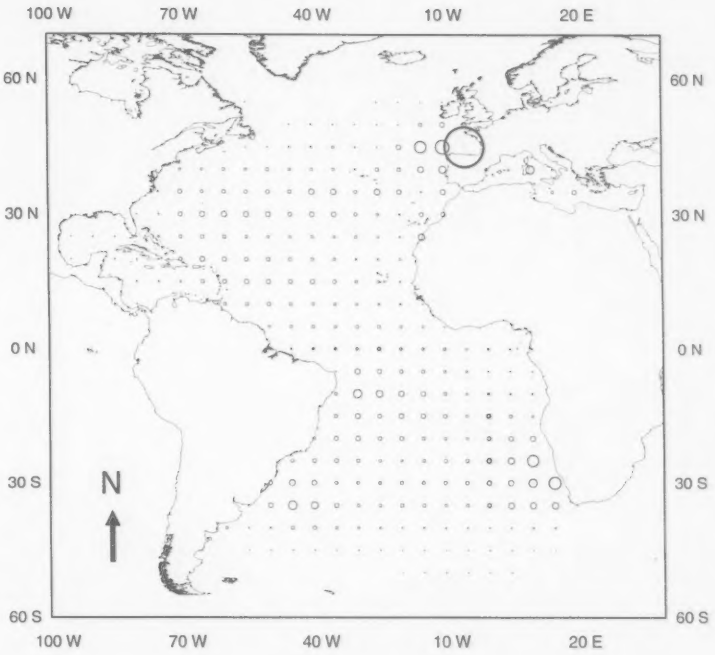

Figure 1

Spatial distribution of Atlantic and Mediterranean albacore (*Thunnus alalunga*) catches (ICCAT, 2001). The size of the circles is proportional to the square root of the total catch at each location.

Stock assessment under the assumption that there is migration between stocks

Blood group frequency data in Arrizabalaga et al. (2004) were used, with the assumption that the sample in the Gulf of Guinea was within the currently accepted range limit for both stocks, and therefore that it may be made up of a mixture of albacore belonging to the northern and southern populations. The proportion that each population would contribute to the mixture was calculated according to Cavalli-Sforza and Bodmer (1981) as

$$x_m = mx_A + (1-m)x_B, \quad (1)$$

where m = the fraction of population A in the mixture;
x_m = the allelic frequency in the mixture; and
x_A and x_B = the allelic frequencies in populations A and B, respectively.

The variance of m is given by

$$\sigma_m^2 = \frac{1}{(x_A - x_B)^2}\left[\sigma_{xm}^2 + m^2\sigma_{xA}^2 + (1-m)^2\sigma_{xB}^2\right], \quad (2)$$

where, σ_{xm}^2, σ_{xA}^2 and σ_{xB}^2 are the variances of the allelic frequencies in the mixture and populations A and B,

[1] ICCAT (International Commission for the Conservation of Atlantic Tunas). Website: http://www.iccat.int/ (accessed 31 June 2005).

[2] ICCAT (International Commission for the Conservation of Atlantic Tunas). 2001. Report of the ICCAT SCRS albacore stock assessment session (Madrid, Spain; October 9 to 15, 2000). Collect. Vol. Sci. Pap. ICCAT, 52, p. 1283–1390. International Commission for the Conservation of Atlantic Tunas, Corazón de María 8, 28002 Madrid, Spain.

respectively. When several diallelic loci are analyzed, the fraction of population A in the mixture can be computed as a weighted average:

$$\bar{m} = \frac{\sum \frac{m}{\sigma_m^2}}{\sum \frac{1}{\sigma_m^2}}. \quad (3)$$

Using three lectins, for which the positive lectin binding proportion in the Gulf of Guinea was intermediate between the proportions for the northern and southern populations as described in Arrizabalaga et al. (2004), we obtained m values shown in Table 1. The weighted mean proportion indicated that 79% of the fish present in the Gulf of Guinea would belong to the northern Atlantic population, and this result was used to formulate plausible migration hypotheses for the two stocks. The mean historical (1975–99) catch around the equator (between lat. 5°N and lat. 5°S) has been 1218 metric tons (t) per year, and therefore 974 t would belong to fish from the North Atlantic population and 244 t to fish from the South Atlantic population. In reference to the average total catch in each stock (38,960 t and 27,111 t in the northern and southern stocks, respectively), these quantities would imply that about 2.5% of the fish from the North Atlantic and 0.9% from the South Atlantic are present in the Gulf of Guinea every year. Assuming that albacore in this area are migrating from one stock to the other, these percentages would, in broad terms, represent the yearly transfer rates between stocks.

Table 1

Proportion of albacore (*Thunnus alalunga*), with a given blood group in the North Atlantic, Gulf of Guinea, and South Atlantic determined with three different lectins (Con A: *Concanavaline A*; WGA: *Triticum vulgare*; ECA: *Eritrina cristagally*; from Arrizabalaga et al., 2004) and estimated mixing proportions in the Gulf of Guinea. m=proportion of northern origin fish in the Gulf of Guinea sample; $\bar{m}$=weighted average proportion. Standard deviation of m and $\bar{m}$ is given in parentheses.

Lectin	Con A	WGA	ECA
North Atlantic	0.2500	0.4500	0.0500
Gulf of Guinea	0.2174	0.3913	0.0435
South Atlantic	0.0357	0.2857	0
m	0,8478 (0,5553)	0,6427 (0,7794)	0,8695 (1,2006)
$\bar{m}$		0,7900 (0.4232)	

Several scenarios were established and tested. Scenario number 1 reflects the above situation (2.5% and 0.9% annual migration rates from north to south and south to north, respectively). However, high variances for mixing proportions were obtained because no diagnostic loci was detected, and those precision estimates could, in fact, be overestimated because not all fish were sampled from different schools in the study of Arrizabalaga et al. (2004). This overestimation may indicate that annual migration rates vary considerably from those in scenario 1. Thus, a range of alternative migration scenarios were explored in which additional biological or fishery aspects were taken into account. Scenarios 2, 3, 7, and 8, reflected the situation in which migration occurs only in one direction (5% yearly from north to south and south to north in scenarios 2 and 3, respectively, and 10% from north to south and south to north in scenarios 7 and 8, respectively). Because no fishing effort targeting albacore exists in the equatorial area, the real migration rate may be higher than the one inferred from catches in that area. Accordingly, in scenario 4, twice the migration rates of scenario 1 (5% from north to south and 1.8% from south to north) were adopted. In scenario 5, migration was considered to be limited to the adult fraction of the stock (ages 5–8+), as size distributions in this area indicated, and finally in scenarios 6 and 9, high rates of migration (5% and 10%, respectively) in both directions were chosen. Although these scenarios are believed to be representative of the true nature of mixing between the stocks, it should be stressed that they represent only some of many different possible mixing scenarios.

All scenarios were tested by assuming an overlap migration model (fish return back to the area of origin for spawning) and using the VPA-2box program (Porch et al., 2001). No diffusive migration was considered because it is not consistent with observed genetic differentiation. Results for all scenarios were compared (in terms of spawning stock biomass trends and the small sample bias-adjusted version of the Akaike information criteria ([AICc, Hurvich and Tsai, 1995]) with the base case where no migration was assumed to occur between stocks.

Results

Stock assessment under the assumption of alternative boundaries between stocks

Best fits for northern and southern stocks were obtained by assuming different stock boundaries, at lat. 5°S and lat. 5°N, respectively. However, estimated abundance and fishing mortalities, with the assumption of any of the alternative stock limits, showed minor differences with respect to the base case (Table 2). The effect of considering the limit in lat. 0°N or in lat. 5°S was practically the same because most of the catch in the equatorial area happens in the Northern Hemisphere (between lat. 5°N and lat. 0°N). All coefficients of variation (CV) were below 15%, except for the F_{5+}^{87-99} in the south Atlantic, which were between 15% and 30%.

Table 2

Results of model fits for alternative boundaries between stocks of albacore (*Thunnus albacore*). Instantaneous fishing mortality (F) and abundance (N, in millions of individuals) estimates are averaged by age groups (subscripts) and time periods (superscripts). Corresponding mean coefficients of variation are given within parentheses. n = number of data points; p = number of estimated parameters; AICc = adjusted Akaike information criteria (Hurvich and Tsai, 1995).

	North Atlantic albacore			South Atlantic albacore		
Limit	5°N	0°N	5°S	5°N	0°N	5°S
-logL	66.68	66.74	66.52	80.85	81.98	82.20
Deviance	117.04	117.01	116.92	61.95	61.97	62.02
n	117.00	117.00	117.00	62.00	62.00	62.00
p	14.00	14.00	14.00	12.00	12.00	12.00
AICc	149.15	149.12	149.04	92.31	92.34	92.39
F_1^{75-86}	0.11 (0.2%)	0.11 (0.23%)	0.11 (0.19%)	0.00 (0.75%)	0.00 (0.86%)	0.00 (0.92%)
F_1^{87-96}	0.16 (3.87%)	0.16 (4.27%)	0.16 (3.97%)	0.01 (6.84%)	0.01 (6.87%)	0.01 (6.63%)
F_{2-4}^{75-86}	0.39 (0.19%)	0.37 (0.22%)	0.37 (0.18%)	0.11 (0.8%)	0.11 (1.02%)	0.11 (1.12%)
F_{2-4}^{87-99}	0.44 (10.44%)	0.41 (10.91%)	0.4 (9.9%)	0.2 (8.44%)	0.2 (8.95%)	0.21 (8.46%)
F_{5+}^{75-86}	0.3 (0.21%)	0.3 (0.24%)	0.3 (0.19%)	0.16 (0.86%)	0.15 (1.12%)	0.15 (1.24%)
F_{5+}^{87-99}	0.2 (11.48%)	0.21 (13.97%)	0.22 (11.17%)	0.3 (18.46%)	0.26 (29.39%)	0.25 (22.42%)
N_1^{75-86}	10.37 (0.19%)	10.6 (0.22%)	10.67 (0.18%)	8.23 (0.87%)	8.17 (1.05%)	8.16 (1.14%)
N_1^{87-96}	8.76 (3.94%)	9.02 (4.33%)	9.12 (4.16%)	7.55 (8.6%)	7.37 (8.52%)	7.3 (9%)
N_{2-4}^{75-86}	12.51 (0.15%)	12.87 (0.18%)	12.97 (0.15%)	13.64 (0.78%)	13.68 (0.99%)	13.69 (1.09%)
N_{2-4}^{87-99}	9.07 (7.97%)	9.47 (8.5%)	9.62 (7.99%)	11.96 (7.97%)	11.56 (8.14%)	11.61 (8.33%)
N_{5+}^{75-86}	3.29 (0.17%)	3.35 (0.2%)	3.36 (0.16%)	4.31 (0.83%)	4.37 (1.07%)	4.41 (1.19%)
N_{5+}^{87-99}	1.65 (7.87%)	1.81 (8.4%)	1.85 (7.67%)	3.57 (10.04%)	3.57 (10.19%)	3.59 (10.12%)

Stock assessment under the assumption of migration between stocks

Fits under several migration scenarios were more parsimonious than under the assumption of no migration between stocks (Table 3). Scenarios 1 (p_{NS}=0.025, p_{SN}=0.009), 2 (p_{NS}=0.05, p_{SN}=0), 3 (p_{NS}=0, p_{SN}=0.05), 4 (p_{NS}=0.05, p_{SN}=0.018), 6 (p_{NS}=0.05, p_{SN}=0.05), and 7 (p_{NS}=0.1, p_{SN}=0) showed lower AICc values than in the base case (BC).

Spawning stock biomass (SSB) values and trends under scenarios 1, 2, 3, 4, 5, 6, and 7 were similar to the ones observed in the base case, especially in the second half of the study period (except for the SSB of the southern stock over the last two years, which showed more variability, Fig. 2). In contrast, scenarios 8 and 9 showed a very different pattern in the last half of the series. In the north Atlantic, after the decline of the SSB during the beginning of the 1980s, the recovery was much more effective under these two scenarios, reaching higher values at the end of the 1990s than in the 1970s. Meanwhile, the SSB values for the southern stock were only slightly lower than those under the assumption of no migration, and under scenario 9 they were higher than in the base case over the last two years (Fig. 2).

Table 3

Considered overlap migration scenarios and associated results of model fits for albacore (*Thunnus alalunga*). n = 179; p = 25; AICc = adjusted Akaike information criteria (Hurvich and Tsai, 1995); BC = base case; p_{NS} = annual migration rate from north to south; p_{SN} = annual migration rate from south to north.

Scenario	p_{NS}	p_{SN}	Age range (yr)	AICc
BC	0	0	1–8+	18.76
1	0.025	0.009	1–8+	13.74
2	0.05	0	1–8+	15.12
3	0	0.05	1–8+	18.03
4	0.05	0.018	1–8+	13.10
5	0.05	0.018	5–8+	19.41
6	0.05	0.05	1–8+	17.67
7	0.1	0	1–8+	12.77
8	0	0.1	1–8+	37.58
9	0.1	0.1	1–8+	46.81

Discussion

The method used to assess the uncertainty in the stock assessments that is due to the assumed stock structure

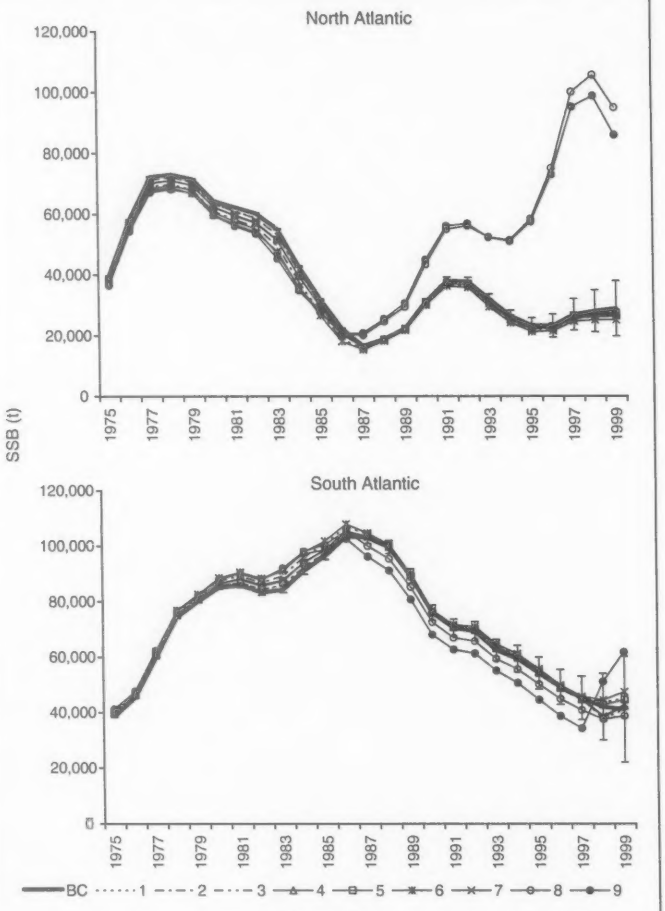

Figure 2

Historical evolution of north and south Atlantic albacore (*Thunnus alalunga*) spawning stock biomass (SSB) estimated under different overlapping migration scenarios (see Table 3 for details). Vertical bars indicate 95% confidence intervals for the spawning stock biomass in the base case. BC = base case.

is based on a simple sensitivity analysis conducted by testing alternative stock structure hypotheses. When plausible hypotheses are generated from the cumulated knowledge on the biology and fisheries of the species, the effect of these hypotheses on the assessment results can be studied. However, it is also important to consider a range of alternative hypotheses so that they produce significantly different results in the assessment, in reference to the base case. The wide range of results allows us to discern the level of migration that is of concern for assessment purposes and shows the level of migration that is not likely to be realistic, given the available catch and effort data. However, several other sources of uncertainty should be taken into account at this stage. The analysis could be extended to future biomass projections under different management strategies in order to indicate those management strategies that are more robust to violation of stock structure assumptions. This kind of study should run parallel to other studies where additional sources of uncertainty (e.g., in biological parameters or fishery data) are quantified because this approach would show their relative importance so that research could be prioritized with the goal of providing improved information on stock status.

In the case of Atlantic albacore, recent genetic studies indicate that, either the limit between both popula-

tions is not at lat. 5°N, but farther south, or that some amount of migration exists between them. Because no diagnostic loci were found by Arrizabalaga et al. (2004), the estimated proportions from each stock in the Gulf of Guinea sample could not be precisely determined and the true nature of mixing between north and south Atlantic albacore has yet to be fully determined. In spite of this uncertainty, the present exercise has made it possible to explore the response of biomass trends in different plausible discrete-stock scenarios and stock-mixing scenarios.

Although it is not possible to determine where the real limit lies between populations, we can conclude from our knowledge about the current low level of reported equatorial catch and the size structure of this catch, that assuming the population limit is 0°N or 5°S, instead of 5°N (as currently assumed), our perception about the stock status does not change significantly. On the other hand, several migration scenarios fitted the observed catch-at-age and abundance indices better than the scenario of no migration. In all these scenarios, SSB trends were very similar and values did not differ significantly from the ones in the base case; therefore it can be concluded that, although some rate of migration between stocks likely exists, the perception that we have about stock status, assuming there is no migration, is quite realistic. In other words, uncertainty in northern and southern Atlantic albacore stock assessments associated with the assumed stock structure does not seem to be important, given current biological knowledge and fishery data.

The highest variations in SSB were observed for northern Atlantic albacore in scenarios with high migration rates from south to north, showing high levels of SSB at the end of the study period. However, the observed difference in SSB levels with respect to the base case in the South Atlantic was not that pronounced, showing that northern Atlantic albacore biomass is more sensitive to biomass input from the south than vice versa. This result occurs because the minimum level of SSB in the north Atlantic in 1987 coincides in time with the maximum SSB in the southern stock, which is an order of magnitude higher. In this case, a migration rate of 10% from south to north would imply the input of approximately half the biomass present in the north at that moment, leading to a more rapid recovery of historic levels than under the null migration assumption. However, the existence of such important migration rates from south to north seems unlikely given the observed catch-at-age and abundance indices for both stocks.

The present analysis allows for the increase in confidence levels regarding stock assessment results for northern and southern Atlantic albacore obtained within ICCAT, assuming that stocks are separated at lat. 5°N and that there is no migration between them. This information is essential in order that the catch- and effort-related management measures that are in force for Atlantic albacore remain effective. Nevertheless, additional hypotheses, such as migration between North Atlantic and Mediterranean albacore, or between South Atlantic and Indian Ocean albacore, should be investigated further as future research findings are made available. Moreover, it should be noted that migration between stocks could vary among years, and a yearly based assessment of genetic mixture, based on DNA analysis, would be more useful for quantitative stock assessments.

Acknowledgments

We are grateful to Clay Porch for his help in the use of VPA-2box and statistical considerations regarding the interpretation of the results. Mauricio Ortiz, Hilario Murua, Dorleta Garcia, two anonymous referees, and the scientific editor also made helpful suggestions. We are also grateful to the Spanish "Comisión de Ciencia y Tecnología" (CICYT) and the "Departamento de Agricultura y Pesca" of the Basque Government for the funding of the MAR98-0233 and RP2002023 research projects, respectively.

Literature cited

Allendorf, F. W., N. Ryman, and F. M. Utter.
1987. Genetics and fishery management: past, present and future. *In* Population genetics and fishery management (N. Ryman and F. M. Utter, eds.), p. 1–19. Univ. Washington Press, Seattle and London.

Arrizabalaga, H., E. Costas, J. Juste, A. González-Garcés, B. Nieto, and V. López-Rodas.
2004. Population structure of albacore *Thunnus alalunga* inferred from blood groups and tag-recapture analyses. Mar. Ecol. Prog. Ser. 282:245–252.

Bard, F. X.
1981. Atlantic albacore tuna (*Thunnus alalunga* Bonnaterre 1788). From population dynamics to demographic strategy. Ph.D. diss, 333 p. [In French.] Universite Pierre et Marie Curie, Paris, France.

Beardsley, G. L.
1969. Proposed migrations for albacore, *Thunnus alalunga*, in the Atlantic Ocean. Trans. Am. Fish. Soc. 98:589–598.

Begg, G. A., K. D. Friedland, and J. B. Pearce.
1999. Stock identification and its role in stock assessment and fisheries management: an overview. Fish. Res. 43:1–8.

Cavalli-Sforza, L. L., and W. F. Bodmer.
1981. The genetics of human populations, 942 p. Freeman and Com., San Francisco, CA.

González-Garcés, A.
1997. Contribution to knowledge about north Atlantic albacore (*Thunnus alalunga*, Bonn. 1788) population dynamics. Ph.D. diss., 200 p. [In Spanish.] Universidad Complutense de Madrid, Ciudad Universitaria, Madrid, Spain.

Hurvich, C. M., and C. L. Tsai.
1995. Relative rates of convergence for efficient model selection criteria in linear regression. Biometrika 35:418–425.

Kell, L. T., W. W. Crozier, and C. M. Legault.
2004a. Mixed and multi-stock fisheries: Introduction. ICES J. Mar. Sci. 61:1330.

Kell, L. T., R. Scott, and E. Hunter.
2004b. Implications for current management advice for North Sea plaice: Part I. Migration between the North Sea and English Channel. J. Sea Res. 51:287–299.

Koto, T.
1969. Studies on the albacore—XIV. Distribution and movement of the albacore in the Indian and the Atlantic Oceans based on the catch statistics of Japanese tuna longline fishery. Bull. Far Seas Fish. Res. Lab.. 1:115–129.

NRC (National Research Council).
1994. An assessment of Atlantic bluefin tuna, 166 p. National Academy Press, Washingon D.C.

Pawson, M. G., and S. Jennings.
1996. A critique of methods for stock identification in marine capture fisheries. Fish. Res. 25:203–217.

Porch, C. E., S. C. Turner, and J. E. Powers.
2001. Virtual population analyses of Atlantic bluefin tuna with alternative models of transatlantic migration: 1970–1997. Collect. Vol. Sci. Pap. ICCAT 52:1022–1045.

Ricker, W. E.
1981. Changes in the average size and average age of Pacific salmon. Can. J. Fish. Aquat. Sci. 38: 1636–1656.

Rosenberg, A. A., and V. R. Restrepo.
1995. Uncertainty and risk evaluation in stock assessment advice for U.S. marine fisheries. Can. J. Fish. Aquat. Sci. 51: 2715–2720.

Sarralde, R., F. X. Bard, and A. Hervé.
2002. Update of tropical east Atlantic albacore (*Thunnus alalunga*) purse seine bycatch information. [In Spanish.] Collect. Vol. Sci. Pap. ICCAT 55:245–250.

Shiohama, T.
1971. Studies on measuring changes in the character of the fishing effort of the tuna longline fishery. Concentrations of the fishing effort to particular areas and species in the japanese Atlantic fishery. Bull. Far Seas Fish. Res. Lab. 5:107–130.

Stephenson, R. L.
1999. Stock complexity in fisheries management: a perspective of emerging issues related to population subunits. Fish. Res. 43:247–249.

Suzuki, A.
1962. Serological studies of the races of tuna. VI. Bigeye-3 antigen occurred in the albacore. Rep. Nankai Reg. Fish. Res. Lab. 16:67–70.

Takagi, M., T. Okamura, S. Chow, and N. Taniguchi.
2001. Preliminary study of albacore (*Thunnus alalunga*) stock identification inferred from microsatellite DNA analysis. Fish. Bull. 99:697–701.

Turner, S. C.
1998. Stock structure and mixing. Collect. Vol. Sci. Pap. ICCAT 50:17–23.

Ueyanagi, S.
1971. Larval distribution of tunas and billfishes in the Atlantic Ocean. FAO Fisheries report 71:297–305.

Uozumi, Y.
1996. A historical review of Japanese longline fishery and albacore catch in the Atlanic ocean. Collect. Vol. Sci. Pap. ICCAT 43:261–268.

Ward, R. D.
2000. Genetics in fisheries management. Hydrobiologia 420:191–201.

New information from fish diets on the importance of glassy flying squid (*Hyaloteuthis pelagica*) (Teuthoidea: Ommastrephidae) in the epipelagic cephalopod community of the tropical Atlantic Ocean

Yves Cherel (contact author)[1]
Richard Sabatié[2]
Michel Potier[3]
Francis Marsac[4]
Frédéric Ménard[4]

[1] Centre d'Etudes Biologiques de Chizé
UPR 1934 du Centre National de la Recherche Scientifique BP 14
79360 Villiers-en-Bois, France
Email address for Y. Cherel: cherel@cebc.cnrs.fr

[2] Pôle Halieutique
Laboratoire d'Ecologie Halieutique, Agrocampus-Rennes
65 rue de Saint Brieuc
35042 Rennes Cedex, France

[3] Institut de Recherche pour le Développement
Centre de La Réunion
UR 109 Thetis, BP 172
97492 Sainte Clotilde Cedex, Isle de La Réunion, France

[4] Institut de Recherche pour le Développement
Centre de Recherche Halieutique Méditerranéenne et Tropicale
UR 109 Thetis, BP 171
34203 Sète Cedex, France

Squids of the family Ommastrephidae are a vital part of marine food webs and support major fisheries around the world. They are widely distributed in the open ocean, where they are among the most abundant in number and biomass of nektonic epipelagic organisms. In turn, seven of the 11 genera of this family (*Dosidicus, Illex, Martialia, Nototodarus, Ommastrephes, Sthenoteuthis,* and *Todarodes*) are heavily preyed upon by top marine predators, i.e., birds, mammals, and fish, and currently support fisheries in both neritic and oceanic waters (Roper and Sweeney, 1984; Rodhouse, 1997). Their commercial importance has made the large ommastrephids the target of many scientific investigations and their biology is consequently reasonably well-known (Nigmatullin et al., 2001; Zuyev et al., 2002; Bower and Ichii, 2005). In contrast, much less information is available on the biology and ecological role of the smaller, unexploited species of ommastrephids (e.g., *Eucleoteuthis, Hyaloteuthis, Ornithoteuthis,* and *Todaropsis*).

Hyaloteuthis pelagica (Bosc, 1802), the glassy flying squid, is the smallest ommastrephid, reaching a maximum mantle length of 90 mm (Nesis, 1987). It appears to be an epipelagic species that is probably distributed in all tropical and subtropical oceans (Nesis and Nigmatullin, 1979; Wormuth, 1998). *Hyaloteuthis pelagica* is rarely captured, but was caught in large numbers during a cruise off Brazil, where it was the dominant ommastrephid captured in nets (Warneke-Cremer, 1986). Almost nothing is known about its trophic relationships, either as prey or predator (Nesis and Nigmatullin, 1979). Numerous remains of *H. pelagica*—from a few intact squids to a fairly large number of accumulated beaks—were found in the stomachs of large predatory fishes during research cruises in the central Atlantic Ocean in autumn 2000. In this note, we describe the importance of *H. pelagica* in fish diets, thus adding new information about the abundance and trophic role of a poorly known ommastrephid species.

Materials and methods

Fieldwork was carried out in the central Atlantic Ocean during three cruises of the Japanese RV *Shoyo Maru* in October–December 2000 (Fig. 1). Cruise I took place in temperate waters of the north equatorial current (between 8–21°N and 42–29°W) and cruises II and III took place in tropical waters of the south equatorial divergence (between 2N–10°S and 13–26°W, and between 7–9°S and 9–24°W). Cruises were a part of the Bigeye Tuna Year Program (BETYP) that was undertaken under the auspices of the International Commission for the Conservation of Atlantic Tunas (ICCAT). The purpose of the cruises was to tag live tunas caught by longlines in order to investigate their migration pattern and behavior in relation to fish aggregating devices.

Fish were measured (eye-fork length for billfishes and fork length for other species) and dissected onboard. In the laboratory, each fish stomach was thawed, opened, and both accumulated (cephalopod beaks with no flesh attached) and fresh items were sorted. Fresh remains were divided into broad prey classes (fish, cephalopods, crustaceans, and others), and weighed to calculate their proportion by mass in the diet. Identification of cephalopod prey relied on the external morphological features of either intact specimens or beaks. Beaks

Manuscript submitted 2 March 2006 to the Scientific Editor's Office.
Manuscript approved for publication 24 May 2006 by the Scientific Editor.
Fish. Bull. 105:147–152 (2007).

(both lower and upper) were identified by reference to features given by Clarke (1986) and by comparison with material held in our own reference collection.

Well-preserved specimens of *H. pelagica* were identified from the special arrangement of luminous spots on the ventral side of the mantle (Nesis, 1987). Beaks from those specimens identified from the spots (reference beaks) allowed us to identify almost all ommastrephid beaks found in fish samples as belonging to *H. pelagica*. Importantly, wings of the lower beaks darkened at a small size, thus precluding misidentification with beaks of other ommastrephid species that darken at larger sizes, e.g., *Sthenoteuthis pteropus* (Clarke, 1986). Lower rostral length (LRL) of beaks was measured to 0.1 mm with a vernier caliper and the allometric equations given by Clarke (1986) were used to estimate dorsal mantle length (ML) and whole wet mass (M) from LRL. Specimens of *H. pelagica* were assumed to be adults at 46 mm ML and larger (Dunning and Brandt, 1985).

Dietary data are presented by using two calculation techniques, namely the frequency of occurrence and the percentage by number of each prey type. Data were statistically analyzed by using SYSTAT 9 (SPSS, Chicago, IL). Values given are means (±SD).

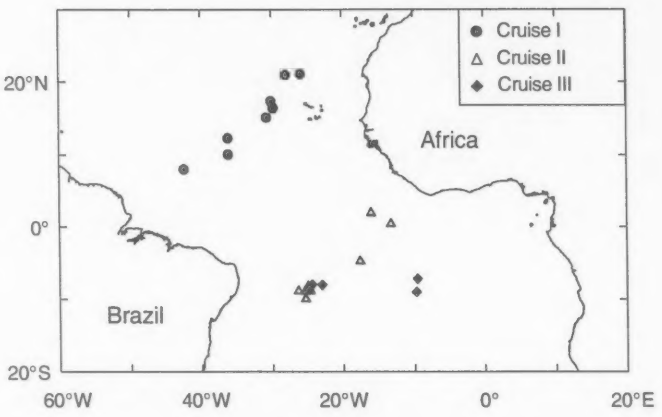

Figure 1

Locations of longline sets carried out in the central Atlantic Ocean during three cruises of the RV *Shoyo Maru* between October and December 2000.

Results

Most (97%) of the fish caught on longlines belonged to 10 different species of large oceanic predatory fishes, including longnose lancetfish (*Alepisaurus ferox*), four scombrids (wahoo [*Acanthocybium solandri*], albacore [*Thunnus alalunga*], yellowfin tuna [*T. albacares*], and bigeye tuna [*T. obesus*]), swordfish (*Xiphias gladius*), and four istiophorids (sailfish [*Istiophorus albicans*], blue marlin [*Makaira nigricans*], and white marlin [*Tetrapturus albidus*], and longbill spearfish [*T. pfluegeri*]). Most of the fish (93%) contained fresh remains in their stomachs. Fish prey dominated the diet by mass (>50%) of eight predator species (Table 1). Fish and cephalopod items were almost equally important in the diet of white marlin, whereas fish, cephalopods, and crustaceans were the main food sources of albacore.

Cephalopods amounted to slightly more than 50% of the diet by mass in one fish species (white marlin) only. They were an important prey class (>10%) in five other species and were still a minor, but significant (≥5–10%), portion of the food of the four remaining fishes (Table 1). Overall, cephalopods (both fresh and accumulated items) were found in most of the individuals (76%) and a total of 2701 cephalopod beaks were identified from the stomach of 105 fish. *Hyaloteuthis pelagica* was by far the most important cephalopod prey of the community of large predatory fishes, amounting to more than 50% of the total number of cephalopods (up to 93%) in six species (Table 2). Indeed, it was found to be the main cephalopod prey in all the fishes, except in bigeye tuna and lancetfish where it ranked second and third, respectively. *Hyaloteuthis pelagica* was much more abundant in the diet of fish caught in tropical waters (cruises II and III) than in the diet of individuals fished in temperate waters (cruise I) (n=1937 and 15 beaks, respectively).

Other important cephalopod prey (>10% by number) included the small onychoteuthid squid *Walvisteuthis* (= *Onykia*) *rancureli* in the diets of bigeye tuna and albacore, and the pelagic octopuses *Japetella diaphana* and common blanket octopus *Tremoctopus violaceus* in those of yellowfin and bigeye tunas, respectively. Three other ommastrephid squids were identified from fish stomach contents; they were two rare prey species, the Atlantic bird squid *Ornithoteuthis antillarum* and the orangeback flying squid *Sthenoteuthis pteropus*, as well as the bait, Argentine shortfin squid *Illex argentinus*.

All fishes fed upon the same size range of *H. pelagica*, including both juvenile and adult squids (Table 3, Fig. 2), but overall they segregated by preying on squids of different sizes (ANOVA on LRL, $F_{(6,907)}$=16.36, P<0.0001). *Post hoc* Tukey multiple comparison tests showed three groups of predators: yellowfin tuna and sailfish fed on smaller squids (51 mm and 3.9 g on average), bigeye tuna, white marlin, and longbill spearfish fed on larger individuals (60, 59, and 58 mm; 6.6, 6.2, and 5.7 g, respectively), and albacore and blue marlin fed on squids of intermediate sizes (54 mm and 4.7–4.8 g). Accordingly, bigeye tuna, white marlin, and longbill spearfish fed more on adult squids (89%, 92%, and 93% of the total number of *H. pelagica*, respectively) than did albacore and blue marlin (85% and 77%) and yellowfin tuna and sailfish (62% and 73%) (Table 3).

Table 1

Frequency of occurrence (FO) and proportion by mass (%) of four broad prey classes (fish, cephalopods, crustaceans, and others) recovered from the stomach contents of 10 species of predatory fishes sampled between October and December 2000 in the central Atlantic Ocean.

Species	No. of specimens	Length ±SD (cm)	No. of stomachs with fresh remains	Fish		Cephalopods		Crustaceans		Others	
				FO	Mass	FO	Mass	FO	Mass	FO	Mass
Alepisauridae											
Alepisaurus ferox	29	120 ±15	26	18	67.8	9	9.8	19	13.6	9	8.8
Scombridae											
Acanthocybium solandri	7	136 ±18	7	6	63.5	2	7.5	0	0.0	6	29.0
Thunnus alalunga	16	109 ±6	15	11	31.5	9	31.7	15	29.7	5	7.1
Thunnus albacares	6	147 ±7	6	6	77.2	5	5.8	5	12.1	2	4.9
Thunnus obesus	24	107 ±22	24	24	77.0	17	20.2	13	2.7	2	0.1
Xiphiidae											
Xiphias gladius	8	126 ±32	6	6	89.3	3	10.3	2	0.4	0	0.0
Isiophoridae											
Istiophorus albicans	4	152 ±13	4	3	85.7	4	13.1	0	0.0	1	1.2
Makaira nigricans	8	180 ±25	5	3	95.2	2	4.7	0	0.0	3	0.2
Tetrapturus albidus	7	130 ±10	7	7	48.2	6	51.2	0	0.0	4	0.6
Tetrapturus pfluegeri	30	143 ±6	29	25	86.8	23	13.0	4	0.0	4	0.1

Table 2

Number (and %composition by number) of the main cephalopod prey species found in the diet of Scombridae and Istiophoridae from the tropical Atlantic Ocean between October and December 2000. Only prey species contributing more than 5% by number are reported. *n* = number of stomachs examined.

Species	*Thunnus alalunga* *n=15*	*Thunnus albacares* *n=5*	*Thunnus obesus* *n=19*	*Istiophorus albicans* *n=4*	*Makaira nigricans* *n=5*	*Tetrapturus albidus* *n=7*	*Tetrapturus pfluegeri* *n=29*
Ommastrephidae							
Hyaloteuthis pelagica	194 (51.5)	133 (61.6)	45 (19.8)	78 (80.4)	101 (75.4)	481 (92.9)	897 (85.8)
Onychoteuthidae							
Onychoteuthis banksi	21 (5.6)	4 (1.9)	2 (0.9)	0 (0.0)	2 (1.5)	1 (0.2)	12 (1.1)
Walvisteuthis rancureli	63 (16.7)	5 (2.3)	62 (27.3)	1 (1.0)	9 (6.7)	0 (0.0)	7 (0.7)
Grimalditeuthidae							
Grimalditeuthis bonplandi	4 (1.1)	2 (0.9)	17 (7.5)	0 (0.0)	0 (0.0)	2 (0.4)	0 (0.0)
Tremoctopodidae							
Tremoctopus violaceus	3 (0.8)	35 (16.2)	3 (1.3)	8 (8.2)	7 (5.2)	11 (2.1)	19 (1.8)
Argonautidae							
Argonauta argo	6 (1.6)	15 (6.9)	2 (0.9)	8 (8.2)	4 (3.0)	21 (4.1)	82 (7.8)
Bolitaneidae							
Japetella diaphana	34 (9.0)	5 (2.3)	28 (12.3)	0 (0.0)	1 (0.7)	0 (0.0)	7 (0.7)
Other cephalopods	52 (13.8)	17 (7.9)	68 (30.0)	2 (2.1)	10 (7.5)	2 (0.4)	21 (2.0)
Total	377 (100.0)	216 (100.0)	227 (100.0)	97 (100.0)	134 (100.0)	518 (100.0)	1045 (100.0)

Discussion

This study is the first, to our knowledge, to point out the abundance of *H. pelagica* in the tropical pelagic ecosystem. In the central Atlantic Ocean, *H. pelagica* was found as a prey of all the fish species that were investigated. When looking at both the proportion by mass of cephalopods in the fish diet (Table 1) and the proportion by number of *H. pelagica* in their cephalopod diet (Table 2), *H. pelagica* was a major prey of white

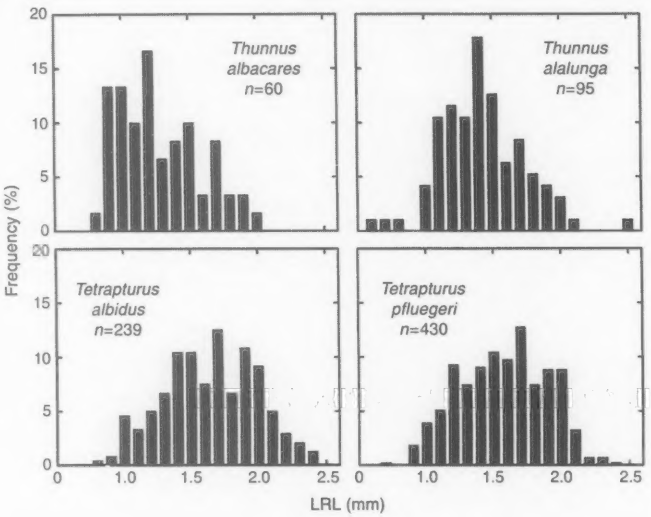

Figure 2

Frequency distribution of lower rostral lengths (LRL) (mm) of *Hyaloteuthis pelagica* glassy flying squid eaten by yellowfin tuna (*Thunnus albacares*), albacore (*Thunnus alalunga*), white marlin (*Tetrapturus albidus*), and longbill spearfish (*Tetrapturus pfluegeri*) in the tropical Atlantic Ocean.

Table 3

Characteristics of *Hyaloteuthis pelagica* eaten by large predatory fish from the tropical Atlantic Ocean. Values given are means (±SD) with ranges in parentheses. LRL=lower rostral length, ML=mantle length, M=body mass.

Species	Number (*n*)	Measured LRL (mm)	Estimated ML (mm)	Estimated M (g)	Adults (ML >46 mm) (%)
Alepisauridae					
Alepisaurus ferox	2	1.6–1.8	60–64	6.1–7.3	100.0
Scombridae					
Acanthocybium solandri	3	2.1 ±0.2 (1.9–2.3)	71 ±5 (67–77)	9.7 ±2.0 (8.5–12.0)	100.0
Thunnus alalunga	95	1.4 ±0.3 (0.5–2.5)	54 ±8 (34–81)	4.7 ±2.1 (0.8–14.0)	85.2
Thunnus albacares	60	1.2 ±0.3 (0.8–1.9)	51 ±7 (39–67)	3.9 ±1.8 (1.5–8.5)	61.7
Thunnus obesus	18	1.6 ±0.5 (0.8–2.3)	60 ±11 (39–77)	6.6 ±3.2 (1.5–12.0)	88.9
Xiphiidae					
Xiphias gladius	5	1.9 ±0.2 (1.6–2.2)	67 ±6 (59–75)	8.4 ±2.0 (5.9–11.3)	100.0
Istiophoridae					
Istiophorus albicans	33	1.3 ±0.2 (0.9–1.8)	51 ±5 (42–64)	3.9 ±1.3 (2.0–7.3)	72.7
Makaira nigricans	39	1.4 ±0.4 (0.5–2.0)	54 ±9 (34–69)	4.8 ±2.2 (0.8–9.2)	76.9
Tetrapturus albidus	239	1.6 ±0.3 (0.7–2.3)	59 ±8 (38–78)	6.2 ±2.4 (1.4–12.4)	92.1
Tetrapturus pfluegeri	430	1.5 ±0.3 (0.7–2.4)	58 ±8 (37–79)	5.7 ±2.2 (1.2–12.8)	92.6

marlin, a common food item of albacore, longbill spearfish, and sailfish and a minor prey for the remaining fishes. However, more information is needed to assess the spatiotemporal importance of *H. pelagica* in the fish community, because 1) all fish were caught during a relatively short period of time, and 2) a medium to low number of specimens per fish species were collected during the cruises.

The ommastrephid *Sthenoteuthis pteropus*, usually abundant in the tropical Atlantic Ocean, was surprisingly absent in fish diets in the present study. Two hypotheses may account for that apparent absence: either fish selected *H. pelagica* rather than *S. pteropus*, or *S. pteropus* was not an important and available nektonic prey organism at the time of sampling. The latter hypothesis is likely to be the best explanation because tunas and billfishes are known to be opportunistic predators. Moreover, the geographical distribution of *S. pteropus* shows that juvenile squids are not abundant in the central Atlantic Ocean where cruises of the present investigation took place (Warneke-Cremer, 1986; Zuev and Nikolsky, 1993). Instead, our study underlines the numerical importance of *H. pelagica*, together with *O. antillarum* (Vaske et al., 2004), in the area, and our numbers are in agreement with the large catches of the species with nets between 20°S and 31°S off Brazil during 1966 and 1968 (Warneke-Cremer, 1986).

The present study documents the largest number of *H. pelagica* ever reported, thus emphasizing the usefulness of marine predators to gain valuable information on the biology of their prey (Clarke, 1980; Cherel et al., 2004). Other ommastrephid species are important food items of various fishes, seabirds, and marine mammals (Clarke, 1996; Cherel and Klages, 1998), but *H. pelagica* was previously found only as a rare prey of squids (Shchetinnikov, 1992), fishes (Matthews et al., 1977; Okutani and Tsukada, 1988; Vaske et al., 2004), birds (Harrison et al., 1983), and cetaceans (Robertson and Chivers, 1997). In the same way, the squid *Grimalditeuthis bonplandi* and the pelagic octopods *T. violaceus* and *J. diaphana* were rarely found in significant numbers in the diet of cephalopod predators (Okutani and Tsukada, 1988; Le Corre et al., 2003), but we commonly found them as fish prey. Consequently, our study shows that these poorly known cephalopods, together with adults of *H. pelagica*, constitute a link in the transfer of energy from lower trophic levels (most likely mesozooplankton) to higher trophic levels (including tunas and billfishes) in the tropical Atlantic Ocean).

Acknowledgments

The authors thank P. Borsa, P. Dewals, and O. Maury for their help to collect scientific samples on board, and the captain and crew of the RV *Shoyo-Maru*.

Literature cited

Bower, J. R., and T. Ichii.
2005. The red flying squid (*Ommastrephes bartramii*): a review of recent research and the fishery in Japan. Fish. Res. 76:39–55.

Cherel, Y., G. Duhamel, and N. Gasco.
2004. Cephalopod fauna of subantarctic islands: new information from predators. Mar. Ecol. Prog. Ser. 266:143–156.

Cherel., Y., and N. Klages.
1998. A review of the food of albatrosses. *In* Albatross biology and conservation (G. Robertson, and R. Gales, eds.), p 113–136. Surrey Beatty and Sons, Chipping Norton, Australia.

Clarke, M. R.
1980. Cephalopoda in the diet of sperm whales of the Southern Hemisphere and their bearing on sperm whale biology. Discovery Rep. 37:1–324.
1986. A handbook for the identification of cephalopod beaks, 273 p. Clarendon Press, Oxford, England.
1996. The role of cephalopods in the world's oceans. Phil. Trans. R. Soc. Lond. B 351:977–1112.

Dunning, M., and S. B. Brandt.
1985. Distribution and life history of deep-water squid of commercial interest from Australia. Aust. J. Mar. Freshw. Res. 36:343–359.

Harrison, C. S., T. S. Hida, and M. P. Seki.
1983. Hawaiian seabird ecology. Wildl. Monogr. 85: 1–71.

Le Corre, M., Y. Cherel, F. Lagarde, H. Lormée, and P. Jouventin.
2003. Seasonal and interannual variation in the feeding ecology of a tropical oceanic seabird, the red-tailed tropicbird *Phaethon rubricauda*. Mar. Ecol. Prog. Ser. 255:289–301.

Matthews, F. D., D. M. Damkaer, L. W. Knapp, and B. B. Collette.
1977. Food of western North Atlantic tunas (*Thunnus*) and lancetfishes (*Alepisaurus*). NOAA Tech. Rep. NMSF SSRF-706, 19 p.

Nesis, K. N.
1987. Cephalopods of the world. Squids, cuttlefishes, octopuses, and allies, 351 p. TFH Publs., Neptune City, NJ.

Nesis, K. N., and C. M. Nigmatullin.
1979. The distribution and biology of the genus *Ornithoteuthis* Okada, 1927 and *Hyaloteuthis* Gray, 1849 (Cephalopoda: Oegopsida). Bull. Moscow Soc. Nat. 84:50–63. [In Russian.]

Nigmatullin, C. M., K. N. Nesis, and A. I. Arkhipkin.
2001. A review of the biology of the jumbo squid *Dosidicus gigas* (Cephalopoda:Ommastrephidae). Fish. Res. 54:9–19.

Okutani, T., and S. Tsukada.
1988. Squids eaten by lancetfish and tunas in the tropical Indo-Pacific Ocean. J. Tokyo Univ. Fish. 75:1–44.

Robertson, K. M., and S. J. Chivers.
1997. Prey occurrence in pantropical spotted dolphins, *Stenella attenuata*, from the eastern tropical Pacific. Fish. Bull. 95:334–348.

Rodhouse, P. G.
1997. Large and meso-scale distribution of the ommastrephid squid *Martialia hyadesi* in the Southern Ocean: a synthesis of information relevant to fishery forecasting and management. Korean J. Polar Res. 8:145–154.

Roper, F. E., and M. J. Sweeney.
1984. Cephalopods of the world. An annotated and illustrated catalogue of species of interest to fisheries. FAO Species Catalogue 3:1–277.

Shchetinnikov, A. S.
1992. Feeding spectrum of squid *Sthenoteuthis oualaniensis* (Oegopsida) in the eastern Pacific. J. Mar. Biol. Assoc. U.K. 72:849–860.

Vaske Jr., T., C. M. Vooren, and R. P. Lessa.
2004. Feeding habits of four species of Istiophoridae (Pisces: Perciformes) from northeastern Brazil. Environ. Biol. Fishes 70:293–304.

Warneke-Cremer, C.
1986. Contributions to the systematics of ommastrephid squid (Mollusca, Cephalopoda, Teuthoidea) and their distribution in the Atlantic, based on the catches of FFS "Walter Herwig" made during 1966 and 1968. Mitteil. Inst. Seefisch. Hamburg 40:1–116. [In German.]

Wormuth, J. H.
1998. Workshop deliberations on the Ommastrephidae: a brief history of their systematics and a review of the systematics, distribution, and biology of the Genera *Martialia* Rochebrune and Mabille, 1889, *Todaropsis* Girard, 1890, *Dosidicus* Steenstrup, 1857, *Hyaloteuthis* Gray, 1849, and *Eucleoteuthis* Berry, 1916. Smithsonian Contrib. Zool. 586:373–383.

Zuev, G. V., and V. N. Nikolsky.
1993. Ecological mechanisms related to intraspecific structure of the nektonic squid *Sthenoteuthis pteropus* (Steenstrup). *In* Recent advances in fisheries biology (T. Okutani, R. K. O'Dor, and T. Kubodera, eds.), p. 653–664. Tokai Univ. Press, Tokyo, Japan.

Zuyev, G., Ch. Nigmatullin, M. Chesalin, and K. Nesis.
2002. Main results of long-term worldwide studies on tropical nektonic oceanic squid genus *Sthenoteuthis*: an overview of the Soviet investigations. Bull. Mar. Sci. 71:1019–1060.

Measurements of total scattering spectra from bocaccio (*Sebastes paucispinis*)

Stéphane G. Conti (contact author)[1]
Benjamin D. Maurer[1]
Mark A. Drawbridge[2]
David A. Demer[1]

Email address for S. G. Conti: sconti@ucsd.edu

[1] Southwest Fisheries Science Center
8604 La Jolla Shores Drive
La Jolla, California 92037

Present address for S. G. Conti: Marine Physical Laboratory
Scripps Institute of Oceanography
University of California San Diego
9500 Gilman Drive
La Jolla, California 92093-0238

[2] Hubbs-SeaWorld Research Institute
2595 Ingraham St.
San Diego, California 92109

Marine sportfishing in southern California is a huge industry with annual revenues totaling many billions of dollars. However, the stocks of lingcod and six rockfish species have been declared overfished by the Pacific Fisheries Management Council. As part of a multifaceted fisheries management plan, marine conservation areas, covering many million square nautical miles, have been mandated. To monitor the recovery of the rockfish stocks in these areas, scientists are faced with the following challenges: 1) multiple species of rockfish exist in these areas; 2) the species reside near or on the bottom at depths of 80 to 300 m; and 3) they are low in numerical density. To meet these challenges, multifrequency echosounders, multibeam sonar, and cameras mounted on remotely operated vehicles are frequently used (Reynolds et al., 2001). The accuracy and precision of these echosounder results are largely dependent upon the accuracy of the species classification and target strength estimation (MacLennan and Simmonds, 1992).

Broad bandwidth characterization of sound scatter from marine organisms has some potential for remotely classifying fish species (Conti and Demer, 2003), shapes and sizes (Conti et al., 2005), behaviors (Conti et al., 2006b), and to validate models for target strength estimation (Demer and Conti, 2003). All of these studies have employed variants of a new method for measuring the broad bandwidth total scattering cross section (σ_T) of animals moving in a reverberant tank.

With the new method, the total scattering cross section (σ_T) of live animals in tanks is obtained from a comparison of the coherent and incoherent acoustical intensities reverberated in a tank (de Rosny and Roux, 2001, 2003). The accuracy of this measurement technique was shown by using standard metal spheres (Demer et al., 2003). This technique was successfully used on krill (Demer and Conti, 2003; Conti et al., 2006a), fish (Conti and Demer, 2003), and humans (Conti et al., 2004). In our study, we explored the potential and limitations of the method to characterize the broad bandwidth sound scattering from bocaccio (*Sebastes paucispinis*).

Materials and methods

The total scattering cross section, σ_T, of bocaccio was measured over acoustic frequencies ranging from 10 to 150 kHz with a group of fish (n=20) swimming freely in a large, insulated fiberglass tank at Hubbs-SeaWorld Research Institute, San Diego, CA, on 1 and 2 July 2004. The tank had 5.1 cm of foam insulation on the exterior, measured 2.44 m in diameter, and was filled with seawater to a depth of 1.37 m (V [volume]=6.4 m^3). The pool was thermostated at approximately 12°C. The acoustic measurement technique and a variety of its applications have been well documented (de Rosny and Roux, 2001; Conti and Demer, 2003; Demer and Conti, 2003; Demer et al., 2003; Conti et al., 2004). However, the general procedure and details of these experiments are presented here for convenience and clarity.

Each of the 20 fish was handled one time, a week prior to the experiment, to measure their weight (W) and total length (L). These data were summarized and plotted in graphs (Table 1, Fig. 1).

An emitter transmitted M acoustical pulses into the tank every other second (δT=2s). The corresponding reverberation time-series $h_k(t)$ were simultaneously recorded on multiple receivers while the fish were swimming between consecutive shots. The boundaries, volume, as well as the positions of the emitter and the receivers in the tank remained identical during the measurements.

The time series $h_k(t)$ were composed of echoes from the boundaries of the tank and the fish. For two consecutive time series $h_k(t)$ and $h_{k+1}(t)$, the contributions from the boundaries of the tank were identical, whereas the contributions from the fish were not. The coherent

$$S_c(t)=\frac{1}{M}\sum_{k=1}^{M}h_k(t)h_{k+1}(t)$$

and incoherent

$$S_i(t)=\frac{1}{M}\sum_{k=1}^{M}h_k^2(t)$$

Manuscript submitted 19 July 2005 to the Scientific Editor.

Manuscript approved for publication 7 July 2006.

Fish. Bull. 105:153–157 (2007).

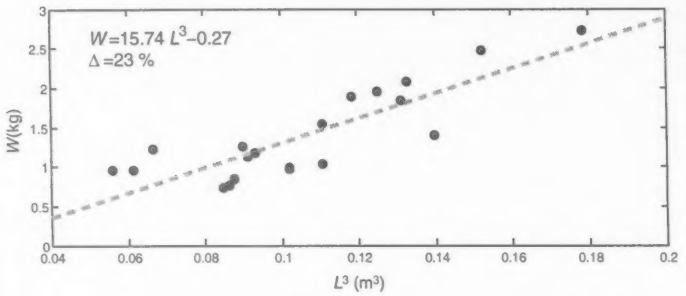

Figure 1

Weight (W) of each boccacio (*Sebastes paucispinis*) versus length-to-the-third power (L^3) (dark dots), and linear least-squares fit (dashed line), and the mean deviation Δ is shown below the equation.

intensities in the tank were estimated from the M recorded time series. The coherent component represents the acoustical intensity reverberated by the fixed boundaries of the tank. The incoherent component also accounted for the acoustical intensity scattered by the fish. When the positions of the fish were uncorrelated between consecutive pulses, the ratio $S(t)$ of the coherent to the incoherent intensities decreased exponentially with the scattering mean free path l_s of the fish (de Rosny and Roux, 2001):

$$S(t)=\left[\frac{S_c(t)}{S_i(t)}\right]\approx\exp\left(-t\frac{c}{l_s}\right)\approx\exp\left(-t\frac{cN\sigma_T}{V}\right),$$

where the bracketing [ ] designates the average for multiple receivers.

The scattering mean free path is related to the total scattering cross section of a single fish in the tank (σ_T), the sound speed (c), the number of fish (N). and the volume (V). Multiple receivers may be used simultaneously to reduce the heterogeneities of the acoustical field on the coherent and incoherent intensities in the tank. Knowing N, c, and V, σ_T (normalized to a single fish) was estimated from the exponential decay of $S(t)$. Thus, σ_T averaged over 10 to 150 kHz was estimated for a single bocaccio, and its total scattering spectrum was similarly estimated after filtering the recorded time series $h_k(t)$ into twenty narrow frequency bands. Each band corresponded to the bandwidth of the transmitted chirp, divided by twenty.

The signal acquisition system (Fig. 2) consisted of a function generator CompuGen 1100 (GageApplied, Montreal, Canada) internally clocked with two 16-bit CompuScope 1610 (GageApplied, Montreal, Canada) dual-channel acquisition boards in a portable computer. The internal clocking of the function generator and the acquisition boards allowed perfect timing between the emitted and the recorded signals. Ensembles of M=100 chirps were transmitted over 50 ms every other second for three frequency bandwidths from 10 to 40 kHz with an ITC1001B emitter (f_c=25 kHz); 30 to 70 kHz with an ITC1032 emitter (f_c=50kHz); and 60 to 150 kHz with

Table 1

Total length (L) and weight (W), and the mean and standard deviation of each,, for the 20 boccacio (*Sebastes paucispinis*) used to measure the total scattering cross section over acoustic frequencies from 10 to 150 kHz in a laboratory tank at Hubbs SeaWorld Research Institute, San Diego, CA.

Fish number	Total length (L, mm)	Weight (W, kg)
1	467	0.99
2	444	0.85
3	480	1.03
4	467	0.97
5	453	1.18
6	442	0.77
7	519	1.4
8	439	0.73
9	450	1.13
10	500	1.95
11	448	1.25
12	510	2.08
13	480	1.54
14	508	1.84
15	534	2.47
16	563	2.73
17	491	1.88
18	394	0.95
19	382	0.95
20	405	1.23
Mean	468	1.37
Standard deviation	45.5	0.57

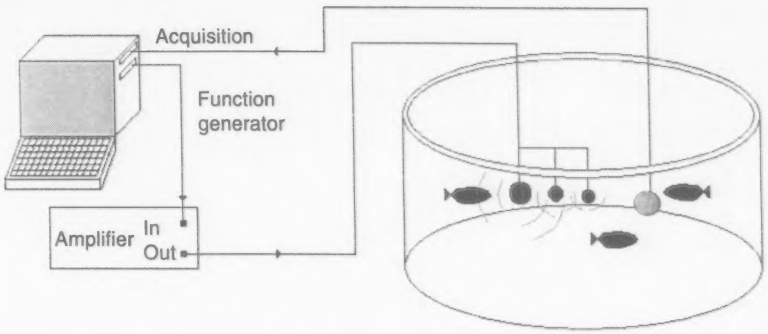

Figure 2

Diagram of the experimental setup: a computer with integrated function generator (CompuGen 1100, GageApplied, Montreal, Canada) and analog to digital acquisition system (CompuScope 1610, GageApplied, Montreal, Canada) connected to the emitters in black (ITC1001B, ITC1032, ITC1042; ITC Transducers Company, Santa Barbara, CA) and receivers in gray (one ITC1001, one ITC1032, and two ITC1042; ITC Transducers Company, Santa Barbara, CA) in the tank. The transmitted signal is amplified with a power amplifier (Krohn-Hite 7500, Krohn-Hite Corporation, Brockton, MA).

an ITC1042 emitter (f_c=105 kHz) (ITC Transducers Company, Santa Barbara, CA). The transducers were inserted from the top of the aquarium. The amplitude of the chirps from the function generator was 1 volt peak-to-peak, amplified 100 times (40 dB) with a Krohn-Hite 7500 amplifier (Krohn-Hite Corporation, Brockton, MA). The corresponding reverberation time series were recorded at a 500-kHz sampling rate, for at least 90 ms on a four transducer array consisting of one ITC1001, one ITC1032, and two ITC1042 transducers.

To increase the signal-to-noise ratio, the recorded reverberation time series were cross correlated with the transmitted signal to obtain the impulse responses $h_k(t)$. The measurements for the lowest (f_c=25 kHz) and highest (f_c=105 kHz) frequencies bands were repeated 11 times. The measurements for the center frequency (f_c=50 kHz) band were repeated 20 times. For f_c=25, 50, and 105 kHz, the total scattering cross sections were estimated from the signals on the ITC1001, ITC1032, and two ITC1042 receivers, respectively.

Results

The mean weight (W) and total length (L) of the 20 bocaccio were 1.37 kg (ranging from 0.73 to 2.73 kg; standard deviation (SD)=0.57 kg), and 468 mm (ranging from 382 to 563 mm; SD=45.5 cm), respectively (Table 1). Fish masses did not correlate well to fish lengths (Fig. 1). The mean deviation was about 25%, for fish weight to fish length-to-the-third-power. This fit may indicate heterogeneity in the shapes (i.e., long and thin versus short and wide) and could be observed from visual inspection of the fish.

Because the fish were not moving very actively during the experiments, the time between consecutive shots δT had to be increased to assure uncorrelated positions of the fish. This was effectively achieved by considering the shots k and k+20 instead of k and k+1 to estimate S_c(t), resulting in δ_T=40 s between the shots. By increasing the time between shots, the measured total scattering cross section reached a stable plateau at σ_T=0.01 m^2 for each of the considered frequency bands (Fig. 3). This plateau indicated that the positions of the fish were uncorrelated between shots, and the measured total scattering cross section was not biased by the correlation of fish positions (Conti et al., 2006a). The measurement variance was conspicuously higher in the lowest and highest frequency bands because of decreased signal-to-noise ratios. The differences in signal-to-noise ratio with frequency was due to the experimental setup at high frequency, and the lack of acoustic modes propagating in the tank at low frequencies. The total scattering cross section was equivalent to the one expected for a rigid sphere of diameter 90 mm in water (Fig. 4; Faran, 1951), which is of the order of the size of the swimbladder for the fish in the tank (Foote, 1979). The largest discrepancies between the measurements and expectations were at the lowest and highest frequencies, again because of lower signal-to-noise ratios.

The total scattering cross-sectional area was virtually the same for each of the three frequency bands because all three measurements were in the geometric scattering domain for these fish. In other words, in all three frequency bands the radius of the equivalent scattering sphere was greater than half the wavelength. In the geometric domain, the scattering cross-section increased with the square of the frequency, in contrast

to the frequency to the fourth power in the Rayleigh domain. For these fish, the transition from the Rayleigh to geometric regimes occurred at frequencies around 15 kHz (Fig. 4).

The spectra of σ_T are shown for over 60 narrow bandwidths (Fig. 4) after we averaged the results from all of the experiments. Each of the three frequency bands were resolved into 20 narrow bandwidths. Further narrowing of the filters on the reverberation time series served only to increase the standard deviation of the measurements without providing more information on the spectra. The mean σ_T was in agreement with the previous broad bandwidth average. The σ_T and its standard deviation increased at the lowest and highest frequencies, likely because of a decrease in signal-to-noise ratios.

The back scattering target strength $TS=10\log_{10}(\sigma_{bs})$ for these fish can be compared to the target strength from a rigid sphere in water of radius a for which the resonances are damped by the surrounding flesh. For this type of scatterer, the target strength at high

$$ka=\frac{2\pi f}{c}a$$

is equal to $10\log_{10}(\pi a^2)$. For a rigid sphere in water of diameter 90 mm, $10\log_{10}(\pi a^2)=-22$dB. The swimbladder is gas filled and can be considered a hard scatterer and its resonances are damped by the surrounding flesh. As a first-order approximation, the theoretical predictions for the air bubble can be used to estimate the target strength of the fish by adjusting the radius of the rigid sphere to the size of the fish swimbladder.

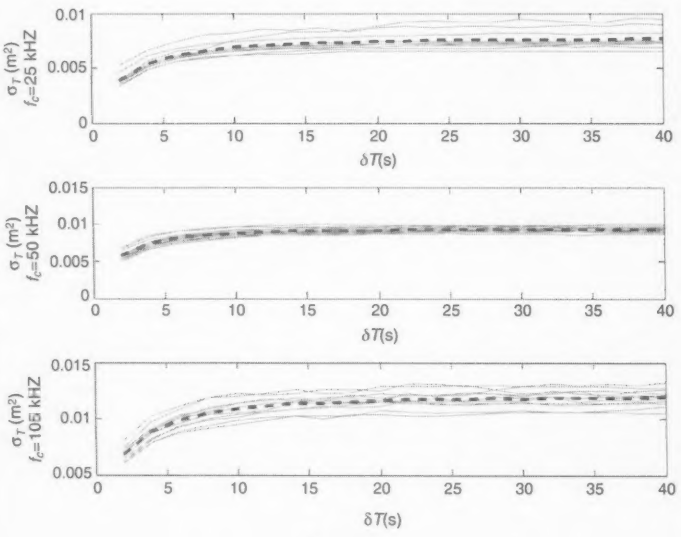

Figure 3

Total scattering cross section σ_T, normalized to one bocaccio (*Sebastes paucispinis*), versus time between shots, δT, for three frequency bands. The measurements (dotted lines) for the lowest and highest frequencies band were repeated 11 times, and 20 times for the center frequencies band, and averaged (dashed dark lines). For short time between shots, σ_T was biased because of slow fish motion. The measurements stabilized with increasing time between shots, δT.

Discussion

The mean σ_T from 10 to 150 kHz was measured from boccacio with a mean length of 468 mm. It is roughly equivalent to that from a 90-mm-diameter rigid sphere in water. This result is in agreement with the approximate size of their swimbladder. Thus, the spectrum of the total scattering cross section for boccacio can be measured with this technique.

Despite these positive results, the following should be considered for future experiments. These measurements were made against the frequency from a heterogeneous-size group of a single species of fish. As such, the results do not permit comparisons of σ_T with frequency, and animal species and morphological features (e.g., size, shape, length, sex, etc.). Measurements should be made of individual fish.

It should also be noted that the bocaccio in these experiments moved very slowly. Simply increasing the time to achieve incoherence between pulses may itself introduce systematic and random measurement error because of instabilities in the medium. That is, some additional incoherence can result from bubbles and fluctuations in the water temperature, sound speed, volume, and water surface. The magnitude of this incoherence could eclipse the differences in σ_T between individual fish. In these measurements, bubbles and motion of the air-water interface caused by breaking bubbles and fish motion were noticeable visually but had only minor effects on the data.

The most significant shortcoming of these experiments was a generally low signal-to-noise ratio because of the tank size and material properties. This low ratio caused appreciable measurement uncertainty at the lowest and highest frequencies. The water volume was large for the projected signal intensities, and the fiberglass boundaries were not very reflective in comparison to other materials such as stainless steel and glass used in previous experiments. Therefore, to obtain and compare measurements of σ_T from

rockfish of different species and sizes, future measurements should be made of individual fish in tank volumes appropriate to the size and the frequency range of the fish, insuring high signal-to-noise ratios and reverberation times. Because of fish handling constraints and access to only a single species of rockfish, it was not possible to do to include these measurements in the present study.

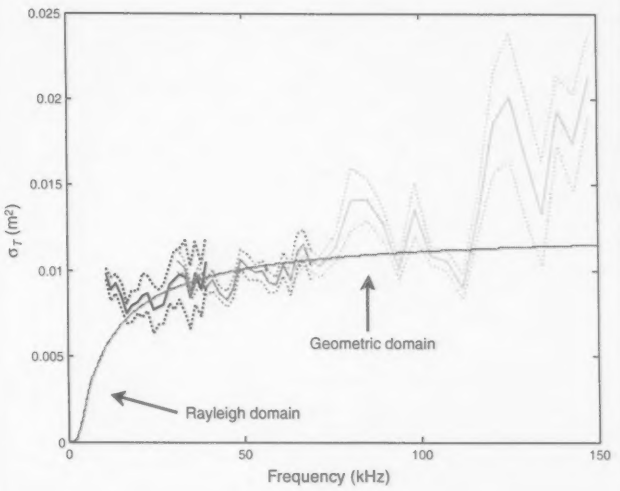

Figure 4

Total scattering spectra σ_T normalized to one boccacio (*Sebastes paucispinis*), over the full frequency band, low to high frequency bands (solid lines from dark to light), and one standard deviation error bounds for these measurements (dashed lines). The spectra were obtained after filtering the data in 20 narrow bands bins for each of the three frequency bands. Theoretical predictions for a 90-mm-diameter rigid sphere in water (Faran, 1951; solid line from 0 to 150 kHz), showing the transition between the Rayleigh and the geometric regimes.

Acknowledgments

We are grateful to P. Sylvia and the rest of the staff at Hubbs-SeaWorld Research Institute for hosting the experiments, and to Chevron Corporation for sponsoring the research.

Literature cited

Conti, S. G., and D. A. Demer.
2003. Wide-bandwidth acoustical characterization of anchovy and sardine from reverberation measurements in an echoic tank. ICES J. Mar. Sci. 60(3):617–624.

Conti, S. G., D. A. Demer, and A. S. Brierley.
2005. Broadbandwidth sound scattering and absorption from krill (*Meganyctiphanes norvegica*), mysids (*Praunus flexuousus* and *Neomysis integer*) and shrimp (*Crangon crangon*). ICES J. Mar. Sci. 62(5):956–965.

Conti, S. G., J. de Rosny, P. Roux, and D. A. Demer .
2006a. Scatterer motion characterization and estimation in a reverberant medium. J. Acoust. Soc. Am. 119(2):769–776.

Conti, S. G., P. Roux, D. A. Demer, and J. de Rosny.
2004. Measurement of the scattering and absorption cross-section of the human body. App. Phy. Let. 84(5):819–821.

Conti, S. G., P. Roux, C. Fauvel, B. D. Maurer, and D. A. Demer.
2006b. Acoustic monitoring of fish density, behavior, and growth rate in a tank. Aquaculture 251(2–4):314–323.

Demer, D. A., and S. G. Conti.
2003. Reconciling theoretical versus empirical target strengths of krill; effects of phase variability on the distorted wave Born approximation. ICES J. Mar. Sci. 60(2):429–434.

Demer, D. A., S. Conti, J. De Rosny, P. Roux.
2003. Absolute measurements of total target strength from reverberation in a cavity. J. Acoust. Soc. Am. 113:1387–1394.

de Rosny, J., and P. Roux.
2001. Multiple scattering in a reflecting cavity: application to fish counting in a tank. J. Ac.Soc. Am. 109:2587–2597.

de Rosny, J., P. Roux, M. Fink, and J. H. Page.
2003. Field fluctuation spectroscopy in a reverberant cavity with moving scatterers. Phy. Rev. Let. 90:9–4302.

Faran, J. J.
1951. Sound scattering by solid cylinders and spheres. J. Ac. Soc. Am. 23(4):405–418.

Foote, K. G.
1979. Fish target-strength-to-length regressions for application in fisheries research. Proceedings of the Ultrasonic International 19, Graz, Austria, 327–333 p. IPC Science and Technology Press Ltd., Guilford, England.

MacLennan, D. N., and E. J. Simmonds.
1992. Fisheries acoustics, 325 p. Chapman and Hall, London.

Reynolds, J. R., R. C. Highsmith, B. Konar, C. G. Wheat, and D. Doudna.
2001. Fisheries and fisheries habitat investigations using undersea tehnologies, OCEANS. MTS/IEEE Conference and Exhibition. *In* Proceedings of the Oceans 2001 conference; 5–8 November 2000, Honolulu, HI. Hawaiian Sea Grant Program, Univ. Hawaii at Manoa, Manoa, HI.

Fishery Bulletin

Guidelines for authors

Content of manuscripts

Contributions published in Fishery Bulletin describe original research in marine fishery science, fishery engineering and economics, as well as the areas of marine environmental and ecological sciences (including modeling). Although all contributions are subject to peer review, responsibility for the contents of papers rests upon the authors and not upon the editor or publisher. *Submission of an article implies that the article is original and is not being considered for publication elsewhere.* Manuscripts must be written in English. Authors whose native language is not English are strongly advised to have their manuscripts checked by English-speaking colleagues prior to submission. **Articles** may range from relatively short contributions (10–15 typed, double-spaced pages, tables and figures not included) to extensive contributions (20–30 typed pages). **Notes** are reports of 5 to 10 pages without an abstract and describe methods or results not supported by a large body of data.

Manuscript preparation

Title page should include authors' full names and mailing addresses and the senior author's telephone, fax number, and e-mail address, and a list of key words to describe the contents of the manuscript. **Abstract** should be limited to 150 words (one-half typed page), state the main scope of the research, and emphasize the author's conclusions and relevant findings. Do not review the methods of the study or list the contents of the paper. Because abstracts are circulated by abstracting agencies, it is important that they represent the research clearly and concisely. **Text** must be typed in 12 point Times New Roman font throughout. A brief introduction should convey the broad significance of the paper; the remainder of the paper should be divided into the following sections: **Materials and methods, Results, Discussion (or Conclusions),** and **Acknowledgments**. Headings within each section must be short, reflect a logical sequence, and follow the rules of multiple subdivision (i.e., there can be no subdivision without at least two items). The entire text should be intelligible to interdisciplinary readers; therefore, all acronyms, abbreviations, and technical terms should be written out in full the first time they are used. Include FAO common names for species in the list of keywords and in the introduction. Regional common names may be used throughout the rest of the text if they are different from FAO common names which can be found at http://www.fishbase.org/search.html. Follow the U.S. Government Printing Office Style Manual (1984 ed.) and the CBE Style Manual (6th ed.) for editorial style; for fish nomenclature follow the most current issue of the American Fisheries Society's Common and Scientific Names of Fishes from the United States and Canada. Dates should be written as follows: 11 November 2000. Measurements should be expressed in metric units, e.g., 58 metric tons (t); if other units of measurement are used, please make this fact explicit to the reader. Write out the numbers zero through nine unless they form part of measurement units (e.g., nine fish but 9 mm).

Text footnotes should be inserted in 9-point font at the bottom of the page that displays the first citation of the footnote. Footnotes should be formatted in the same manner as citations. Footnote all personal communications, unpublished data, and unpublished manuscripts with full address of the communicator or author, or, as in the case of unpublished data, where the data are on file. Authors are advised to avoid references to nonstandard (gray) literature (such as internal, project, processed, or administrative reports, ICES Council Minutes, IWC Minutes or Working Papers, any "research" or "working" documents, laboratory or contract reports, Management Council reports, and manuscripts in review) wherever possible. If these references are used, present them as footnotes and list whether they are available at NTIS (National Technical Information Service) or at some other public depository. Cite all software and special equipment or chemical solutions used in the study, not in a footnote but within parentheses in the text (e.g., SAS, vers. 6.03, SAS Inst., Inc., Cary, NC).

Literature cited comprises published works and those accepted for publication in peer-reviewed literature (in press). Follow the name and year system for citation format in the "Literature cited" section. If there is a sequence of citations in the text, list chronologically: (Smith, 1932; Green, 1947; Smith and Jones, 1985). Abbreviations of serials should conform to abbreviations given in the Serial Sources for the BIOSIS Previews Database. Authors are responsible for the accuracy and completeness of all citations. Literature citation format: Author (last name, followed by first-name initials). Year. Title of report or manuscript. Abbreviated title of the series to which it belongs. Always include number of pages. If the authorship for a sequence of citations is identical, list works chronologically.

Tables and figures—general format

- Zeros should precede all decimal points for values less than one.
- Sample size, *n*, should be italicized.
- Capitalize the first letter of the first word in all labels within figures.
- Do not use overly large font sizes in maps and for units of measurements along axes in figures.
- Do not use bold fonts or bold lines in figures.
- Do not place outline rules around graphs.
- Do not use horizontal lines in graphs to indicate measurement units on axes.
- Use a comma in numbers of five digits or more (e.g. 13,000 but 3000).
- Maps should have a North arrow (or compass sign) and degrees latitude-longitude (e.g., 170°E)

Tables are often overused in scientific papers; it is seldom necessary or even desirable to present all the data associated with a study. Tables should not be excessive in size and must be cited in numerical order in the text. Headings should be short but ample enough to allow the table to be intelligible on its own. All unusual symbols must be explained in the table legend. Other incidental comments may be footnoted with italic footnote markers. Use asterisks to indicate probability in statistical data. Do not type table legends on a separate page; place them on the same page as the table data. *Do not submit tables in photo mode.*

Figures include line illustrations, photographs (or slides), and computer-generated graphs and must be cited in numerical order in the text. Graphics will aid in the comprehension of the text, but they should be limited to presenting patterns rather than raw data. Figures are costly to print and should be limited to six. Figures must be labeled with author's name and number of figure. Avoid placing labels vertically (except on *y*-axis). Figure legends should explain all symbols and abbreviations and should be double-spaced on a separate page at the end of the manuscript. Please note that we do not print graphs in color.

FAILURE TO FOLLOW THESE GUIDELINES WILL DELAY PUBLICATION OF A MANUSCRIPT

Copyright law does not apply to *Fishery Bulletin*, which falls within the public domain. However, if an author reproduces any part of an article from *Fishery Bulletin* in his or her work, reference to source is considered correct form (e.g., Source: Fish. Bull 97:105).

Reprints are available free of charge to the senior author (50 copies) and to his or her laboratory (50 copies).

Submission

The Scientific Editorial Office encourages authors to submit their manuscripts as a *single* PDF (preferred), or Word (zipped) document by e-mail to Fishery.Bulletin@noaa.gov. Please use the subject heading "Fishery Bulletin manuscript submission." *Do not* send encrypted files. For further details on electronic submission, please contact the Scientific Editorial Office directly (see address below). Or you may send your manuscript on compact disc in one of the above formats along with four printed copies (one original plus three copies [stapled]) to the Scientific Editor, at the address shown below.

Dr. Adam Moles
Scientific Editor, *Fishery Bulletin*
11305 Glacier Hwy
Juneau, AK 99801-8626

Once the manuscript has been accepted for publication, you will be asked to submit a final software copy of your manuscript. When requested, the text and tables should be submitted in Word or Word Rich Text Format. Figures should be sent as PDF files, Windows metafiles, tiff files, or as EPS files. Send a copy of figures in original software if conversion to any of these formats yields a degraded version.

Fishery Bulletin

Subscription form

Superintendent of Documents **Publications** Order Form

*5178

☐ YES, please send me the following publications:

____ Subscriptions to *Fishery Bulletin*
for $36.00 per year ($50.40 foreign)

The total cost of my order is $ _____ . Prices include regular domestic postage and handling and are subject to change.

_____
(Company or Personal Name) (Please type or print)

_____
(Additional address/attention line)

_____
(Street address)

_____
(City, State, ZIP Code)

_____
(Daytime phone including area code)

_____
(Purchase Order No.)

Charge your order. IT'S EASY!

VISA

MasterCard

Please Choose Method of Payment:

☐ Check Payable to the Superintendent of Documents

☐ GPO Deposit Account ☐☐☐☐☐☐–☐

☐ VISA or MasterCard Account

☐☐☐☐☐☐☐☐☐☐☐☐☐☐☐☐

☐☐☐☐ (Credit card expiration date)

To fax your orders (202) 512-2250

_____
(Authorizing Signature)

Thank you for your order!

Mail To: Superintendent of Documents
P.O. Box 371954, Pittsburgh, PA 15250-7954

Also available online at http://bookstore.gpo.gov/collections/fishery-bulletin